# VULCAN: Network Analysis of ER-α activation reveals reprogramming of GRHL2

Andrew N. Holding[1,3,*], Federico M. Giorgi[1,3], Amanda Donnelly[1], Amy E. Cullen[1], Luke A. Selth[2], and Florian Markowetz[1]

[1] CRUK Cambridge Institute, University of Cambridge, Robinson Way, Cambridge, CB2 0RE
[2] Dame Roma Mitchell Cancer Research Laboratories and Freemasons Foundation Centre for Men's Health, Adelaide Medical School, The University of Adelaide, SA, Australia

[3] These authors contributed equally to this work.

*Corresponding Author

# Abstract

VULCAN utilises network analysis of genome-wide DNA binding data to predict regulatory interactions of transcription factors. We benchmarked our approach against alternative methods and found improved performance in all cases. VULCAN analysis of estrogen receptor (ER) activation in breast cancer highlighted key components of the ER signalling axis and identified a novel interaction with GRHL2, validated by ChIP-seq and quantitative proteomics. Mechanistically, we show E2-responsive GRHL2 binding occurs concurrently with increases in eRNA transcription and GRHL2 negatively regulates transcription at these sites. These findings provide new insight into ER action in breast cancer and validate VULCAN as a powerful tool.

**100/100**



**Keywords:** Breast Cancer, Network Analysis, Dynamics, ER, Master Regulator, ChIP-seq, VULCAN, GRHL2, Squelching, P300

# Introduction

**Network Analysis of ChIP-seq to infer Transcription Factor (TF) activity**

Usage of gene regulatory networks to analyse biological systems has witnessed an exponential increase in the last decade, due to the ease of obtaining genome-wide expression data [1–3]. Recently, the VIPER approach to interrogate these network models has been proposed to infer transcription factor activity using the expression of a collection of their putative targets, *i.e.* their regulon [4]. In the VIPER algorithm, gene-level *differential expression* signatures are obtained for either individual samples (relative to the mean of the dataset) or between groups of samples, and regulons are tested for enrichment.

Several tools exist to integrate ChIP-seq binding events to increase statistical power and to support the interpretation of data. These methods typically provide information in the context of biological pathways and established gene sets [5,6] or through motif analysis [7]. In contrast, we developed an extension of the VIPER algorithm, called "**V**irt**U**a**L** **C**hIP-seq **A**nalysis through **N**etworks" (VULCAN), to reveal and specifically analyse potential interactions of TFs in ChIP-seq experiments. Previously, the strategies employed by VIPER were limited to the analysis of transcription data. By developing VULCAN to overlay co-expression networks established from patient tumour data onto ChIP-seq data, we are able to provide candidate coregulators of the response to a given stimulus (**Figure 1**). Unlike previous method, the results of our analysis are therefore focused on discovering tissue or disease specific interactions in the context of these networks. Further, as VULCAN builds on master regulator analysis, the output from the pipeline provides the end user with information in terms of the activity of potentially interacting TFs, rather than in terms of pathways. The combination of disease specific context and TF activity information presents a significant step forward in providing valuable information for the elucidation of on-chromatin interactions from ChIP-seq experiments over previous strategies.

**The estrogen receptor as a model for systems biology**

Breast cancer is the most common form of cancer in women in North America and Europe. The majority of breast cancers are associated with deregulated signalling by the Estrogen Receptor-alpha (ER), which drives tumour growth. ER is the key prognostic marker in the clinic and the target of the first lines of treatment in estrogen receptor positive (ER+) tumors. ER-targeting pharmacological strategies include SERMs (Selective Estrogen Receptor Modulators e.g. tamoxifen) and SERDs (estrogen receptor degraders, e.g. fulvestrant) and aromatase inhibitors that block the production of estrogens in the body [8]

On activation, ER binds to promoter and enhancer regions containing Estrogen-Response Elements (ERE) [9] to stimulate the transcription of hundreds of genes [10,11]. Gene expression is driven by both the recruitment of the basal transcription machinery to these loci and through longer range interactions [12]. Analysis of ER-target genes showed that many are proliferative in function and drive the growth of the tumour [13]

On the treatment of ER+ cells with estra-2-diol (E2), ER recruits several cofactors to form a complex on the chromatin. FOXA1 is of particular interest as the protein shares nearly 50% of its genomic binding sites with ER and has been shown to operate as a pioneer factor before ER activation [14]. It is through FOXA1 and other cofactors [15,16], e.g. SRC-1, that ER is able to recruit RNA Polymerase II at the gene promoter sites in order to initiate transcription [17].

Early studies have shown that, after stimulation with E2, ER binding to EREs can occur within minutes [18]. Maximum ER occupancy at promoters of target genes such as CTSD and TFF1 is achieved after 45’ in MCF7 cells. Roughly 90’ after estradiol treatment, ER is partially released from the promoters of the target gene, only to reoccupy the site again at 135’ and release them at 180’, in a 45’ phase cyclical manner [19]. The 90’ occupancy phase has been shown to be independent of new protein synthesis, and is therefore thought to operate at the

post-translational level. This cyclic, proteasome-mediated turnover of unliganded and liganded ER-α on responsive promoters is an integral feature of estrogen signaling [20,21].

Given the three features discussed above, ER is a prime target for systems biology. By applying VULCAN to ChIP-seq time-course data of ER activation, our study provides new temporal insights into ER cofactors on a genome-wide scale.

# Results

The development of VULCAN to infer changes in cofactor activity from differential ChIP-seq analysis using network analysis led to novel insights into key coregulators of the ER binding process. An implementation of VULCAN in R is available on Bioconductor.org [https://bioconductor.org/packages/release/bioc/html/vulcan.html] and the scripts to replicate our analysis are available as a supplementary Rmarkdown file. Unless otherwise specified, all p-values were Bonferroni-corrected.

## Regulatory network analysis to detect ER cofactors

VULCAN was developed in order to understand which TF or co-factors could be responsible for the temporal behavior of ER. To develop VULCAN, we combined co-expression networks, established from breast cancer tumour biopsy transcriptional data, with a modified version of the VIPER algorithm [4] to enable master regulator analysis on differential binding signatures acquired from ChIP-seq analysis.

We generated co-expression networks using the most recent implementation of ARACNe [22] on the METABRIC dataset [23] and the independent TCGA dataset [24]. Briefly, ARACNe generates gene networks by estimating putative regulatory interactions between transcription factors and target genes using mutual information between gene expression

profiles. As an example, **Figure 1C** shows an ARACNe-inferred targets of ESR1. The sets of targets of each TF (i.e. its regulon) were merged in a genome-wide transcriptional regulation network, as shown in a minimal diagram in **Figure 1D**.

Master regulator analysis [25] is an algorithm developed to identify transcription factors whose regulon is enriched within a list of differentially expressed genes. VULCAN extends the VIPER approach to use differential binding profiles rather than differential expression profiles. In this way, VULCAN can test the enrichment of TF regulons in ER occupancy signatures derived from ChIP-seq experiments (**Figure 1E**).

## Comparison of VULCAN to existing methods

### Comparing VULCAN's Mutual Information networks to Partial Correlation networks

VULCAN uses mutual information networks like VIPER [4]. To test the robustness of our approach to different underlying networks, we compared mutual information networks with partial correlation networks using different correlation thresholds. We generated several partial correlation networks from the TCGA Breast Cancer data using the same input as the ARACNe network used by VULCAN. We tested the overlap of every partial correlation network with the ARACNe network using the Jaccard Index (JI) criterion (**Suppl. Figure 33**). Finally, we show how the Jaccard Index between partial correlation networks and the ARACNe network is always significantly higher than expected by selecting random network edges (**Suppl. Figure 34**). This confirms previous observations that partial correlation and mutual information networks are highly similar [26]

### Comparing VULCAN with alternative methods for target enrichment analysis

We compared VULCAN's Gene Set Enrichment Analysis (GSEA) approach [27] with three independent methods previously applied to benchmark VIPER [4]. The first implemented a t-test

based method, which takes the targets of a TF and integrates their p-value in a specific contrast. The method is similar to VIPER but involves a Fisher p-value integration step. The integrated test lacks stringency and results in nearly all regulons as significantly enriched (**Suppl. Figure 35**). Second, we implemented a fraction of targets method, defining for every TF the fraction of their targets that are also differentially bound. This alternative to VULCAN ignores the MI strength of interaction and the individual strengths of differential bindings, reducing the resolving power of the algorithm (**Suppl. Figure 36**). Finally, we compared to a Fisher's Exact Method, which assesses the overlap between networks and significant differential binding. This method is too stringent (as observed in the original VIPER paper) [4] and even without p-value correction there are no significant results, even at low stringency, demonstrating the low sensitivity of the using a Fisher's Exact Method method (**Suppl. Figure 37**). In summary, VULCAN outperformed all three alternative methods we tested (t-test based; fraction of targets method; and Fisher's Exact Method) in our dataset.

**Comparing VULCAN with Online Tools (GREAT, ISMARA & ChIP-Enrich)**

To further validate our method, we compared the output of our GSEA analysis with different versions of promoter-enrichment approaches implemented by GREAT [5], ISMARA [7] and ChIP-Enrich [6]. The VULCAN analysis shows a significant overlap in terms of detected pathways with the GREAT method (**Suppl. Figure 38**). ChIP-Enrich identifies enrichment of a number of TFs also predicted by VULCAN, but it fails to identify ESR1 as the top transcription factor affected by our experiment (**Suppl. Figure 39**). ISMARA succeeds at identifying ESR1 using a motif-based analysis, but does not identify other candidate binding TFs (**Suppl. Figure 40**). In summary, VULCAN outperforms both ISMARA and ChIP-Enrich, and significantly overlaps with GREAT, but provides additional value through inference of TF factor activity.

# VULCAN analysis of ER activation

**Differential Binding Analysis**

We performed four replicated ChIP-seq experiments for ER at three timepoints: 0, 45 and 90' after estradiol treatment **(Figure 2)** in the MCF7 breast cancer cell line**.** The binding profile of ER at each time point was then compared between time points using differential binding analysis. Differential binding analysis (**Figure 2B,C**) identified 18,900 statistically significant binding events at 45' ($p < 0.05$). We observed the previously reported reduction of ER binding at 90' [20] on a genome-wide level (17,896 significant binding events), but with a smaller amplitude than previous gene-specific assays [21]. A potential cause for the smaller amplitude we observed in ER cycling may relate to the fact that ChIP-seq is not inherently quantitative, and hence the typical normalisation strategies applied to ChIP-seq data are likely to suppress global changes [28,29]. We therefore validated the ER binding behaviour with ChIP-qPCR (**Figure 2A**) and observed the same reduction in amplitude at specific binding events as was predicted by ChIP-seq. Another potential reason for the difference in amplitude was we did not treat α-Amanitin prior to treatment with E2 [21] as this perturbation would further separate the experimental condition from clinical interpretation**.**

We performed motif enrichment analysis (HOMER software) on ER binding sites detected by differential binding analysis. This analysis confirmed a strong enrichment for a single element, ERE, bound at both 45 and 90', with a corrected p-value of 0.0029 (**Figure 3F**). When clustered according to peak intensity, samples cluster tightly in two groups: treated and untreated (**Suppl. Figures 2, 3 and 4**), but treatment at 45 and 90' is detectably different on a genome-wide scale, as highlighted by Principal Component Analysis (**Suppl. Figures 5 and 6**).

**VULCAN groups genes by temporal dynamics of ER binding**

We leveraged the information contained in mutual information networks to establish TF networks enriched in the differential binding patterns induced by estradiol. From our temporal analysis of ER binding, we established four classes of binding pattern: early responders, repressed transcription factors, late responders and candidate cyclic genes (**Figure 3).**

Using VULCAN, we defined TF network activity of occupied regulatory regions (**Figure 3A**) according to the binding of ER within their promoter and enhancer regions (limited to 10kb upstream of the Transcription Starting Site to ensure gene specificity). We define as early responders TFs whose network is upregulated at both 45 and 90' (**Figure 3B**); these genes include AR, SP1 and CITED1. TFs with opposite behaviour (namely TFs whose negative/repressed targets in the ARACNe model are occupied by ER), or "repressed TFs", include GLI4, MYCN and RAD21 (**Figure 3C**). Some TFs appear to have their targets bound at 45', but then unoccupied at 90'. This "updown" behaviour is consistent with the cyclic properties of certain components of the ER DNA-binding complex observed previously, and therefore we dubbed them "candidate cyclic TFs" (**Figure 3D**). We also define a "late responders" category, defined as  TFs active at 90 but not at 45'. While this category exists, and notably contains both ESR1 and the known ESR1 interactor GATA3, it is just below the significance threshold at 45' (**Figure 3E**).

**Validating VULCAN results on independent data**

We repeated our TF network activity analysis of ER activation (Figure 3A-E) on an independent data from TCGA (**Suppl. Figures 16–20**). We again found enrichment for ESR1 as a later responder. GATA3 was detected as an early responder, likely as a result of the METABRIC result being only slightly below the significance threshold at 45'. Notably, PGR was shifted from an early responder to a late responder.

To ensure the robustness of results, we performed a joint analysis of data obtained from both networks. At 45' (**Figure 4A**) and 90' (**Figure 4B**) we identified robust candidates,

specifically the ESR1, GATA3 and RARA networks were consistently activated by ER in both time points. On the other hand, some factors, including HSF1 and GRHL2, were significantly repressed in the joint analysis.

As a negative control, we used a different context ARACNe network, derived from the TCGA AML dataset. This network shows globally weaker enrichment scores and a weak positive correlation with the results obtained through breast cancer regulatory models (**Suppl. Figure 22**).

**Pathway analysis of regulatory region binding**

We performed a Gene Set Enrichment Analysis [27] and an associated Rank Enrichment Analysis [4] using the differential binding at gene regulatory regions (with time 0 as reference). Individual differential binding signatures for GSEA were calculated using a negative binomial test implemented by DiffBind [30]. The collective contribution of differentially bound sites highlights several ER-related pathways [31–33] (**Suppl. Figure 23**) in both the GSEA and aREA analyses. The strongest upregulated pathway in both time points (**Table S2 and S5**) was derived via RNA-seq in an MCF7 study using estradiol treatment [32], confirming the reproducibility of our dataset.

**Validating VULCAN results by quantitative proteomics**

We tested the performance of VULCAN against a complementary experimental approach called RIME [34] combined with TMT [35] (qPLEX-RIME), which aims at identifying interactors of ER within the ER-chromatin complex. We generated ER qPLEX-RIME data from MCF7 cells treated with estradiol at both 45 and 90’ and compared this with the VULCAN dataset, with the aim of identifying TFs upstream of the observed differential binding (**Suppl. Figure 31**). We found known ESR1 interactors with both methods, namely HDAC1, NCOA3, GATA3 and RARA with positive Network Enrichment Score (NES) [4], implying the TF’s regulon is over-

represented within the differentially bound genes. Conversely, GRHL2 was discovered with a negative NES. A negative NES implies the regulon is either significantly depleted within the set of differentially bound genes or that TF is established by ARACNe as having a negative correlation to the genes regulated at these differentially bound sites.

## The GRHL2 Transcription Factor

In our analysis of ER dynamics, the GRHL2 transcription factor stood out. In both the METABRIC and TGCA networks, GRHL2 was significantly repressed; yet in our proteomics analysis, the protein was significantly increased. GRHL2 is a transcription factor that is important for maintaining epithelial lineage specificity in multiple tissues [36,37]. It has previously been predicted to exist in ER-associated enhancer protein complexes [38], but its function in the ER signalling axis is unknown. Therefore, we set out to experimentally validate GRHL2 as an ESR1 cofactor, possibly with repression properties for the ER complex.

Our analysis shows that the genes occupied by the ER complex do not form part of the GRHL2 regulon, using both TCGA-derived and METABRIC-derived regulatory models. Our analysis highlights the small overlap between the ESR1 (Estrogen Receptor) and GRHL2 networks (**Suppl. Figure 28**), hinting at complementary signals not dependent on global network overlaps. In fact, there is only a weak, positive correlation between ESR1 and GRHL2 expression in the TCGA breast cancer dataset (**Suppl. Figure 29**) and also in the METABRIC breast cancer dataset (**Suppl. Figure 30**). Furthermore, GRHL2 has a visibly lower variance than ESR1: it does not change significantly in different PAM50 subtypes, although it is lower in normal compared to malignant tissue.

The low overlap between networks and the low correlation in expression profiles could be explained by the fact that GRHL2's role may not be related to its function as a transcription

factor; rather, it may be controlled by other mechanisms like phosphorylation, subcellular localisation or on-chromatin interactions.

**GRHL2 activity before and after stimulation with E2**

Differential ChIP-seq analysis of GRHL2 binding between 0 and 45' indicated that GRHL2 binding is altered on treatment with E2 **(Figure 5A)**. VULCAN analysis of the GRHL2 differential binding showed a consistent Network Enrichment Score for both the TCGA- and METABRIC-derived networks for ER, but not for FOXA1 or GRHL2 **(Figure 5B)**. Individual analysis of peaks show that typically ER promoter sites, e.g. RARa, were not the target of this redistribution of GRHL2, as these sites were occupied by GRHL2 before E2 stimulation. Motif analysis of the sites within increased GRHL2 occupancy showed enrichment for the full ERE (p-value = $1 \times 10^{-86}$) and the GRHL2 binding motif (p-value = $1 \times 10^{-31}$).

qPLEX-RIME analysis of GRHL2 interactions showed high coverage of the bait protein (>59%) and, in both the estrogen-free and estrogenic conditions, high levels of transcription-related protein interactors including HDAC1 (p-value = $6.4 \times 10^{-9}$), TIF1A (p-value = $6.4 \times 10^{-9}$), PRMT (p-value = $6.4 \times 10^{-9}$) and GTF3C2 (p-value = $4.6 \times 10^{-9}$). P-values given for estrogenic conditions and estrogen-free conditions were comparable. The only protein differentially bound to GRHL2 in estrogen-free versus estrogenic conditions was ER.

The specific nature of the detected ER-GRHL2 interaction suggests that ER does not regulate or interact with GRHL2 through the recruitment of alternative cofactors. This implies instead that ER recruits GRHL2 to certain genomic loci for a specific function. We therefore undertook a comparison of GRHL2 binding with public datasets. **(Figure 5C).** Our analysis showed that GRHL2 sites that responded to E2 were enriched for ER binding sites (in agreement with our qPLEX-RIME data) and FOXA1 (compatible with either an ER interaction or the previously reported interaction with MLL3 [38]). To establish, therefore, if the reprogramming of GRHL2 was primarily related to a transcriptional function or the previously

described interaction with MLL3, we overlapped our GRHL2 data with that of published H3K4me1/3 [38] and P300 [39] cistromes. While H3K4me occupancy was consistent between conditions, we found P300 binding to be enriched at the E2 responsive GRHL2 sites. A more detailed analysis of the GRHL2 overlap with P300 sites showed the greatest co-occupancy of GRHL2/P300 sites was when both TFs were stimulated by E2 **(Figure 5D).** Moreover**,** overlap of GRHL2 peaks with ER ChIA-PET data [ENCSR000BZZ] showed that the GRHL2 responsive sites were enriched at enhancers over promoters **(Figure 5E).**

These findings suggested that the GRHL2-ER interaction was involved in transcription at ER enhancer sites. To explore this concept further, we investigated the transcription of enhancer RNAs at these sites using publicly available GRO-seq data [40] [GSE43836] **(Figure 5F).** At E2 responsive sites**,** eRNA transcription was strongly increased by E2 stimulation; by contrast, eRNA transcription was largely independent of E2 stimulation when the entire GRHL2 cistrome was considered. Analysis of a second GRO-seq dataset, GSE45822, corroborated these results **(Suppl. Figure S92)**.

To further explore how GRHL2 regulates ER enhancers, we measured eRNA expression at the GREB1, TFF1 and XBP1 enhancers after over-expression of GRHL2. At TFF1 and XBP1, increased GRHL2 resulted in reduced eRNA transcription **(Figure 6)** ($p < 0.05$, paired-sample, t-test). Conversely, eRNA production at the TFF1, XBP1 and GREB1 enhancers was moderately increased after GRHL2 knockdown **(Suppl. Figure 106).** Combining data from all three sites established the effect as significant by paired-sample rank test ($p = 0.04$, one-tailed paired-sample, wilcoxon test). Collectively, these data demonstrate that GRHL2 constrains specific ER enhancers.

Analysis of mRNA expression levels of TFF1, XBP1 and GREB1 by RT-qPCR revealed that overexpression of GRHL2 also led to a significant reduction in TFF1 and XBP1 ($p < 0.05$, paired-sample, t-test), while knockdown of GRHL2 led to a significant increase in GREB1 transcription ($p < 0.05$, paired-sample, t-test) **(Suppl. Figure 107)**.

# Discussion

## VirtUaL ChIP-seq Analysis through Networks – VULCAN

The VULCAN method is valuable for the discovery of transcription factors which have a role in the regulation of protein complexes that would otherwise remain hidden. The challenge of highlighting cofactors from a ChIP-seq experiment lays in the infeasibility of reliable proteomic characterisation of DNA-bound complexes at specific regions. On the other hand, while RNA-seq is arguably the most efficient technique to obtain genome-wide quantitative measurements, any transcriptomic approach cannot provide a full picture of cellular responses for stimuli that are provided on a shorter timescale than mRNA synthesis speed, such as the estradiol administration described in our study. VULCAN, by combining RNA-seq derived networks and ChIP-seq cistrome data, aims at overcoming limitations of both. Most notably, our method can work in scenarios where candidate cofactors do not have a well characterised binding site or do not even bind DNA directly.

By developing VULCAN, we have been able to rediscover known cofactors of the estradiol-responsive ER complex and predict and experimentally validate a novel protein-protein interaction.

## Reprogramming of GRHL2 by ER

In the 4T1 tumour model, GRHL2 was found to be significantly downregulated in cells that had undergone EMT [36]. The same study showed that knockdown of GRHL2 in MCF10A – an ER-negative cell line – lead to loss of epithelial morphology. Overall, this suggested that the GRHL2 transcription factor plays an essential role in maintaining the epithelial phenotype of breast cells. Similar results were observed with the MDA-MB-231 model, where expression of GRHL2

resulted in reversal of EMT [37]. This result has been recapitulated in hepatocytes, where GRHL2 was found to suppress EMT by inhibiting P300 [41]

Survival data for ER+ breast cancer (KMplotter, use gene expression, p=0.001) and ER- (KMplotter, use gene expression, p=0.035) shows that high GRHL2 has a negative impact on survival time in both contexts. The ability to suppress EMT has also been noted in prostate cancer, another cancer driven by a steroid hormone receptor (AR), and the genes regulated by GRHL2 are linked to disease progression [42].

Combined, these earlier data indicate a significant role for GRHL2 in the progression of breast cancer, but its role in the ER signalling axis has, until now, been unknown. Here, we show that GRHL2 constrains activity at a subset of ER enhancers. Overexpression of GRHL2 resulted in a significant decrease in eRNA production at the TFF1 and XBP1 enhancers and, in agreement with previous studies that correlate eRNA transcription with gene expression [43–45], we found the measured eRNA decrease was concurrent with a significant downregulation in the expression of the corresponding gene.

These results are consistent with previous findings that GRHL2 inhibits P300 [41] and, while the ER complex results in the activation of eRNA transcription at these sites, that GRHL2 plays a role in fine-tuning or modulating this process.

In breast cancer, GRHL2 has previously been shown to directly interact with FOXA1, which may contribute to tethering of the histone methyltransferase MLL3 and, consequently, epigenetic marks at GRHL2/FOXA1 binding sites [38]. Our analysis, however, showed no particular enrichment for H3K4me1/3 marks at E2 responsive GRHL2 sites compared to other GRHL2 binding sites and our proteomic analysis of interactors showed a strong association with proteins related to transcription. Therefore, while GRHL2 ChIP-seq analysis shows that GRHL2 is already bound to a proportion of FOXA1 sites before treatment of cells with E2, we still observed an increase in GRHL2 binding at 45’. We proposed that these ER responsive sites are related to a role of GRHL2 in a transcriptional process independent of its interaction with

MLL3. This was supported by evidence of a significant overlap with binding of the coactivator P300 and a pronounced increase in eRNA transcription on activation at E2 responsive GRHL2 sites.

# Conclusion

VULCAN is built on state-of-the-art network analysis tools previously applied to RNA-seq data. By adapting network-based strategies to ChIP-seq data, we have been able to reveal novel information regarding the regulation of breast cancer in a model system.

The VULCAN algorithm can be applied generally to ChIP-seq for the identification of new key regulator interactions. Our method provides a novel approach to investigate chromatin occupancy of cofactors that are too transient or for which no reliable antibody is available for direct ChIP-seq analysis.

VULCAN enabled us to identify the reprogramming of GRHL2 by the ER on stimulation with E2. Further analysis showed the process to be unrelated to the previously reported interaction with FOXA1 and MLL3 [38]. Our conclusion, therefore, is that GRHL2 has a second, previously undescribed, role: negatively regulating levels of transcription at estrogen responsive enhancers **(Figure 7)**. Given the central role of the ER in breast cancer development and GRHL2's own ability to regulate EMT, the discovery that ER recruits GRHL2, leading to the constraint of eRNA transcription, is an important step in enhancing our understanding of breast cancer and tumourigenesis.

# Methods

## Sample preparation

MCF7 cells were obtained from the CRUK Cambridge Institute collection, authenticated by STR genotyping and confirmed free of mycoplasma. All cells were maintained at 37 $^{o}$C, 5% $CO_2$. For each individual ChIP pull-down, we cultured 8 x $10^7$ MCF7 cells (ATCC) across four 15 cm diameter plates in DMEM with 10% FBS, Glutamine and Penicillin/Streptomycin (Glibco). Five days before the experiment, the cells were washed with phosphate buffered saline (PBS) and the media was replaced with clear DMEM supplemented with charcoal treated serum. The media was refreshed every 24 hours, which halted the growth of the cells and ensured that majority ER within the cell was not active. On day 5, the cells were treated with estradiol (100 nM). At the appropriate time point, the cells were washed with ice cold PBS twice and then fixed by incubating with 10mL per plate of 1% formaldehyde in unsupplemented clear media for 10 minutes. The reaction was stopped by the addition of 1.5mL of 2.5 M glycine and the plates were washed twice with ice cold PBS. Each plate was then scraped in 1 mL of PBS with protease inhibitors (PI) into a 1.5 mL microcentrifuge tube. The cells were centrifuged at 8000 rpm for 3 minutes at 4 $^{o}$C and the supernatant removed. The process was repeated for a second wash in 1 mL PBS+PI and the PBS removed before storing at -80 $^{o}$C.

## ChIP-Seq

Frozen samples were processed using established ChIP protocols [46] to obtain DNA fragments of ~300 bp in length. The libraries were prepared from the purified DNA using a Thruplex DNA-seq kit (Rubicon Genomics) and sequenced on the Illumina HiSeq Platform. Sequencing data is available from Gene Expression Omnibus, accession GSE109820.

## Differential binding analysis

Sequencing data was aligned using BWA[47] to the human genome (hg19). Reads from within the DAC Blacklisted Regions was removed before peak calling with MACS 2.1 [48] on default parameters. The aligned reads and associated peak files were then analyzed using DiffBind [30] to identify significant changes in ER binding.

## Gene Set Enrichment Analysis (GSEA)

Gene Set Enrichment Analysis (GSEA) was performed as described by *Subramanian et al*. [49] using the curated pathway collection (C2) from MSIGDB v 5.0 with 1000 set permutations for each pathway investigated, followed by Benjamini Hochberg P-value correction.

## Motif analysis

Motif analysis of the binding regions was undertaken with Homer v4.4 [50] using default parameters. Motif logo rendering was performed using Weblogo v2.8.2 [51]

## VULCAN analysis

We reconstructed a regulatory gene network using ARACNe-AP as described by Alvarez [26]. RNA-Seq breast cancer data was downloaded from TCGA on January 2015 and VST-Normalized as described by Anders and Huber [52]. The ARACNe transcriptional regulation network was imported into R using the *viper* BioConductor package and it was interrogated using the differential binding profiles from our ChIP-Seq experiment as signatures, 45’ vs control and 90’ vs control. The peak-to-promoter assignment was performed using a 10kb window with respect to the transcription starting site (TSS) of every gene on the hg19 human genome. The algorithm *msVIPER* (multi-sample Virtual Inference of Protein activity by Enriched

Regulon analysis) was then applied, leveraging the full set of eight replicates per group, with 1000 signature permutations and default parameters.

# qPLEX-RIME

Samples were prepared as previously described for RIME[34], protocol was modified to include TMT isobaric labels for quantification (manuscript under review). qPLEX-RIME data and analysis pipeline is available as part of the supplementary Rmarkdown.

# TF Binding Overlap

Publically available data was downloaded as described in the source publication [38–40,53] and overlap was calculated with bedtools (v2.25.0). Presented data was normalised as a percentage of GRHL2 sites.

# Code availability

Code for data analysis is provided as an Rmarkdown document and supporting data is avalible from https://github.com/andrewholding/VULCANSupplementary. For convenience, we have provide VULCAN as a BioConductor package https://bioconductor.org/packages/release/bioc/html/vulcan.html along with a supporting data package https://bioconductor.org/packages/release/data/experiment/html/vulcandata.html.

# eRNA quantification

MCF7 cells were transfected with Smart Pool siRNA (Dharmacon, L-014515-02), siControl, GRHL2 overexpression vector (Origene, RC214498) or empty control vector using Lipofectamine 3000 (Thermo Fisher Scientific) according to the manufacturer's protocol in 6 well format. Expression was monitored by rtPCR using TaqMan assay with GAPHD as a control transcript. Knockdown efficiency was ~75% and the GRHL2 overexpression vector led a 730-fold increase in expression over control plasmid. 1 ug of purified RNA was reverse transcribed with Superscript III reverse transcriptase (Thermo Fisher Scientific, 18080085) using random primers (Promega, C1181) according to manufacturer instructions. eRNAs were quantified with qPCR using Power SYBR™ Green PCR Master Mix (Thermo Fisher Scientific, 4367660) and denoted as relative eRNA levels after normalizing with UBC mRNA levels.

| **Primer name** | **Sequences** | **Reference** |
|---|---|---|
| eGREB1 F | ACTGCGGCATTTCTGTGAGA | This study |
| eGREB1 R | ACTGCAGTTTGCCTGTCACT | This study |
| eXBP1 F | TGTGAGCACTTGGCATCCAT | Nagarajan et al 2014 |
| eXBP1 R | ACAGGGCCTCATTCTCCTCT | Nagarajan et al 2014 |
| eTFF1 F | AGGGGATGTGTGTGAGAAGG | Li et al 2013 |
| eTFF1 R | GCTTCGAGACAGTGGGAGTC | Li et al 2013 |
| UBC F | ATTTGGGTCGCGGTTCTTG | Peña et al 2009 |

| | | |
|---|---|---|
| UBC R | TGCCTTGACATTCTCGATGGT | Peña et al 2009 |

# Author Contributions

ANH, FMG, LAS & FM conceived and designed the experiments, ANH undertook ER experimentation, ANH & FMG undertook the analysis of ER data, ANH & FMG designed VULCAN, FMG implemented the VULCAN analysis, AEC & AD undertook GRHL2 experimentation. ANH, AEC & LAS undertook analysis of GRHL2 data. ANH, FMG, LAS and FM wrote the manuscript.

# Acknowledgements

We would like to acknowledge the support of the University of Cambridge, Cancer Research UK and Hutchison Whampoa Limited.

Parts of this work were funded by CRUK core grant [grant numbers C14303/A17197, A19274] to FM; Breast Cancer Now Award [grant number 2012NovPR042] to FM.

We would like to acknowledge the contribution from the CRUK Genomics, Proteomics and Bioinformatic core facilities in supporting this work.

# Materials & Correspondence

All materials requests & correspondence should be addressed to Dr Andrew N. Holding.

# Competing interests.

The authors have no competing interests to declare.

# Abbreviations

| | |
|---|---|
| AR | Androgen Receptor |
| ARACNe-AP | AccuRate Algorithm for reConstruction of Network through Adaptive Partitioning |
| CCLE | Cancer Cell Line Encyclopedia |
| ChIP | Chromatin ImmunoPrecipitation |
| ER | Estrogen Receptor-Alpha |
| ERE | Estrogen-Response Elements |
| GSEA | Gene Set Enrichment Analysis |
| GRHL2 | Grainyhead Like Transcription Factor 2 |
| METABRIC | MolEcular TAxonomy of BReast cancer International Consortium |
| PBS | Phosphate Buffered Saline |
| PI | Protease Inhibitors |
| PR | Progesterone Receptor |
| TCGA | The Cancer Genome Atlas |
| TF | Transcription Factor |
| VIPER | Virtual Inference of Protein activity by Enriched Regulon analysis |
| VULCAN | VirtUaL ChIP-Seq Analysis through Networks |

# Declarations

Parts of this work were funded by CRUK core grant C14303/A17197 and A19274 (to FM), and by Breast Cancer Now Award (2012NovPR042). None of the authors have any competing interests to declare. Data supporting this manuscript is available from the GEO accession GSE109820.

# Figure Legends

## Figure 1: An overview of VULCAN

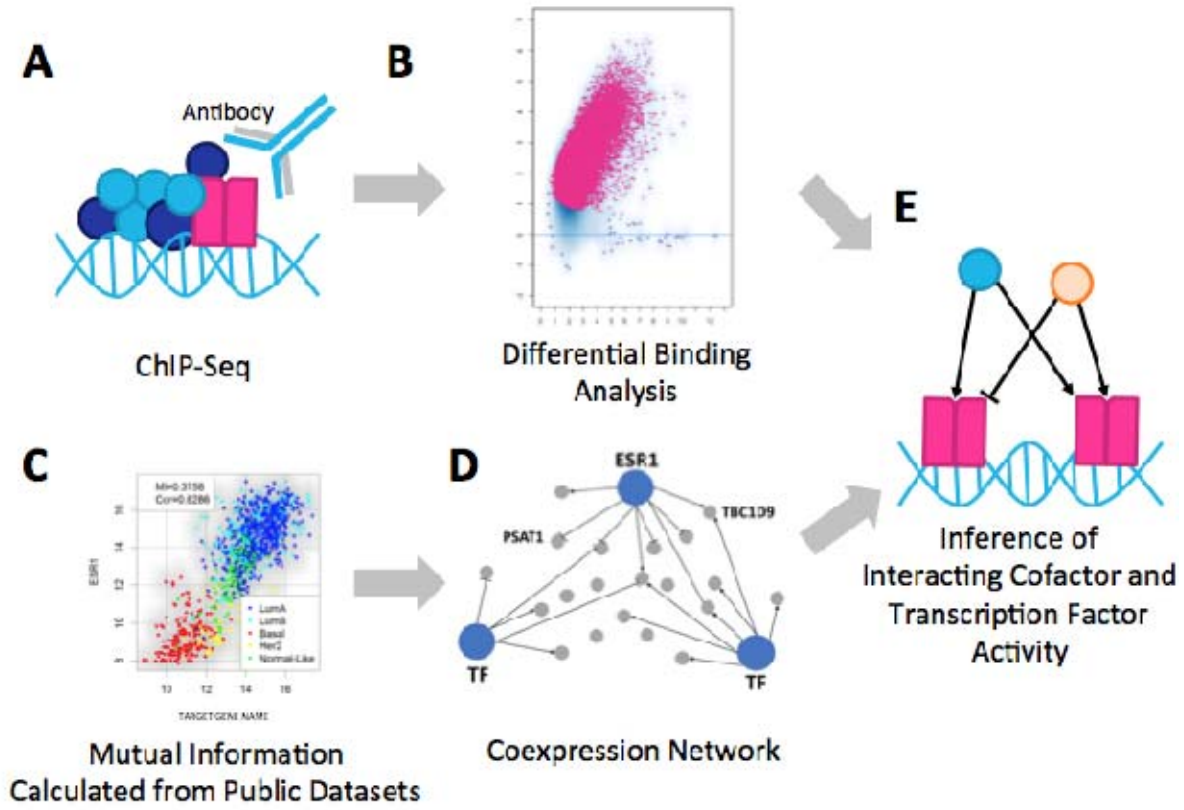


A: ChIP-Seq analysis from multiple conditions is undertaken to generate cistrome data at multiple timepoints (or conditions). B: Binding events are then compared using differential binding analysis to establish log-fold change values for individual binding events between each timepoint. C: ARACNe-AP infers all pairwise TF-target coexpression. In the example, the TCGA breast dataset is shown to infer A putative target that is correlated with ESR1. D: Minimalistic representation of the ARACNe-AP network, highlighting negative and positive regulation of targets by transcription factors. E: All the targets of a specific TF are divided in positive and negative, and tested on a differential binding signature through the msVIPER algorithm [4]

# Figure 2: Dynamic behaviour during early activation of ER

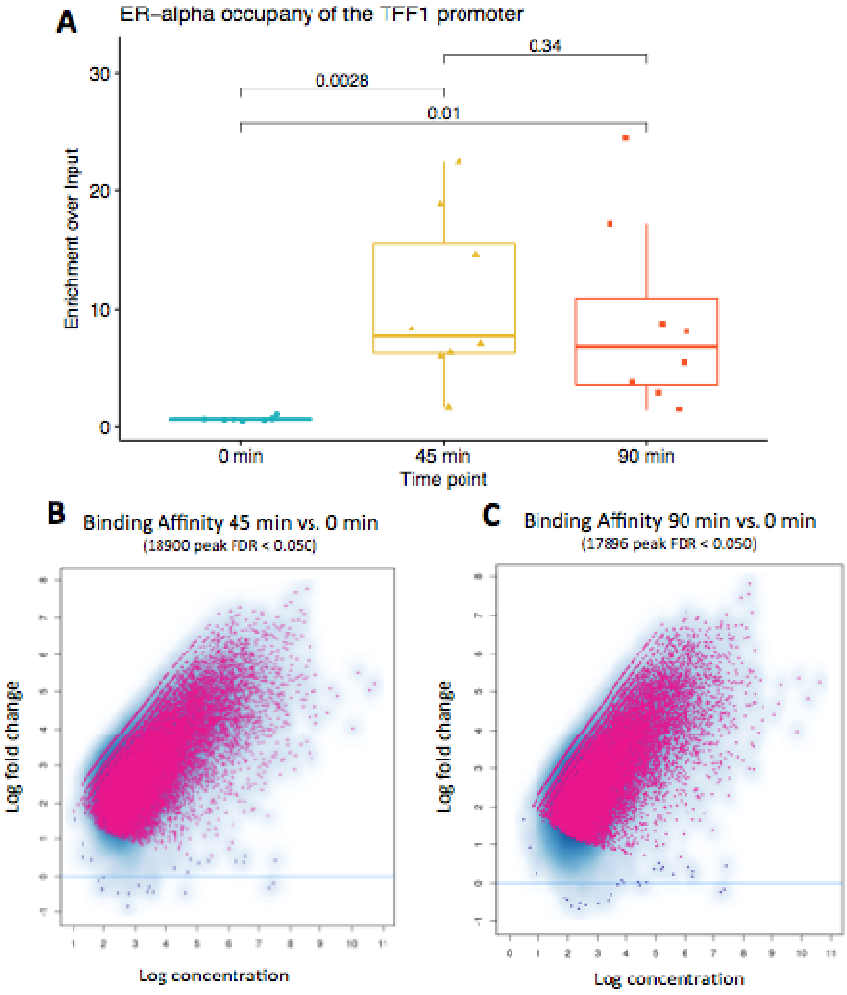


ChIP-qPCR of the TFF1 gene (A) at 3 time points shows increased binding of ER at 45 minutes after MCF7 cells are stimulated by estra-2-diol. The previously reported maximum is followed by a decrease in the TFF1 promoter occupancy at 90 minutes. P-values are generated by one-tailed t-test. The maximal point at 90 minutes was identified as an outlier ( > median + 2 x IQR); however removal did not alter the significance of results. (B) Differential binding analysis of ChIP-Seq data at three time points to monitor the activation of ERa. The ER a strong increase in binding at 45 minutes vs. 0 minutes (C) and the majority of sites still display binding at 90 minutes.

Figure 3: ER occupancy after estradiol treatment in terms of TF network activity

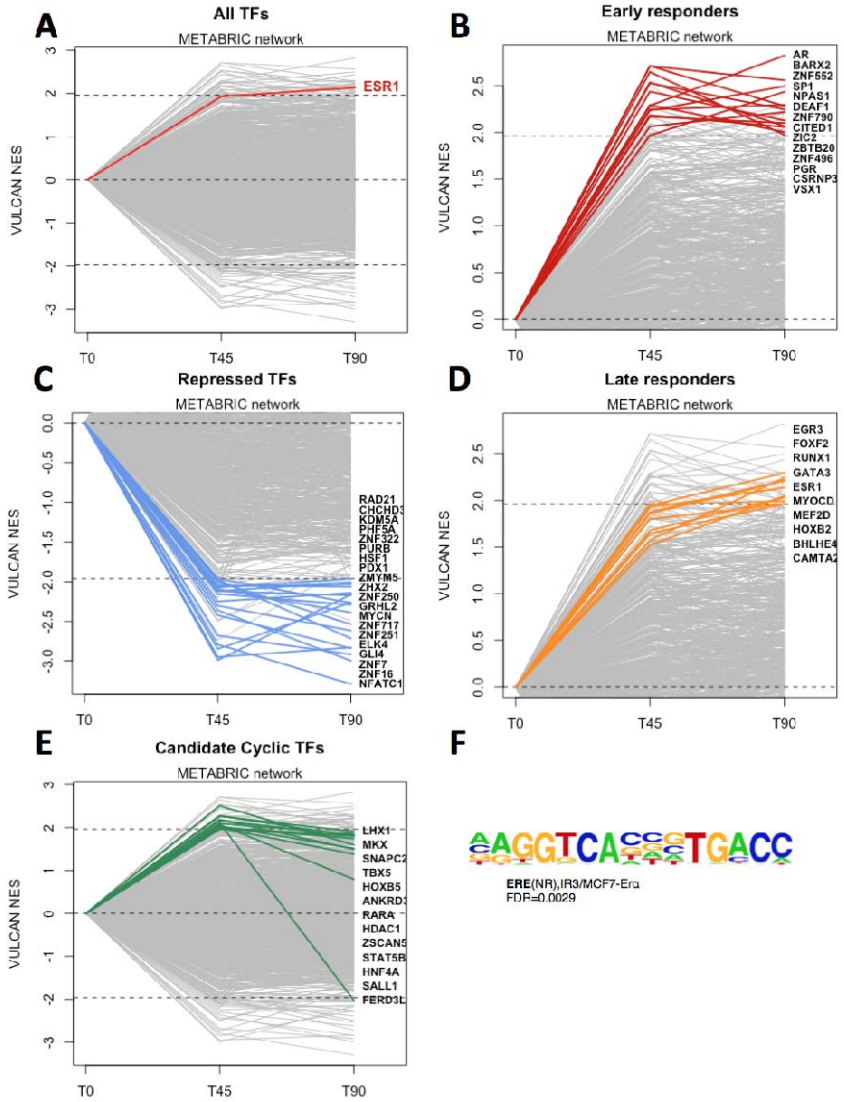


**A**: Global TF network behavior as predicted by VULCAN in our ChIP-Seq dataset, highlighting the ESR1 TF at time 0 and 45/90minutes after estradiol treatment.
**B**: Global TF activity after Estradiol Treatment in MCF7 cells, inferred using the METABRIC network, highlighting TFs significantly upregulated at 45 minutes and 90 minutes
**C**: Global TF activity after Estradiol Treatment in MCF7 cells, inferred using the METABRIC network, highlighting TFs significantly downregulated at 45 minutes and 90 minutes
**D**: Global TF activity after Estradiol Treatment in MCF7 cells, inferred using the METABRIC network, highlighting TFs significantly upregulated at 45 minutes but not at 90 minutes
**E**: Global TF activity after Estradiol Treatment in MCF7 cells, inferred using the METABRIC network, highlighting TFs significantly upregulated at 90 minutes but not at 45 minutes
**F**: Most enriched motif in peaks upregulated at both 45 and 90 minutes after estradiol treatment, as predicted by HOMER.

Figure 4: Global TF activity after estradiol treatment using different network models.

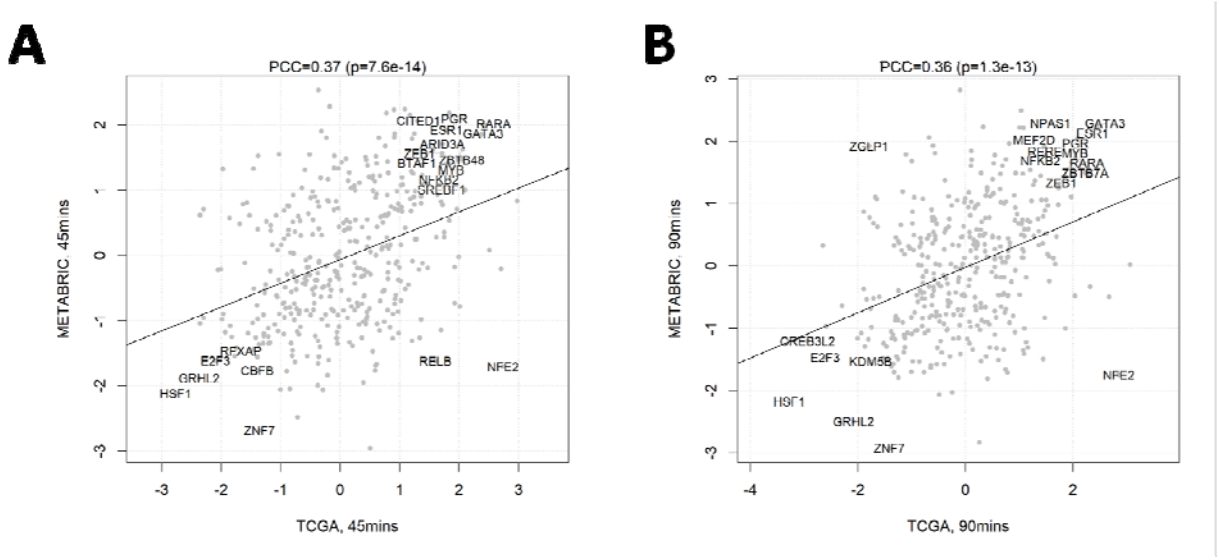


XY Scatter showing the TF activity as calculated by VULCAN for our differential ChIP-Seq analysis of ER binding at 45 minutes (A) and at 90 minutes (B) after stimulation with 100 nM E2. Comparison of results calculated using the METABRIC (y-axis) and TCGA (x-axis) networks shows consistent results know ER interactors including PGR, RARA, GATA3 and GRHL2. GRHL2 activity is notably enriched against. The regulon of ER is also consistently enriched in both networks.

# Figure 5: GRHL2 Differential ChIP-Seq between 0 and 45 minutes.

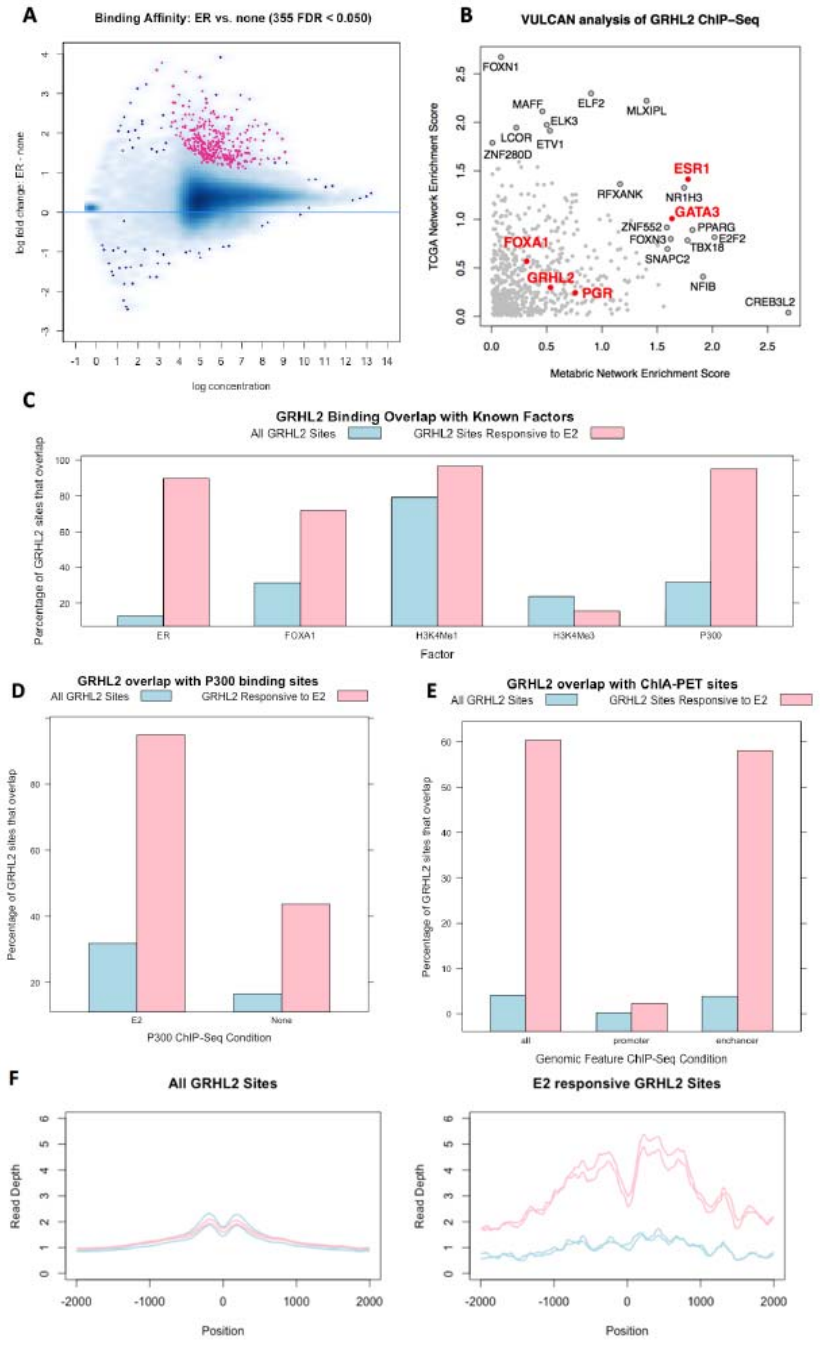


**(A)** Activation of the ER with estro-2-diol results in a genome wide increase in GRHL2 binding. **(B)** VULCAN Analysis of the same data show a significant enrichment for ESR1 sites in both

the context of the METABRIC and TGCA networks. The regulon for FOXA1 is also not enriched. Inspection of known FOXA1/GRHL2 sites (e.g. RARa promoter) shows GRHL2 already bound.

**(C)** Overlap of GRHL2 binding with public datasets shows that E2 responsive GRHL2 sites show considerable overlap with ER, FOXA1 and P300 sites, H3K4Me1 and H3K4Me3 show little enrichment.

**(D)** Analysis of P300 binding showed a greater overlap of GRHL2 ER responsive sites in the presence of E2 than in control conditions

**(E)** Overlap with ER ChIA-PET sites showed enrichment for GRHL2 sites at ER enhancers.

**(F)** Analysis of Gro-SEQ data (GSE43836) at GRHL2 sites. Blue lines are control samples, Pink are samples after stimulation with E2. In general GRHL2 sites (left) show no change in the levels of transcription on addition of E2; however, E2 responsive GRHL2 sites (right) show a robust increase in transcription on the activation of the ER.

## Figure 6: Effect of overexpression of GRHL2 on eRNA at E2 responsive binding sites.

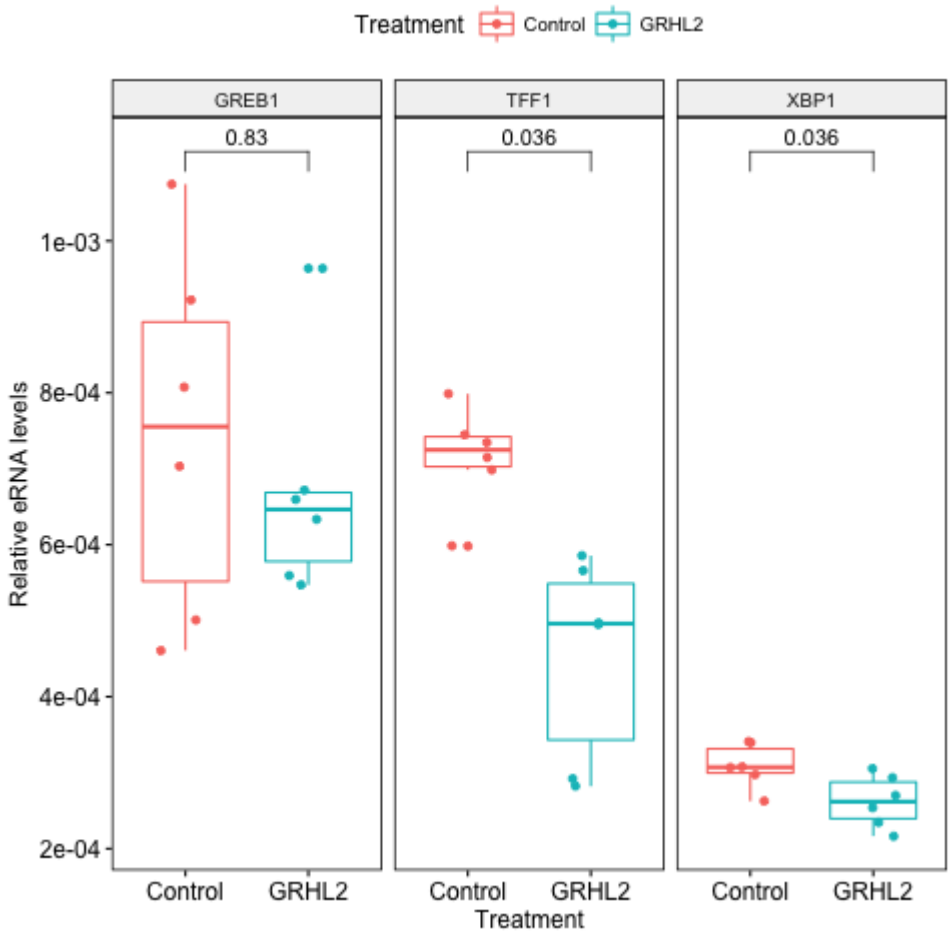


Overexpression of GRHL2 in MCF7 resulted in a reduction of eRNA transcribed from the GREB1, TFF1 and XBP1 enhancers. The effect was significant at TFF1 and XBP1 enhancers ($p < 0.05$, Wilcoxon paired-test).

## Figure 7: Overview of the role of GRHL2 in ER activation

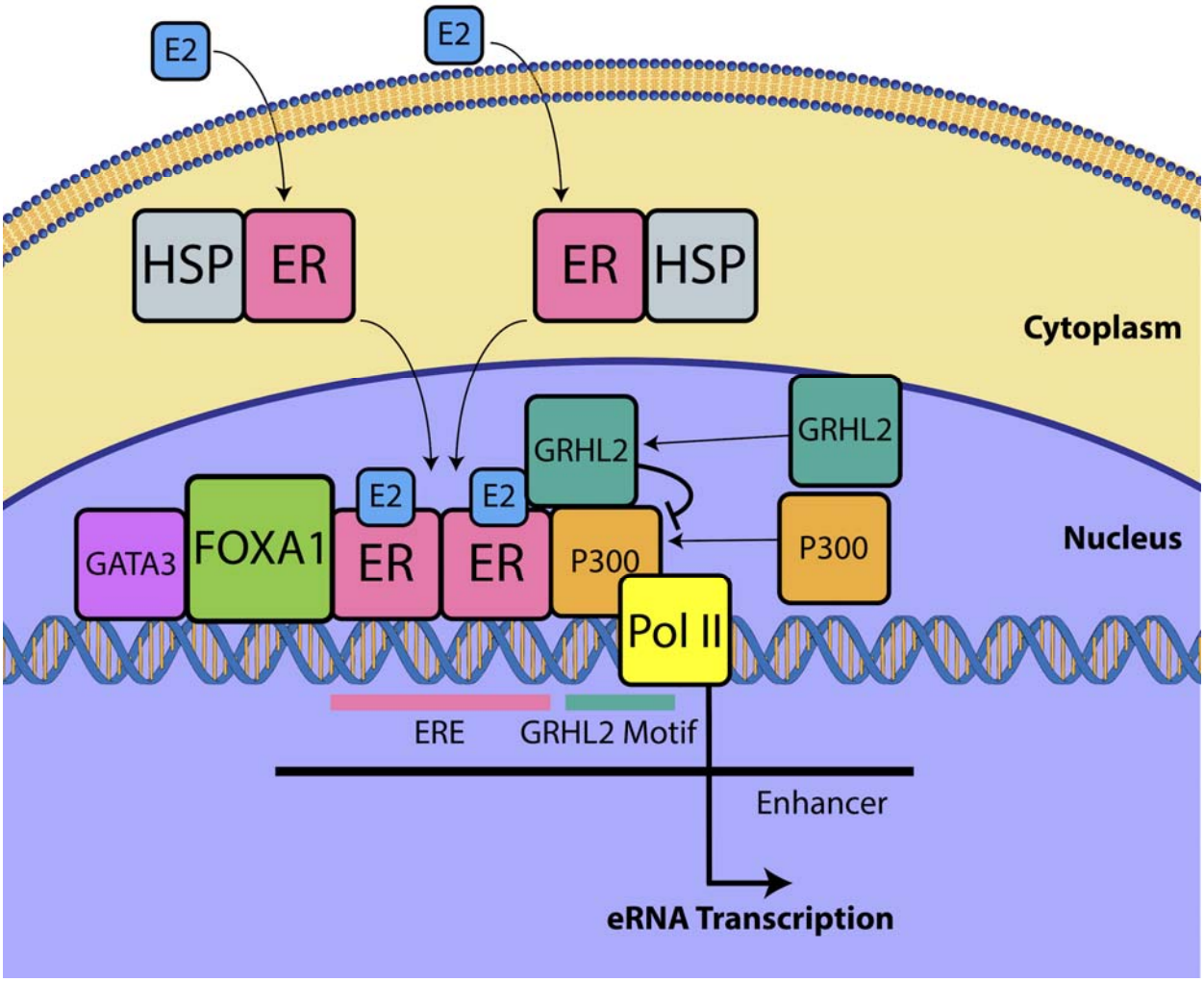


On activation of the ER by the ligand E2 the protein is released from a complex containing HSPs and translocates to the nucleus. The holo-ER dimer forms a core complex at Estrogen Response Elements (ERE) with FOXA1 (pioneer factor) and GATA3. ER further recruits P300 and GRHL2. GRHL2 has an inhibitory effect on P300 (a transcriptional activator interacting with TFIID, TFIIB, and RNAPII) thereby reducing the level of eRNA transcription at enhancer sites. Overexpression of GRHL2 further suppresses transcription, while knockdown of GRHL2 reverses the process.

**References:**

1. Basso K, Margolin A, Stolovitzky G, Klein U, Dalla-Favera R, Califano A. Reverse engineering of regulatory networks in human B cells. Nat Genet. Nature Publishing Group; 2005;37:382–90.
2. Giorgi FM, Del Fabbro C, Licausi F. Comparative study of RNA-seq- and Microarray-derived coexpression networks in Arabidopsis thaliana. Bioinformatics. 2013;29.
3. Castro MAA, de Santiago I, Campbell TM, Vaughn C, Hickey TE, Ross E, et al. Regulators of genetic risk of breast cancer identified by integrative network analysis. Nat. Genet. 2016;48:12–21.
4. Alvarez MJ, Shen Y, Giorgi FM, Lachmann A, Ding BB, Ye BH, et al. Functional characterization of somatic mutations in cancer using network-based inference of protein activity. Nat. Genet. 2016;48:838–47.
5. McLean CY, Bristor D, Hiller M, Clarke SL, Schaar BT, Lowe CB, et al. GREAT improves functional interpretation of cis-regulatory regions. Nat. Biotechnol. 2010;28:495–501.
6. Welch RP, Lee C, Imbriano PM, Patil S, Weymouth TE, Smith RA, et al. ChIP-Enrich: gene set enrichment testing for ChIP-seq data. Nucleic acids Res. 2014;42:e105.
7. Balwierz PJ, Pachkov M, Arnold P, Gruber AJ, Zavolan M, van Nimwegen E. ISMARA: automated modeling of genomic signals as a democracy of regulatory motifs. Genome Res. 2014;24:869–84.
8. Carroll JS. Mechanisms of oestrogen receptor (ER) gene regulation in breast cancer. Eur. J. Endocrinol. 2016;175:R41–9.
9. Lin C-Y, Vega VB, Thomsen JS, Zhang T, Kong SL, Xie M, et al. Whole-genome cartography of estrogen receptor alpha binding sites. PLoS Genet. 2007;3:e87.
10. Driscoll MD, Sathya G, Muyan M, Klinge CM, Hilf R, Bambara RA. Sequence requirements for estrogen receptor binding to estrogen response elements. J. Biol. Chem. 1998;273:29321–30.
11. Carroll JS, Meyer C a, Song J, Li W, Geistlinger TR, Eeckhoute J, et al. Genome-wide analysis of estrogen receptor binding sites. Nat. Genet. 2006;38:1289–97.
12. Carroll JS, Liu XS, Brodsky AS, Li W, Meyer CA, Szary AJ, et al. Chromosome-Wide Mapping of Estrogen Receptor Binding Reveals Long-Range Regulation Requiring the Forkhead Protein FoxA1. Cell. 2005;122.
13. Frasor J, Danes JM, Komm B, Chang KCN, Lyttle CR, Katzenellenbogen BS. Profiling of estrogen up- and down-regulated gene expression in human breast cancer cells: insights into gene networks and pathways underlying estrogenic control of proliferation and cell phenotype. Endocrinology. 2003;144:4562–74.
14. Zaret KS, Carroll JS. Pioneer transcription factors: establishing competence for gene expression. Genes & Dev. 2011;25:2227–41.
15. Horwitz KB, Jackson TA, Bain DL, Richer JK, Takimoto GS, Tung L. Nuclear receptor coactivators and corepressors. Mol. Endocrinol. 1996;10.
16. Glass CK, Rose DW, Rosenfeld MG. Nuclear receptor coactivators. Curr. Opin. cell Biol. 1997;9:222–32.
17. Green KA, Carroll JS. Oestrogen-receptor-mediated transcription and the influence of co-factors and chromatin state. Nat. Rev. Cancer. 2007;7:713–22.
18. Klinge CM. Estrogen receptor interaction with estrogen response elements. Nucleic acids Res. 2001;29:2905–19.
19. Shang Y, Hu X, DiRenzo J, Lazar MA, Brown M. Cofactor dynamics and sufficiency in estrogen receptor-regulated transcription. Cell. 2000;103:843–52.

20. Reid G, Hubner MR, Metivier R, Brand H, Denger S, Manu D, et al. Cyclic, proteasome-mediated turnover of unliganded and liganded ER alpha on responsive promoters is an integral feature of estrogen signaling. Mol. Cell. 2003;11:695–707.
21. Métivier R, Penot G, Hübner MR, Reid G, Brand H, Kos M, et al. Estrogen receptor-alpha directs ordered, cyclical, and combinatorial recruitment of cofactors on a natural target promoter. Cell. 2003;115:751–63.
22. Lachmann A, Giorgi FM, Lopez G, Califano A. ARACNe-AP: gene network reverse engineering through adaptive partitioning inference of mutual information. Bioinforma. 2016;32:2233–5.
23. Curtis C, Shah SP, Chin S-F, Turashvili G, Rueda OM, Dunning MJ, et al. The genomic and transcriptomic architecture of 2,000 breast tumours reveals novel subgroups. Nature. 2012;486:346–52.
24. Cancer Genome Atlas Network. Comprehensive molecular portraits of human breast tumours. Nature. 2012;490:61–70.
25. Lefebvre C, Rajbhandari P, Alvarez MJ, Bandaru P, Lim WK, Sato M, et al. A human B-cell interactome identifies MYB and FOXM1 as master regulators of proliferation in germinal centers. Mol. Syst. Biol. 2010;6:377.
26. Lachmann A, Giorgi FM, Lopez G, Califano A. ARACNe-AP: gene network reverse engineering through adaptive partitioning inference of mutual information. Bioinformatics. 2016;32.
27. Subramanian A, Tamayo P, Mootha VK, Mukherjee S, Ebert BL, Gillette MA, et al. Gene set enrichment analysis: a knowledge-based approach for interpreting genome-wide expression profiles. Proc. Natl. Acad. Sci. United States Am. 2005;102:15545–50.
28. Orlando DA, Chen MW, Brown VE, Solanki S, Choi YJ, Olson ER, et al. Quantitative ChIP-Seq normalization reveals global modulation of the epigenome. Cell reports. 2014;9:1163–70.
29. Guertin MJ, Markowetz F, Holding AN. Novel Quantitative ChIP-seq Methods Measure Absolute Fold-Change in ER Binding Upon Fulvestrant Treatment. bioRxiv. 2017;
30. Ross-Innes CS, Stark R, Teschendorff AE, Holmes KA, Ali HR, Dunning MJ, et al. Differential oestrogen receptor binding is associated with clinical outcome in breast cancer. Nature. 2012;481:389–93.
31. Stein RA, Chang C-Y, Kazmin DA, Way J, Schroeder T, Wergin M, et al. Estrogen-related receptor alpha is critical for the growth of estrogen receptor-negative breast cancer. Cancer Res. 2008;68:8805–12.
32. Bhat-Nakshatri P, Wang G, Appaiah H, Luktuke N, Carroll JS, Geistlinger TR, et al. AKT alters genome-wide estrogen receptor alpha binding and impacts estrogen signaling in breast cancer. Mol. Cell. Biol. 2008;28:7487–503.
33. Gozgit JM, Pentecost BT, Marconi SA, Ricketts-Loriaux RSJ, Otis CN, Arcaro KF. PLD1 is overexpressed in an ER-negative MCF-7 cell line variant and a subset of phospho-Akt-negative breast carcinomas. Br. J. Cancer. 2007;97:809–17.
34. Mohammed H, D'Santos C, Serandour AA, Ali HR, Brown GD, Atkins A, et al. Endogenous purification reveals GREB1 as a key estrogen receptor regulatory factor. Cell reports. 2013;3:342–9.
35. Thompson A, Schäfer J, Kuhn K, Kienle S, Schwarz J, Schmidt G, et al. Tandem Mass Tags: A Novel Quantification Strategy for Comparative Analysis of Complex Protein Mixtures by MS/MS. Anal. Chem. 2003;75.
36. Xiang X, Deng Z, Zhuang X, Ju S, Mu J, Jiang H, et al. Grhl2 determines the epithelial phenotype of breast cancers and promotes tumor progression. PloS one. 2012;7:e50781.
37. Cieply B, Riley P, Pifer PM, Widmeyer J, Addison JB, Ivanov AV, et al. Suppression of the epithelial-mesenchymal transition by Grainyhead-like-2. Cancer Res. 2012;72:2440–53.

38. Jozwik KM, Chernukhin I, Serandour AA, Nagarajan S, Carroll JS. FOXA1 Directs H3K4 Monomethylation at Enhancers via Recruitment of the Methyltransferase MLL3. Cell reports. 2016;17:2715–23.
39. Zwart W, Theodorou V, Kok M, Canisius S, Linn S, Carroll JS. Oestrogen receptor-co-factor-chromatin specificity in the transcriptional regulation of breast cancer. EMBO J. 2011;30:4764–76.
40. Hah N, Murakami S, Nagari A, Danko CG, Kraus WL. Enhancer transcripts mark active estrogen receptor binding sites. Genome Res. 2013;23:1210–23.
41. Pifer PM, Farris JC, Thomas AL, Stoilov P, Denvir J, Smith DM, et al. Grainyhead-like 2 inhibits the coactivator p300, suppressing tubulogenesis and the epithelial-mesenchymal transition. Mol. Biol. cell. 2016;27:2479–92.
42. Paltoglou S, Das R, Townley SL, Hickey TE, Tarulli GA, Coutinho I, et al. Novel Androgen Receptor Coregulator GRHL2 Exerts Both Oncogenic and Antimetastatic Functions in Prostate Cancer. Cancer Res. 2017;77:3417–30.
43. Cheng J-H, Pan DZ-C, Tsai ZT-Y, Tsai H-K. Genome-wide analysis of enhancer RNA in gene regulation across 12 mouse tissues. Sci. reports. 2015;5:12648.
44. Rahman S, Zorca CE, Traboulsi T, Noutahi E, Krause MR, Mader S, et al. Single-cell profiling reveals that eRNA accumulation at enhancer-promoter loops is not required to sustain transcription. Nucleic acids Res. 2017;45:3017–30.
45. Kim T-K, Hemberg M, Gray JM, Costa AM, Bear DM, Wu J, et al. Widespread transcription at neuronal activity-regulated enhancers. Nature. 2010;465:182–7.
46. Holmes KA, Brown GD, Carroll JS. Chromatin Immunoprecipitation-Sequencing (ChIP-seq) for Mapping of Estrogen Receptor-Chromatin Interactions in Breast Cancer. Methods Mol. Biol. 2016;1366:79–98.
47. Li H, Durbin R. Fast and accurate short read alignment with Burrows-Wheeler transform. Bioinformatics. 2009;25.
48. Zhang Y, Liu T, Meyer CA, Eeckhoute J, Johnson DS, Bernstein BE, et al. Model-based analysis of ChIP-Seq (MACS). Genome Biol. 2008;9:137.
49. Subramanian A, Tamayo P, Mootha VK, Mukherjee S, Ebert BL, Gillette MA, et al. Gene set enrichment analysis: a knowledge-based approach for interpreting genome-wide expression profiles: a knowledge-based approach for interpreting genome-wide expression profiles. Proc. Natl. Acad. Sci. United States Am. National Acad Sciences; 2005;102:15545–50.
50. Heinz S, Benner C, Spann N, Bertolino E, Lin YC, Laslo P, et al. Simple combinations of lineage-determining transcription factors prime cis-regulatory elements required for macrophage and B cell identities. Mol. cell. 2010;38:576–89.
51. Crooks GE, Hon G, Chandonia J-M, Brenner SE. WebLogo: a sequence logo generator. Genome Res. 2004;14:1188–90.
52. Anders S, Huber W. Differential expression analysis for sequence count data. Genome Biol. BioMed Central Ltd; 2010;11:106.
53. Hurtado A, Holmes KA, Ross-Innes CS, Schmidt D, Carroll JS. FOXA1 is a key determinant of estrogen receptor function and endocrine response. Nat Genet. Nature Publishing Group; 2010;43:27–33.

# VULCAN Analysis Combined

*Andrew Holding*

*1/22/2018*

## Contents

**1 Introduction** **3**

**2 Estrogen Receptor-alpha qPCR Analysis** **3**
2.1 Delta-delta ct Calculation . . . 3
2.2 Box plot of Raw Data . . . 5

**3 Estrogen Receptor-alpha ChIP-Seq and VULCAN Analysis** **6**
3.1 Introduction . . . 6
3.2 Software setup . . . 8
3.3 Import ChIP-Seq data using Vulcan . . . 8
3.3.1 Initial import . . . 8
3.3.2 Annotation . . . 9
3.3.3 Normalization . . . 9
3.3.4 Dataset Sample Clustering . . . 9
3.3.5 MA plots . . . 13
3.4 Apply a coregulatory network over a ChIP-Seq profile . . . 16
3.4.1 Running the core Vulcan function . . . 20
3.4.2 Visualize the relative TF activity . . . 21
3.5 Pathway enrichment analysis . . . 37
3.6 The GRHL2 Transcription Factor . . . 44
3.6.1 Network similarity between ESR1 and GRHL2 . . . 44
3.6.2 Correlation between ESR1 and GRHL2 expression in breast cancer datasets . . . 47
3.6.3 Enrichment of GRHL2 network for gene pathways . . . 51
3.7 Comparing VULCAN results with other tools and approaches . . . 54
3.7.1 VULCAN and qPLEX-RIME . . . 54
3.7.2 Comparing Mutual Information and Partial Correlation networks . . . 60
3.7.3 Comparing alternative methods for target enrichment analysis . . . 63
3.7.4 Comparing VULCAN with online tools . . . 72

**4 Estrogen Receptor-alpha qPLEX-RIME Analysis** **77**
4.1 Introduction . . . 80
4.2 Peptide intensity data . . . 80
4.2.1 Missing intensity values . . . 81
4.3 Normalization of intensity data . . . 81
4.4 Protein-level quantification . . . 86
4.5 Principal Component Analysis . . . 86
4.6 Differential Binding . . . 86
4.6.1 ER 45min vs ER 0min, excluding peptides with missing intensities, no normalization . 91
4.6.2 ER 45min vs ER 0min, excluding peptides with missing intensities, quantile normalization 95
4.6.3 ER 45min vs ER 0min, excluding peptides with missing intensities, quantile normalization excluding IgG control . . . 99
4.6.4 ER 45min vs ER 0min, excluding peptides with missing intensities, scale normalization 103
4.6.5 ER 45min vs ER 0min, excluding peptides with missing intensities, scale normalization using top 10 IgG peptides . . . 107

4.6.6 ER 45min vs ER 0min, KNN nearest neighbour averaging imputation of missing values, quantile normalization . . . 111
4.7 Comparison of differential binding analysis approaches . . . 115
4.7.1 Removal of missing values vs KNN imputation (quantile normalization in both) . . . 116
4.7.2 Removal of missing values vs lowest value imputation (quantile normalization in both) 118
4.7.3 Quantile vs Scale normalization (missing values excluded in both) . . . 120
4.7.4 Scale normalization based on all peptides vs peptides with highest IgG intensities (missing values excluded in both) . . . 122
4.8 Comparisoin of variance between specfic and non-specific binding . . . 124
4.9 Differential binding results tables . . . 127
4.9.1 ER 45min vs ER 0min . . . 128
4.9.2 ER 90min vs ER 0min . . . 130
4.9.3 ER 90min vs ER 45min . . . 132
4.9.4 FOXA1 45min vs FOXA1 0min . . . 133
4.9.5 FOXA1 90min vs FOXA1 0min . . . 135
4.9.6 FOXA1 90min vs FOXA1 45min . . . 136

**5 GRHL2 ChIP-Seq Analysis 137**
5.1 Pre-processing . . . 137
5.1.1 Download files . . . 137
5.1.2 Removal of reads in blacklisted sites . . . 137
5.1.3 Peak Calling . . . 137
5.2 Differntial binding analysis . . . 138
5.2.1 MA plot . . . 138
5.2.2 PCA . . . 138
5.2.3 Table of differntiall bound sites . . . 138
5.2.4 Number of sites with increased or decreased binding . . . 141
5.3 Quality Control . . . 141
5.3.1 Reproducability of peaks . . . 141
5.4 VULCAN Analysis . . . 141
5.4.1 Transcription factor activity . . . 148
5.4.2 METABRIC TGCA comparison . . . 149
5.5 Motif Analysis . . . 150
5.5.1 Export bed files . . . 150
5.5.2 Homer . . . 152
5.5.3 Generate promoter locations . . . 152
5.6 Ovlerap of GRHL2 binding sites with published data . . . 152
5.6.1 Extract ChIA-PET Data . . . 152
5.6.2 Find overlapping sites . . . 152
5.6.3 Count number of overlaping sites . . . 154
5.6.4 Table of number of overlaping sites for each factor . . . 154
5.6.5 GRHL2 binding overlap with known factors . . . 155
5.6.6 GRHL2 binding overlap with P300 binding sites . . . 155
5.6.7 GRHL2 overlap with ChIA-PET sites . . . 158
5.6.8 GRHL2 overlap with Gro-SEQ data . . . 158
5.6.9 GRHL2 overlap with Gro-SEQ data is reproducible between studies . . . 158

**6 GRHL2 qPLEX-RIME Analysis 161**
6.1 Introduction . . . 161
6.2 Raw data QC . . . 161
6.2.1 Coverage plot . . . 161
6.2.2 Intensity Plot . . . 161
6.2.3 Peptide intensities for GHRL2 . . . 161
6.2.4 Correlation Plot . . . 161

6.2.5 Hierichical clustering dendrogram . . . 166
6.2.6 PCA Plot . . . 166
6.2.7 QC Conclusion . . . 166
6.3 Full data set analysis . . . 168
6.3.1 Effect of within group normalisation . . . 168
6.3.2 Differential analysis results . . . 168
6.4 Remove sample Ctrl 1 . . . 170
6.4.1 Effect of within group normalisation . . . 170
6.4.2 ER - Ctrl . . . 170
6.4.3 Ctrl - IgG . . . 172
6.4.4 ER - IgG . . . 172

**7 Effect of GRHL2 expression on eRNA and mRNA 172**
7.1 Effect of GRHL2 overexpression on eRNA transcription . . . 172
7.2 Effect of GRHL2 knockdown on eRNA transcription . . . 174
7.2.1 siRNA combined test . . . 174
7.3 Effect of GRHL2 overexpression on mRNA transcription . . . 174

**8 Technical Session Info 177**

# 1 Introduction

To reduce the overall size of this project read count and network data is stored within Rdata files. These are avalible from https://github.com/andrewholding/VULCANSupplementary. The raw data is avalible from the gene expression omnibus if reprocessing is required. The following script will download all the required files and rebuild the network file. The Rmd files are designed to recreate the processed data from the raw data if the processed data is not found.

```
git clone https://github.com/andrewholding/VULCANSupplementary.git

#Rebuild network
cd ChIP-seq_ER/data/
cat brca-expmat.rda.part1 brca-expmat.rda.part2 > brca-expmat.rda
```

# 2 Estrogen Receptor-alpha qPCR Analysis

## 2.1 Delta-delta ct Calculation

```
#Set varibles to make time points easier to spot
time0 <- 1
time45 <- 2
time90 <- 3

#Input raw data
qpcr <- list()
qpcr[[time0]] <- read.table("qpcr-0.txt",
                            header = T,
                            sep = "\t",
                            as.is = T)
qpcr[[time45]] <-
```

```r
    read.table("qpcr-45.txt",
               header = T,
               sep = "\t",
               as.is = T)
qpcr[[time90]] <-
    read.table("qpcr-90.txt",
               header = T,
               sep = "\t",
               as.is = T)

for (time_point in time0:time90)
{
    qpcr[[time_point]][qpcr[[time_point]] == "No Ct"] <- NA
}


#Prepare lists
ct_values <- list()
ct_values_means <- list()
d_ct_values_means <- list()
input_values <- list()
input_mean <- list()
d_input_mean <- list()
dd_ct_values_means <- list()


for (time_point in time0:time90)
{
    #Create object
    ct_values[[time_point]] <- matrix(NA, 0, 2)

    #Add reps 1:8 to object
    for (rep in 1:8) {
        y_coord <- rep * 12 - 11
        ct_values[[time_point]] <- rbind(ct_values[[time_point]],
                                         cbind(
                                             as.numeric(qpcr[[time_point]]$Ct..dR[y_coord:(y_coord + 4)]
                                             as.numeric(qpcr[[time_point]]$Ct..dR[(y_coord + 5):(y_coord
                                                                                                        9)]
                                         ))
    }



    #Average techical reps from same isogenic replicate
    ct_values_means[[time_point]] <- matrix(NA, 0, 2)
    for (rep in 1:8) {
        y_coord <- rep * 5 - 4
        ct_values_means[[time_point]] <-
            rbind(ct_values_means[[time_point]], colMeans(ct_values[[time_point]][y_coord:(y_coord +
                                                                                                  4), 1:2])
    }
```

```r
    #Import Input from time_point mins


    input_values[[time_point]] <- cbind(as.numeric(qpcr[[time_point]]$Ct..dR[12 *
                                                                                (0:4) + 11]),
                                        as.numeric(qpcr[[time_point]]$Ct..dR[12 *
                                                                                (0:4) + 12]))

    #Calucate Average of technical reps.
    input_mean[[time_point]] <-
        colMeans(input_values[[time_point]], na.rm = T)

    if (time_point == 2)
    {
        #Plate layout is reversed wrt control and target primers. See lab book.
        d_ct_values_means[[time_point]] <-
            ct_values_means[[time_point]][, 2] - ct_values_means[[time_point]][, 1]
        d_input_mean[[time_point]] <-
            input_mean[[time_point]][2] - input_mean[[time_point]][1]

        dd_ct_values_means[[time_point]] <-
            d_ct_values_means[[time_point]] - d_input_mean[[time_point]]
    } else {
        d_ct_values_means[[time_point]] <-
            ct_values_means[[time_point]][, 1] - ct_values_means[[time_point]][, 2]
        d_input_mean[[time_point]] <-
            input_mean[[time_point]][1] - input_mean[[time_point]][2]

        dd_ct_values_means[[time_point]] <-
            d_ct_values_means[[time_point]] - d_input_mean[[time_point]]
    }
}

df_ct <- data.frame(cbind(
    2 ^ dd_ct_values_means[[time0]],
    2 ^ dd_ct_values_means[[time45]],
    2 ^ dd_ct_values_means[[time90]]
))
colnames(df_ct) <- c("0 min", "45 mins", "90 mins")
```

## 2.2 Box plot of Raw Data

```r
library("ggpubr")
```

```
## Warning: package 'ggpubr' was built under R version 3.4.2

## Loading required package: ggplot2

## Loading required package: magrittr
```

```r
tp1<-cbind(df_ct["0 min"],rep("0 min",8))
tp2<-cbind(df_ct["45 mins"],rep("45 min",8))
tp3<-cbind(df_ct["90 mins"],rep("90 min",8))
```

```
colnames(tp1)<-c("Enrichment","Time")
colnames(tp2)<-c("Enrichment","Time")
colnames(tp3)<-c("Enrichment","Time")

df<-rbind(tp1,tp2,tp3)


#Code to remove data points more than 2*IQR from median. P-value are one-sided Wilcoxon rank test. Look
#tp3<-tp3[!(df$Enrichment[df$Time=="90 min"]>median(df$Enrichment[df$Time=="90 min"])+IQR(df$Enrichment
#tp2<-tp2[!(df$Enrichment[df$Time=="45 min"]>median(df$Enrichment[df$Time=="45 min"])+IQR(df$Enrichment

df<-rbind(tp1,tp2,tp3)

 p <- ggboxplot(df, x = "Time", y = "Enrichment",
                color = "Time", palette =c("#00AFBB", "#E7B800", "#FC4E07"),
                add = "jitter", shape = "Time",
                outlier.shape=NA,
                 main = "ER-alpha occupany of the TFF1 promoter",
                ylab = "Enrichment over Input",
                xlab = "Time point",
                show.legend=FALSE) +theme(legend.position="none")

 my_comparisons <- list(c("90 min", "0 min"), c("45 min", "0 min"),  c("45 min", "90 min") )

p + stat_compare_means(comparisons = my_comparisons,
                       method="t.test",
                       label = "p-value",
                       show.legend=FALSE,
                       method.args=list(alternative="greater"))
```

# 3 Estrogen Receptor-alpha ChIP-Seq and VULCAN Analysis

## 3.1 Introduction

Vulcan (VirtUaL ChIP-Seq Analysis through Networks) is a pipeline that combines ChIP-Seq data and regulatory networks to obtain transcription factors that are likely affected by a specific stimulus. In order to do so, our package combines strategies from different BioConductor packages: *DESeq* for data normalization, *ChIPpeakAnno* and *DiffBind* for annotation and definition of ChIP-Seq genomic peaks, *csaw* to define optimal peak width and *viper* for applying a regulatory network over a differential binding signature. Usage of gene regulatory networks to analyze biological systems has witnessed an exponential increase in the last decade, due to the ease of obtaining genome-wide expression data (Margolin et al., 2005; Giorgi et al., 2013; Castro et al., 2015). Recently, the VIPER approach to interrogate these network models has been proposed to infer transcription factor activity using the expression of a collection of their putative targets, i.e. their regulon (Alvarez et al., 2016). In the VIPER algorithm, gene-level differential expression signatures are obtained for either individual samples (relative to the mean of the dataset) or between groups of samples, and regulons are tested for enrichment. Ideally, TF regulons can be tested on promoter-level differential binding signatures generated from ChIP-Seq experiments, in order to ascertain the global change in promoter occupancy for gene sets. In our study, we propose an extension of the VIPER algorithm to specifically analyze TF occupancy in ChIP-Seq experiments. Our VULCAN algorithm uses ChIP-Seq data obtained for a given TF to provide candidate coregulators of the response to a given stimulus. The analysis is based on identifying differentially bound genes and testing their enrichment in the regulon of potential co-regulatory factors.

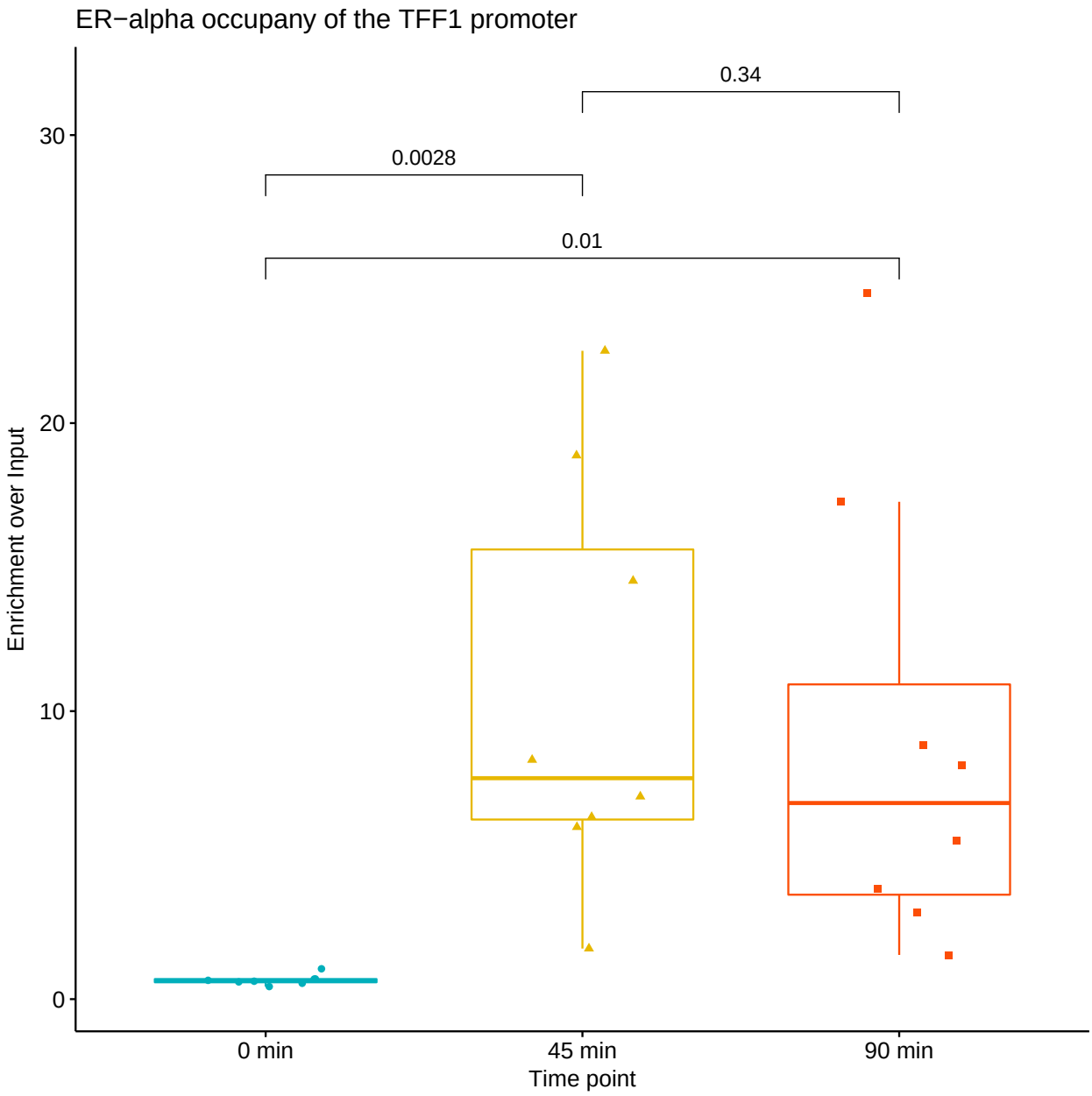


Figure 1: Box Plot showing ChIP enrichment over control loci for ER at 0, 45 and 90 minutes after stimuation with 100nM E2

## 3.2 Software setup

VULCAN is conveniently provided as an R package available from the Bioconductor repository.

```
#source("http://bioconductor.org/biocLite.R")
#biocLite("vulcan")
library(vulcan)
```

Other packages are required for the execution of the analysis and the visualization of the results. A *results* folder will be also created to store intermediate steps of the analysis.

```
library(gplots) # for heatmap.2
library(org.Hs.eg.db)
library(gridExtra) # for the pathway part
library(GeneNet) # to generate partial correlation networks
if(!file.exists("results")){dir.create("results")}
```

Finally, we will define here some convenience functions, such as those to convert from gene symbols to entrez ids, and viceversa.

```
list_eg2symbol<-as.list(org.Hs.egSYMBOL[mappedkeys(org.Hs.egSYMBOL)])
e2s<-function(ids){
  ids <- as.character(ids)
  outlist <- list_eg2symbol[ids]
  names(outlist) <- ids
  outlist[is.na(outlist)] <- paste("unknown.", ids[is.na(outlist)], sep = "")
  outlist <- gsub("unknown.unknown.", "", outlist)
  return(outlist)
}
list_symbol2eg <- as.character(org.Hs.egSYMBOL2EG[mappedkeys(org.Hs.egSYMBOL2EG)])
s2e<-function(ids){
  ids <- as.character(ids)
  outlist <- list_symbol2eg[ids]
  names(outlist) <- ids
  outlist[is.na(outlist)] <- paste("unknown.", ids[is.na(outlist)], sep = "")
  outlist <- gsub("unknown.unknown.", "", outlist)
  return(outlist)
}
```

## 3.3 Import ChIP-Seq data using Vulcan

ChIP-Seq data was generated using a cell line model of ER+ breast cancer, MCF7, at 0', 45' and 90' after stimulation with estradiol. The binding profile of ER at each timepoint was then compared between time points using differential binding analysis. From the temporal comparison ER binding we established four classes of binding pattern: early responders, repressed transcription factors, late responders and candidate cyclic genes.

The first part of our analysis highlights how to import ChIP-Seq data using the VULCAN adn DiffBind packages, provided alignment files (BAM format) and peak files (BED format) for each of the samples. In our dataset, we have 4 replicates for each time point.

### 3.3.1 Initial import

VULCAN requires an input sheet file in CSV format describing the samples and the location of the individual input files

```r
sheetfile<-"chipseq/holding/sheet.csv"

fname<-"results/001_input.rda"
if(!file.exists(fname)){
  vobj<-vulcan.import(sheetfile)
  save(vobj,file=fname)
} else {
  load(fname)
}
```

### 3.3.2 Annotation

VULCAN identifies the location of each peak in each sample, and according to the selected method, assigns a score to each gene promoter. There are a few methods available.

- ***sum***: when multiple peaks are found, sum their contributions
- ***closest***: when multiple peaks are found, keep only the closest to the TSS as the representative one
- ***strongest***: when multiple peaks are found, keep the strongest as the representative one
- ***farthest***: when multiple peaks are found, keep only the closest to the TSS as the representative one
- ***topvar***: when multiple peaks are found, keep the most varying as the representative one
- ***lowvar***: when multiple peaks are found, keep the least varying as the representative one

```r
vobj<-vulcan.annotate(vobj,lborder=-10000,rborder=10000,method="sum")
```

### 3.3.3 Normalization

At this step, genes are quantified according to the number of reads that could be associated to their promoters. The algorithms within VULCAN (*viper* and *DESeq2*) require however data to be normalized via Variance-Stabilizing Transformation (Anders and Huber, 2010).

```r
vobj<-vulcan.normalize(vobj)
save(vobj,file="results/001_vobj.rda")
```

### 3.3.4 Dataset Sample Clustering

Here, we show how the samples cluster together using peak raw counts, VST-normalized peak raw counts and peak RPKMs. In the following heatmaps, there are 4288 rows, one per gene promoter, and 16 columns, one per sample. The sample name indicates the time point in minutes (T0, T45 or T90) and the number of replicate (_1, _2, _3, _4).

```r
heatmap.2(vobj$rawcounts,scale="row",
          col=colorpanel(1000,"navy","white","red3"),tracecol="black",labRow="")
mtext("Raw Counts")
```

```r
heatmap.2(vobj$normalized,
          col=colorpanel(1000,"navy","white","red3"),tracecol="black",labRow="")
mtext("VST-normalized")
```

```r
heatmap.2(vobj$rpkms,scale="row",
          col=colorpanel(1000,"navy","white","red3"),tracecol="black",labRow="")
mtext("RPKMs")
```

Principal Component Analysis further confirms the clustering of replicates in two distinct groups: untreated (T0) and treated (T45/T90).

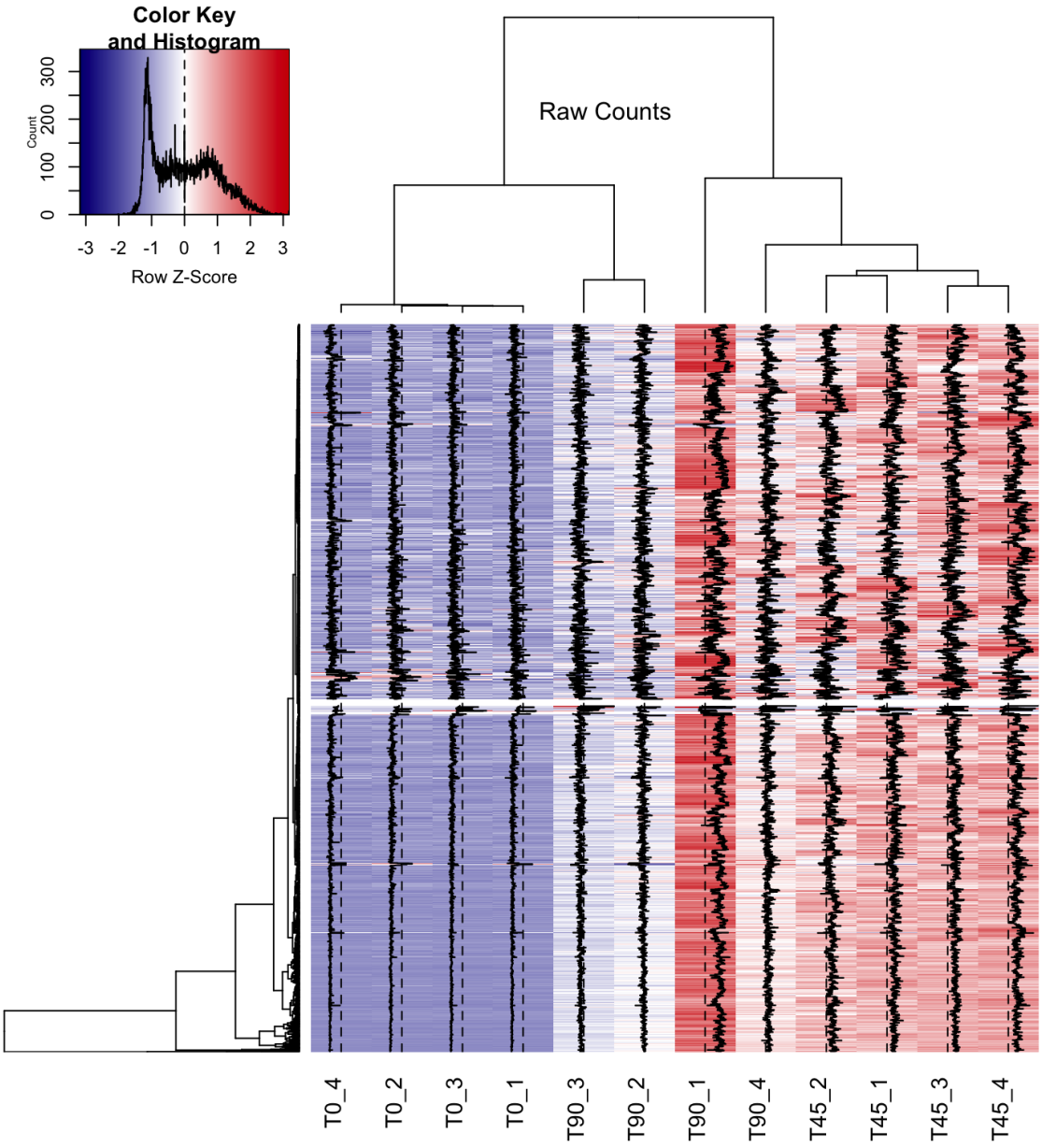


Figure 2: Dataset clustering with Raw Counts

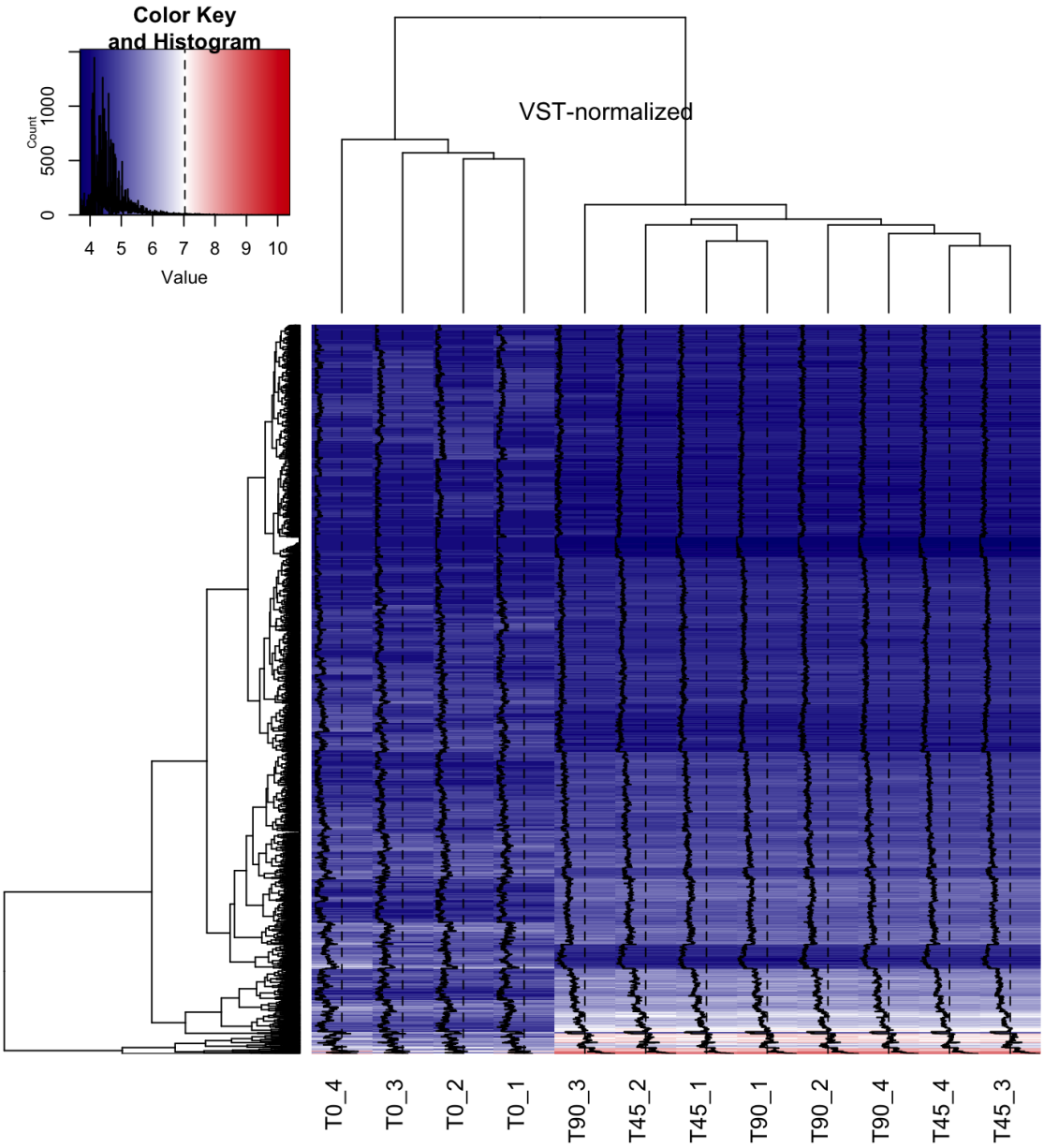


Figure 3: Dataset clustering with VST-normalized Counts

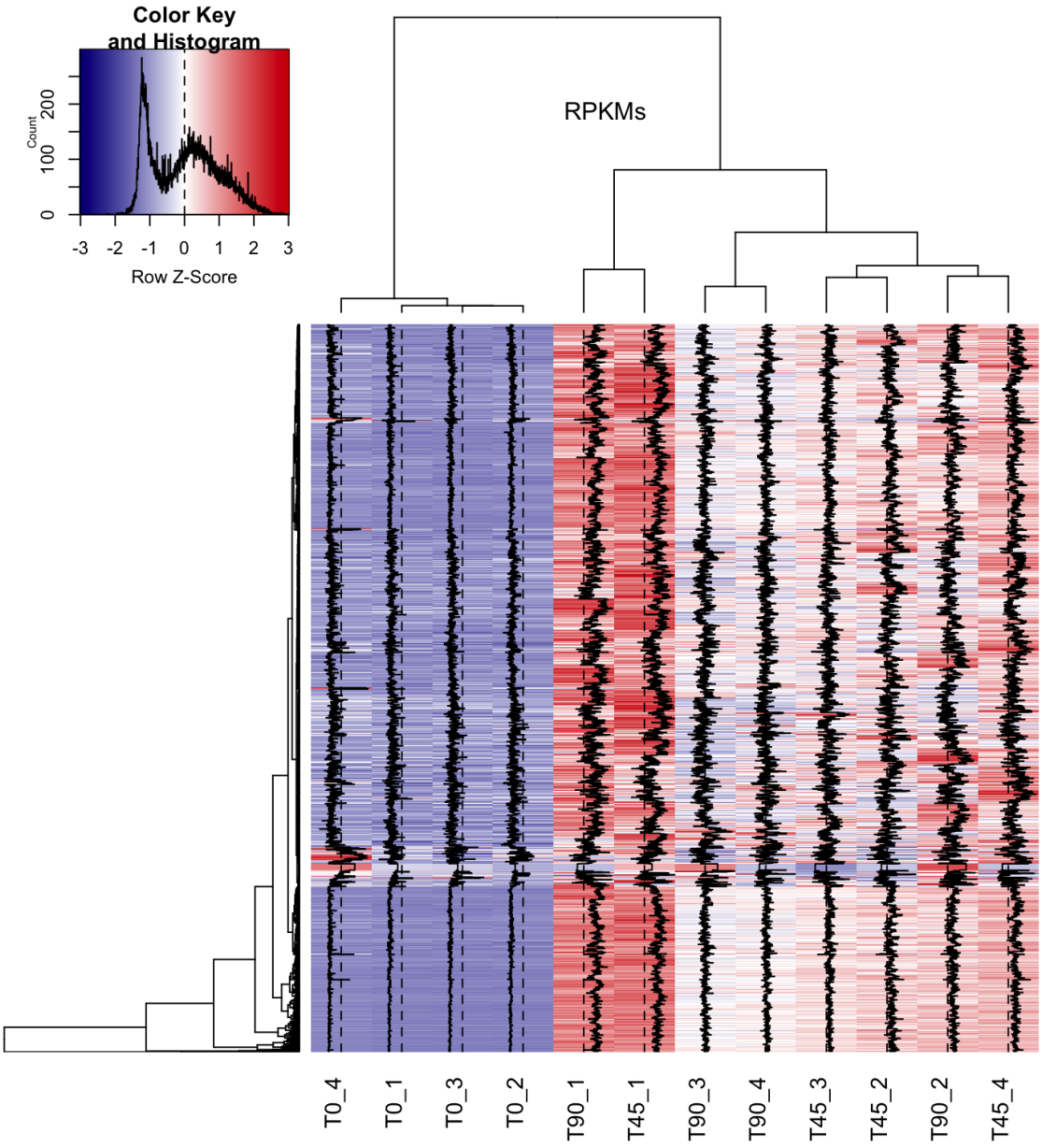


Figure 4: Dataset clustering with RPKMs

```
topvar<-apply(vobj$normalized[,],1,var)
topvar<-sort(topvar,dec=TRUE)[1:500]
submat<-vobj$normalized[names(topvar),]
pca<-prcomp(t(submat))
vars<-100*(pca$sdev^2)/sum(pca$sdev^2)
vars<-signif(vars,3)

p1<-1
p2<-2
plot(pca$x[,p1],pca$x[,p2],
     xlab=paste0("PC",p1," (Var.Explained: ",vars[p1],"%)"),
     ylab=paste0("PC",p2," (Var.Explained: ",vars[p2],"%)"),
     type="p",main="PC Analysis",pch=20,col="grey",
     xlim=c(min(pca$x[,p1])*1.1,max(pca$x[,p1])*1.1)
)
mtext("VST-Normalized data",cex=0.8)
textplot2(pca$x[,p1],pca$x[,p2],new=FALSE,
          words=gsub("_[0-9]","",rownames(pca$x),perl=TRUE)
)
grid()
```

A clearer distinction of T45 and T90 is highlighted by PC5:

```
p1<-1
p2<-5
plot(pca$x[,p1],pca$x[,p2],
     xlab=paste0("PC",p1," (Var.Explained: ",vars[p1],"%)"),
     ylab=paste0("PC",p2," (Var.Explained: ",vars[p2],"%)"),
     type="p",main="PC Analysis",pch=20,col="grey",
     xlim=c(min(pca$x[,p1])*1.1,max(pca$x[,p1])*1.1)
)
mtext("VST-Normalized data",cex=0.8)
textplot2(pca$x[,p1],pca$x[,p2],new=FALSE,
          words=gsub("_[0-9]","",rownames(pca$x),perl=TRUE)
)
grid()
```

### 3.3.5 MA plots

Without changing the format of the input data, we can use the Bioconductor DiffBind package to visualize the amplitude of changes in ER binding between time points. One way to do this is an MA plot, which shows the differences between measurements taken in two groups (e.g. 45' vs 00'), by transforming the promoter peak intensity data onto M (log ratio) and A (mean average) scales.

We will process the data using the DiffBind package and then use the *dba.plotMA* function to visualize the contrasts (which we can extract using the *dba.contrast* function).

```
sheetfile<-"chipseq/holding/sheet.csv"
fname<-"results/001_diffbind.rda"
if(!file.exists(fname)){
  # Load a sample sheet
  chipseqSamples<-read.csv(sheetfile)
  dbaobj<-dba(sampleSheet=chipseqSamples)
```

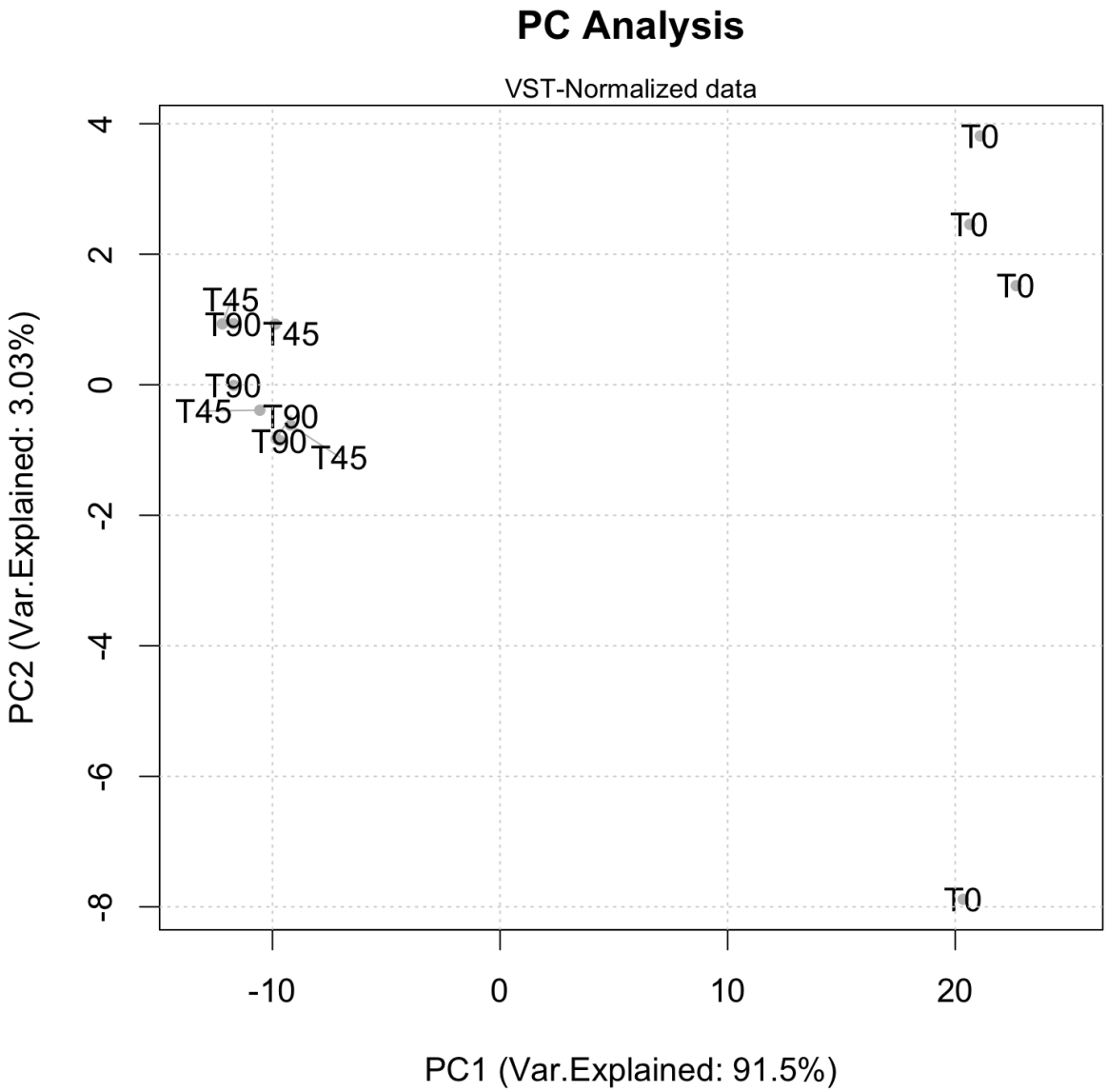


Figure 5: Principal Component Analysis of the dataset, highlighting components 1 and 2

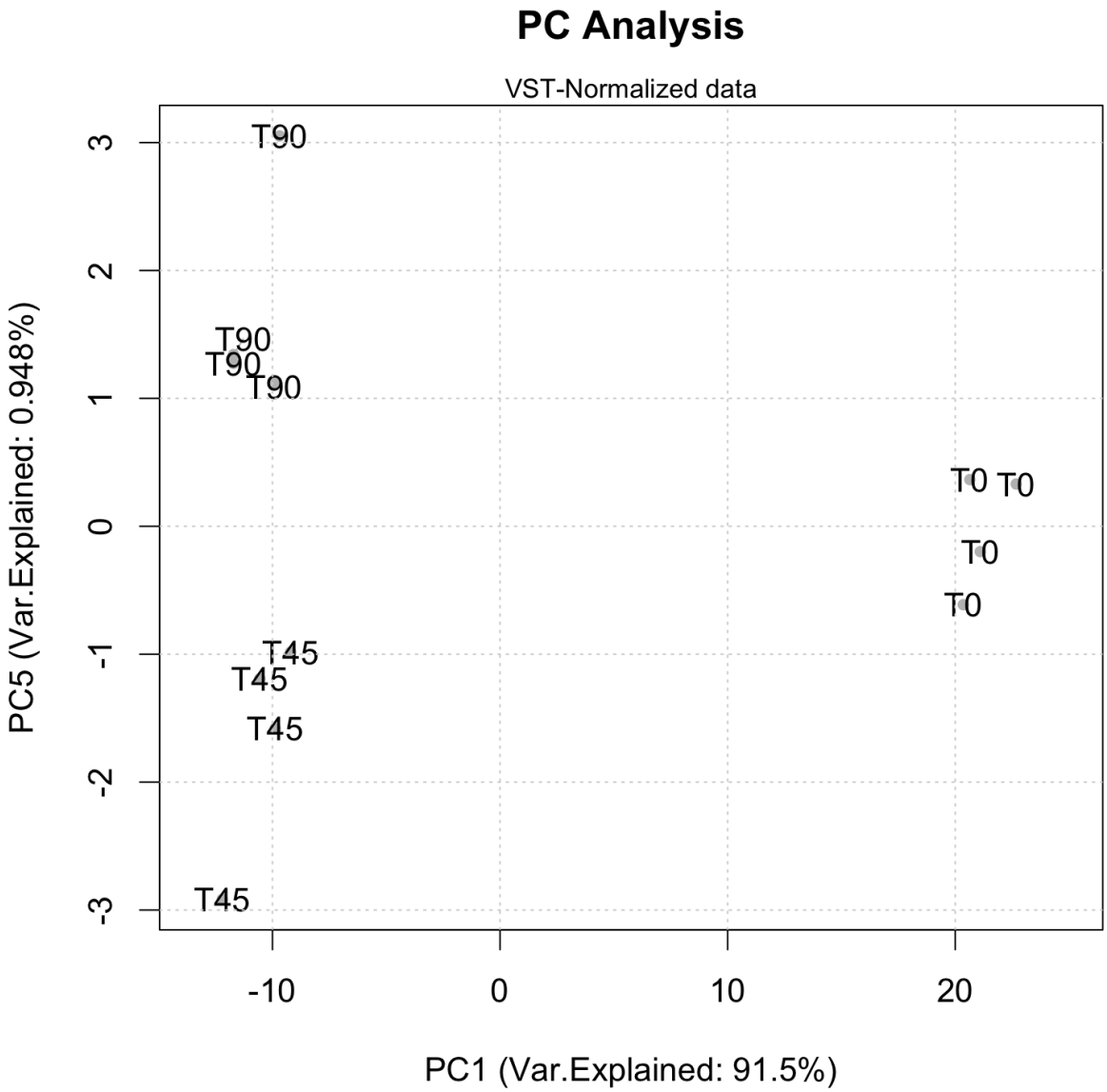


Figure 6: Principal Component Analysis of the dataset, highlighting components 1 and 5

```r
  # Count reads 500bp either side of summits, a peak is considered a peak
  # if it is found in 3 samples out of loaded samples.
  dbaobj<-dba.count(dbaobj,minOverlap=3,summits=500)

  # Define contrasts
  dbaobj<-dba.contrast(dbaobj, categories=DBA_CONDITION)

  # Calculate differential binding using the DESeq2 engine within DiffBind
  dbaobj<-dba.analyze(dbaobj,method=DBA_DESEQ2)

  # Save the DiffBind object
  save(dbaobj,file=fname)
} else {
  load(fname)
}

# Visualize each contrast
dba.contrast(dbaobj)
```

```
## 12 Samples, 19351 sites in matrix:
##       ID Tissue Factor Condition Replicate Caller Intervals FRiP
## 1  T90_1   MCF7     ER       t90         1 counts     19351 0.15
## 2  T90_2   MCF7     ER       t90         2 counts     19351 0.12
## 3  T90_3   MCF7     ER       t90         3 counts     19351 0.09
## 4  T90_4   MCF7     ER       t90         4 counts     19351 0.09
## 5  T45_1   MCF7     ER       t45         1 counts     19351 0.16
## 6  T45_2   MCF7     ER       t45         2 counts     19351 0.11
## 7  T45_3   MCF7     ER       t45         3 counts     19351 0.11
## 8  T45_4   MCF7     ER       t45         4 counts     19351 0.13
## 9   T0_1   MCF7     ER        t0         1 counts     19351 0.01
## 10  T0_2   MCF7     ER        t0         2 counts     19351 0.01
## 11  T0_3   MCF7     ER        t0         3 counts     19351 0.01
## 12  T0_4   MCF7     ER        t0         4 counts     19351 0.02
##
## 3 Contrasts:
##   Group1 Members1 Group2 Members2
## 1    t90        4    t45        4
## 2    t90        4     t0        4
## 3    t45        4     t0        4
```

```r
dba.plotMA(dbaobj,contrast=1,method=DBA_DESEQ2)
```

```r
dba.plotMA(dbaobj,contrast=2,method=DBA_DESEQ2)
```

```r
dba.plotMA(dbaobj,contrast=3,method=DBA_DESEQ2)
```

### 3.4 Apply a coregulatory network over a ChIP-Seq profile

Once the data has been loaded, VULCAN applies a regulatory network over differential binding signatures to define Transcription Factors whose networks are most affected by the treatment. In our analysis, we will be using three different networks generated via ARACNe (Margolin et al., 2006): two are breast cancer-specific and are derived from the TCGA and METABRIC data collection, respectively. A third network is used as a negative control, highlighting regulatory mechanisms derived from the Amyloid Leukemia dataset (TCGA).

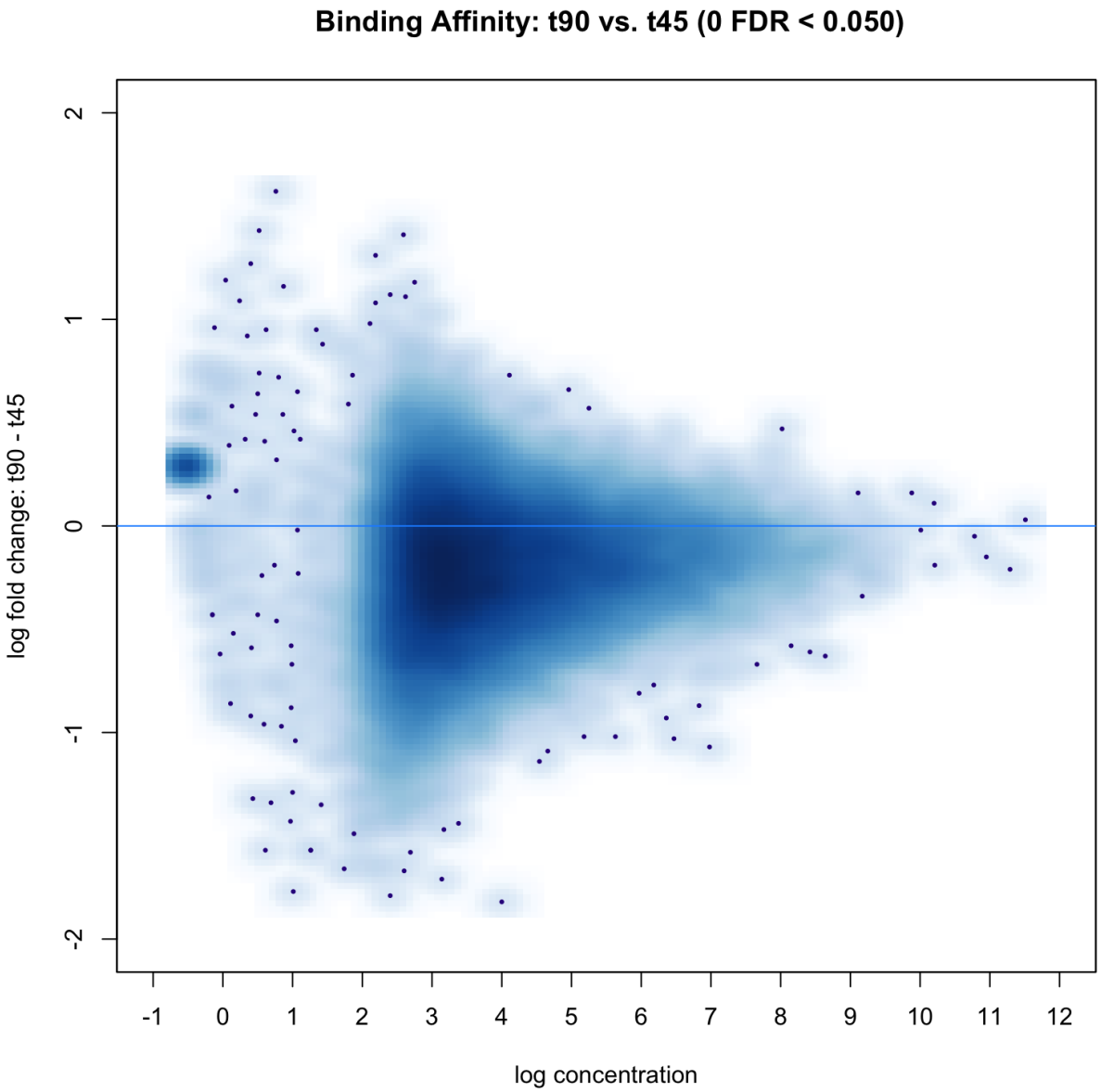


Figure 7: MA plot for Contrast 90mins vs 45mins, highlighting each individual peak. Significant peaks are highlighted in red

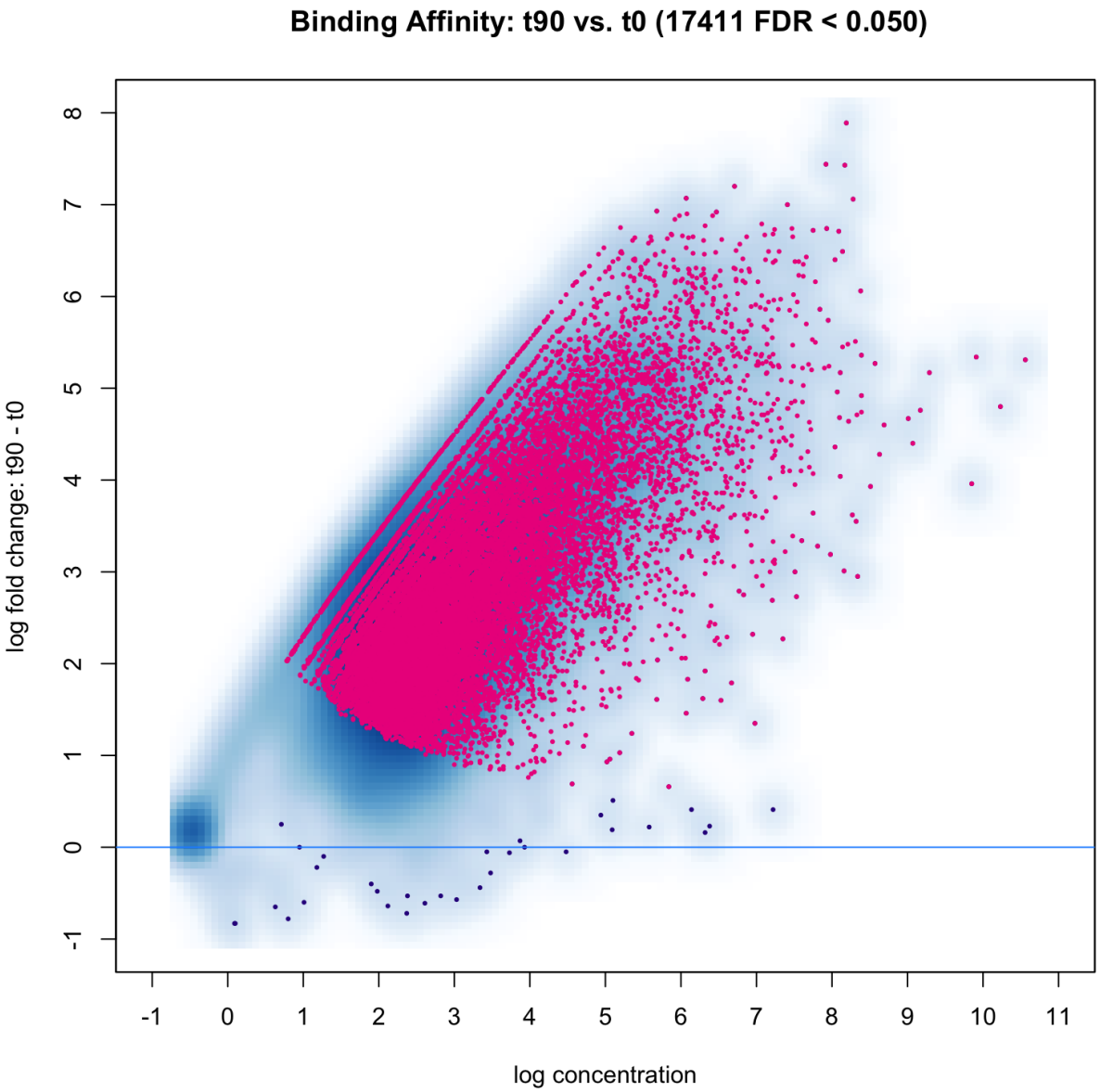


Figure 8: MA plot for Contrast 90mins vs 00mins, highlighting each individual peak. Significant peaks are highlighted in red

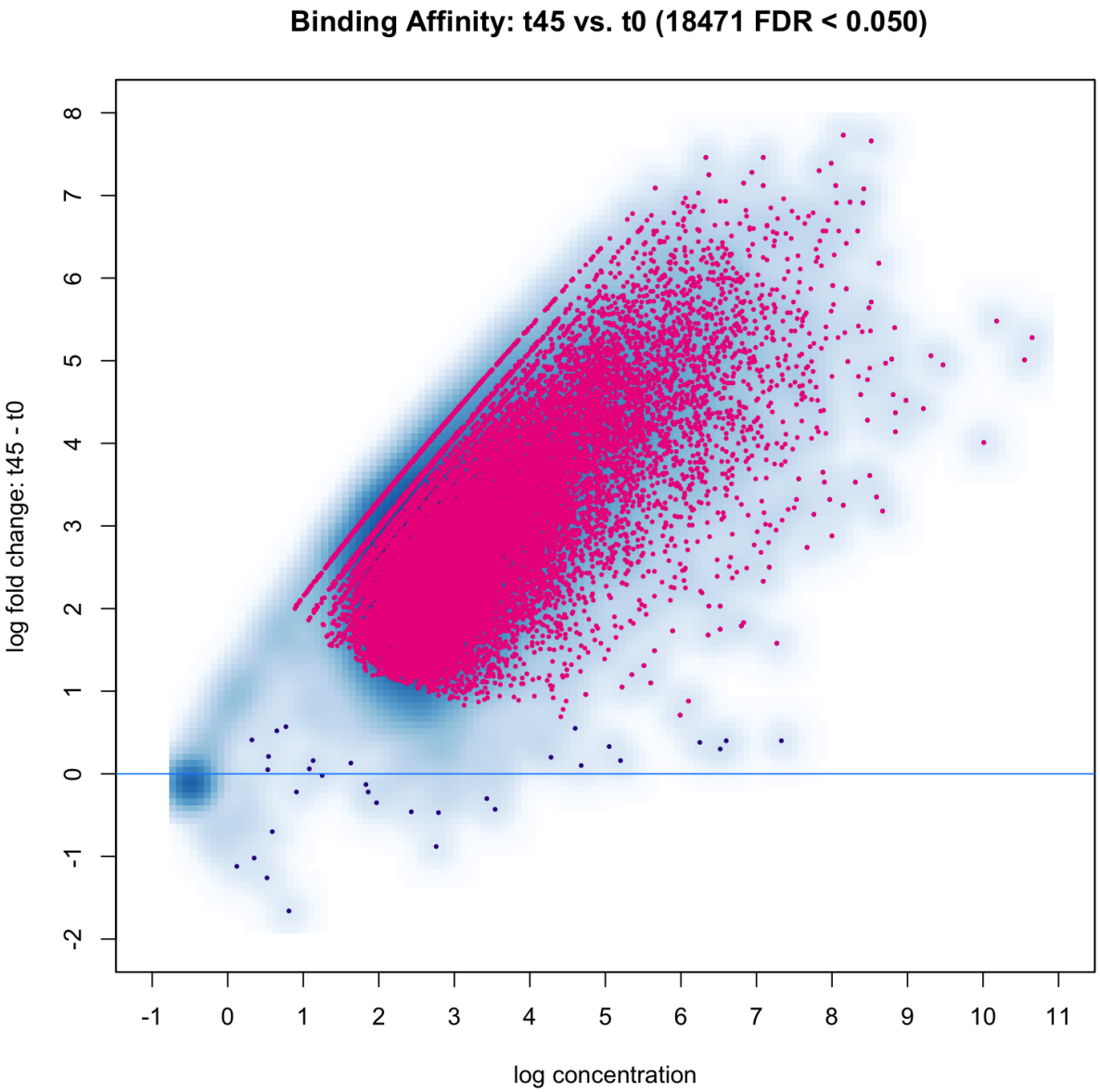


Figure 9: MA plot for Contrast 45mins vs 00mins, highlighting each individual peak. Significant peaks are highlighted in red

### Loading the input networks and processed data First, we will load the output from the previous paragraphs (chipseq data annotated and normalized) and the three networks.

```
# Load imported vulcan object
load("results/001_vobj.rda")

# Vulcan Analysis (multiple networks)
## Networks
load("networks/laml-tf-regulon.rda")
laml_regulon<-regul
rm(regul)

load("networks/brca-tf-regulon.rda")
tcga_regulon<-regul
rm(regul)

load("networks/metabric-regulon-tfs.rda")
metabric_regulon<-regulon
rm(regulon)
```

Accessing the vulcan object /texit{vobj} can give us informations on the sample groups thereby contained.

```
names(vobj$samples)
```

```
## [1] "t90" "t45" "t0"
```

#### 3.4.1 Running the core Vulcan function

The final Vulcan pipeline step requires three input objects:

- The annotated and normalized chipseq data (/texit{vobj})
- A specific binding signature defined by a contrast between two sample groups
- A regulatory network

```
fname<-"results/002_vobj_networks.rda"
list_eg2symbol<-as.list(org.Hs.egSYMBOL[mappedkeys(org.Hs.egSYMBOL)])
if(!file.exists(fname)){
  vobj_tcga_90<-vulcan(vobj,network=tcga_regulon,contrast=c("t90","t0"),annotation=list_eg2symbol)
  vobj_tcga_45<-vulcan(vobj,network=tcga_regulon,contrast=c("t45","t0"),annotation=list_eg2symbol)
  vobj_metabric_90<-vulcan(vobj,network=metabric_regulon,contrast=c("t90","t0"),annotation=list_eg2symbo
  vobj_metabric_45<-vulcan(vobj,network=metabric_regulon,contrast=c("t45","t0"),annotation=list_eg2symbo
  vobj_negative_90<-vulcan(vobj,network=laml_regulon,contrast=c("t90","t0"),annotation=list_eg2symbol)
  vobj_negative_45<-vulcan(vobj,network=laml_regulon,contrast=c("t45","t0"),annotation=list_eg2symbol)
  save(
    vobj_tcga_90,
    vobj_tcga_45,
    vobj_metabric_90,
    vobj_metabric_45,
    vobj_negative_90,
    vobj_negative_45,
    file=fname
  )
} else {
  load(fname)
}
```

### 3.4.2 Visualize the relative TF activity

Vulcan has now generated activity scores for each Transcription Factor, which specify the global ER binding strength on the promoters of their targets.

#### 3.4.2.1 METABRIC results

The following line plot shows the relative network activity for every TF at two time points. On the y-axis, the Normalized Enrichment Score of Vulcan is provided. Dashed lines indicate a p=0.05 significance threshold for up- and down-regulation.

```
threshold<-p2z(0.05)
metabric_90=vobj_metabric_90$mrs[,"NES"]
metabric_45=vobj_metabric_45$mrs[,"NES"]
tfs<-names(metabric_45)
metabricmat<-cbind(rep(0,length(metabric_45)),metabric_45[tfs],metabric_90[tfs])
colnames(metabricmat)<-c("T0","T45","T90")
## All TFs
matplot(t(metabricmat),type="l",col="grey",ylab="VULCAN NES",xaxt="n",lty=1,main="All TFs",xlim=c(1,3.3
axis(1,at=c(1:3),labels=colnames(metabricmat))
abline(h=c(0,threshold,-threshold),lty=2)
matplot(t(t(metabricmat["ESR1",])),type="l",col="red",lty=1,lwd=2,add=TRUE)
text(3,metabricmat["ESR1",3],label="ESR1",pos=4,cex=1,font=2,col="red3")
mtext("METABRIC network")
```

These TFs can be grouped in classes. For example, TFs whose activity is already significant after 45mins and remains significant at 90 minutes after estradiol treatment can be dubbed **early responders**.

```
threshold<-p2z(0.05)
tfclass<-tfs[metabricmat[,"T45"]>=threshold&metabricmat[,"T90"]>=threshold]
matplot(t(metabricmat),type="l",col="grey",ylab="VULCAN NES",xaxt="n",lty=1,main="Early responders",xlim
axis(1,at=c(1:3),labels=colnames(metabricmat))
abline(h=c(0,threshold,-threshold),lty=2)
matplot(t(metabricmat[tfclass,]),type="l",col="red3",lty=1,lwd=2,add=TRUE)
# Repel a bit
plabels<-tfclass
oricoords<-sort(setNames(metabricmat[plabels,3],plabels))
newcoords<-setNames(seq(min(oricoords)*0.7,max(oricoords),length.out=length(oricoords)),names(oricoords
text(3,newcoords,label=names(oricoords),pos=4,cex=0.8,font=2)
text(3,newcoords["ESR1"],label="ESR1",pos=4,cex=1,font=2,col="red3")
mtext("METABRIC network")
```

TFs whose *repressed* targets are bound will yield a negative activity score. These **repressed TFs** are symmetrically opposite to early responder TFs.

```
threshold<-p2z(0.05)
tfclass<-tfs[metabricmat[,"T45"]<=-threshold&metabricmat[,"T90"]<=-threshold]
matplot(t(metabricmat),type="l",col="grey",ylab="VULCAN NES",xaxt="n",lty=1,main="Repressed TFs",xlim=c
axis(1,at=c(1:3),labels=colnames(metabricmat))
abline(h=c(0,threshold,-threshold),lty=2)
matplot(t(metabricmat[tfclass,]),type="l",col="cornflowerblue",lty=1,lwd=2,add=TRUE)
# Repel a bit
plabels<-c(tfclass,"GRHL2")
oricoords<-sort(setNames(metabricmat[plabels,3],plabels))
newcoords<-setNames(seq(min(oricoords),max(oricoords)*0.5,length.out=length(oricoords)),names(oricoords
```

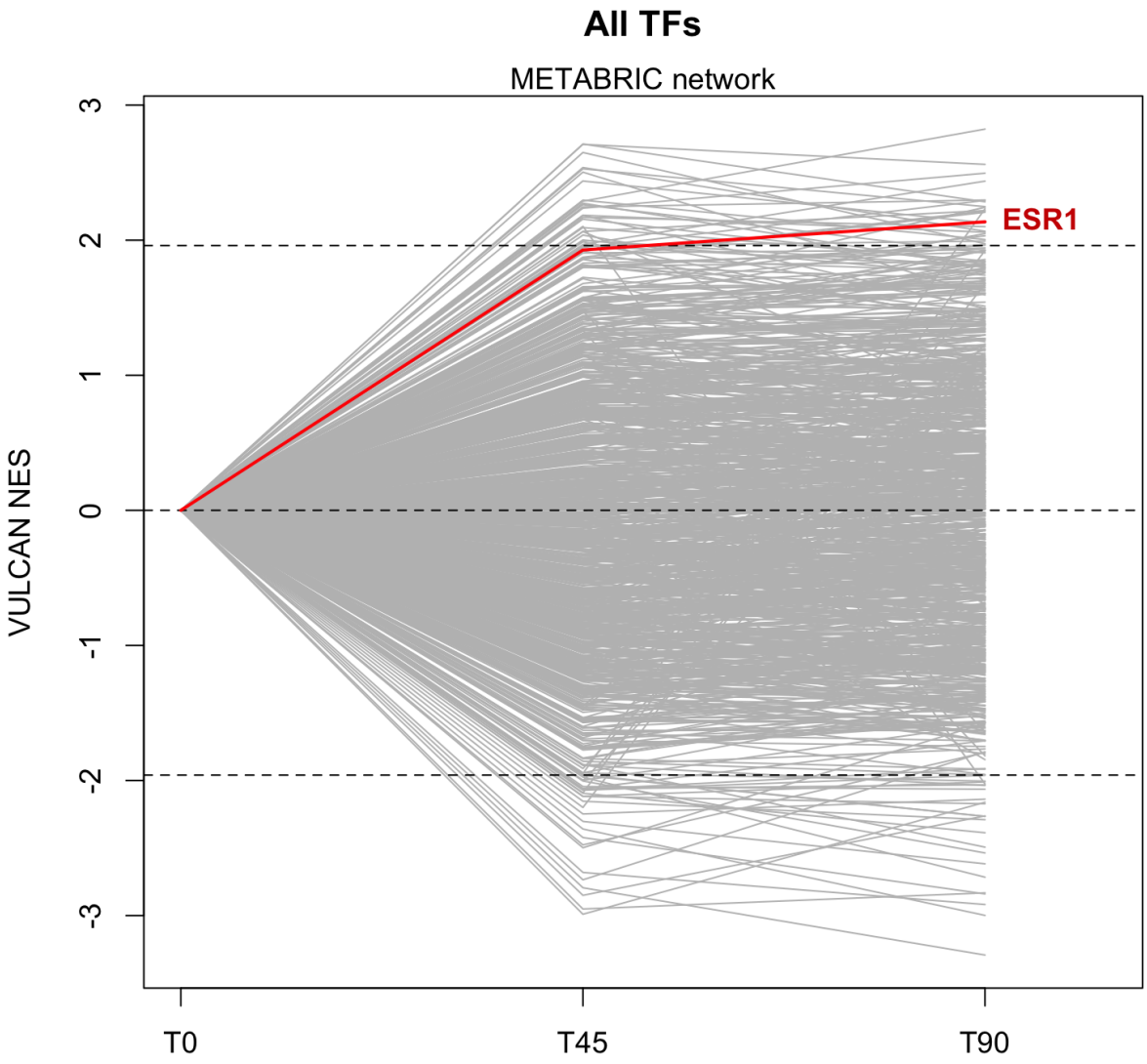


Figure 10: Global TF activity after Estradiol Treatment in MCF7 cells, inferred using the METABRIC network, highlighting the ESR1 TF as an example

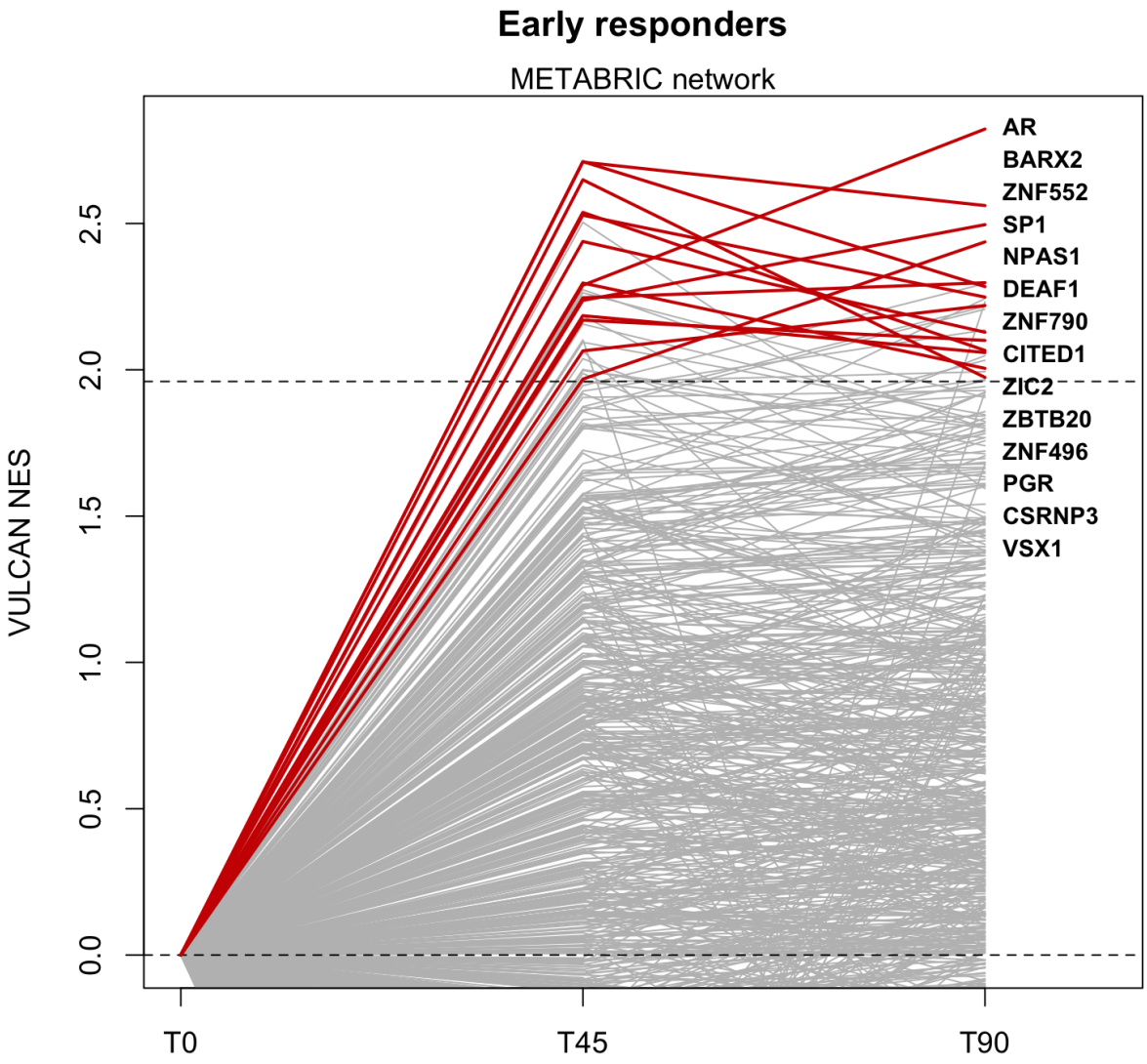


Figure 11: Global TF activity after Estradiol Treatment in MCF7 cells, inferred using the METABRIC network, highlighting TFs significantly upregulated at 45 minutes and 90 minutes

```
text(3,newcoords,label=names(oricoords),pos=4,cex=0.8,font=2)
mtext("METABRIC network")
```

Some TFs appear to have their targets bound at 45 minutes, but then unoccupied at 90 minutes. This "updown" behavior is consistent to what observed in previous literature about the cyclic properties of certain components of the ER DNA-binding complex, and therefore we dubbed them **candidate cyclic TFs**.

```
threshold<-p2z(0.05)
tfclass<-tfs[metabricmat[,"T45"]>=threshold&metabricmat[,"T90"]<=threshold]
matplot(t(metabricmat),type="l",col="grey",ylab="VULCAN NES",xaxt="n",lty=1,main="Candidate Cyclic TFs"
axis(1,at=c(1:3),labels=colnames(metabricmat))
abline(h=c(0,threshold,-threshold),lty=2)
matplot(t(metabricmat[tfclass,]),type="l",col="seagreen",lty=1,lwd=2,add=TRUE)
# Repel a bit
plabels<-tfclass
oricoords<-sort(setNames(metabricmat[plabels,3],plabels))
newcoords<-setNames(seq(min(oricoords),max(oricoords),length.out=length(oricoords)),names(oricoords))
text(3,newcoords,label=names(oricoords),pos=4,cex=0.8,font=2)
mtext("METABRIC network")
```

Finally, a category of TFs appear to be activated but at 90 minutes only. We call this category of TFs **late responders**.

```
threshold<-p2z(0.05)
tfclass<-tfs[metabricmat[,"T45"]<=threshold&metabricmat[,"T45"]>0&metabricmat[,"T90"]>=threshold]
matplot(t(metabricmat),type="l",col="grey",ylab="VULCAN NES",xaxt="n",lty=1,main="Late responders",xlim=
axis(1,at=c(1:3),labels=colnames(metabricmat))
abline(h=c(0,threshold,-threshold),lty=2)
matplot(t(metabricmat[tfclass,]),type="l",col="darkorange",lty=1,lwd=2,add=TRUE)
# Repel a bit
plabels<-tfclass
oricoords<-sort(setNames(metabricmat[plabels,3],plabels))
newcoords<-setNames(seq(min(oricoords)*0.7,min(oricoords)*1.4,length.out=length(oricoords)),names(orico
text(3,newcoords,label=names(oricoords),pos=4,cex=0.8,font=2)
mtext("METABRIC network")
```

#### 3.4.2.2 TCGA results

All the TFs and the four categories of TFs were inferred also using the TCGA network.

```
tcga_90=vobj_tcga_90$mrs[,"NES"]
tcga_45=vobj_tcga_45$mrs[,"NES"]
tfs<-names(tcga_45)
tcgamat<-cbind(rep(0,length(tcga_45)),tcga_45[tfs],tcga_90[tfs])
colnames(tcgamat)<-c("T0","T45","T90")
## All TFs
matplot(t(tcgamat),type="l",col="grey",ylab="VULCAN NES",xaxt="n",lty=1,main="All TFs",xlim=c(1,3.3),yl
axis(1,at=c(1:3),labels=colnames(tcgamat))
abline(h=c(0,threshold,-threshold),lty=2)
matplot(t(t(tcgamat["ESR1",])),type="l",col="red",lty=1,lwd=2,add=TRUE)
text(3,tcgamat["ESR1",3],label="ESR1",pos=4,cex=0.6,font=2,col="red3")
mtext("TCGA network")
```

```
threshold<-p2z(0.05)
tfclass<-tfs[tcgamat[,"T45"]>=threshold&tcgamat[,"T90"]>=threshold]
matplot(t(tcgamat),type="l",col="grey",ylab="VULCAN NES",xaxt="n",lty=1,main="Early responders",xlim=c(
```

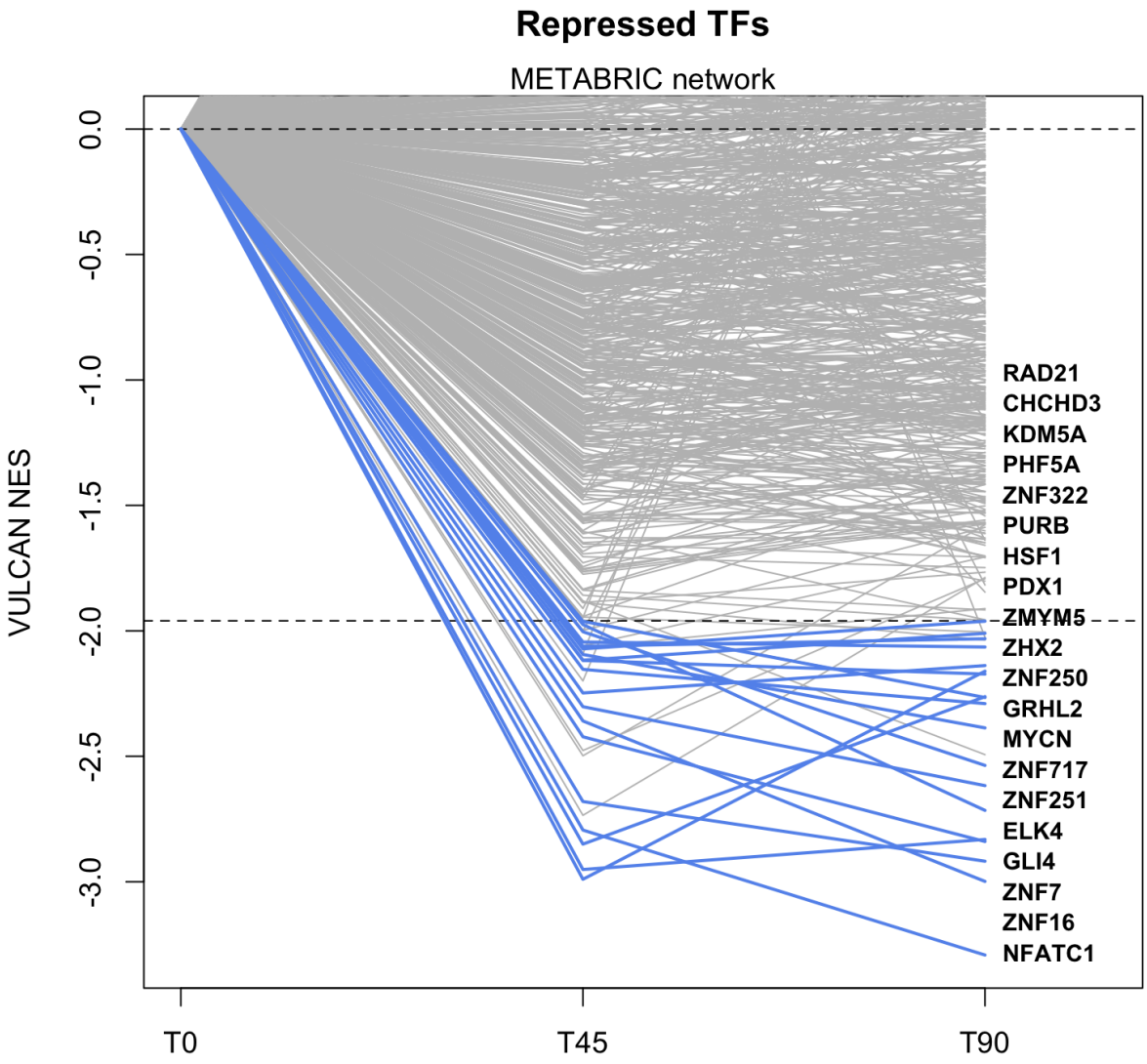


Figure 12: Global TF activity after Estradiol Treatment in MCF7 cells, inferred using the METABRIC network, highlighting TFs significantly downregulated at 45 minutes and 90 minutes

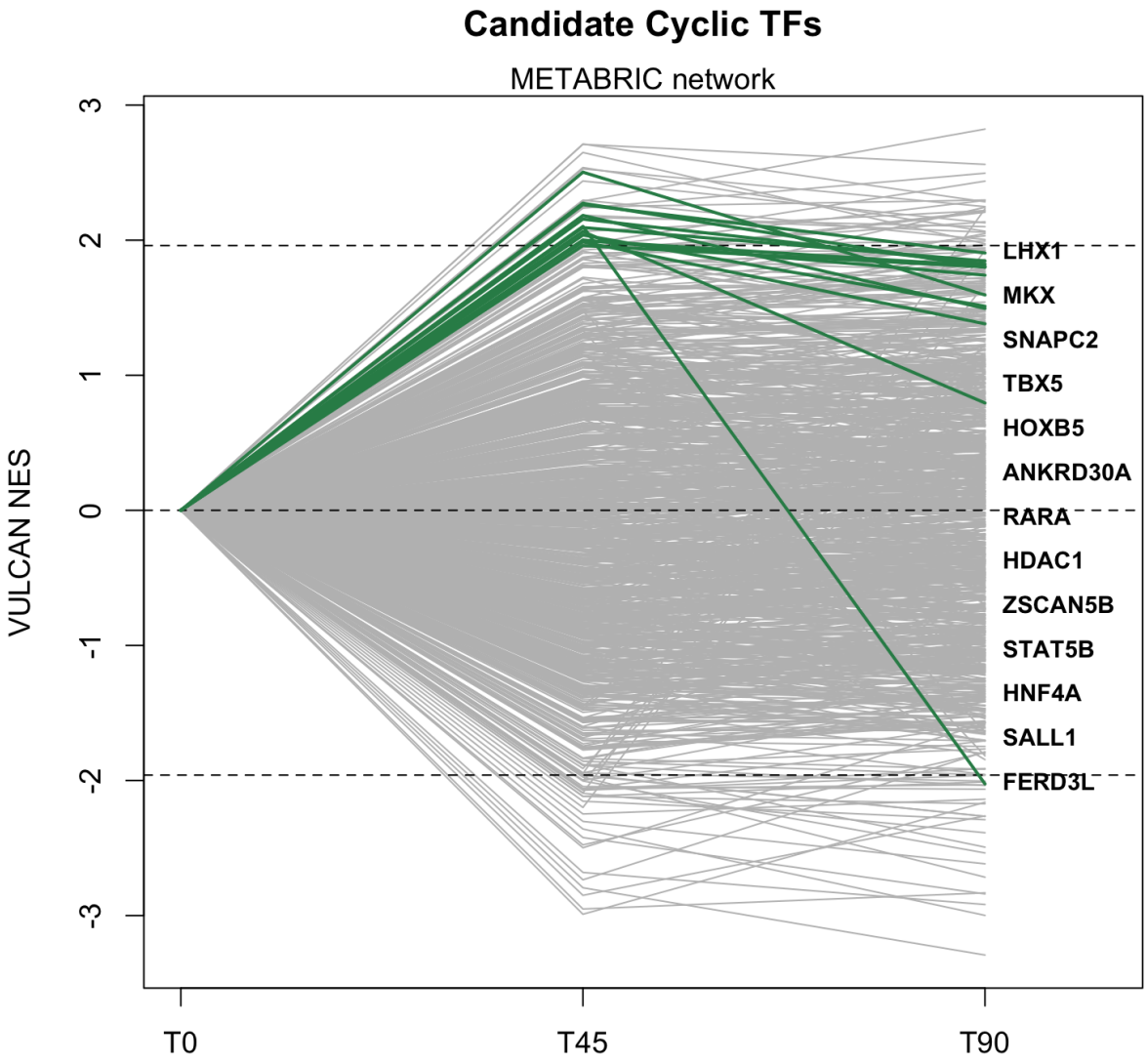


Figure 13: Global TF activity after Estradiol Treatment in MCF7 cells, inferred using the METABRIC network, highlighting TFs significantly upregulated at 45 minutes but not at 90 minutes

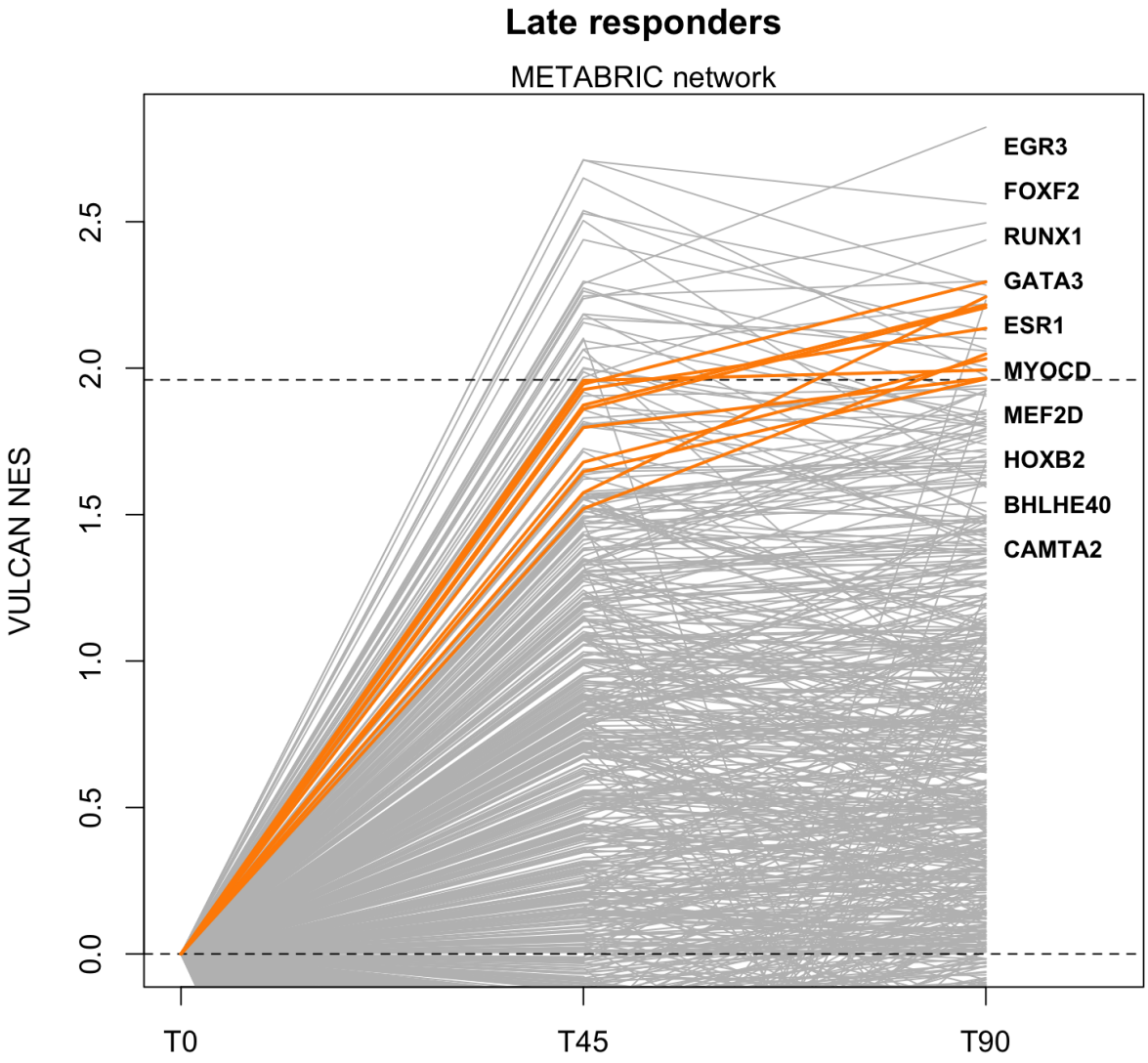


Figure 14: Global TF activity after Estradiol Treatment in MCF7 cells, inferred using the METABRIC network, highlighting TFs significantly upregulated at 90 minutes but not at 45 minutes

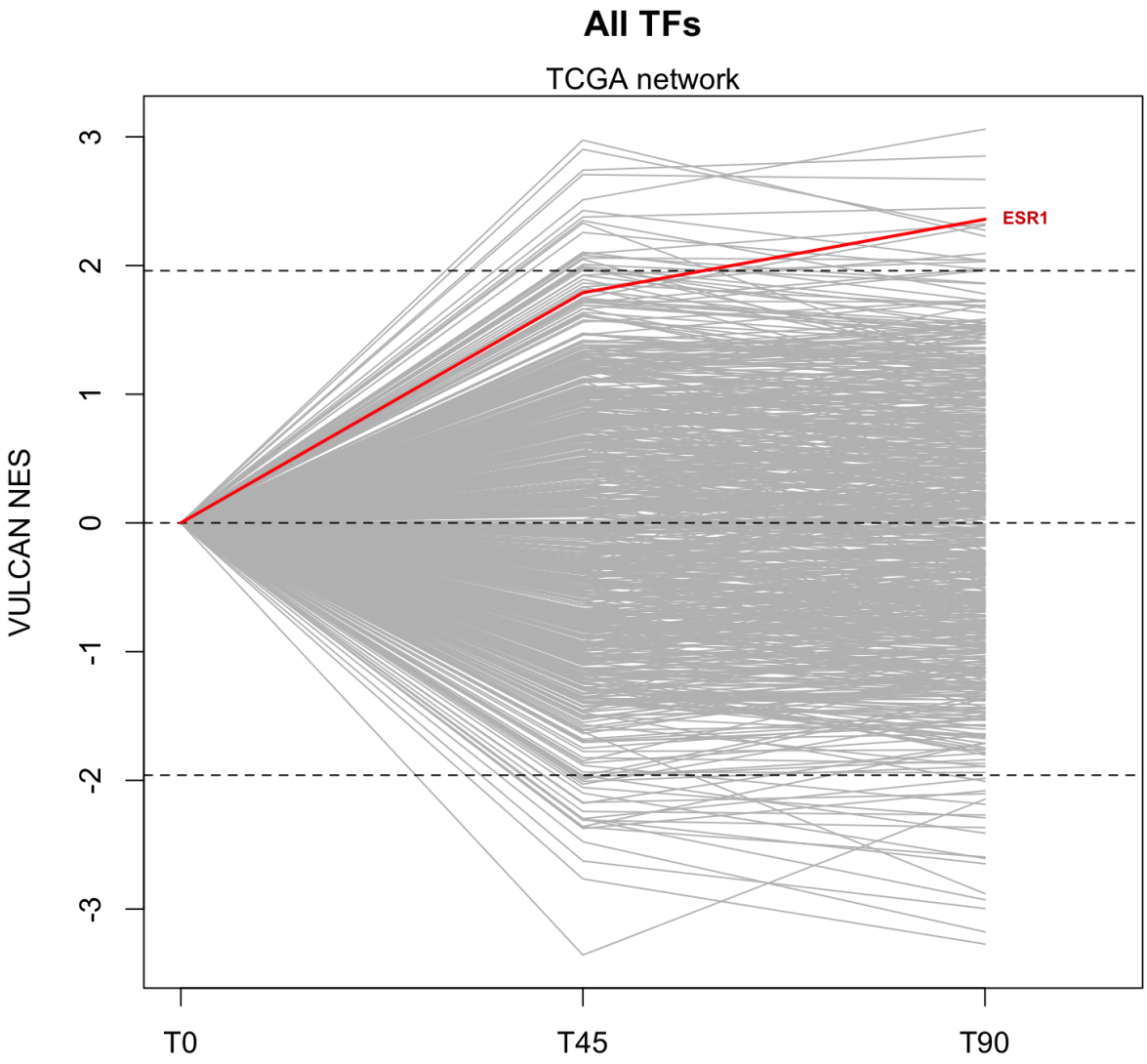


Figure 15: Global TF activity after Estradiol Treatment in MCF7 cells, inferred using the TCGA network, highlighting the ESR1 TF as an example

```
axis(1,at=c(1:3),labels=colnames(tcgamat))
abline(h=c(0,threshold,-threshold),lty=2)
matplot(t(tcgamat[tfclass,]),type="l",col="red3",lty=1,lwd=2,add=TRUE)
# Repel a bit
plabels<-tfclass
oricoords<-sort(setNames(tcgamat[plabels,3],plabels))
newcoords<-setNames(seq(min(oricoords),max(oricoords),length.out=length(oricoords)),names(oricoords))
text(3,newcoords,label=names(oricoords),pos=4,cex=0.6,font=2)
text(3,newcoords["ESR1"],label="ESR1",pos=4,cex=0.6,font=2,col="red3")
mtext("TCGA network")
```

```
threshold<-p2z(0.05)
tfclass<-tfs[tcgamat[,"T45"]<=-threshold&tcgamat[,"T90"]<=-threshold]
matplot(t(tcgamat),type="l",col="grey",ylab="VULCAN NES",xaxt="n",lty=1,main="Repressed TFs",xlim=c(1,3
axis(1,at=c(1:3),labels=colnames(tcgamat))
abline(h=c(0,threshold,-threshold),lty=2)
matplot(t(tcgamat[tfclass,]),type="l",col="cornflowerblue",lty=1,lwd=2,add=TRUE)
# Repel a bit
plabels<-tfclass
oricoords<-sort(setNames(tcgamat[plabels,3],plabels))
newcoords<-setNames(seq(min(oricoords),max(oricoords),length.out=length(oricoords)),names(oricoords))
text(3,newcoords,label=names(oricoords),pos=4,cex=0.6,font=2)
mtext("TCGA network")
```

```
threshold<-p2z(0.05)
tfclass<-tfs[tcgamat[,"T45"]>=threshold&tcgamat[,"T90"]<=threshold]
matplot(t(tcgamat),type="l",col="grey",ylab="VULCAN NES",xaxt="n",lty=1,main="Candidate Cyclic TFs",xlim
axis(1,at=c(1:3),labels=colnames(tcgamat))
abline(h=c(0,threshold,-threshold),lty=2)
matplot(t(tcgamat[tfclass,]),type="l",col="seagreen",lty=1,lwd=2,add=TRUE)
# Repel a bit
plabels<-tfclass
oricoords<-sort(setNames(tcgamat[plabels,3],plabels))
newcoords<-setNames(seq(min(oricoords),max(oricoords),length.out=length(oricoords)),names(oricoords))
text(3,newcoords,label=names(oricoords),pos=4,cex=0.6,font=2)
mtext("TCGA network")
```

```
## Dn-Up TF class
threshold<-p2z(0.05)
tfclass<-tfs[tcgamat[,"T45"]<=threshold&tcgamat[,"T45"]>0&tcgamat[,"T90"]>=threshold]
matplot(t(tcgamat),type="l",col="grey",ylab="VULCAN NES",xaxt="n",lty=1,main="Late responders",xlim=c(1
axis(1,at=c(1:3),labels=colnames(tcgamat))
abline(h=c(0,threshold,-threshold),lty=2)
matplot(t(tcgamat[tfclass,]),type="l",col="darkorange",lty=1,lwd=2,add=TRUE)
# Repel a bit
plabels<-tfclass
oricoords<-sort(setNames(tcgamat[plabels,3],plabels))
newcoords<-setNames(seq(min(oricoords),min(oricoords)*1.2,length.out=length(oricoords)),names(oricoords
text(3,newcoords,label=names(oricoords),pos=4,cex=0.6,font=2)
mtext("TCGA network")
```

#### 3.4.2.3 Comparing TCGA and METABRIC results

The following scatterplots compare the activity inferred by VULCAN using two alternative networks, derived

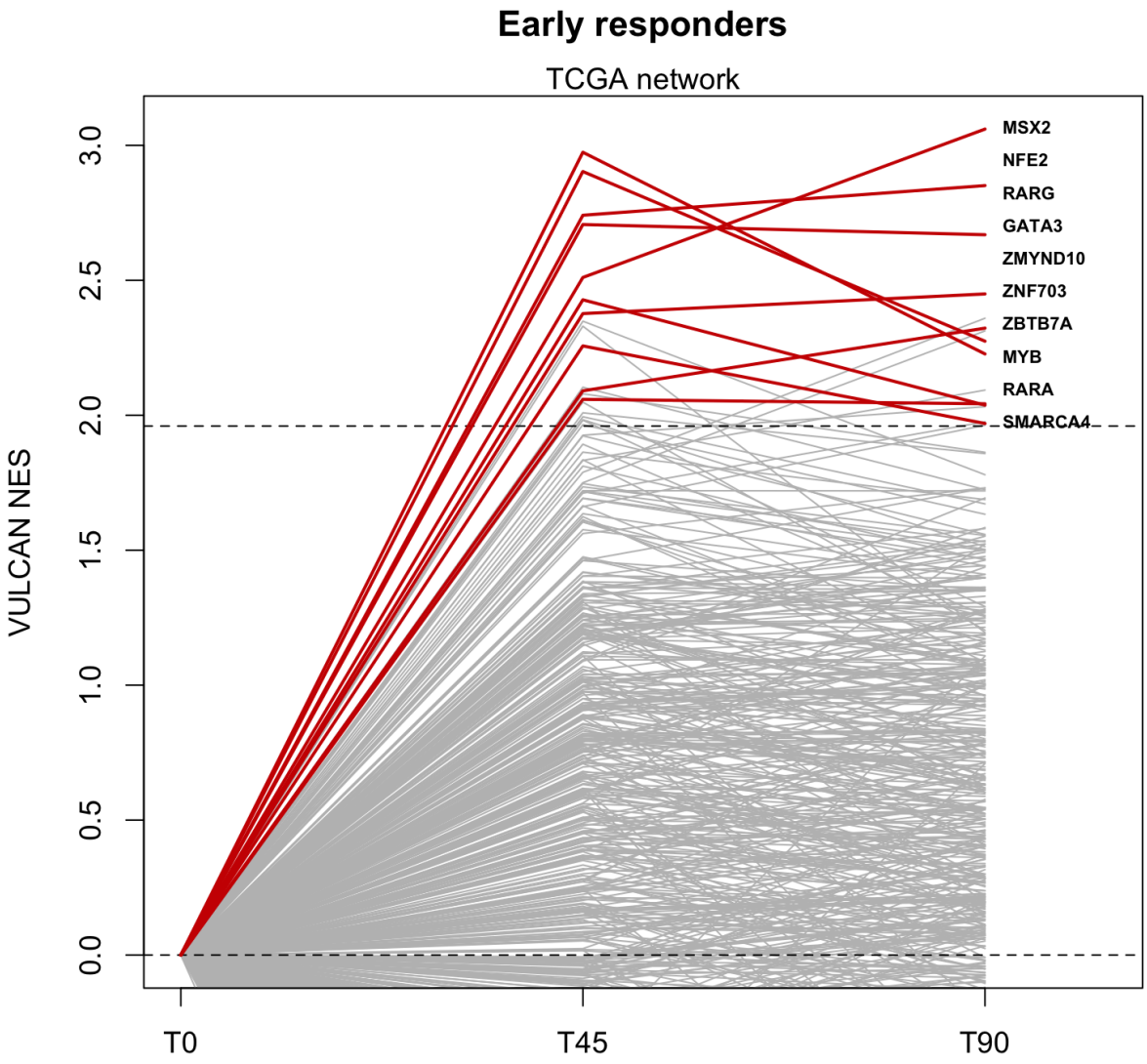


Figure 16: Global TF activity after Estradiol Treatment in MCF7 cells, inferred using the TCGA network, highlighting TFs significantly upregulated at 45 minutes and 90 minutes

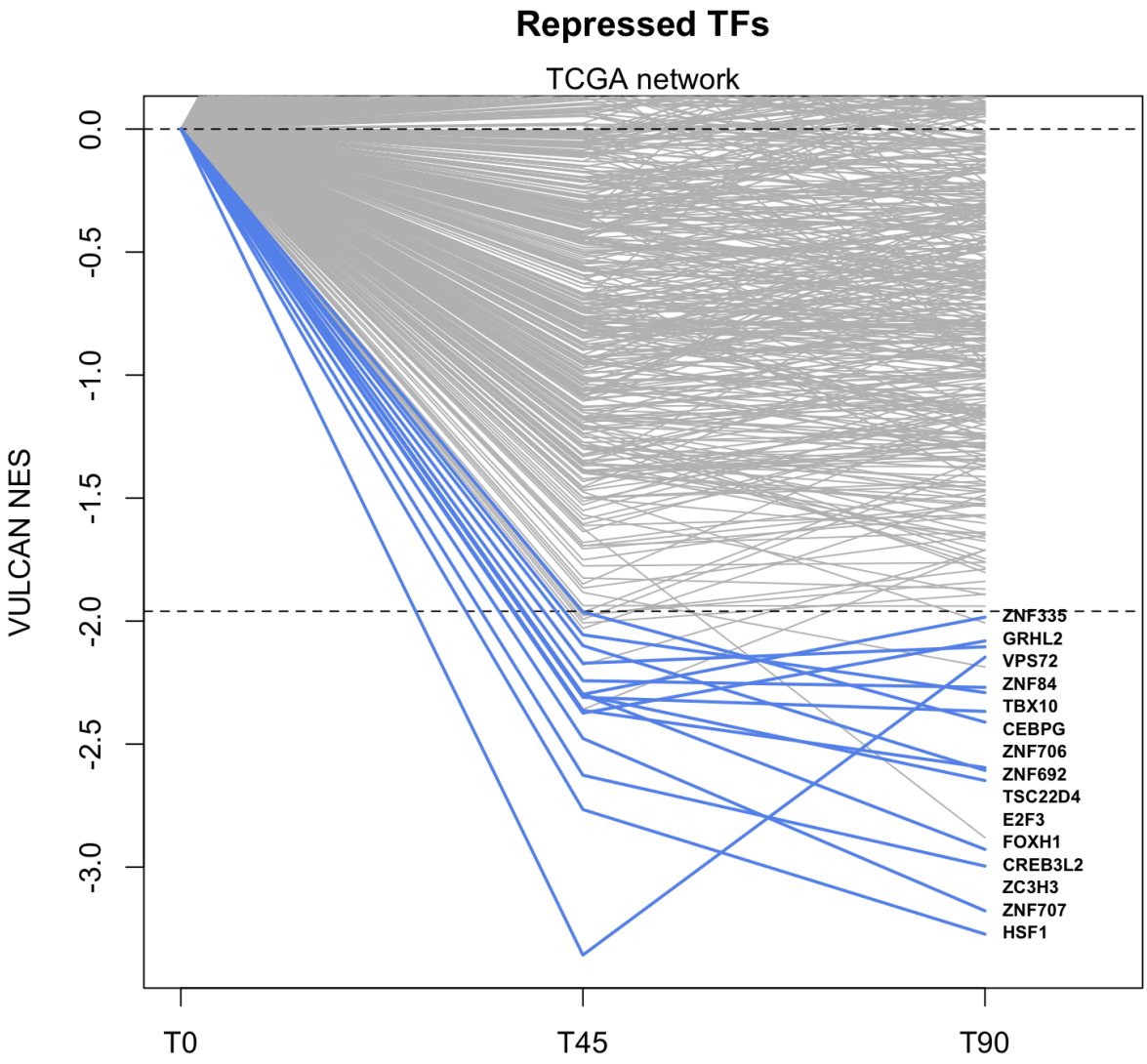


Figure 17: Global TF activity after Estradiol Treatment in MCF7 cells, inferred using the TCGA network, highlighting TFs significantly downregulated at 45 minutes and 90 minutes

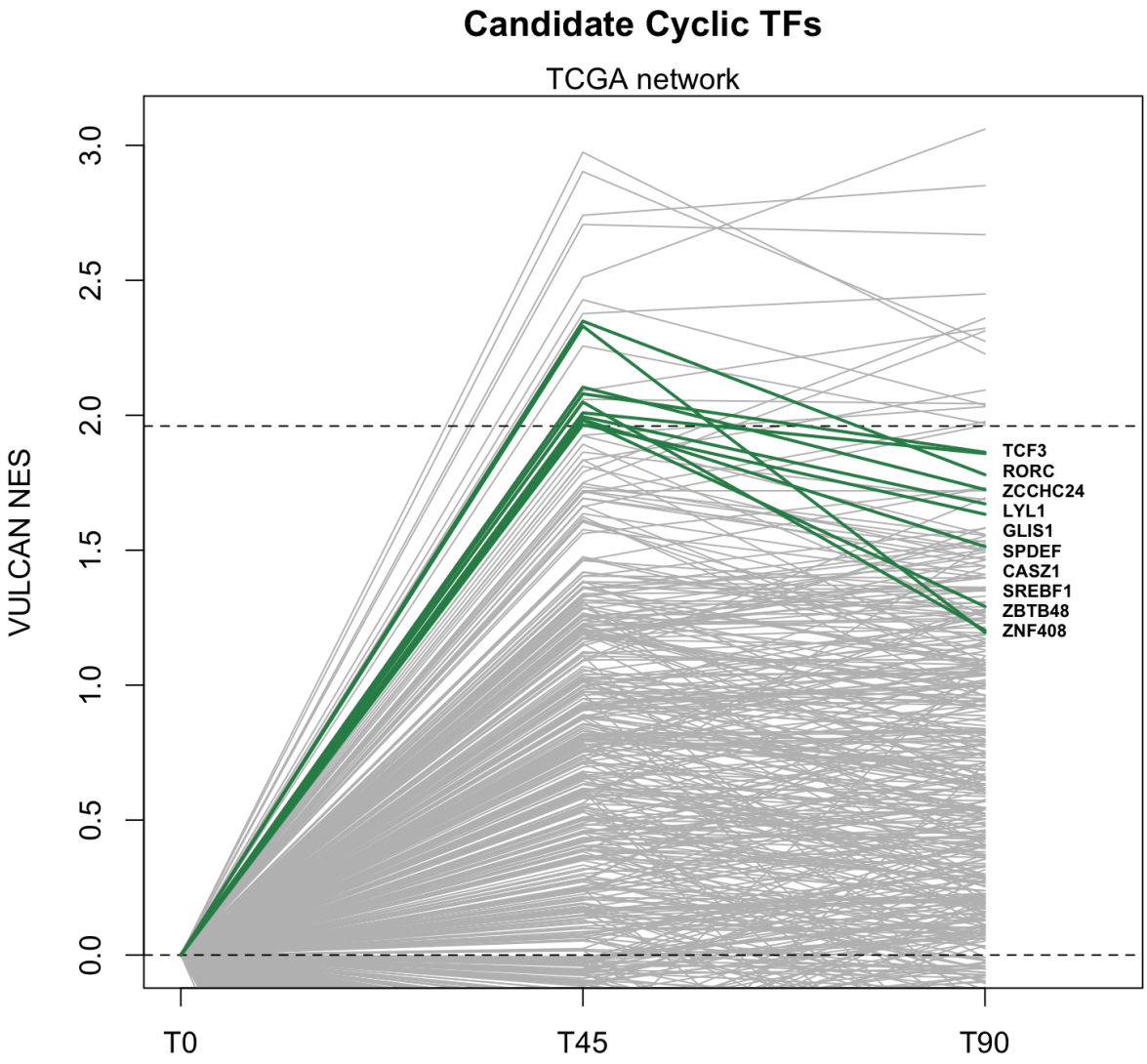


Figure 18: Global TF activity after Estradiol Treatment in MCF7 cells, inferred using the TCGA network, highlighting TFs significantly upregulated at 45 minutes but not at 90 minutes

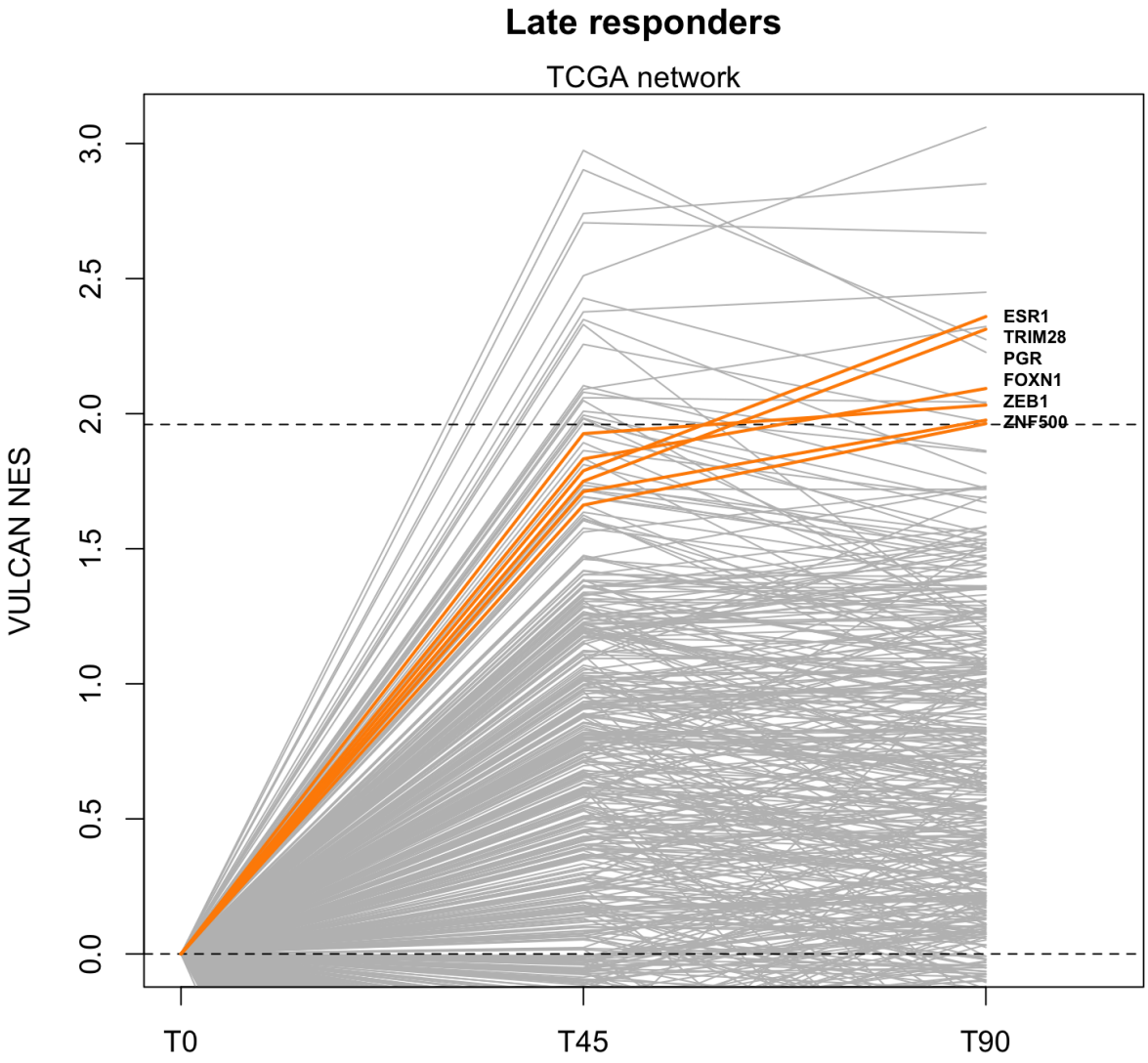


Figure 19: Global TF activity after Estradiol Treatment in MCF7 cells, inferred using the TCGA network, highlighting TFs significantly upregulated at 90 minutes but not at 45 minutes

from the TCGA and METABRIC breast cancer datasets using ARACNe-AP (Giorgi et al., 2016) with default parameters.

```
common<-intersect(rownames(tcgamat),rownames(metabricmat))
set.seed(1)
x<-tcgamat[common,"T45"]
y<-metabricmat[common,"T45"]
plot(x,y,xlab="TCGA, 45mins",ylab="METABRIC, 45mins",pch=20,col="grey",xlim=c(min(x)*1.2,max(x)*1.2))
grid()
#toshow<-c("ESR1","GATA3","RARA","HSF1")
toshow<-names(which(rank(rank(-abs(x))+rank(-abs(y)))<=20))
#toshow<-unique(c(toshow,names(sort(rank(-abs(x))[1:10])),names(sort(rank(-abs(y)))[1:10])))
textplot2(x[toshow],y[toshow],words=toshow,new=FALSE,cex=0.8)
lm1<-lm(y~x)
abline(lm1$coef)
pcc<-cor.test(x,y)
mtext(paste0("PCC=",signif(pcc$estimate,2)," (p=",signif(pcc$p.value,2),")"))
```

```
x<-tcgamat[common,"T90"]
y<-metabricmat[common,"T90"]
plot(x,y,xlab="TCGA, 90mins",ylab="METABRIC, 90mins",pch=20,col="grey",xlim=c(min(x)*1.2,max(x)*1.2))
grid()
#toshow<-c("ESR1","GATA3","RARA","HSF1")
toshow<-names(which(rank(rank(-abs(x))+rank(-abs(y)))<=20))
#toshow<-unique(c(toshow,names(sort(rank(-abs(x))[1:10])),names(sort(rank(-abs(y)))[1:10])))
textplot2(x[toshow],y[toshow],words=toshow,new=FALSE,cex=0.8)
lm1<-lm(y~x)
abline(lm1$coef)
pcc<-cor.test(x,y)
mtext(paste0("PCC=",signif(pcc$estimate,2)," (p=",signif(pcc$p.value,2),")"))
abline(lm1$coef)
```

#### 3.4.2.4 Testing with a different context network as a negative control

Regulatory networks can be tissue-specific, and so we built a third network using the same parameters as the two breast cancer data-based ones. The third network is built on leukemic samples from the TCGA AML dataset. Our results show a weaker activity for all TFs, which is only weakly correlated to that inferred via the TCGA breast cancer network.

```
negative_90=vobj_negative_90$mrs[,"NES"]
negative_45=vobj_negative_45$mrs[,"NES"]
tfs<-names(negative_45)
negativemat<-cbind(rep(0,length(negative_45)),negative_45[tfs],negative_90[tfs])
colnames(negativemat)<-c("T0","T45","T90")

common<-intersect(rownames(tcgamat),rownames(negativemat))

par(mfrow=c(1,2),oma=c(0,0,2,0))
# Scatterplot, negative vs tcga 45mins
x<-tcgamat[common,"T45"]
y<-negativemat[common,"T45"]
plot(x,y,xlab="TCGA, 45mins",ylab="negative, 45mins",pch=20,col="grey",xlim=c(min(x)*1.2,max(x)*1.2))
grid()
lm1<-lm(y~x)
abline(lm1$coef)
```

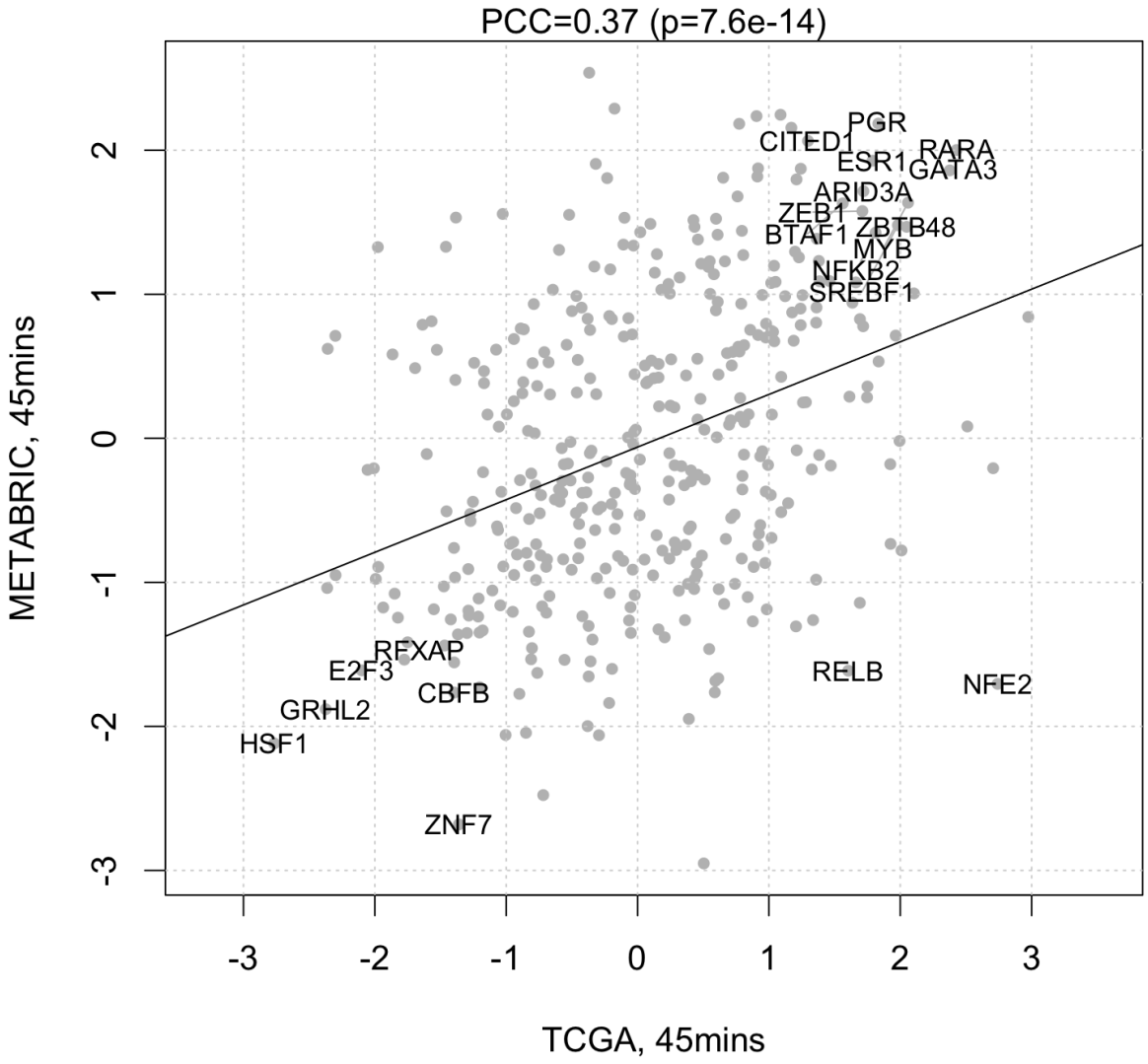


Figure 20: Comparing TF activities inferred by VULCAN using two different breast cancer dataset-derived networks on the ER 45 minutes signature. PCC indicates the Pearson Correlation Coefficient

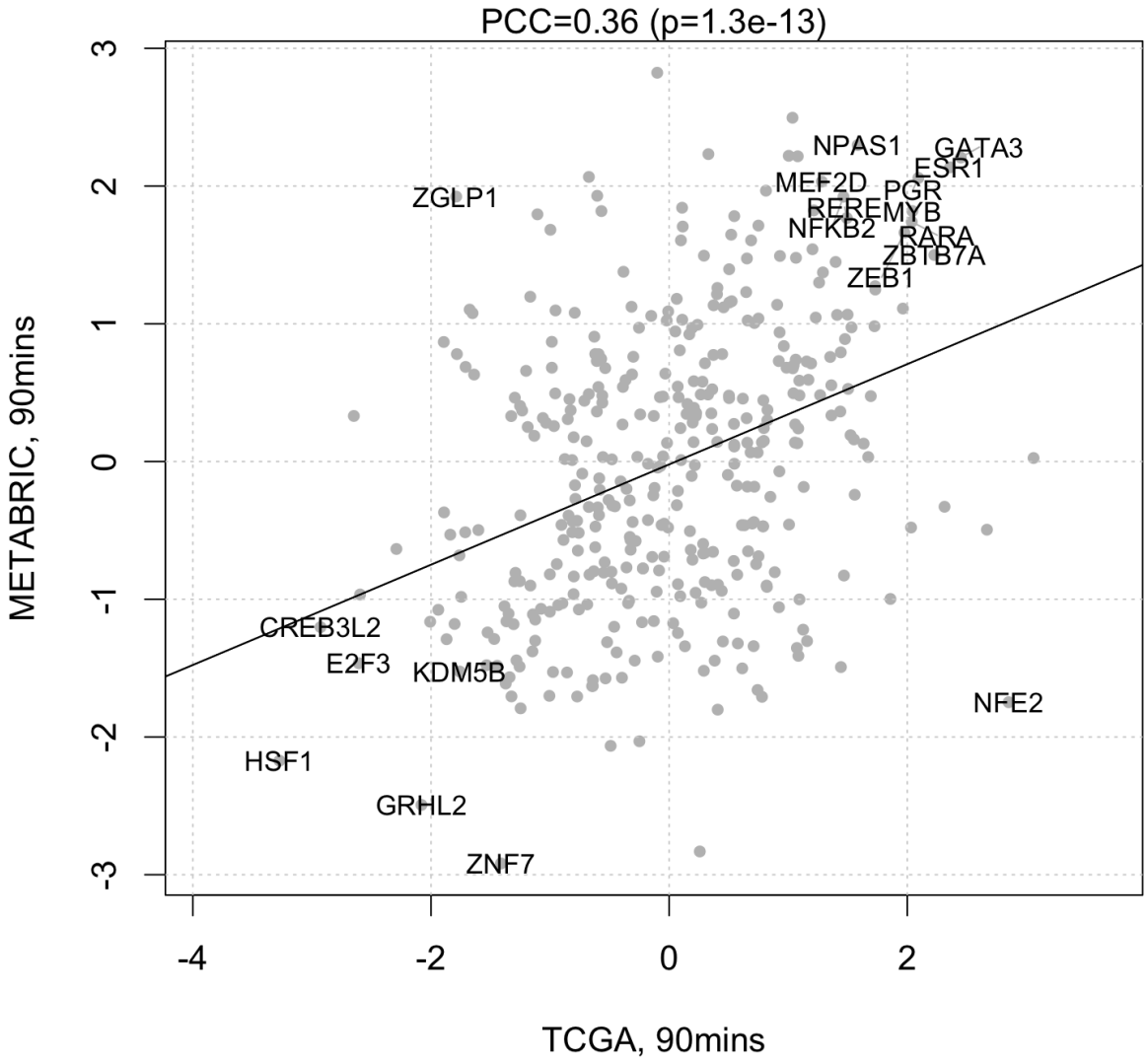


Figure 21: Comparing TF activities inferred by VULCAN using two different breast cancer dataset-derived networks on the ER 90 minutes signature. PCC indicates the Pearson Correlation Coefficient

```
pcc<-cor.test(x,y)
mtext(paste0("PCC=",signif(pcc$estimate,2)," (p=",signif(p.adjust(pcc$p.value,method="bonferroni",n=1000

abline(lm1$coef)


# Scatterplot, negative vs tcga 90mins
x<-tcgamat[common,"T90"]
y<-negativemat[common,"T90"]
plot(x,y,xlab="TCGA, 90mins",ylab="negative, 90mins",pch=20,col="grey",xlim=c(min(x)*1.2,max(x)*1.2))
grid()
lm1<-lm(y~x)
abline(lm1$coef)
pcc<-cor.test(x,y)
mtext(paste0("PCC=",signif(pcc$estimate,2)," (p=",signif(p.adjust(pcc$p.value,method="bonferroni",n=1000
abline(lm1$coef)

title("Comparison with Negative Network", outer=TRUE)
```

### 3.5 Pathway enrichment analysis

In the previous paragraphs we generated signatures of differential binding centered around the peaks extracted by VULCAN using the *vulcan.annotate* function. We apply two methods that assess the enrichment of gene pathways over continuous signatures: GSEA (Subramaniam et al., 2004) and aREA (Alvarez et al., 2016). First, we will load the VULCAN object containing our dataset:

```
# Load imported vulcan object
load("results/001_vobj.rda")
```

Then, we need gene pathways. A manually annotated and very exhaustive list is available from the MsiGDB database by the Broad Institute

```
# Load MsigDB
load("msigdb/MSigDB_v5.0_human.rda")
pathways<-msigDBentrez$c2.all.v5.0.entrez.gmt
```

First, we compare aREA and GSEA. Despite being similar in purpose, the two methods differ in their core algorithm and implementations. Notably, aREA processes the entire analysis in one go, by virtue of matrix multiplications. We expect aREA to be faster, while using more RAM than GSEA. Both GSEA and aREA are implemented in the VULCAN package. Here we calculate GSEA on the 90' vs 00' signature:

```
fname<-"results/003_pathwayComparison_GSEA_90.rda"
if(!file.exists(fname)){
  start<-Sys.time()
  results_gsea_90<-vulcan.pathways(vobj,pathways,contrast=c("t90","t0"),method="GSEA",np=1000)
  end<-Sys.time()
  time_gsea<-end-start
  save(results_gsea_90,time_gsea,file=fname)
} else {
  load(fname)
}
```

Then, we calculate aREA on the same 90' vs 00' signature:

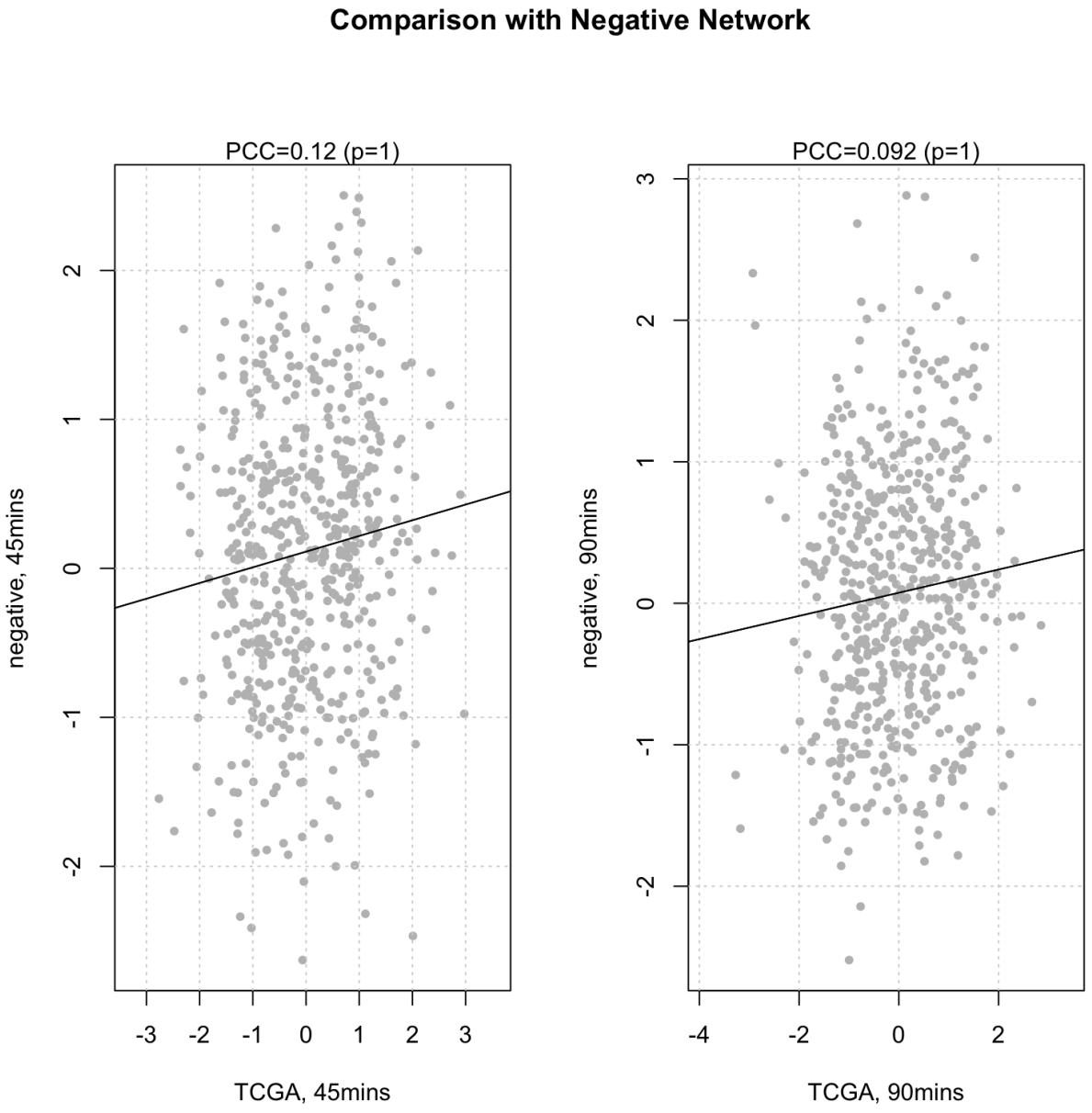


Figure 22: Comparison between activities inferred through a breast cancer TCGA dataset and the AML dataset. PCC indicates the Pearson Correlation Coefficient

```
fname<-"results/003_pathwayComparison_REA_90.rda"
if(!file.exists(fname)){
  start<-Sys.time()
  results_rea_90<-vulcan.pathways(vobj,pathways,contrast=c("t90","t0"),method="REA")[,1]
  end<-Sys.time()
  time_rea<-end-start
  save(results_rea_90,time_rea,file=fname)
} else {
  load(fname)
}
```

We then compare GSEA and aREA:

```
plot(results_rea_90,results_gsea_90,xlab="aREA enrichment score",ylab="GSEA enrichment score",pch=20,ma
     ylim=c(-max(abs(results_gsea_90)),max(abs(results_gsea_90))),col="grey")
th<-p2z(0.1)
abline(h=c(th,-th),v=c(th,-th),lty=2)
lm1<-lm(results_gsea_90~results_rea_90)
abline(lm1$coef,lwd=2)
pcc<-cor(results_rea_90,results_gsea_90,method="p")
mtext(paste0("PCC=",signif(pcc,3),", run on ",length(pathways)," pathways"))
# Estrogen
keywords<-c("ESTROGEN","ESTRADIOL","ESR1")
keypaths<-c()
for(keyword in keywords){
  keypaths<-c(keypaths,grep(keyword,names(pathways),value=TRUE))
}
keypaths<-unique(keypaths)
# Breast Cancer
keywords<-c("BREAST_CANCER")
keypaths2<-c()
for(keyword in keywords){
  keypaths2<-c(keypaths2,grep(keyword,names(pathways),value=TRUE))
}
keypaths2<-unique(keypaths2)

points(results_rea_90[keypaths],results_gsea_90[keypaths],pch=16,col="red3")
points(results_rea_90[keypaths2],results_gsea_90[keypaths2],pch=16,col="navy")
legend("topleft",pch=16,col=c("red3","navy"),cex=1,legend=c("Estrogen-Related Pathways","Breast Cancer
legend("bottomright",
       legend=c(
         paste0("REA: ",signif(time_rea,2)," ",units(time_rea)),
         paste0("GSEA: ",signif(time_gsea,2)," ",units(time_gsea))
       ),
       title="Runtime"
)
```

aREA appears to be faster. Therefore, we will use it to calculate the 45' signature as well:

```
fname<-"results/003_pathwayComparison_REA_45.rda"
if(!file.exists(fname)){
  start<-Sys.time()
  results_rea_45<-vulcan.pathways(vobj,pathways,contrast=c("t45","t0"),method="REA")[,1]
  end<-Sys.time()
  time_rea<-end-start
```

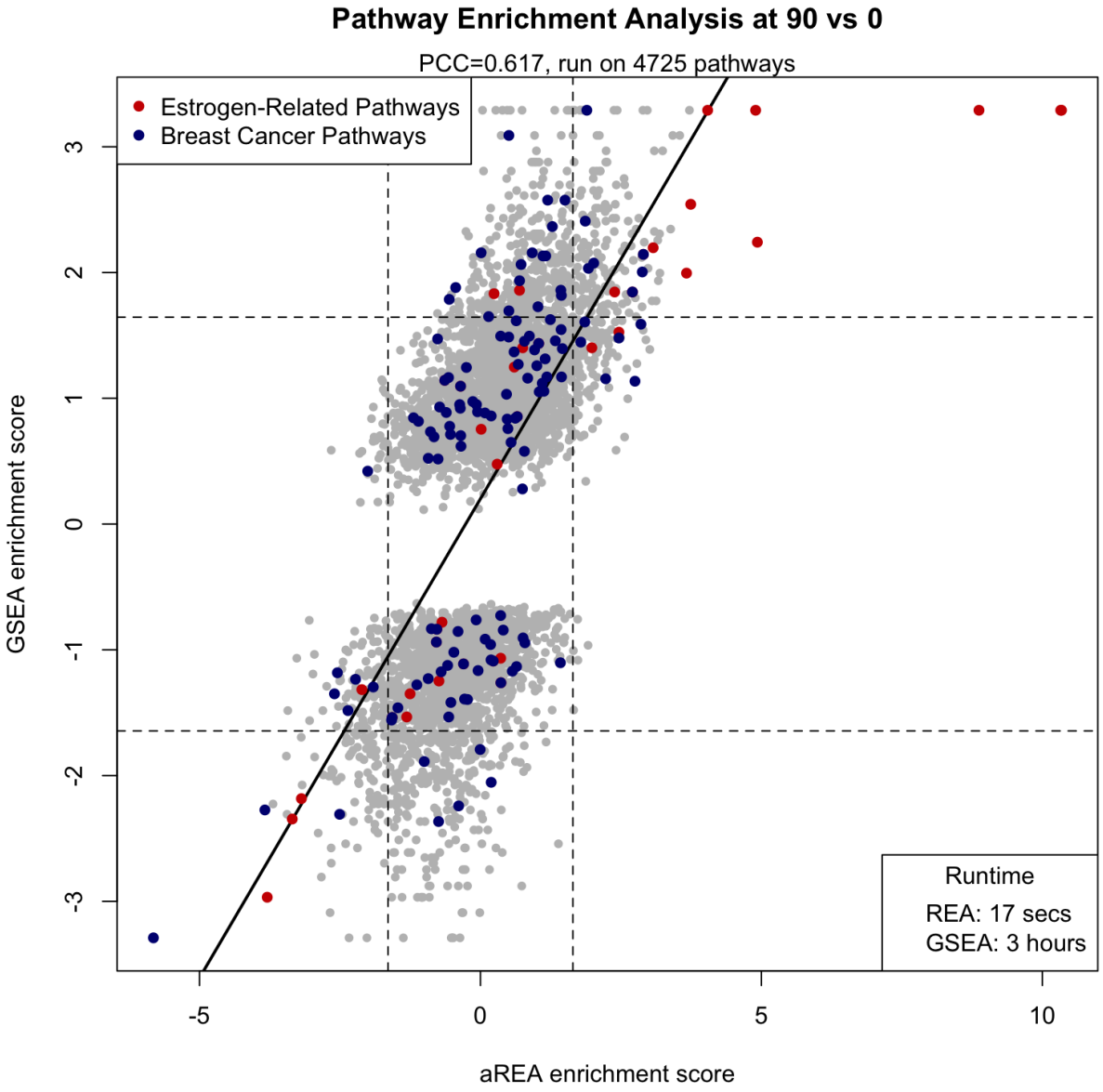


Figure 23: Comparison of GSEA and aREA on a differential binding signature

```
  save(results_rea_45,time_rea,file=fname)
} else {
  load(fname)
}
```

The results of aREA in both 90'vs00' and 45'vs00' signatures show the presence of known Estrogen-related pahtways:

```
topdn<-sort(results_rea_90)[1:20]
topup<-sort(results_rea_90,dec=TRUE)[1:20]

topdn<-cbind(topdn,z2p(topdn))
topup<-cbind(topup,z2p(topup))
colnames(topdn)<-colnames(topup)<-c("NES, 90' vs 0'","pvalue")

rownames(topdn)<-tolower(rownames(topdn))
rownames(topup)<-tolower(rownames(topup))
rownames(topdn)<-gsub("_"," ",rownames(topdn))
rownames(topup)<-gsub("_"," ",rownames(topup))
topdn[,1]<-signif(topdn[,1],3)
topup[,1]<-signif(topup[,1],3)
topdn[,2]<-signif(topdn[,2],2)
topup[,2]<-signif(topup[,2],2)

firstup <- function(x) {
  substr(x, 1, 1) <- toupper(substr(x, 1, 1))
  x
}
rownames(topdn)<-firstup(rownames(topdn))
rownames(topup)<-firstup(rownames(topup))
```

```
# Plot your table with table Grob in the library(gridExtra)
grid.newpage()
grid.table(topup)
```

```
grid.newpage()
grid.table(topdn)
```

```
topdn<-sort(results_rea_45)[1:20]
topup<-sort(results_rea_45,dec=TRUE)[1:20]

topdn<-cbind(topdn,z2p(topdn))
topup<-cbind(topup,z2p(topup))
colnames(topdn)<-colnames(topup)<-c("NES, 45' vs 0'","pvalue")

rownames(topdn)<-tolower(rownames(topdn))
rownames(topup)<-tolower(rownames(topup))
rownames(topdn)<-gsub("_"," ",rownames(topdn))
rownames(topup)<-gsub("_"," ",rownames(topup))
topdn[,1]<-signif(topdn[,1],3)
topup[,1]<-signif(topup[,1],3)
topdn[,2]<-signif(topdn[,2],2)
topup[,2]<-signif(topup[,2],2)

firstup <- function(x) {
```

| | NES, 90' vs 0' | pvalue |
|---|---|---|
| *Bhat esr1 targets not via akt1 up* | 10.3 | 4.6e-25 |
| *Bhat esr1 targets via akt1 up* | 10.3 | 5.3e-25 |
| *Dutertre estradiol response 6hr up* | 8.87 | 7.1e-19 |
| *Frasor response to estradiol up* | 4.93 | 8.3e-07 |
| *Dutertre estradiol response 24hr up* | 4.9 | 9.7e-07 |
| *Stein esr1 targets* | 4.04 | 5.3e-05 |
| *Stein esrra targets responsive to estrogen dn* | 3.74 | 0.00018 |
| *Creighton endocrine therapy resistance 1* | 3.72 | 2e-04 |
| *Stossi response to estradiol* | 3.67 | 0.00024 |
| *Zwang egf interval dn* | 3.55 | 0.00039 |
| *Creighton endocrine therapy resistance 4* | 3.42 | 0.00062 |
| *Pedrioli mir31 targets up* | 3.38 | 0.00071 |
| *Massarweh tamoxifen resistance dn* | 3.24 | 0.0012 |
| *Lein pons markers* | 3.19 | 0.0014 |
| *Reactome hs gag degradation* | 3.19 | 0.0014 |
| *Jiang tip30 targets dn* | 3.17 | 0.0015 |
| *Kegg glycerophospholipid metabolism* | 3.16 | 0.0016 |
| *Geserick tert targets dn* | 3.13 | 0.0018 |
| *Gross hypoxia via hif1a dn* | 3.09 | 0.002 |
| *Valk aml cluster 6* | 3.09 | 0.002 |

Figure 24: Table S2. aREA results: upregulated MsigDBpathways at 90mins

| | NES, 90' vs 0' | pvalue |
|---|---|---|
| *Nikolsky breast cancer 8q23 q24 amplicon* | -5.82 | 5.9e-09 |
| *Nikolsky breast cancer 1q21 amplicon* | -3.84 | 0.00012 |
| *Dutertre estradiol response 24hr dn* | -3.79 | 0.00015 |
| *Streicher lsm1 targets up* | -3.69 | 0.00022 |
| *Kenny ctnnb1 targets dn* | -3.45 | 0.00055 |
| *Reactome activation of chaperone genes by xbp1s* | -3.44 | 0.00058 |
| *Verrecchia response to tgfb1 c4* | -3.43 | 0.00061 |
| *Frasor response to estradiol dn* | -3.35 | 0.00081 |
| *Pid myc repress pathway* | -3.27 | 0.0011 |
| *Sesto response to uv c4* | -3.19 | 0.0014 |
| *Dutertre estradiol response 6hr dn* | -3.19 | 0.0014 |
| *Reactome degradation of the extracellular matrix* | -3.17 | 0.0015 |
| *Lamb ccnd1 targets* | -3.05 | 0.0023 |
| *Guo targets of irs1 and irs2* | -3.04 | 0.0024 |
| *Vakabayashi adipogenesis pparg rxra bound with h4k20me1 mark* | -2.98 | 0.0029 |
| *Woo liver cancer recurrence up* | -2.96 | 0.0031 |
| *Pid myc pathway* | -2.95 | 0.0032 |
| *Hu angiogenesis dn* | -2.89 | 0.0039 |
| *Reactome unfolded protein response* | -2.83 | 0.0046 |
| *Yamashita liver cancer with epcam dn* | -2.8 | 0.005 |

Figure 25: Table S3. aREA results: downregulated MsigDBpathways at 90mins

```
  substr(x, 1, 1) <- toupper(substr(x, 1, 1))
  x
}
rownames(topdn)<-firstup(rownames(topdn))
rownames(topup)<-firstup(rownames(topup))
```

```
# Plot your table with table Grob in the library(gridExtra)
grid.newpage()
grid.table(topup)
```

```
grid.newpage()
grid.table(topdn)
```

## 3.6 The GRHL2 Transcription Factor

Our analysis shows that the genes repressed by the Transcription Factor GRHL2 are occupied by the ER complex, using both TCGA-derived and METABRIC-derived regulatory models.

### 3.6.1 Network similarity between ESR1 and GRHL2

The following analysis highlights, with a Venn Diagram for both the METABRIC and TCGA ARACNe-derived regulatory models, the overlap between the ESR1 (Estrogen Receptor) and GRHL2 networks

```
# Load networks
load("networks/brca-tf-regulon.rda")
tcga_regulon<-regul
rm(regul)

load("networks/metabric-regulon-tfs.rda")
metabric_regulon<-regulon
rm(regulon)


# Select TFs
tf1<-"ESR1"
tf2<-"GRHL2"


par(mfrow=c(1,2))

# Venn diagram in TCGA
reg1<-tcga_regulon[[list_symbol2eg[[tf1]]]]
reg2<-tcga_regulon[[list_symbol2eg[[tf2]]]]
targets1<-names(reg1$tfmode)
targets2<-names(reg2$tfmode)
vennlist<-list()
vennlist[[tf1]]<-targets1
vennlist[[tf2]]<-targets2
venn(vennlist)
title("Network overlap in TCGA")


# Venn diagram in METABRIC
```

| | NES, 45' vs 0' | pvalue |
|---|---|---|
| *Bhat esr1 targets via akt1 up* | 10.8 | 3e-27 |
| *Bhat esr1 targets not via akt1 up* | 10.4 | 2.8e-25 |
| *Dutertre estradiol response 6hr up* | 8.1 | 5.5e-16 |
| *Frasor response to estradiol up* | 4.54 | 5.6e-06 |
| *Stein esrra targets responsive to estrogen dn* | 4.21 | 2.6e-05 |
| *Dutertre estradiol response 24hr up* | 4.15 | 3.4e-05 |
| *Stein esr1 targets* | 4.03 | 5.6e-05 |
| *Vantveer breast cancer esr1 up* | 3.84 | 0.00012 |
| *Geserick tert targets dn* | 3.69 | 0.00022 |
| *Pedrioli mir31 targets up* | 3.61 | 3e-04 |
| *Reactome glycerophospholipid biosynthesis* | 3.39 | 0.00069 |
| *Zwang egf interval dn* | 3.38 | 0.00072 |
| *Naba ecm affiliated* | 3.31 | 0.00093 |
| *Stossi response to estradiol* | 3.29 | 0.00099 |
| *Lien breast carcinoma metaplastic vs ductal dn* | 3.25 | 0.0011 |
| *Kegg glycerophospholipid metabolism* | 3.25 | 0.0012 |
| *Creighton endocrine therapy resistance 1* | 3.24 | 0.0012 |
| *Reactome hs gag degradation* | 3.21 | 0.0013 |
| *Valk aml cluster 6* | 3.2 | 0.0014 |
| *Massarweh tamoxifen resistance dn* | 3.1 | 0.0019 |

Figure 26: Table S5. aREA results: upregulated MsigDBpathways at 45mins

| | NES, 45' vs 0' | pvalue |
|---|---|---|
| *Nikolsky breast cancer 8q23 q24 amplicon* | -5.39 | 7.2e-08 |
| *Dutertre estradiol response 24hr dn* | -3.97 | 7.2e-05 |
| *Kenny ctnnb1 targets dn* | -3.89 | 1e-04 |
| *Nikolsky breast cancer 1q21 amplicon* | -3.8 | 0.00014 |
| *Streicher lsm1 targets up* | -3.7 | 0.00021 |
| *Wakabayashi adipogenesis pparg rxra bound 8d* | -3.45 | 0.00055 |
| *Boyault liver cancer subclass g23 up* | -3.16 | 0.0016 |
| *Reactome activation of chaperone genes by xbp1s* | -3.13 | 0.0017 |
| *Dutertre estradiol response 6hr dn* | -3.04 | 0.0023 |
| *Sesto response to uv c4* | -3.01 | 0.0026 |
| *Shin b cell lymphoma cluster 2* | -2.96 | 0.003 |
| *Yamashita liver cancer with epcam dn* | -2.91 | 0.0037 |
| *Ichiba graft versus host disease 35d up* | -2.82 | 0.0048 |
| *Chen hoxa5 targets 9hr up* | -2.77 | 0.0057 |
| *Kenny ctnnb1 targets up* | -2.74 | 0.0061 |
| *Kegg sulfur metabolism* | -2.72 | 0.0065 |
| *Laiho colorectal cancer serrated up* | -2.72 | 0.0066 |
| *Reactome unfolded protein response* | -2.68 | 0.0074 |
| *Heidenblad amplicon 8q24 up* | -2.67 | 0.0077 |
| *Nikolsky breast cancer 20q12 q13 amplicon* | -2.65 | 0.008 |

Figure 27: Table S6. aREA results: downregulated MsigDBpathways at 45mins

```
reg1<-metabric_regulon[[list_symbol2eg[[tf1]]]]
reg2<-metabric_regulon[[list_symbol2eg[[tf2]]]]
targets1<-names(reg1$tfmode)
targets2<-names(reg2$tfmode)
vennlist<-list()
vennlist[[tf1]]<-targets1
vennlist[[tf2]]<-targets2
venn(vennlist)
title("Network overlap in METABRIC")
```

```
par<-par.backup
```

### 3.6.2 Correlation between ESR1 and GRHL2 expression in breast cancer datasets

The following analysis assesses the inverse correlation between GRHL2 and ESR1 expressions in TCGA and METABRIC, and highlights the phenomenon for specific tumor subtypes, according to the PAM50 nomenclature (Perou et al., 2000)

```
# TCGA Color annotation
load("data/brca-expmat.rda")
load("data/brca-subtypes.rda")
expmat<-expmat[,names(subtypes)]
colors<-setNames(rep("black",length(subtypes)),subtypes)
colors[subtypes=="Basal"]<-"#FF0000AA"
colors[subtypes=="LumA"]<-"#00FFFFAA"
colors[subtypes=="LumB"]<-"#0000FFAA"
colors[subtypes=="Her2"]<-"#FFFF00AA"
colors[subtypes=="Tumor, Normal-Like"]<-"#00FF00AA"
colors[subtypes=="Normal, Tumor-Like"]<-"#00FF00AA"
colors[subtypes=="Normal"]<-"#00FF00AA"
colors_tcga<-colors
tcga_expmat<-expmat

# METABRIC Color annotation
load("data/metabric-expmat.rda")
load("data/metabric-subtypes.rda")
expmat<-expmat[,names(subtypes)]
colors<-setNames(rep("black",length(subtypes)),subtypes)
colors[subtypes=="Basal"]<-"#FF0000AA"
colors[subtypes=="LumA"]<-"#00FFFFAA"
colors[subtypes=="LumB"]<-"#0000FFAA"
colors[subtypes=="Her2"]<-"#FFFF00AA"
colors[subtypes=="Tumor, Normal-Like"]<-"#00FF00AA"
colors[subtypes=="Normal, Tumor-Like"]<-"#00FF00AA"
colors[subtypes=="Normal"]<-"#00FF00AA"
colors_metabric<-colors
metabric_expmat<-expmat

x<-tcga_expmat[list_symbol2eg[[tf1]],]
y<-tcga_expmat[list_symbol2eg[[tf2]],]
plot(x,y,xlab=tf1,ylab=tf2,pch=20,main="Correlation between GRHL2 and ESR1 expression in TCGA",col=colo
pcc<-cor(x,y)
mtext(paste0("PCC=",signif(pcc,3)))
```

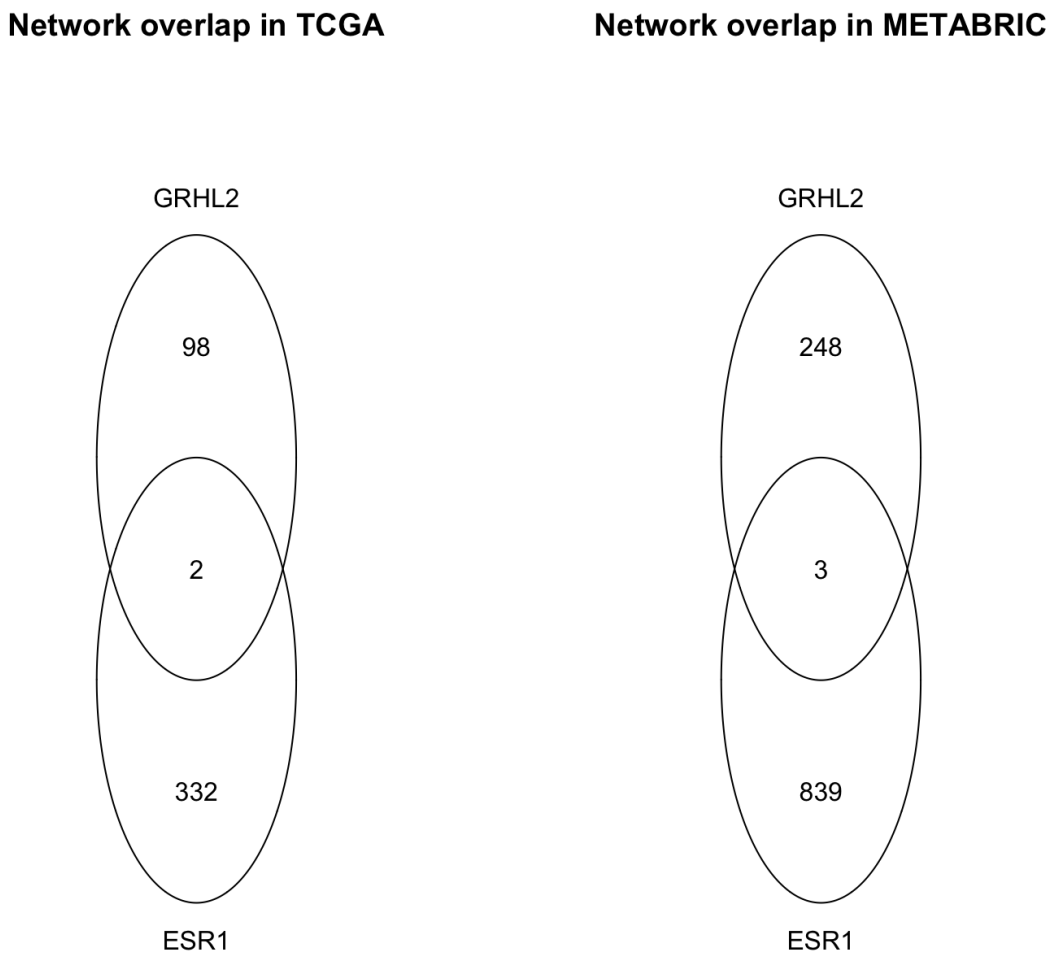


Figure 28: Overlap between ESR1 and GRH2 networks in TCGA (left) and METABRIC (right) networks

```
grid()
legend("bottomright",col=c("red","cyan","blue","yellow","green"),legend=c("Basal","LumA","LumB","Her2",
```

```
x<-metabric_expmat[list_symbol2eg[[tf1]],]
y<-metabric_expmat[list_symbol2eg[[tf2]],]
plot(x,y,xlab=tf1,ylab=tf2,pch=20,main="Correlation between GRHL2 and ESR1 expression in METABRIC",col=c
pcc<-cor(x,y)
mtext(paste0("PCC=",signif(pcc,3)))
grid()
legend("bottomright",col=c("red","cyan","blue","yellow","green"),legend=c("Basal","LumA","LumB","Her2",
```

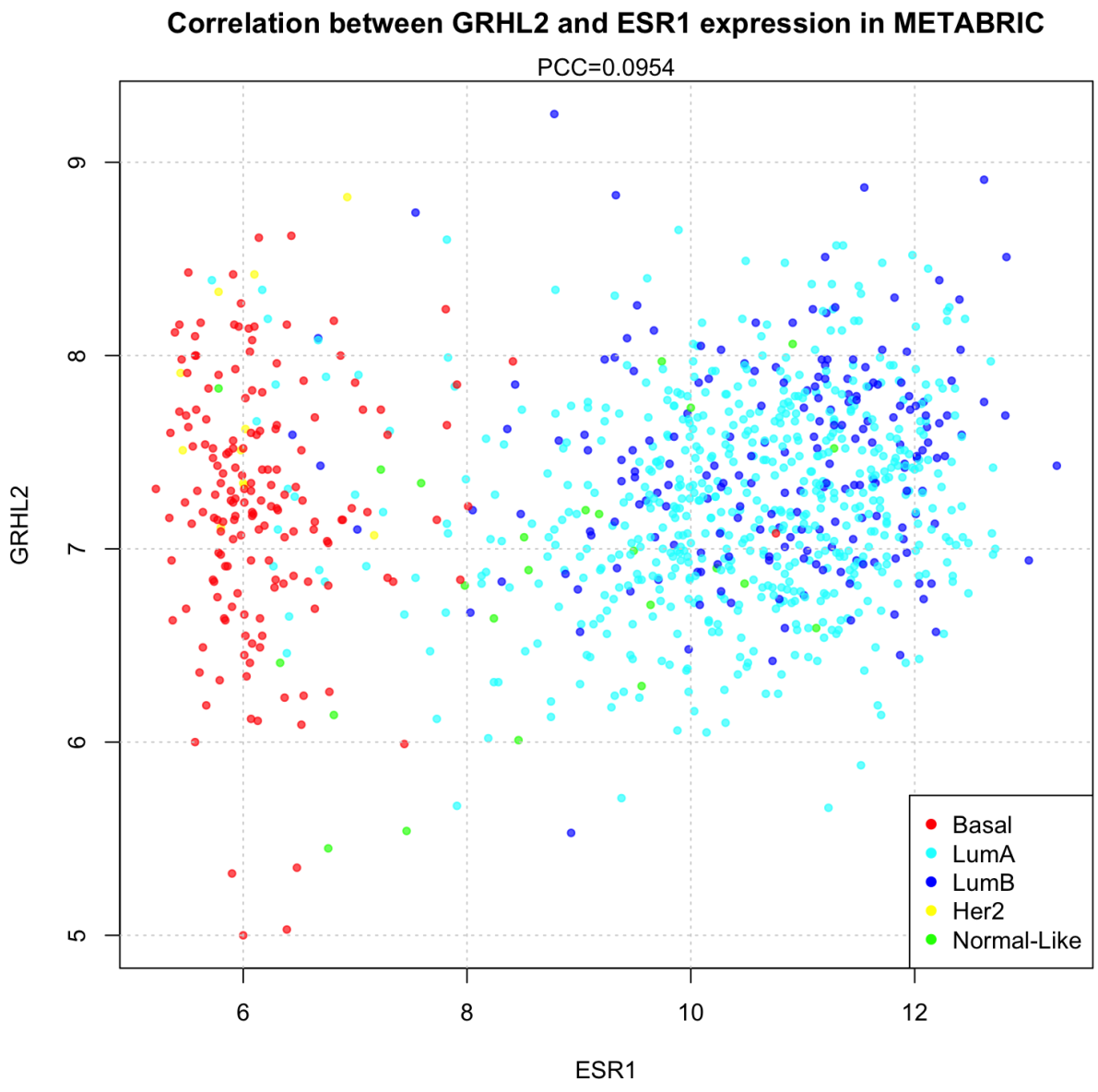

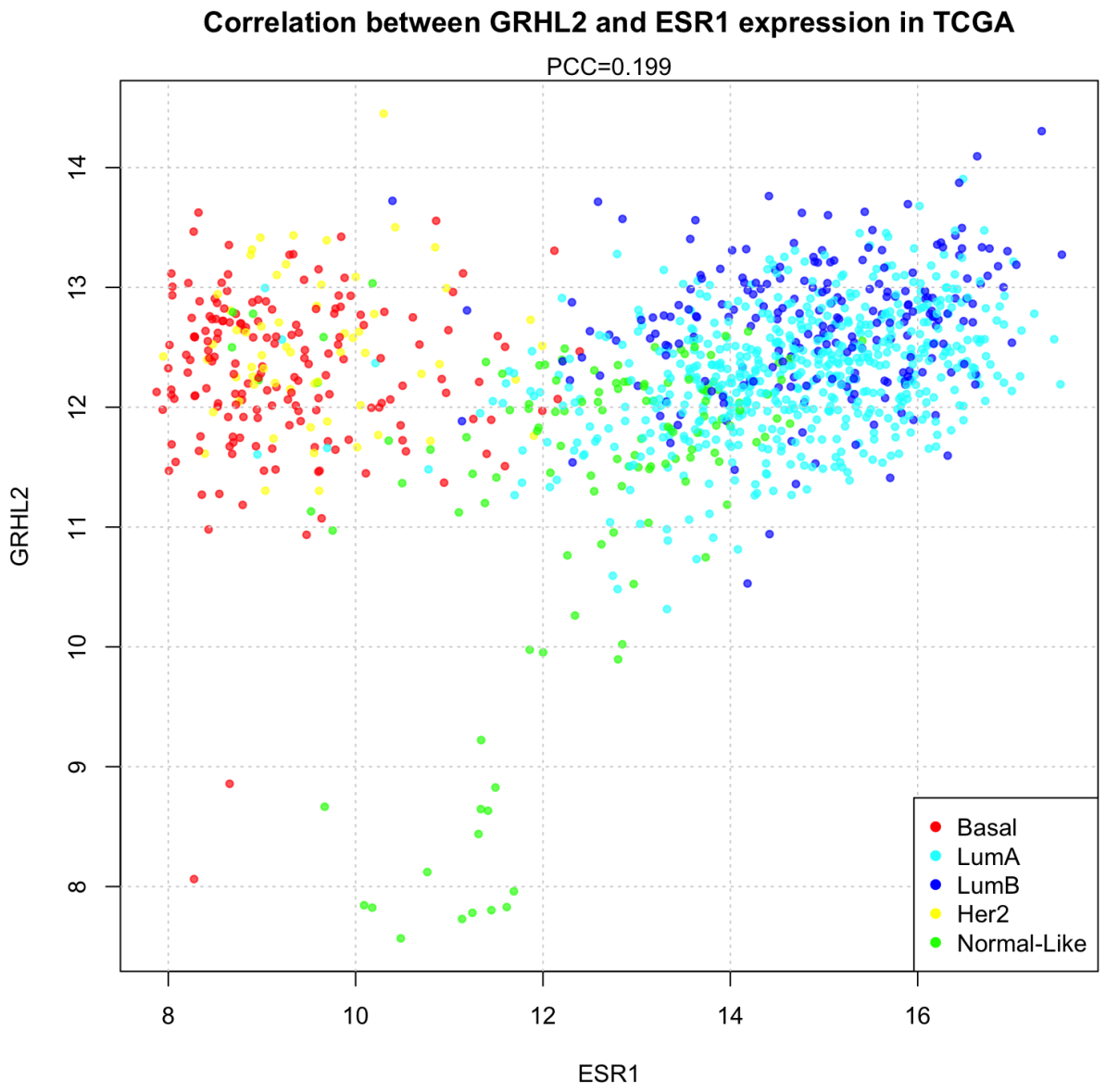


Figure 29: Correlation between GRHL2 and ESR1 expression in the TCGA breast cancer dataset

### 3.6.3 Enrichment of GRHL2 network for gene pathways

In order to analyze the GRHL2 network, we perform a simple hypergeometric test to overlap its targets with all pathways contained in hte manually curated Reactome collection of MsigDB pathways (C2 v5.0).

```
tf<-"GRHL2"
regulon<-tcga_regulon

# Pathways
wass<-load("msigdb/MSigDB_v5.0_human.rda") # "msigDBentrez" "msigDBsymbol"
ngenes<-length(unique(unlist(msigDBentrez$c2.all.v5.0.entrez.gmt)))

### Hypergeometric test implementation
# Hypergeometric enrichment function
enrich<-function(list1,list2,pathway){
  l1<-length(list1)
  l2<-length(list2)
  overlap<-length(intersect(list1,list2))
  q<-overlap-1
  m<-l1
  n<-ngenes-l1
  k<-l2
  p<-phyper(q,m,n,k,lower.tail=FALSE,log.p=FALSE)
  return(p)
}

# Fisher P integration function
fisherp<-function (ps) {
  Xsq <- -2 * sum(log(ps))
  p.val <- pchisq(Xsq, df = 2 * length(ps), lower.tail = FALSE)
  return(p.val)
}

# Regulon vs. pathway
networkUP<-names(regulon[[s2e(tf)]]$tfmode)[regulon[[s2e(tf)]]$tfmode>=0]
networkDN<-names(regulon[[s2e(tf)]]$tfmode)[regulon[[s2e(tf)]]$tfmode<0]

### Enrichment Loop C2
fname<-paste0("results/004_results_hypergeom_C2_",tf,".rda")
#pathways<-msigDBentrez$c2.cp.biocarta.v5.0.entrez.gmt
pathways<-msigDBentrez$c2.all.v5.0.entrez.gmt
if(!file.exists(fname)){
  results<-list()
  ntests<-0
  tfs<-names(regulon)
  pb<-txtProgressBar(0,length(tfs),style=3)
  pbi<-1
  for(tf in tfs){
    plimit<-0.05
    setTxtProgressBar(pb,pbi)
    sublistUP<-setNames(rep(NA,length(pathways)),names(pathways))
    sublistDN<-setNames(rep(NA,length(pathways)),names(pathways))
    i<-1
    for(pathway in pathways){
```

```
      networkUP<-names(regulon[[tf]]$tfmode)[regulon[[tf]]$tfmode>=0]
      networkDN<-names(regulon[[tf]]$tfmode)[regulon[[tf]]$tfmode<0]
      pUP<-enrich(networkUP,pathway,ngenes)
      pDN<-enrich(networkDN,pathway,ngenes)
      ntests<-ntests+1
      sublistUP[i]<-pUP
      sublistDN[i]<-pDN
      i<-i+1
    }
    sublistUP<-sublistUP[sublistUP<=plimit]
    sublistDN<-sublistDN[sublistDN<=plimit]
    results[[tf]]<-list(up=sublistUP,dn=sublistDN)
    pbi<-pbi+1
  }
  save(results,ntests,file=fname)
} else {
  load(fname)
}

### Now, plotting
# Set parameters
topn<-20
subsetting<-"REACTOME_"

## Start plot
# Prepare input results
res<-results[[s2e(tf)]]

# Correct pvalues and integrate
resUP<-p.adjust(res$up,method="none",n=ntests) # convert to bonferroni when deploying
resDN<-p.adjust(res$dn,method="none",n=ntests)
union<-union(names(resUP),names(resDN))
tmptable<-cbind(resUP[union],resDN[union])
tmptable[is.na(tmptable)]<-1
rownames(tmptable)<-union
integrated<-apply(tmptable,1,fisherp)

# Optional subsetting
toshow<-names(sort(integrated))
toshow<-toshow[grep(subsetting,toshow)]
toshow<-toshow[1:topn]


# Prepare input
resUP<--log10(res$up[toshow])
resDN<--log10(res$dn[toshow])
names(resUP)<-toshow
names(resDN)<-toshow
resUP[is.na(resUP)]<-0
resDN[is.na(resDN)]<-0
```

```
# Canvas
upperlim<-ceiling(max(c(resUP,resDN)))
par(mar=c(0,0,0,0))
```

```r
plot(0,col="white",xlim=c(-10,12),ylim=c(-2,topn+3),xaxt="n",yaxt="n",type="n",frame.plot=FALSE,
     xlab="",ylab="",xaxs="i",yaxs="i")
# text(c(0:10),c(0:10),labels=c(0:10),pos=1,offset=0)
# text(c(1,2,2,1),c(1,2,1,2),labels=c("1_1","2_2","2_1","1_2"),pos=1,offset=0)

# Title
regsize<-length(regulon[[s2e(tf)]]$tfmode)
text(5,topn+2.8,paste0("Pathway enrichment of ",tf," regulon"),pos=1,offset=0,font=2)
text(5,topn+2,paste0("regulon size: ",regsize),pos=1,offset=0,font=3,cex=0.8)

# Axis horizontal
abline(h=0)
segments(0:10,0,0:10,-0.3)
text(5,-1,"Hypergeometric -log10(pvalue)",pos=1,offset=0)
text(1:10,-0.5,cex=0.7,
     labels=round(signif(seq(0,upperlim,length.out=11)),2)[2:11]
)

# Axis vertical
abline(v=0)
#segments(0,topn:0,-0.3,topn:0)

# Significance line
abline(v=(-log10(0.05)/upperlim)*10,lty=2)

# Bars
for(i in topn:1){
  upval<-(resUP[i]/upperlim)*10
  dnval<-(resDN[i]/upperlim)*10
  rect(0,i+0.25,upval,i,col="salmon")
  rect(0,i,dnval,i-0.25,col="cornflowerblue")
}


# Pathway labels
pathlabels<-gsub(subsetting,"",toshow)
pathlabels<-tolower(pathlabels)
pathlabels<-gsub("_"," ",pathlabels)
for(i in topn:1){
  text(0,i,pathlabels[i],pos=2,offset=0.1,cex=0.8)
}


# Percentage of pathway overlap
r<-names(regulon[[s2e(tf)]]$tfmode)
percs<-c()
for(i in topn:1){
  p<-pathways[[toshow[i]]]
  intrsct<-intersect(p,r)
  perc<-100*length(intrsct)/length(p)
  percs<-c(percs,perc)
}
names(percs)<-rev(toshow)
```

```
spercs<-(percs/max(percs))*4
lines(spercs,topn:1,lty=1,lwd=2)

# Ruler of pathway overlap
segments(0,topn+1,4,topn+1)
text(2,topn+1.5,pos=1,offset=0,font=3,cex=0.7,labels="% pathway")
segments(0:4,topn+1,0:4,topn+0.8)
text(1:4,topn+0.65,cex=0.5,
     labels=round(seq(0,max(percs),length.out=5),1)[2:5]
)
```

```
par<-par.backup
```

## 3.7 Comparing VULCAN results with other tools and approaches

Our VULCAN results were obtained using independent gene regulatory models and multiple replicates to generate ER-response signatures.

### 3.7.1 VULCAN and qPLEX-RIME

We set to testing the performance of VULCAN against a complementary experimental approach called qPLEX-RIME (Holding et al., submitted), which aims at identifyin interactors of ER within the ER-chromatin complex at estrogen-responding promoters. We have QRIME results for MCF7 cells treated with estradiol at both 45 and 90 minutes, the same experimental setup for the VULCAN input dataset.

```
# Load imported vulcan object
load("results/001_vobj.rda")

#### Vulcan Analysis (multiple networks)
## TCGA network, ARACNe with proteomics centroids
load("aracne/regulon-tcga-centroids.rda")
tcga_regulon<-regulon
rm(regulon)

## METABRIC network, ARACNe with proteomics centroids
load("aracne/regulon-metabric-centroids.rda")
metabric_regulon<-regulon
rm(regulon)

## Specify contrast and network
fname<-"results/005_vobj_networks.rda"
list_eg2symbol<-as.list(org.Hs.egSYMBOL[mappedkeys(org.Hs.egSYMBOL)])
if(!file.exists(fname)){
  vobj_tcga_90<-vulcan(vobj,network=tcga_regulon,contrast=c("t90","t0"),annotation=list_eg2symbol)
  vobj_tcga_45<-vulcan(vobj,network=tcga_regulon,contrast=c("t45","t0"),annotation=list_eg2symbol)
  vobj_metabric_90<-vulcan(vobj,network=metabric_regulon,contrast=c("t90","t0"),annotation=list_eg2symbo
  vobj_metabric_45<-vulcan(vobj,network=metabric_regulon,contrast=c("t45","t0"),annotation=list_eg2symbo
  save(
    vobj_tcga_90,
    vobj_tcga_45,
    vobj_metabric_90,
    vobj_metabric_45,
    file=fname
```

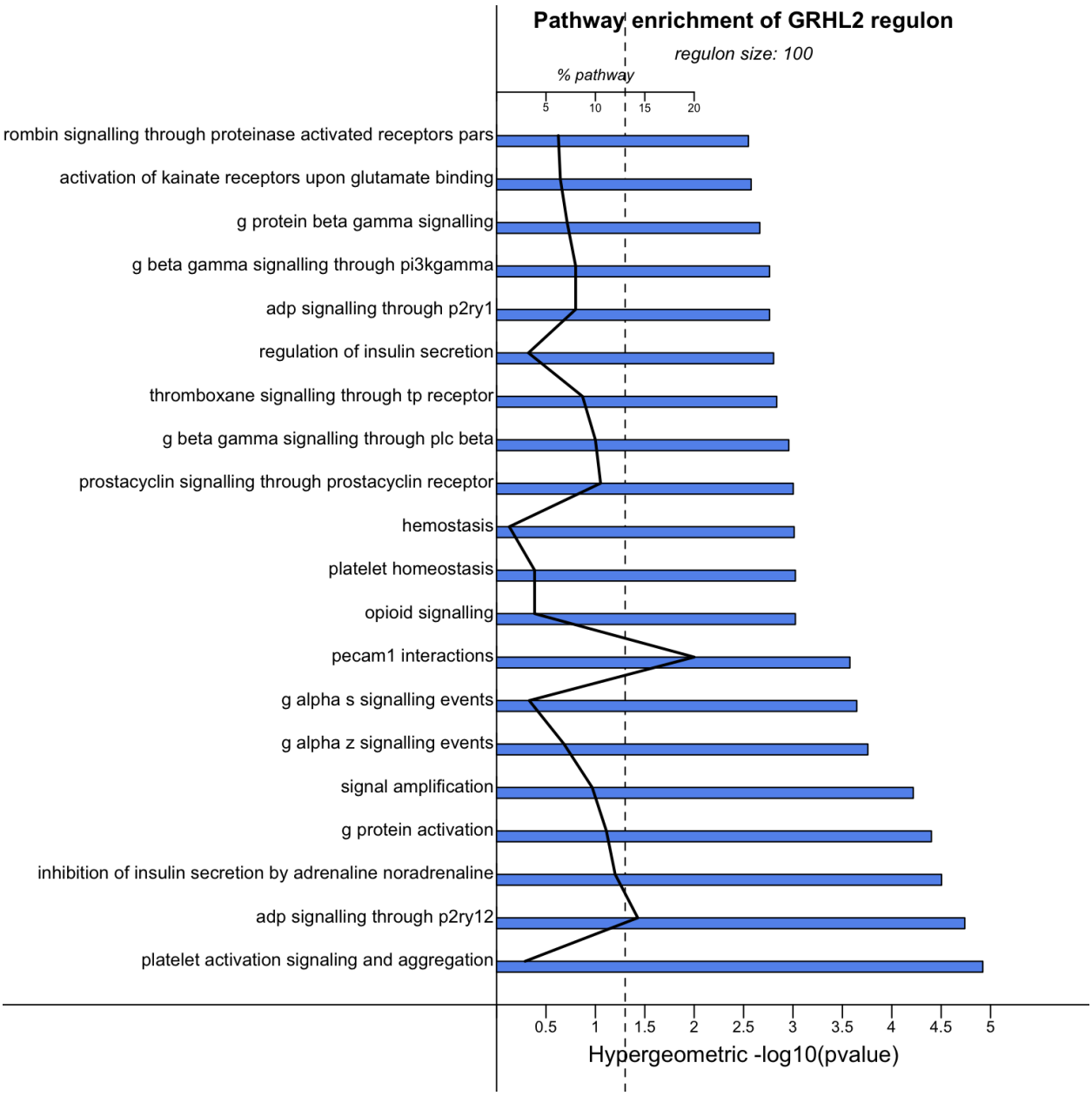


Figure 30: Pathways most significantly overlapping the GRHL2 network

```
  )
} else {
  load(fname)
}

# Merge proteomics and TF aracne results
vobj2_tcga_90<-vobj_tcga_90
vobj2_tcga_45<-vobj_tcga_45
vobj2_metabric_90<-vobj_metabric_90
vobj2_metabric_45<-vobj_metabric_45

fname<-"results/002_vobj_networks.rda"
load(fname)
vobj_tcga_90$mrs<-rbind(vobj_tcga_90$mrs,vobj2_tcga_90$mrs[setdiff(rownames(vobj2_tcga_90),rownames(vob
vobj_tcga_45$mrs<-rbind(vobj_tcga_45$mrs,vobj2_tcga_45$mrs[setdiff(rownames(vobj2_tcga_45),rownames(vob
vobj_metabric_90$mrs<-rbind(vobj_metabric_90$mrs,vobj2_metabric_90$mrs[setdiff(rownames(vobj2_metabric_
vobj_metabric_45$mrs<-rbind(vobj_metabric_45$mrs,vobj2_metabric_45$mrs[setdiff(rownames(vobj2_metabric_

# Metabric Results
metabric_90=vobj_metabric_90$mrs[,"pvalue"]
metabric_45=vobj_metabric_45$mrs[,"pvalue"]
tfs<-names(metabric_45)
metabricmat<-cbind(metabric_45[tfs],metabric_90[tfs])
colnames(metabricmat)<-c("T45","T90")

# TCGA Results
tcga_90=vobj_tcga_90$mrs[,"pvalue"]
tcga_45=vobj_tcga_45$mrs[,"pvalue"]
tfs<-names(tcga_45)
tcgamat<-cbind(tcga_45[tfs],tcga_90[tfs])
colnames(tcgamat)<-c("T45","T90")


## QRIME results
raw45<-read.delim("qrime/Results/ER_45min_vs_ER_0minExcludeMissingValues_QuantileNormalization.txt",as.
qrime45<-setNames(raw45$P.Value,raw45$Gene)
qrime45<-qrime45[!is.na(qrime45)]

raw90<-read.delim("qrime/Results/ER_90min_vs_ER_0minExcludeMissingValues_QuantileNormalization.txt",as.
qrime90<-setNames(raw90$P.Value,raw90$Gene)
qrime90<-qrime90[!is.na(qrime90)]
```

Here, we will compare ER-binding pvalues obtained with QRIME, with the VULCAN results aimed at identifying TFs upstream of the observed differential promoter binding.

```
### Comparisons, pvalues
par(mfrow=c(2,2))
# TCGA 45
main<-"TCGA network, 45 mins"
common<-intersect(rownames(tcgamat),names(qrime45))
x<-qrime45[common]
x<--log10(x)
y<-tcgamat[common,"T45"]
y<--log10(y)
```

```r
plot(x,y,pch=20,xlab="-log10(p) QRIME",ylab="-log10(p) VULCAN",col="grey",main=main,
     xlim=c(min(x)-max(x)*0.3,max(x)*1.1),
     ylim=c(min(y)-max(y)*0.2,max(y)*1.1)
)
topx<-names(sort(x,dec=TRUE))[1:10]
topy<-names(sort(y,dec=TRUE))[1:10]
top<-union(topx,topy)
textplot2(x[top],y[top],words=top,new=FALSE)
grid()

# TCGA 90
main<-"TCGA network, 90 mins"
common<-intersect(rownames(tcgamat),names(qrime90))
x<-qrime90[common]
x<--log10(x)
y<-tcgamat[common,"T90"]
y<--log10(y)
plot(x,y,pch=20,xlab="-log10(p) QRIME",ylab="-log10(p) VULCAN",col="grey",main=main,
     xlim=c(min(x)-max(x)*0.3,max(x)*1.1),
     ylim=c(min(y)-max(y)*0.2,max(y)*1.1)
)
topx<-names(sort(x,dec=TRUE))[1:10]
topy<-names(sort(y,dec=TRUE))[1:10]
top<-union(topx,topy)
textplot2(x[top],y[top],words=top,new=FALSE)
grid()


# METABRIC 45
main<-"METABRIC network, 45 mins"
common<-intersect(rownames(metabricmat),names(qrime45))
x<-qrime45[common]
x<--log10(x)
y<-metabricmat[common,"T45"]
y<--log10(y)
plot(x,y,pch=20,xlab="-log10(p) QRIME",ylab="-log10(p) VULCAN",col="grey",main=main,
     xlim=c(min(x)-max(x)*0.3,max(x)*1.1),
     ylim=c(min(y)-max(y)*0.2,max(y)*1.1)
)
topx<-names(sort(x,dec=TRUE))[1:10]
topy<-names(sort(y,dec=TRUE))[1:10]
top<-union(topx,topy)
textplot2(x[top],y[top],words=top,new=FALSE)
grid()

# METABRIC 90
main<-"METABRIC network, 90 mins"
common<-intersect(rownames(metabricmat),names(qrime90))
x<-qrime90[common]
x<--log10(x)
y<-metabricmat[common,"T90"]
y<--log10(y)
plot(x,y,pch=20,xlab="-log10(p) QRIME",ylab="-log10(p) VULCAN",col="grey",main=main,
```

```r
     xlim=c(min(x)-max(x)*0.3,max(x)*1.1),
     ylim=c(min(y)-max(y)*0.2,max(y)*1.1)
)
topx<-names(sort(x,dec=TRUE))[1:10]
topy<-names(sort(y,dec=TRUE))[1:10]
top<-union(topx,topy)
textplot2(x[top],y[top],words=top,new=FALSE)
grid()
```

```r
# TCGA Results
tcganes_90=vobj_tcga_90$mrs[,"NES"]
tcganes_45=vobj_tcga_45$mrs[,"NES"]
tfs<-names(tcganes_45)
tcganesmat<-cbind(tcganes_45[tfs],tcganes_90[tfs])
colnames(tcganesmat)<-c("T45","T90")

# METABRIC Results
metabricnes_90=vobj_metabric_90$mrs[,"NES"]
metabricnes_45=vobj_metabric_45$mrs[,"NES"]
tfs<-names(metabricnes_45)
metabricnesmat<-cbind(metabricnes_45[tfs],metabricnes_90[tfs])
colnames(metabricnesmat)<-c("T45","T90")




par(mfrow=c(2,2))
# TCGA 45
main<-"TCGA network, 45 mins"
common<-intersect(rownames(tcganesmat),names(qrime45))
x<-qrime45[common]
x<--log10(x)
y<-tcganesmat[common,"T45"]
plot(x,y,pch=20,xlab="-log10(p) QRIME",ylab="NES VULCAN",col="grey",main=main,
     xlim=c(min(x)-max(x)*0.3,max(x)*1.1),
     ylim=c(min(y)-max(y)*0.2,max(y)*1.1)
)
topx<-names(sort(x,dec=TRUE))[1:10]
topy<-names(sort(y,dec=TRUE))[1:10]
top<-union(topx,topy)
textplot2(x[top],y[top],words=top,new=FALSE)
abline(h=c(-p2z(0.05),p2z(0.05)),lty=3)
grid()

# TCGA 90
main<-"TCGA network, 90 mins"
common<-intersect(rownames(tcganesmat),names(qrime90))
x<-qrime90[common]
x<--log10(x)
y<-tcganesmat[common,"T90"]
plot(x,y,pch=20,xlab="-log10(p) QRIME",ylab="NES VULCAN",col="grey",main=main,
     xlim=c(min(x)-max(x)*0.3,max(x)*1.1),
     ylim=c(min(y)-max(y)*0.2,max(y)*1.1)
)
```

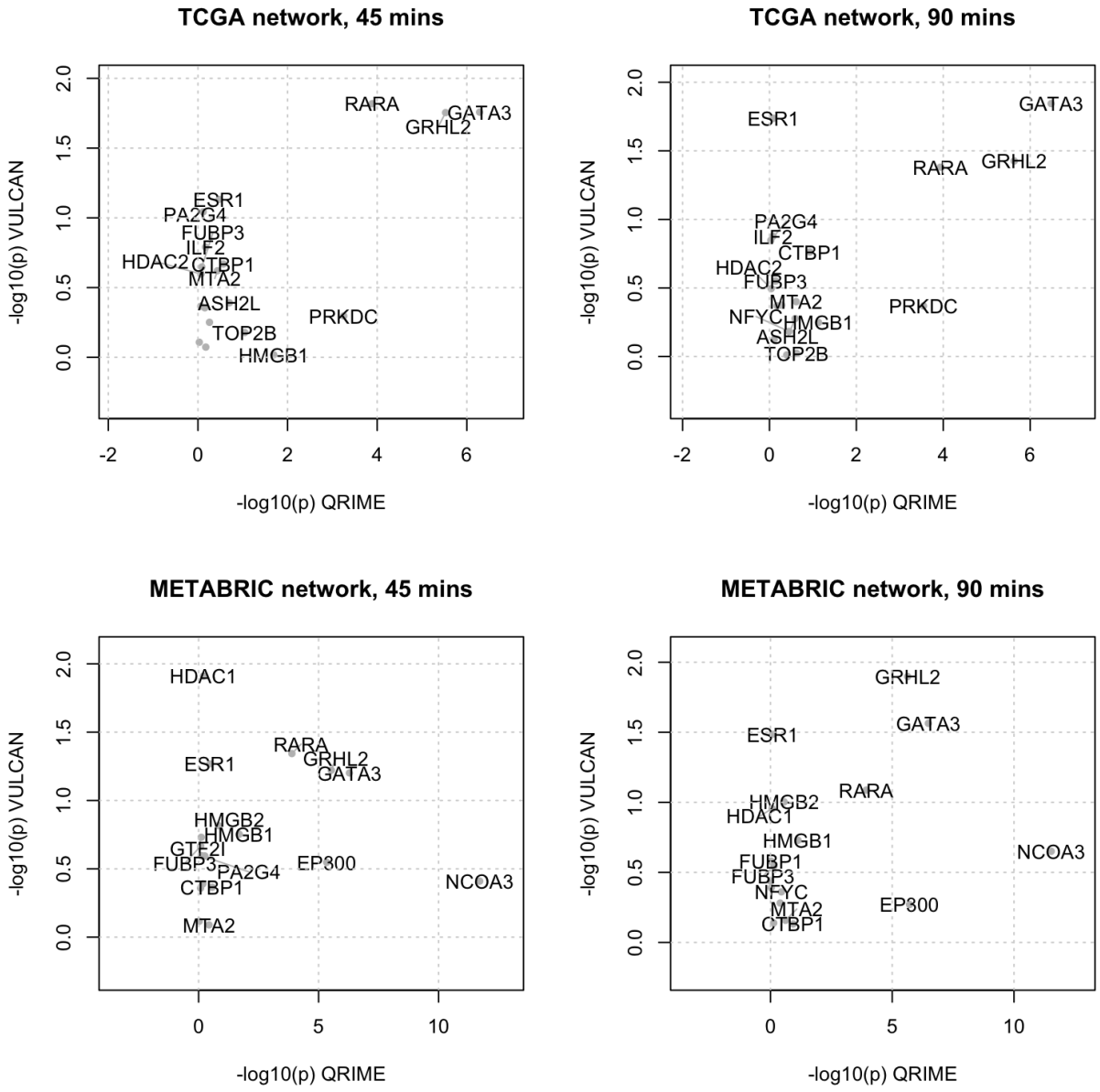


Figure 31: Comparison of significance between the QRIME method (x-axis) and the VULCAN method (y-axis) at two time points using two regulatory networks for VULCAN

```r
topx<-names(sort(x,dec=TRUE))[1:10]
topy<-names(sort(y,dec=TRUE))[1:10]
top<-union(topx,topy)
textplot2(x[top],y[top],words=top,new=FALSE)
abline(h=c(-p2z(0.05),p2z(0.05)),lty=3)
grid()


# METABRIC 45
main<-"METABRIC network, 45 mins"
common<-intersect(rownames(metabricnesmat),names(qrime45))
x<-qrime45[common]
x<--log10(x)
y<-metabricnesmat[common,"T45"]
plot(x,y,pch=20,xlab="-log10(p) QRIME",ylab="NES VULCAN",col="grey",main=main,
     xlim=c(min(x)-max(x)*0.3,max(x)*1.1),
     ylim=c(min(y)-max(y)*0.2,max(y)*1.1)
)
topx<-names(sort(x,dec=TRUE))[1:10]
topy<-names(sort(y,dec=TRUE))[1:10]
top<-union(topx,topy)
textplot2(x[top],y[top],words=top,new=FALSE)
abline(h=c(-p2z(0.05),p2z(0.05)),lty=3)
grid()

# METABRIC 90
main<-"METABRIC network, 90 mins"
common<-intersect(rownames(metabricnesmat),names(qrime90))
x<-qrime90[common]
x<--log10(x)
y<-metabricnesmat[common,"T90"]
plot(x,y,pch=20,xlab="-log10(p) QRIME",ylab="NES VULCAN",col="grey",main=main,
     xlim=c(min(x)-max(x)*0.3,max(x)*1.1),
     ylim=c(min(y)-max(y)*0.2,max(y)*1.1)
)
topx<-names(sort(x,dec=TRUE))[1:10]
topy<-names(sort(y,dec=TRUE))[1:10]
top<-union(topx,topy)
textplot2(x[top],y[top],words=top,new=FALSE)
abline(h=c(-p2z(0.05),p2z(0.05)),lty=3)
grid()
```

### 3.7.2 Comparing Mutual Information and Partial Correlation networks

As shown before in literature, partial correlation and mutual information networks are highly similar. While requiring a mutual information network due to the VIPER engine used by the VULCAN pipeline, we set out here to compare Mutual Information networks with partial correlation ones, using different correlation thresholds.

```r
filename<-"results/006_comparison1_aracne.rda"
if(!file.exists(filename)){
  # Load aracne network
  load("aracne/regulon-tcga-centroids.rda")
```

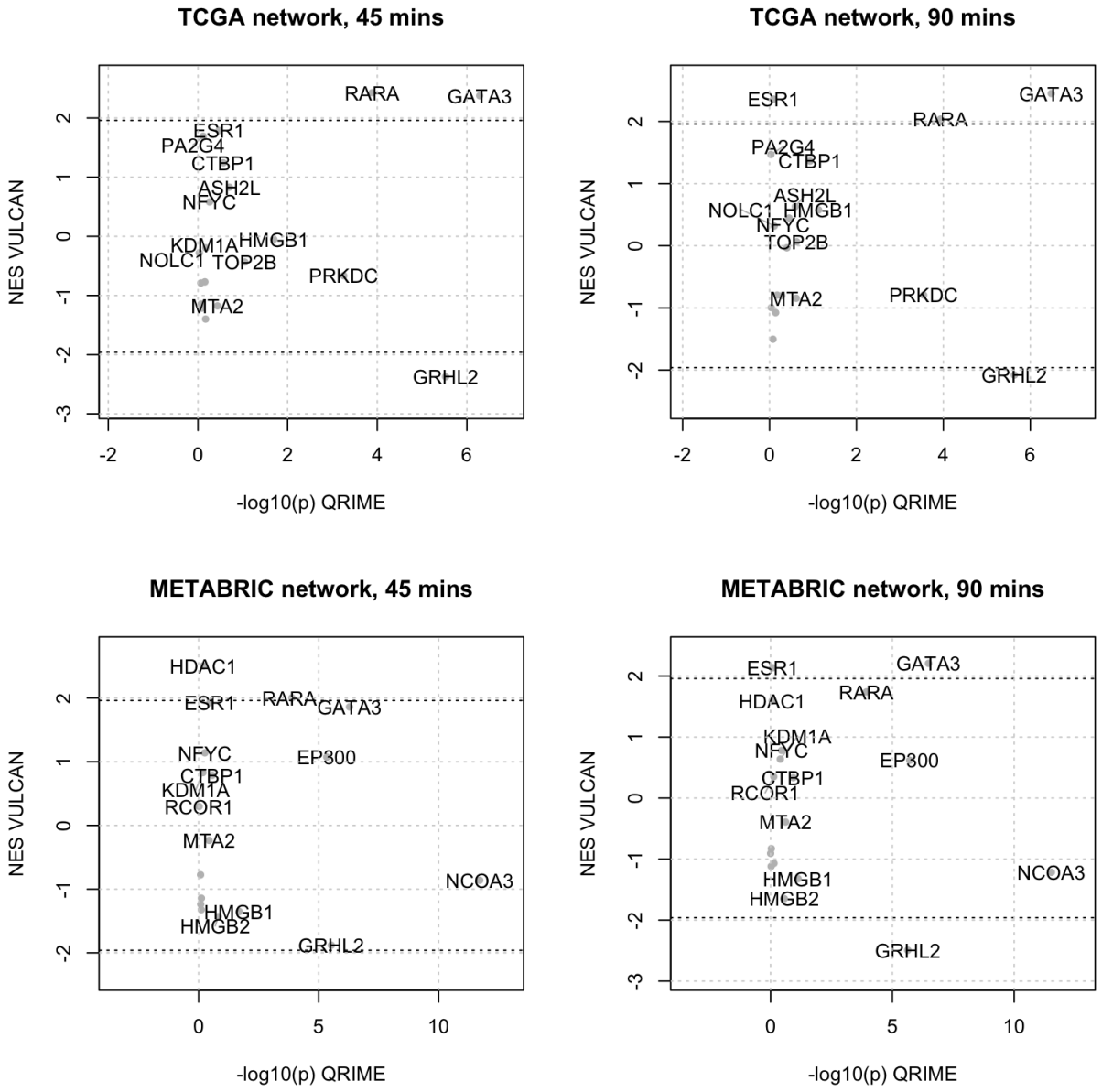


Figure 32: Comparison of Normalized Enrichment Score between the QRIME method (x-axis) and the VULCAN method (y-axis) at two time points using two regulatory networks for VULCAN

```r
# Load expression matrix
expmat<-as.matrix(read.delim("aracne/tcga-expmat.dat",as.is=TRUE,row.names=1))


### Better pipeline
tfs<-names(regulon)
genes<-rownames(expmat)


# Remove zero-SD genes
sds<-apply(expmat,1,sd)
expmat<-expmat[sds>=0.5,]
dim(expmat)



# Build Covariance Matrix
pcormat<-cov(t(expmat))
# Build pcormat
pcormat<-cor2pcor(pcormat)
rownames(pcormat)<-colnames(pcormat)<-rownames(expmat)


# Keep only TFs
diag(pcormat)<-0
tfs<-intersect(tfs,rownames(pcormat))
pcormat<-pcormat[tfs,]

# Transform my network into a vector of edges
myedges<-c()
for(centroid in names(regulon)){
  targets<-names(regulon[[centroid]]$tfmode)
  newedges<-paste0(centroid,"___",targets)
  myedges<-c(myedges,newedges)
}
length(myedges) # 268394

### Loop over rs
jis<-c()
nedges<-c()
rs<-seq(0.05,0.4,by=0.025)
for(r in rs){
  # Transform networks into vectors of edges
  matches<-which(abs(pcormat)>=r,arr.ind=TRUE)
  pcoredges<-paste0(rownames(pcormat)[matches[,1]],"___",colnames(pcormat)[matches[,2]])
  nedges<-c(nedges,nrow(matches))
  # Calculate Jaccard
  ji<-length(intersect(myedges,pcoredges))/length(union(myedges,pcoredges))
  jis<-c(jis,ji)
}
names(jis)<-names(nedges)<-rs
```

```r
  # Generate random network vectors
  random<-list()
  for(ii in 1:length(rs)){
    n<-nedges[ii]
    message("Doing ",rs[ii])
    pb<-txtProgressBar(0,1000,style=3)
    randomjis<-c()
    for(i in 1:1000){
      x<-sample(1:nrow(pcormat),n,replace=TRUE)
      y<-sample(1:ncol(pcormat),n,replace=TRUE)
      matches<-cbind(x,y)
      pcoredges<-paste0(rownames(pcormat)[matches[,1]],"___",colnames(pcormat)[matches[,2]])
      ji<-length(intersect(myedges,pcoredges))/length(union(myedges,pcoredges))
      randomjis<-c(randomjis,ji)
      setTxtProgressBar(pb,i)
    }
    random[[ii]]<-randomjis
  }
  names(random)<-as.character(rs)

  save(jis,rs,nedges,random,file=filename)

} else {
  load(filename)
}
```

We generate several partial correlation networks using the same input as the ARACNe network used by VULCAN (the TCGA breast cancer dataset). We tested the overlap of every partial correlation network with the ARACNe network using the Jaccard Index (JI) criterion.

```r
par(mfrow=c(1,1))
bp<-barplot(jis,xlab="pcor r",ylab="JI",ylim=c(0,max(jis)*1.1))
text(bp[,1],jis,labels=kmgformat(nedges),pos=3,cex=0.7)
mtext("Number of overlapping edges between Pcor and Aracne",cex=0.8)
```

Finally, we show how the Jaccard Index between partial correlation networks and the ARACNe network is always significantly higher than expected by selecting random network edges.

```r
par(mfrow=c(5,3))
for(i in 1:length(random)){
  dd<-density(random[[i]])
  plot(dd,xlim=c(min(random[[i]]),jis[i]*1.1),main=paste0("r=",rs[i]),xlab="Jaccard Index",lwd=2)
  arrows(jis[i],max(dd$y),jis[i],0,lwd=2)
}
```

### 3.7.3 Comparing alternative methods for target enrichment analysis

We developed three independent methods to compare VULCAN with. The first is common, the second is simple but crude, and the third is also common but too stringent.

```r
### Classic vulcan result
# vobj_tcga_90<-vulcan(vobj,network=tcga_regulon,contrast=c("t90","t0"),annotation=list_eg2symbol)
wass<-load("results/002_vobj_networks.rda")
```

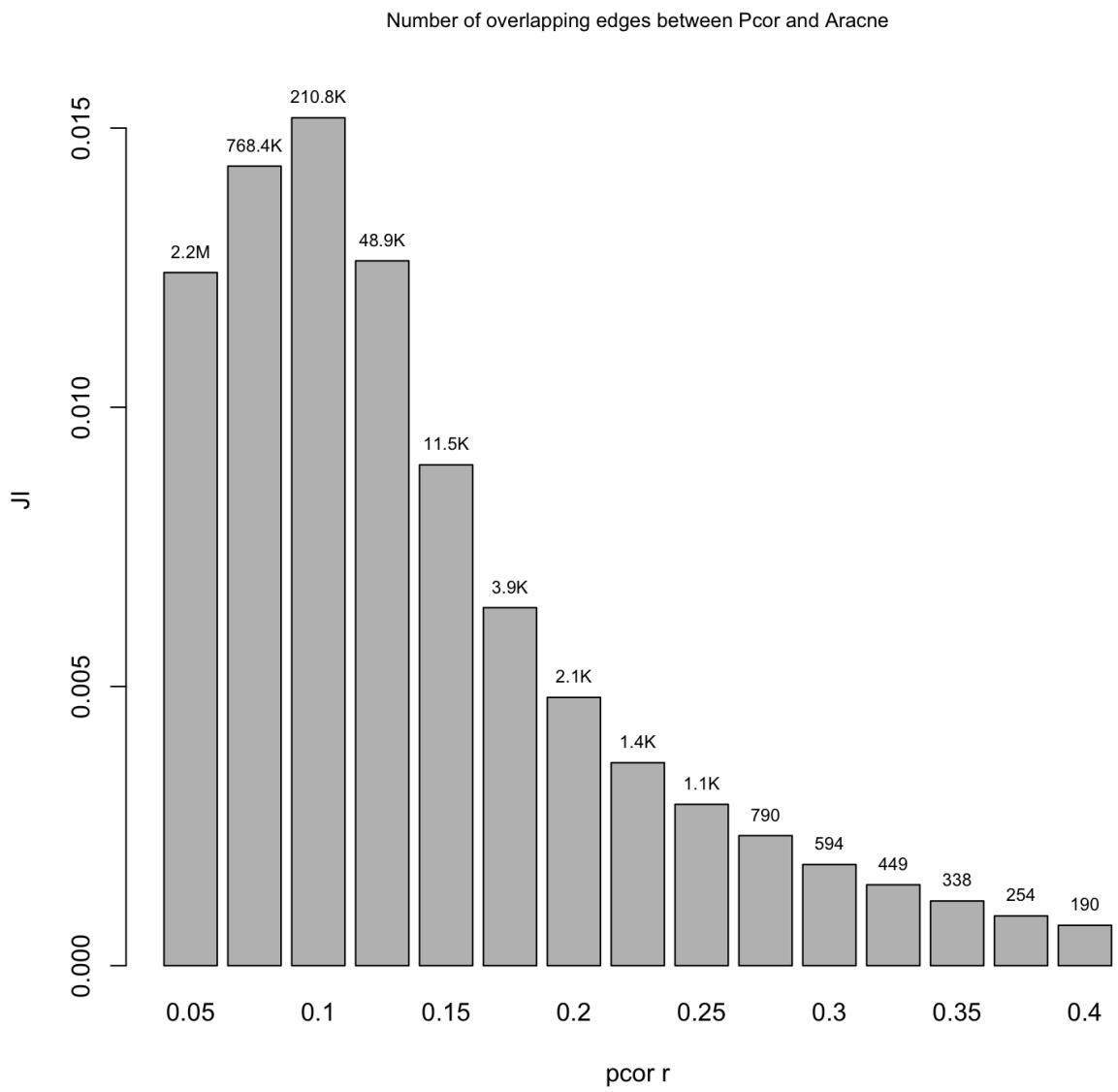


Figure 33: Sheer number of overlapping edges at different Pcor thresholds

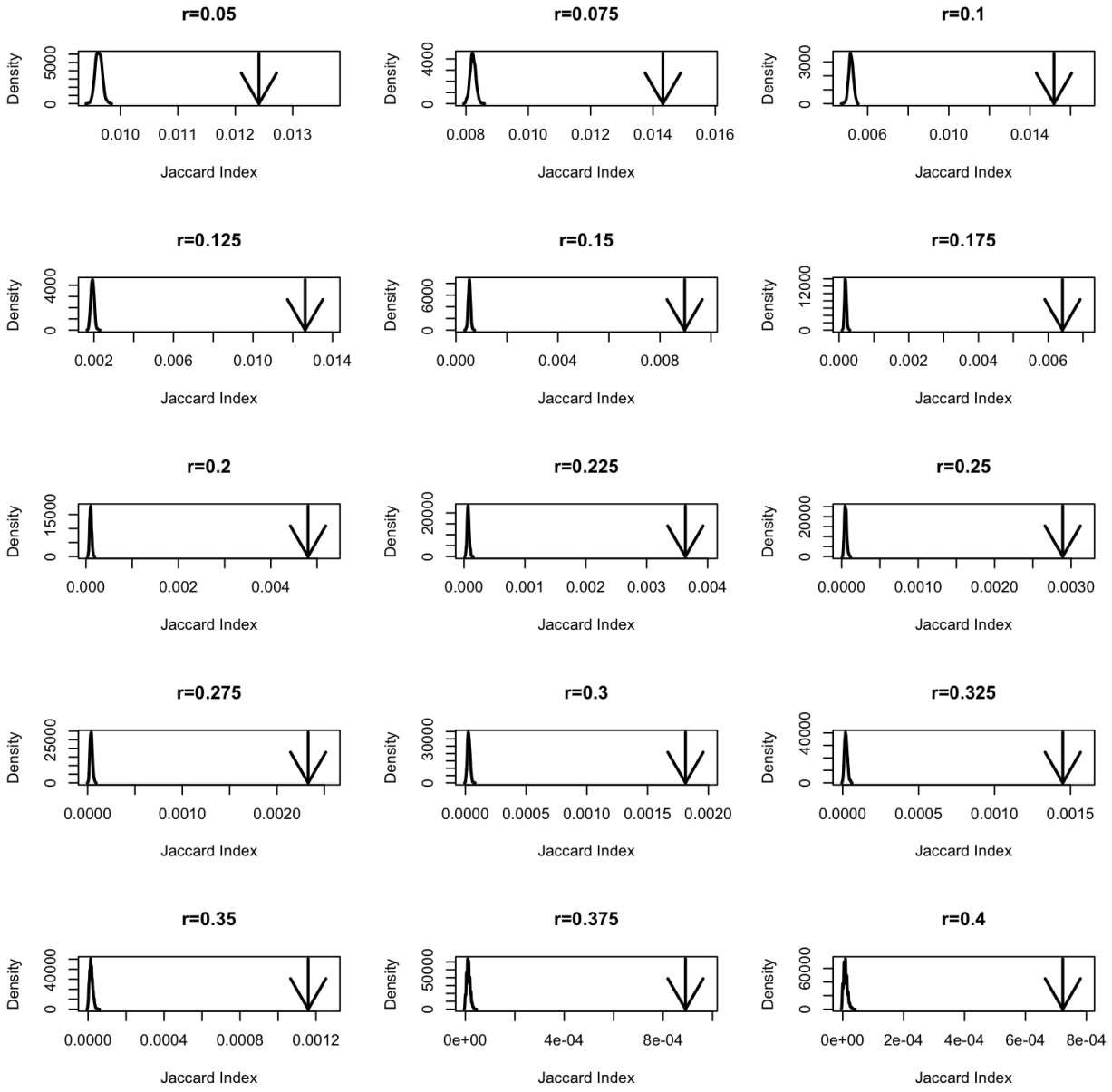


Figure 34: Comparing the Jaccard Index between the ARACNe network and Partial correlation networks (indicated as arrows) and random networks (indicated as distributions)

```r
### Prepare the workspace
# Load imported vulcan object
load("results/001_vobj.rda")

# Network
load("networks/brca-tf-regulon.rda")
tcga_regulon<-regul
rm(regul)

# Entrez to symbol
library(org.Hs.eg.db)
list_eg2symbol<-as.list(org.Hs.egSYMBOL[mappedkeys(org.Hs.egSYMBOL)])
```

1. A T-test based method, that takes the targets of a TF and integrates their pvalue in a specific contrast. Good but hard to keep control over the p-value (the classic integration step using the Fisher's Integration method vastly underestimates them). Also, GRHL2 doesn't shine with this method. Unless differently specified, the p-values are always Bonferroni-corrected

```r
#######################################################
### TTEST INTEGRATION
#######################################################
if(TRUE){
  ### TTest functions
  msvipertt<-function(signature,network,minsize=10){
    # First, convert tscores into pvalues
    psignature<-2*pt(signature[,1], nrow(signature)-2, lower=FALSE)

    # For each regulon, take the targets and integrate their pvalue
    tfpvalues<-c()
    for(tf in names(network)){
      targets<-names(network[[tf]]$tfmode)
      ptargets<-psignature[intersect(targets,names(psignature))]
      if(length(ptargets)>=minsize){
        pt<-fisherp(ptargets)
        tfpvalues<-c(tfpvalues,pt)
        names(tfpvalues)[length(tfpvalues)]<-tf
      }
    }

    return(tfpvalues)
  }
  vulcantt<-function(vobj, network, contrast, annotation = NULL, minsize = 10) {
    tfs <- names(network)
    samples <- vobj$samples
    normalized <- vobj$normalized

    # Prepare output objects
    msvipers <- matrix(NA, ncol = 3, nrow = length(tfs))
    rownames(msvipers) <- tfs
    # Define contrast
    a <- samples[[contrast[1]]]
    b <- samples[[contrast[2]]]
    # Vulcan msviper implementation
    signature <- rowTtest(normalized[, a], normalized[, b])$statistic
```

```
    tfpvalues <- msvipertt(signature, network, minsize = minsize)
    if(!is.null(annotation)){
      names(tfpvalues)<-annotation[names(tfpvalues)]
    }
    return(tfpvalues)
  }

  ### Repeat the same analysis but with TT
  ttp_90<-p.adjust(vulcantt(vobj,network=tcga_regulon,contrast=c("t90","t0"),annotation=list_eg2symbol)
  ttp_45<-p.adjust(vulcantt(vobj,network=tcga_regulon,contrast=c("t45","t0"),annotation=list_eg2symbol)

  ### Compare vulcan and TT
  vulcanp_90<-vobj_tcga_90$msviper$es$p.value
  vulcanp_45<-vobj_tcga_45$msviper$es$p.value

  toshow<-c("ESR1","GATA3","GRHL2")

  par(mfrow=c(1,2))

  common<-intersect(names(ttp_45),names(vulcanp_45))
  x<--log10(vulcanp_45[common]+1e-320)
  y<--log10(ttp_45[common]+1e-320)
  plot(x,y,pch=20,main="Method Comparison, 45' vs 00'",xlab="VULCAN pvalue",ylab="Ttest integration pval
  grid()
  pcc<-cor.test(x,y)
  mtext(paste0("PCC=",signif(pcc$estimate,3)," (p=",signif(pcc$p.value,3),")"))
  textplot2(x[toshow],y[toshow],words=toshow,new=FALSE)

  common<-intersect(names(ttp_90),names(vulcanp_90))
  x<--log10(vulcanp_90[common]+1e-320)
  y<--log10(ttp_90[common]+1e-320)
  plot(x,y,pch=20,main="Method Comparison, 90' vs 00'",xlab="VULCAN pvalue",ylab="Ttest integration pval
  grid()
  pcc<-cor.test(x,y)
  mtext(paste0("PCC=",signif(pcc$estimate,3)," (p=",signif(pcc$p.value,3),")"))
  textplot2(x[toshow],y[toshow],words=toshow,new=FALSE)

  par(mfrow=c(1,1))

}
```

2. A fraction of targets method, defining for every TF the fraction of their targets that are also differentially bound. A crude alternative to VULCAN, which is ignoring the MI strength of interaction and the individual strengths of differential bindings.

```
#######################################################
### FRACTION TEST
#######################################################
if(TRUE){
  ### TTest functions
  msviperfrac<-function(signature,network,minsize=10){
    # First, convert tscores into pvalues
    psignature<-2*pt(signature[,1], nrow(signature)-2, lower=FALSE)
```

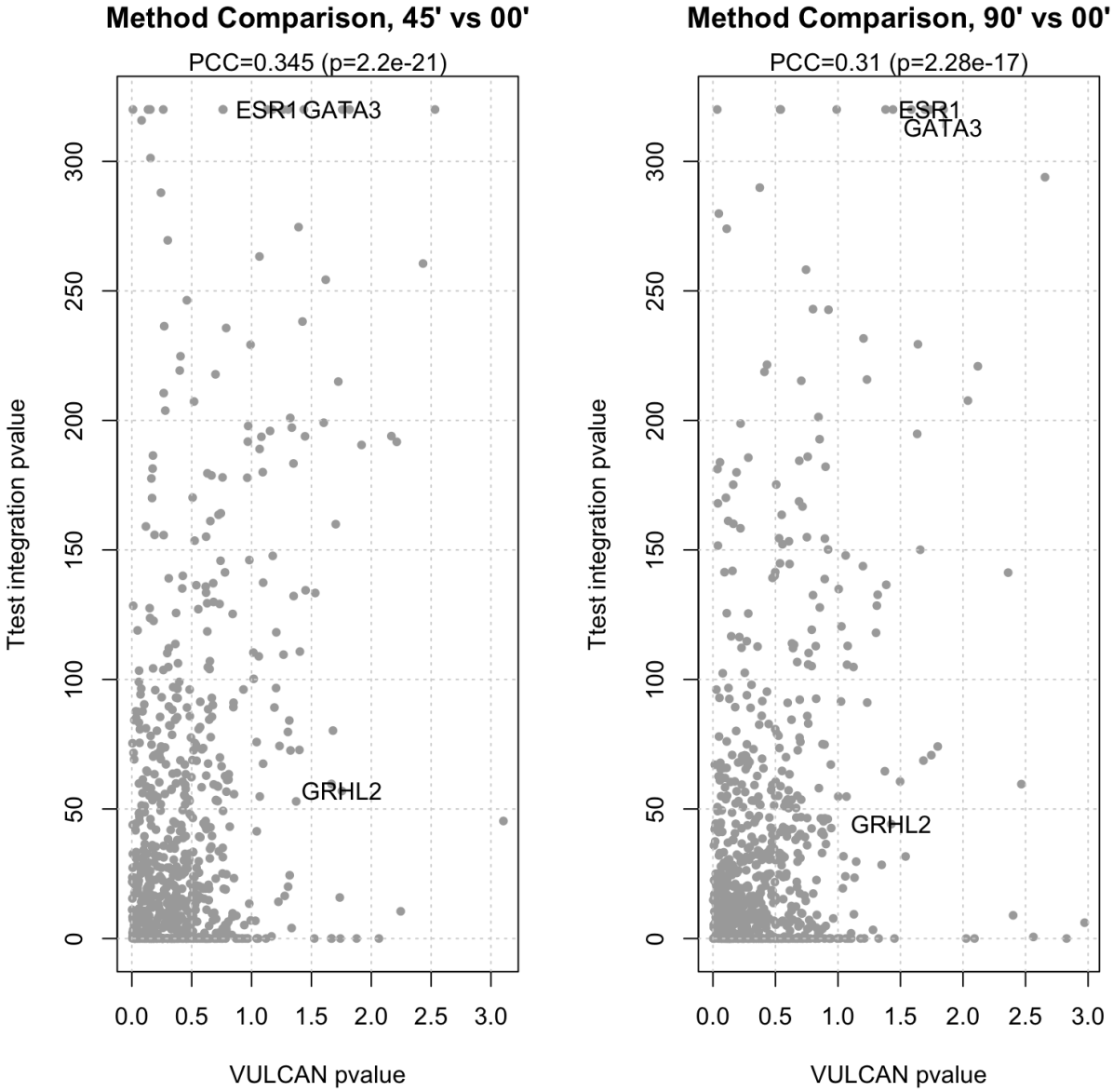


Figure 35: Comparison between VULCAN/VIPER and T-test integration

```r
  # For each regulon, take the targets and integrate their pvalue
  tfpvalues<-c()
  for(tf in names(network)){
    targets<-names(network[[tf]]$tfmode)
    ptargets<-psignature[intersect(targets,names(psignature))]
    ptargets<-ptargets
      frac<-length(ptargets)/length(targets)
      tfpvalues<-c(tfpvalues,frac)
      names(tfpvalues)[length(tfpvalues)]<-tf
  }
  return(tfpvalues)
}
vulcanfrac<-function(vobj, network, contrast, annotation = NULL, minsize = 10) {
  tfs <- names(network)
  samples <- vobj$samples
  normalized <- vobj$normalized

  # Prepare output objects
  msvipers <- matrix(NA, ncol = 3, nrow = length(tfs))
  rownames(msvipers) <- tfs
  # Define contrast
  a <- samples[[contrast[1]]]
  b <- samples[[contrast[2]]]
  # Vulcan msviper implementation
  signature <- rowTtest(normalized[, a], normalized[, b])$statistic
  tfpvalues <- msviperfrac(signature, network, minsize = minsize)
  if(!is.null(annotation)){
    names(tfpvalues)<-annotation[names(tfpvalues)]
  }
  return(tfpvalues)
}

### Repeat the same analysis but with TT
ttp_90<-vulcanfrac(vobj,network=tcga_regulon,contrast=c("t90","t0"),annotation=list_eg2symbol)
ttp_45<-vulcanfrac(vobj,network=tcga_regulon,contrast=c("t45","t0"),annotation=list_eg2symbol)

### Compare vulcan and TT
vulcanp_90<-vobj_tcga_90$msviper$es$p.value
vulcanp_45<-vobj_tcga_45$msviper$es$p.value

toshow<-c("ESR1","GATA3","GRHL2")

par(mfrow=c(1,2))

common<-intersect(names(ttp_45),names(vulcanp_45))
x<--log10(vulcanp_45[common])
y<-ttp_45[common]
plot(x,y,pch=20,main="Method Comparison, 45' vs 00'",xlab="VULCAN pvalue",ylab="Fraction of Differenti
grid()
pcc<-cor.test(x,y)
mtext(paste0("PCC=",signif(pcc$estimate,3)," (p=",signif(pcc$p.value,3),")"))
textplot2(x[toshow],y[toshow],words=toshow,new=FALSE)
```

```
  common<-intersect(names(ttp_90),names(vulcanp_90))
  x<--log10(vulcanp_90[common])
  y<-ttp_90[common]
  plot(x,y,pch=20,main="Method Comparison, 90' vs 00'",xlab="VULCAN pvalue",ylab="Fraction of Differenti
  grid()
  pcc<-cor.test(x,y)
  mtext(paste0("PCC=",signif(pcc$estimate,3)," (p=",signif(pcc$p.value,3),")"))
  textplot2(x[toshow],y[toshow],words=toshow,new=FALSE)

  par(mfrow=c(1,1))

}
```

3. A Fisher's Exact Method (different from the Fisher's Integration!) which assesses the overlap between networks and significant differential binding. Here the problem is that the test is too stringent (as observed in the original VIPER paper) and even without p-value correction we get nothing significant (I tried different threshold of differential binding significance). The plot is uninspiring highlights the non-significance of the results of this method:

```
#######################################################
### FISHER'S EXACT TEST
#######################################################
if(TRUE){
  ### TTest functions
  msviperfet<-function(signature,network,minsize=10){
    # First, convert tscores into pvalues
    psignature<-2*pt(signature[,1], nrow(signature)-2, lower=FALSE)

    # For each regulon, take the targets and calculate how many are significant
    tfpvalues<-c()
    for(tf in names(network)){
      targets<-names(network[[tf]]$tfmode)
      ptargets<-psignature[intersect(targets,names(psignature))]
      if(length(ptargets)>=minsize){
        # Prepare the contingency table
        ul<-names(ptargets)[ptargets<=0.05]
        ur<-setdiff(targets,ul)
        dl<-setdiff(names(psignature)[psignature<=0.05],ul)
        ctable<-rbind(
          c(length(ul),length(ur)),
          c(length(dl),0)
        )
        #ctable[2,2]<-5000-sum(ctable)
        fet<-fisher.test(ctable,alternative="greater")
        pt<-fet$p.value
        tfpvalues<-c(tfpvalues,pt)
        names(tfpvalues)[length(tfpvalues)]<-tf
      }
    }

    return(tfpvalues)
  }
  vulcanfet<-function(vobj, network, contrast, annotation = NULL, minsize = 10) {
    tfs <- names(network)
```

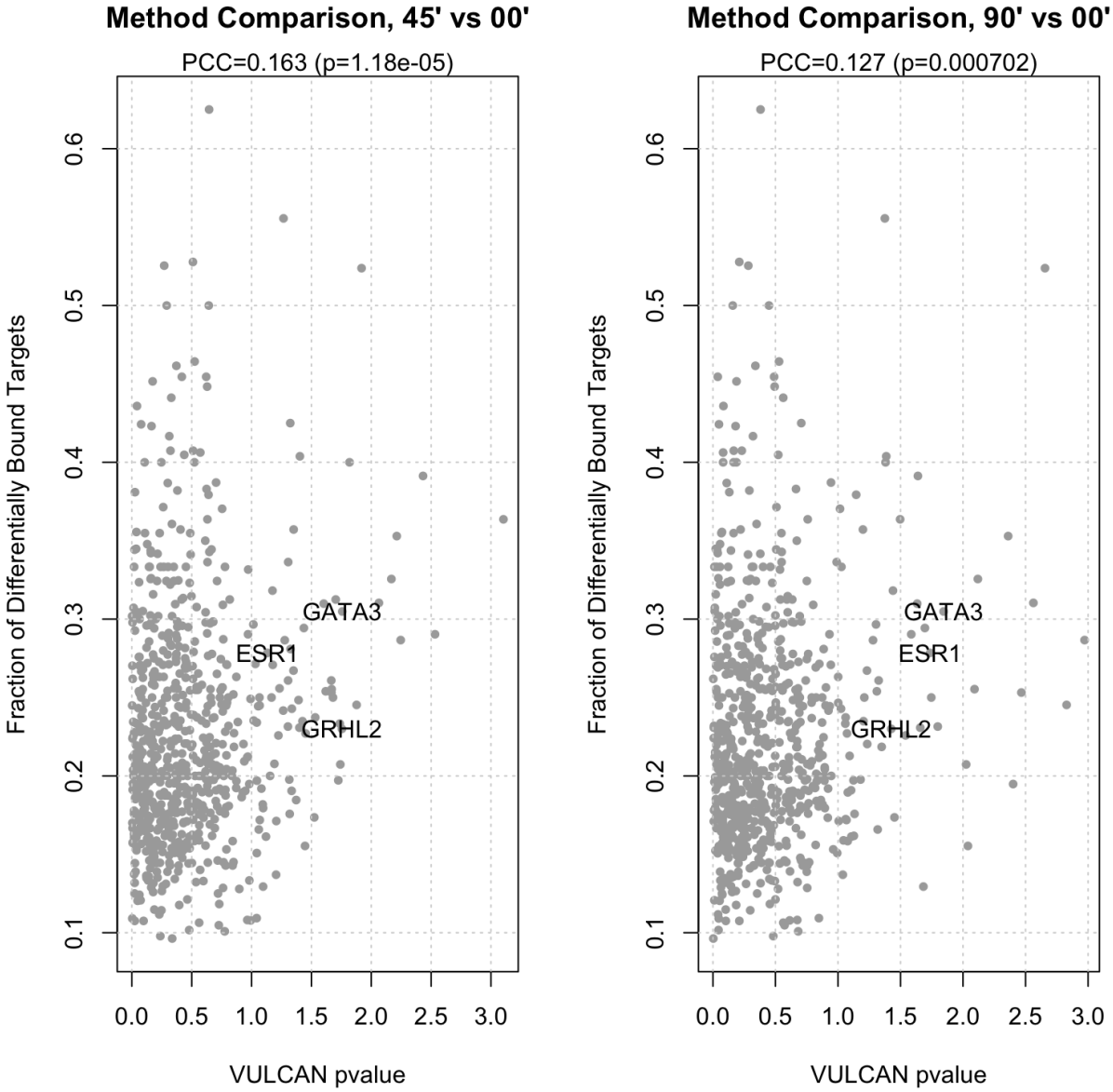


Figure 36: Comparison between VULCAN/VIPER and a fraction of targets found method

```
    samples <- vobj$samples
    normalized <- vobj$normalized

    # Prepare output objects
    msvipers <- matrix(NA, ncol = 3, nrow = length(tfs))
    rownames(msvipers) <- tfs
    # Define contrast
    a <- samples[[contrast[1]]]
    b <- samples[[contrast[2]]]
    # Vulcan msviper implementation
    signature <- rowTtest(normalized[, a], normalized[, b])$statistic
    tfpvalues <- msviperfet(signature, network, minsize = minsize)
    if(!is.null(annotation)){
      names(tfpvalues)<-annotation[names(tfpvalues)]
    }
    return(tfpvalues)
  }

  ### Repeat the same analysis but with FET
  ttp_90<-vulcanfet(vobj,network=tcga_regulon,contrast=c("t90","t0"),annotation=list_eg2symbol)
  ttp_45<-vulcanfet(vobj,network=tcga_regulon,contrast=c("t45","t0"),annotation=list_eg2symbol)

  ### Compare vulcan and TT
  vulcanp_90<-vobj_tcga_90$msviper$es$p.value
  vulcanp_45<-vobj_tcga_45$msviper$es$p.value

  toshow<-c("ESR1","GATA3","GRHL2")

  par(mfrow=c(1,2))

  common<-intersect(names(ttp_45),names(vulcanp_45))
  x<--log10(vulcanp_45[common]+1e-320)
  y<--log10(ttp_45[common]+1e-320)
  plot(x,y,pch=20,main="Method Comparison, 45' vs 00'",xlab="VULCAN pvalue",ylab="Classic Fisher's Exac
  grid()
  textplot2(x[toshow],y[toshow],words=toshow,new=FALSE)

  common<-intersect(names(ttp_90),names(vulcanp_90))
  x<--log10(vulcanp_90[common]+1e-320)
  y<--log10(ttp_90[common]+1e-320)
  plot(x,y,pch=20,main="Method Comparison, 90' vs 00'",xlab="VULCAN pvalue",ylab="Classic Fisher's Exac
  grid()
  textplot2(x[toshow],y[toshow],words=toshow,new=FALSE)

  par(mfrow=c(1,1))
}
```

### 3.7.4 Comparing VULCAN with online tools

We will generate BED files for the peaks, as reported by DiffBind, we will then test the pathway enrichment for each of these peaks using the Great software v3.0.0 (http://bejerano.stanford.edu/great/public/html/), the ChIP-Enrich pipeline (http://chip-enrich.med.umich.edu/) and the ISMARA tool (http://ismara.unibas.ch). Parameters for GREAT: defaults (Basal plus extension, 5.0kb upstream, 1.0 kb downstream) Parameters for

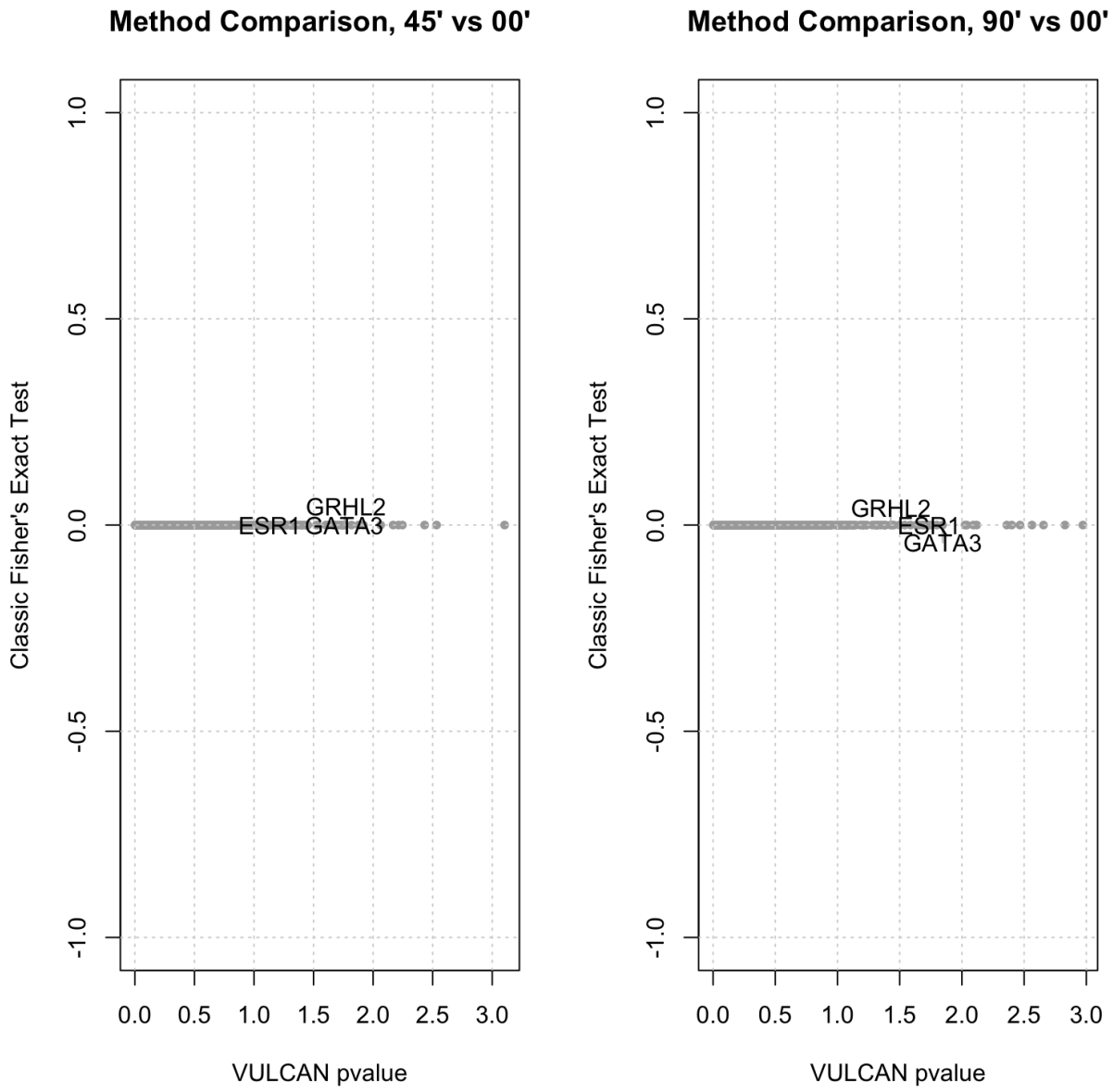


Figure 37: Comparison between VULCAN/VIPER and Fisher's Exact Test method

ChIP-Enrich: defaults (Nearest TSS, pathways size<=2000, Biocarta, KEGG, Reactome, TFs). Parameters for ISMARA: defaults (ChIP-Seq mode, hg19)

The VULCAN analysis shows a significant overlap in terms of significant pathways with the GREAT method. ChIP-enrich computes enrichment for a number of TFs which are amongst the most significant in VULCAN, but it surprisingly fails at identifing ESR1 as the top Transcription Factor affected by our experiment. ISMARA succeeds at identifying ESR1 using a motif-based analysis, but doesn't identify other candidate binding TFs, as expected, being the experiment targeted at the estrogen receptor.

```
### Number of tested pathways (for statistical comparison later)
load("msigdb/MSigDB_v5.0_human.rda")
raw<-msigDBentrez$c2.all.v5.0.entrez.gmt
universe<-names(raw)[grep("BIOCARTA_|REACTOME_|KEGG_|PID_|ST_",names(raw))]

### DiffBind object (containing peak location and intensity)
wass<-load("results/001_diffbind.rda")

### Generate input BEDs for chip enrich and GREAT (ismara takes BAMs as input)
fname<-paste0("results/008_comparison_contrast90vs00_UP_p1.bed")
if(!file.exists(fname)){
  contrasts<-c("contrast45vs00","contrast90vs00","contrast90vs45")
  for (contrast in contrasts) {
    c<-switch(contrast,contrast45vs00=3,contrast90vs00=2,contrast90vs45=1)
    for(pgreat in c(1,0.05)){
      bed<-as.data.frame(dba.report(dbaobj,contrast=c,method=DBA_DESEQ2,bNormalized=TRUE, bCounts=TRUE,
      if(nrow(bed)>0) { # Nothing individually significant if no rows were produced
        bedup<-bed[bed$Fold>0,1:3]
        beddn<-bed[bed$Fold<0,1:3]
        if(nrow(bedup)>0){
          write.table(bedup,
                      file=paste0("results/008_comparison_",contrast,"_UP_p",pgreat,".bed"),
                      row.names=FALSE,col.names=FALSE,sep="\t",quote=FALSE
          )
        }
        if(nrow(beddn)>0){
          write.table(beddn,
                      file=paste0("results/008_comparison_",contrast,"_DN_p",pgreat,".bed"),
                      row.names=FALSE,col.names=FALSE,sep="\t",quote=FALSE
          )
        }
      }
    }
  }
}
```

```
### Pathway Comparison: VULCAN vs. GREAT
load_obj <- function(f){
  env <- new.env()
  nm <- load(f, env)[1]
  env[[nm]]
}
contrasts<-c("45","90")
par(mfrow=c(2,1))
for(c in contrasts){
  # Our REA pathways
```

```
  nes.tpathways<-load_obj(paste0("results/003_pathwayComparison_REA_",c,".rda")) # results_rea_45

  # GREAT pathways
  rawgreat<-read.delim(paste0("results/great/great_",c,"_p1_UP.tsv"),as.is=TRUE,skip=3)
  table(rawgreat[,1])
  rawgreat<-rawgreat[rawgreat[,1]=="MSigDB Pathway",]
  great<-setNames(rawgreat$BinomBonfP,rawgreat[,2])
  great<-great[great<0.1]

  ### Comparison GREAT/VULCAN
  vsig<-nes.tpathways[z2p(nes.tpathways)<0.1]
  venn(list(VULCAN=names(vsig),GREAT=names(great)))
  title(paste0("Comparison VULCAN/GREAT for pathways at ",c," minutes"))
  ctable<-rbind(c(0,0),c(0,0))
  ctable[1,1]<-length(intersect(names(vsig),names(great)))
  ctable[1,2]<-length(setdiff(names(vsig),names(great)))
  ctable[2,1]<-length(setdiff(names(great),names(vsig)))
  ctable[2,2]<-length(universe)-ctable[1,1]-ctable[1,2]-ctable[2,1]
  fp<-signif(fisher.test(ctable)$p.value,4)
  mtext(paste0("FET p-value: ",fp))
  text(100,3,ctable[2,2])

  common<-intersect(names(nes.tpathways),names(great))
}
```

```
par(mfrow=c(1,1))
```

```
### TF and Pathway Comparison: VULCAN vs. ChIP enrich
load("results/002_vobj_networks.rda")
contrasts<-c("45","90")
par(mfrow=c(2,1))
for(c in contrasts){
  # Our VULCAN TF enrichment
  if(c=="45"){
    vulcannes<-vobj_tcga_45$msviper$es$nes
  }
  if(c=="90"){
    vulcannes<-vobj_tcga_90$msviper$es$nes
  }
  # ChIPEnrich pathways + TFs
  rawchipenrich<-read.delim(paste0("results/chipenrichr/",c,"_p1_UP_results.tab"),as.is=TRUE)
  chipenrich_tfs<-rawchipenrich[rawchipenrich[,1]=="Transcription Factors",]
  chipenrich_pathways<-rawchipenrich[rawchipenrich[,1]!="Transcription Factors",]
  t1<-gsub(" ","_",paste0(toupper(chipenrich_pathways[,1]),"_",toupper(chipenrich_pathways[,3])))
  t2<-chipenrich_pathways[,"FDR"]
  chipenrich_pathways<-setNames(t2,t1)

  # TF comparison
  cetfs<-setNames(chipenrich_tfs[,"FDR"],gsub("_.+","",chipenrich_tfs[,"Description"]))
  vutfs<-vulcannes[!is.na(vulcannes)]
  vutfs<-vutfs[vutfs>0]
  common<-intersect(names(vutfs),names(cetfs))

  plot(vutfs,-log10(z2p(vutfs)),xlab="VULCAN NES",ylab="VULCAN -log10(p)",pch=20,col="grey",
```

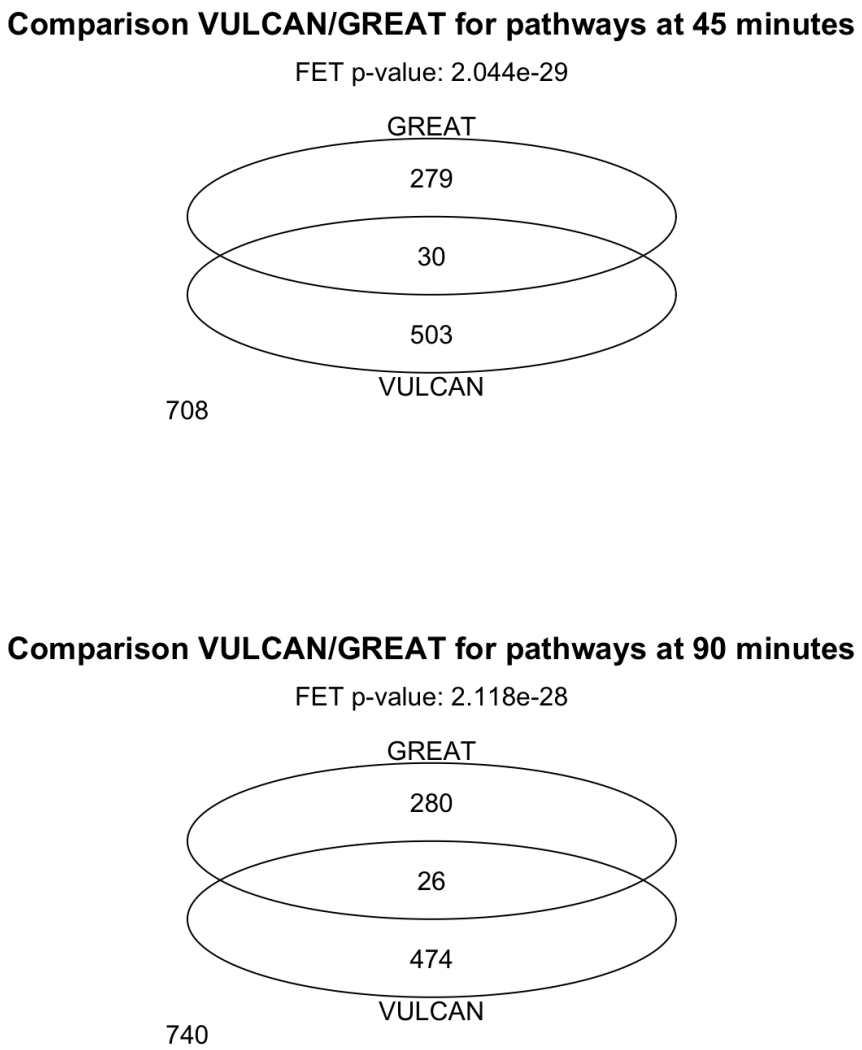


Figure 38: Comparison of results from the VULCAN and GREAT methods

```
      main=paste0("Comparison VULCAN/ChIP-enrich at ",c)
  )
  mtext("Labels indicate significant TFs by ChIP-enrich binding site analysis",cex=0.8)
  set.seed(1)
  textplot2(vutfs[common],-log10(z2p(vutfs))[common],common,new=FALSE)
}
```

```
par(mfrow=c(1,1))
```

```
### Comparison: VULCAN vs. ISMARA
ismara<-t(read.delim("results/ismara/ismara_report/activity_table",as.is=TRUE))
vulcan45<-vobj_tcga_45$msviper$es$nes
vulcan90<-vobj_tcga_90$msviper$es$nes

# Compare VULCAN (x axis) at 45 and 90 minutes with ISMARA (yaxis) average + sd

# Prepare ismara values
i45<-ismara[,grep("45",colnames(ismara))]
i90<-ismara[,grep("90",colnames(ismara))]
i45_mean<-apply(i45,1,mean)
i45_sd<-apply(i45,1,sd)
i90_mean<-apply(i90,1,mean)
i90_sd<-apply(i90,1,sd)

common<-intersect(names(vulcan45),rownames(ismara))
length(common) # 148
```

```
## [1] 148
```

```
# Plots
par(mfrow=c(2,1))

# 45 minutes
x<-vulcan45[common]
y<-i45_mean[common]
uiw<-i45_sd[common]
top<-intersect(names(sort(x,dec=TRUE))[1:20],names(sort(y,dec=TRUE))[1:20])
plotCI(x,y,uiw=uiw,xlab="VULCAN NES",ylab="ISMARA Activity",main="Comparison VULCAN/ISMARA",pch=20,col=
mtext("45 minutes",cex=0.8)
textplot2(x[top],y[top],words=top,new=FALSE,font=2)
# 90 minutes
x<-vulcan90[common]
y<-i90_mean[common]
uiw<-i90_sd[common]
top<-intersect(names(sort(x,dec=TRUE))[1:25],names(sort(y,dec=TRUE))[1:25])
plotCI(x,y,uiw=uiw,xlab="VULCAN NES",ylab="ISMARA Activity",main="Comparison VULCAN/ISMARA",pch=20,col=
mtext("90 minutes",cex=0.8)
textplot2(x[top],y[top],words=top,new=FALSE,font=2)
```

# 4 Estrogen Receptor-alpha qPLEX-RIME Analysis

---

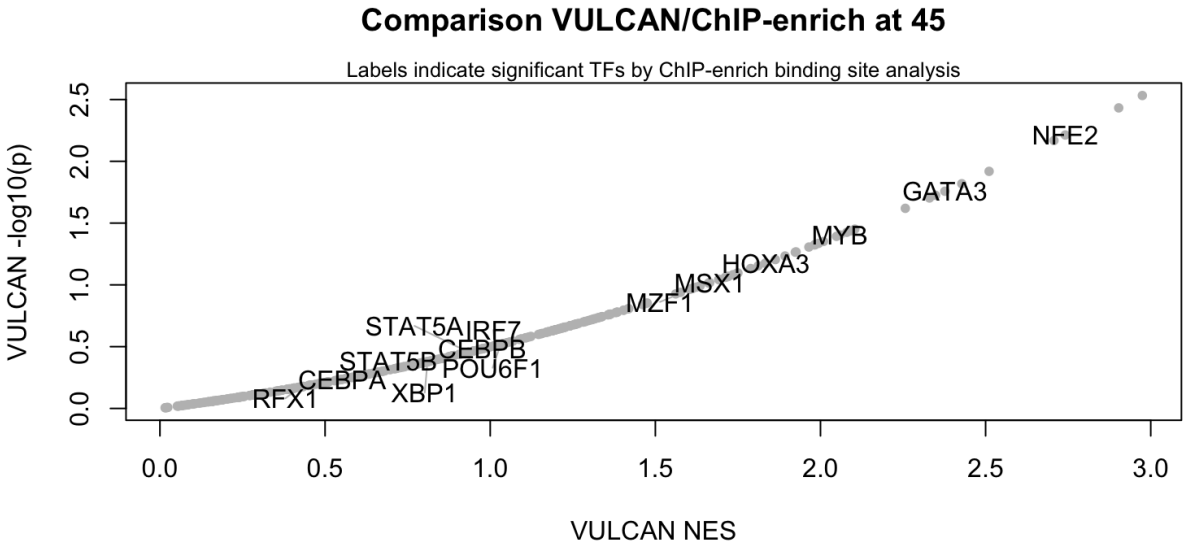


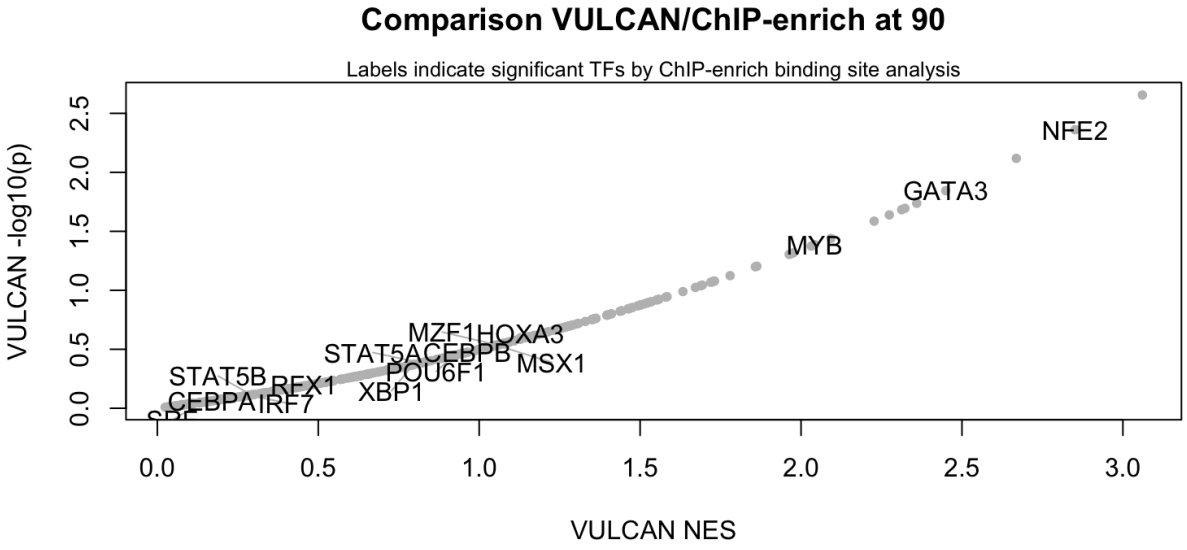


Figure 39: Comparison of results from the VULCAN and ChIP-enrich methods

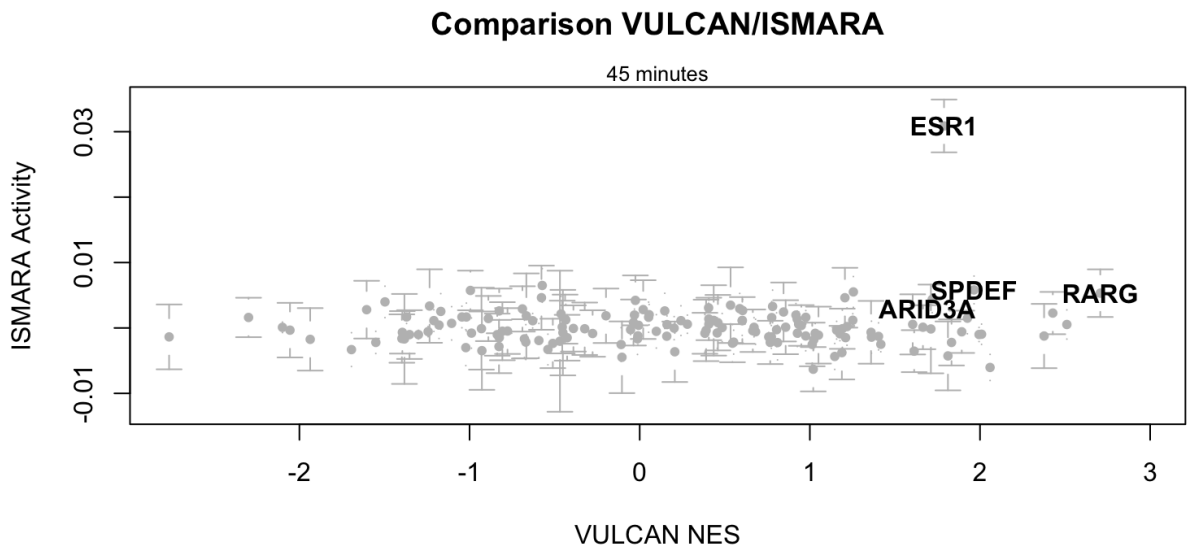


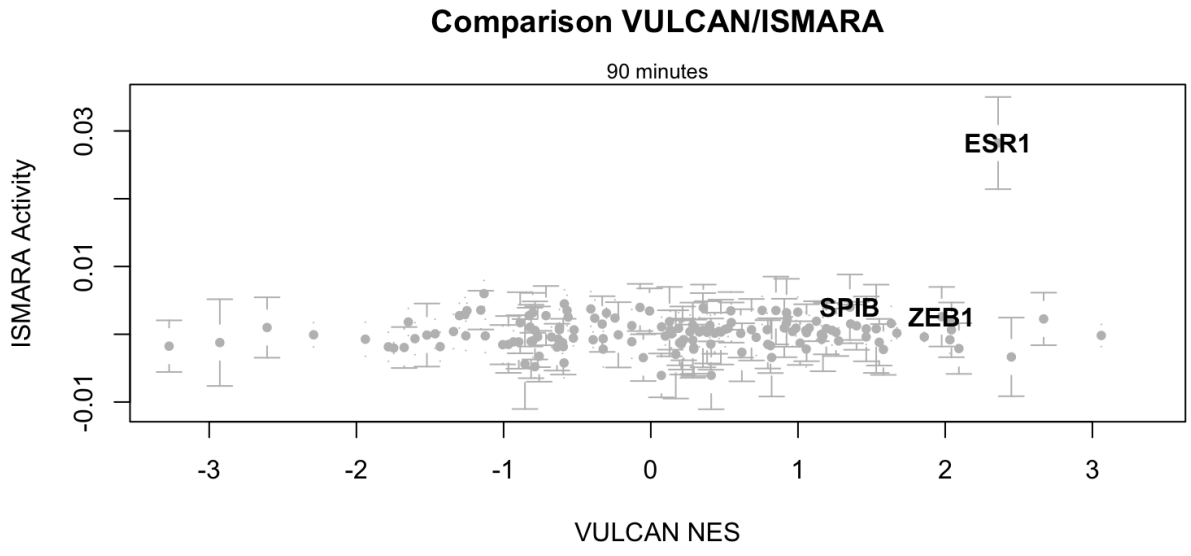


Figure 40: Comparison of results from the VULCAN and ISMARA methods

## 4.1 Introduction

This report is from an analysis of the RIME-TMT proteomics data for an experiment carried out by Andrew Holding to quantify specific interactors of estrogen receptor (ER) and forkhead box protein A1 (FOXA1) in MCF-7 cells.

The RIME (Rapid Immunoprecipitation of Endogenous Proteins) technique was used to pull down ER and FOXA1 and their interacting proteins, which were subsequently assessed and quantitated using mass spectrometry with tandem mass tags (TMT). TMT runs were carried out for 3 biological replicates, estrogen-starved MCF-7 cells from the same cell line at different times/passages, before and after addition of estrogen with samples taken at 3 different time points – 0, 45 and 90 minutes after estrogen addition. A pull down of Immunoglobulin G (IgG) was also run as a control.

The digests from two of the biological replicates (PR622 and PR650) were analyzed with 3 separate runs of the mass spectrometer to increase coverage; data from the repeated runs were combined prior to the analysis carried out here. The other sample (PR590) was run once only.

Table 1 shows the isobaric tags used for each sample within each of the runs.

| Group | PR590 | PR622 | PR650 |
|---|---|---|---|
| ER 0min | 127N | 127N | 128N |
| ER 45min | 128C | 127C | 128C |
| ER 90min | 129N | 128N | 129N |
| FOXA1 0min | 129C | 129C | 129C |
| FOXA1 45min | 130N | 130N | 130N |
| FOXA1 90min | 130C | 130C | 130C |
| IgG | 126 | 126 | 131 |

Table 1: Isobaric tags used for each sample (group) and run.

## 4.2 Peptide intensity data

Raw spectra were processed using Proteome Discover 2.1 to produce peptide-level intensity data with a single set of intensity values per distinct peptide. Only peptides with unique high-confidence protein matches were included.

Multiple peptide-spectrum matches (PSMs) for the same peptide were combined using Proteome Discoverer by summing the PSM-level intensities. Peptide sequences with different modifications are treated as distinct peptides and the data provided contain intensities values for each modification identified for a peptide sequence. Several distinct peptide sequences (with modifications) may have been identified for any given protein.

Table 2 shows the numbers of distinct peptides and proteins obtained in each TMT run. Also given are the numbers of peptides and proteins after filtering peptides with missing intensity values in one or more TMT channels.

| | PR590 | PR622 | PR650 | All |
|---|---|---|---|---|
| Peptides | 5822 | 6952 | 3183 | 9321 |
| Peptides with no missing values | 5702 | 6872 | 3118 | 9179 |
| Proteins | 1125 | 1227 | 656 | 1553 |
| Proteins with no missing values | 1112 | 1218 | 645 | 1541 |

Table 2: Numbers of peptides and proteins observed in each run.

Figure 1 shows the distribution of intensities for each sample within each run.

#### 4.2.1 Missing intensity values

Missing intensity values can result even though ions are present at detectable concentrations due to the stochastic nature of the mass spectrometry acquisition method. It is reasonable to expect that these missing values are randomly distributed in the data. Alternatively, missing values may occur when there is a low abundance of ions, below the limit of detection of the instrument. These biologically relevant missing values are not randomly distributed, affecting only those proteins that are expressed at low levels in the samples analysed. The R/Bioconductor package `MSnBase` provides imputation methods for both types of missing value.

In this analysis, missing values have been handled in 3 different ways. The first approach is to exclude all peptide-level mesasurements where there is a missing value for one or more of the samples within a run. In addition, two imputation methods have been performed: one in which the missing values are set to the smallest non-missing value in the data for that run and the other in which k-nearest neighbour (KNN) averaging is applied.

Figure 2 shows the distribution of intensities for each sample within each run following imputation using the smallest non-missing values. A small hump just below zero on the $\log_2$ scale is clearly visible for each run.

### 4.3 Normalization of intensity data

The intensity distribution for PR622 suggests that the labeled samples have been pooled with differing protein concentrations and that some normalization is required to properly assess differences between groups. Normalization techniques that are commonly applied to microarray expression data and mRNA sequencing data assume that only a few genes, e.g. a few hundred out of tens of thousands, are expressed at very different levels between samples. This assumption may not hold for a RIME experiment where a specific set of interacting proteins is targeted. For example, if the majority of interacting proteins were to bind less strongly at one time point relative to another, quantile normalization or scale normalization approaches would have the effect of removing the general trend. In this case, following normalization, those proteins that bind less strongly may appear to be largely unchanged, while proteins with very similar levels of binding at the different time points would have artificially increased binding levels. Therefore some care is required when interpreting the results of a differential binding analysis for RIME TMT experiments.

In this analysis, quantile normalization and scale normalization were applied for each run separately.

The IgG control was used to assess non-specific binding. The binding of a protein was considered to be non-specific if the binding level of that protein in the condition of interest, e.g. ER at 45 minutes, was not significantly above the level observed for the IgG control. Proteins detected with the IgG control are expressed at lower levels in the PR590 and PR650 runs. Normalization of the IgG control along with the other samples would make it more difficult to distinguish between specific and non-specific binding since the intensities of the IgG control would be scaled to a similar level of those of the other samples.

Among a number of normalization approaches tested here, normalizations were carried out that both include and exclude the IgG control. Figure 3 shows the normalized intensity distributions following scale normalization of all peptide intensities including those with missing values. Figure 4 shows the normalized intensity distributions following scale normalization for all samples except the IgG controls.

A further normalization approach was attempted that scales the data from all samples within a run based on a subset of peptides that are considered most likely to be at similar concentrations between the samples. The assumption is that the peptides with the highest intensity values in the IgG control are the result of non-specific binding and that that binding is consistent across all samples. Similar to the scale normalization applied in the first approach, the median intensity within each sample is computed to determine a scaling

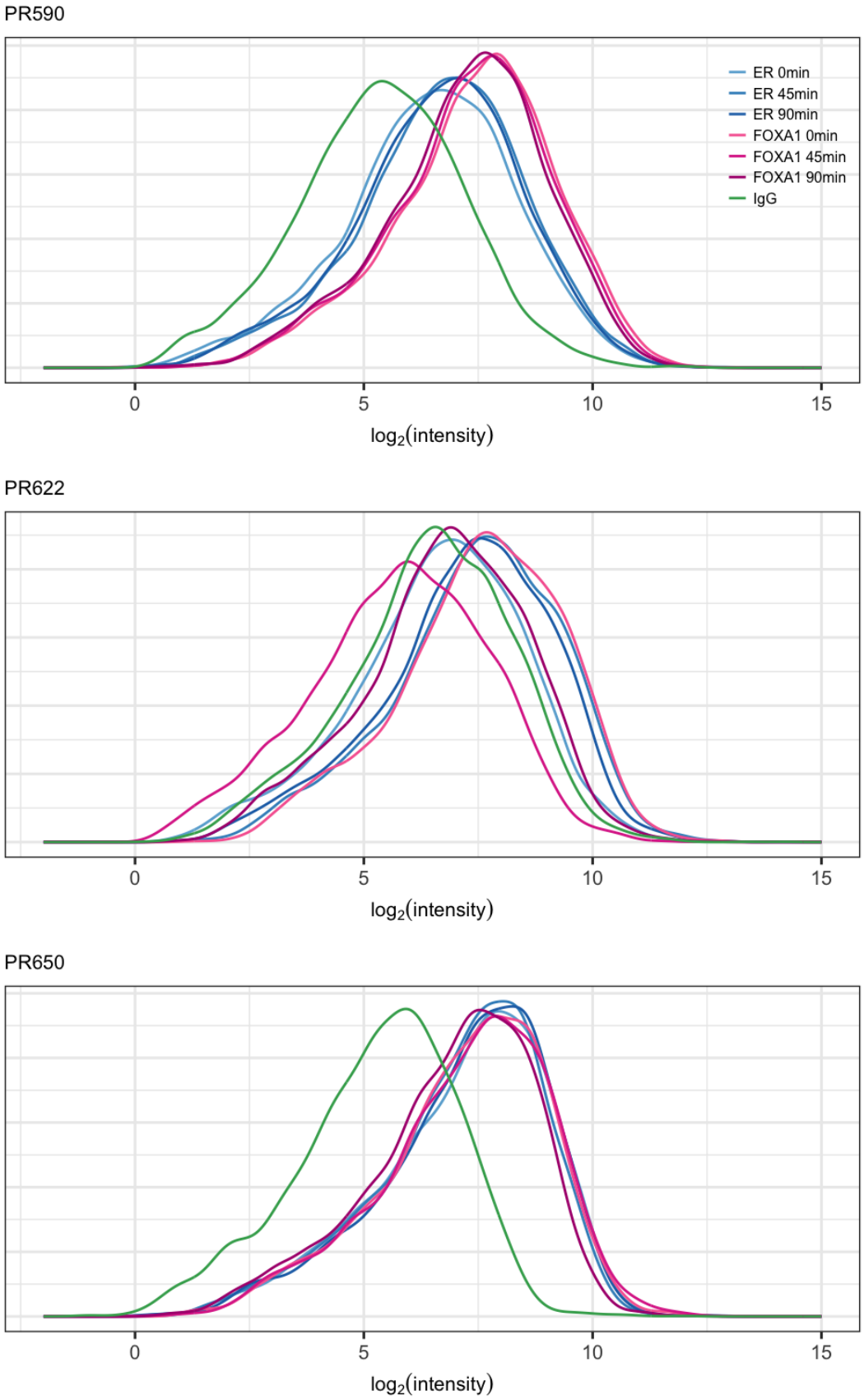


Figure 41: Density plots of intensities from each run.

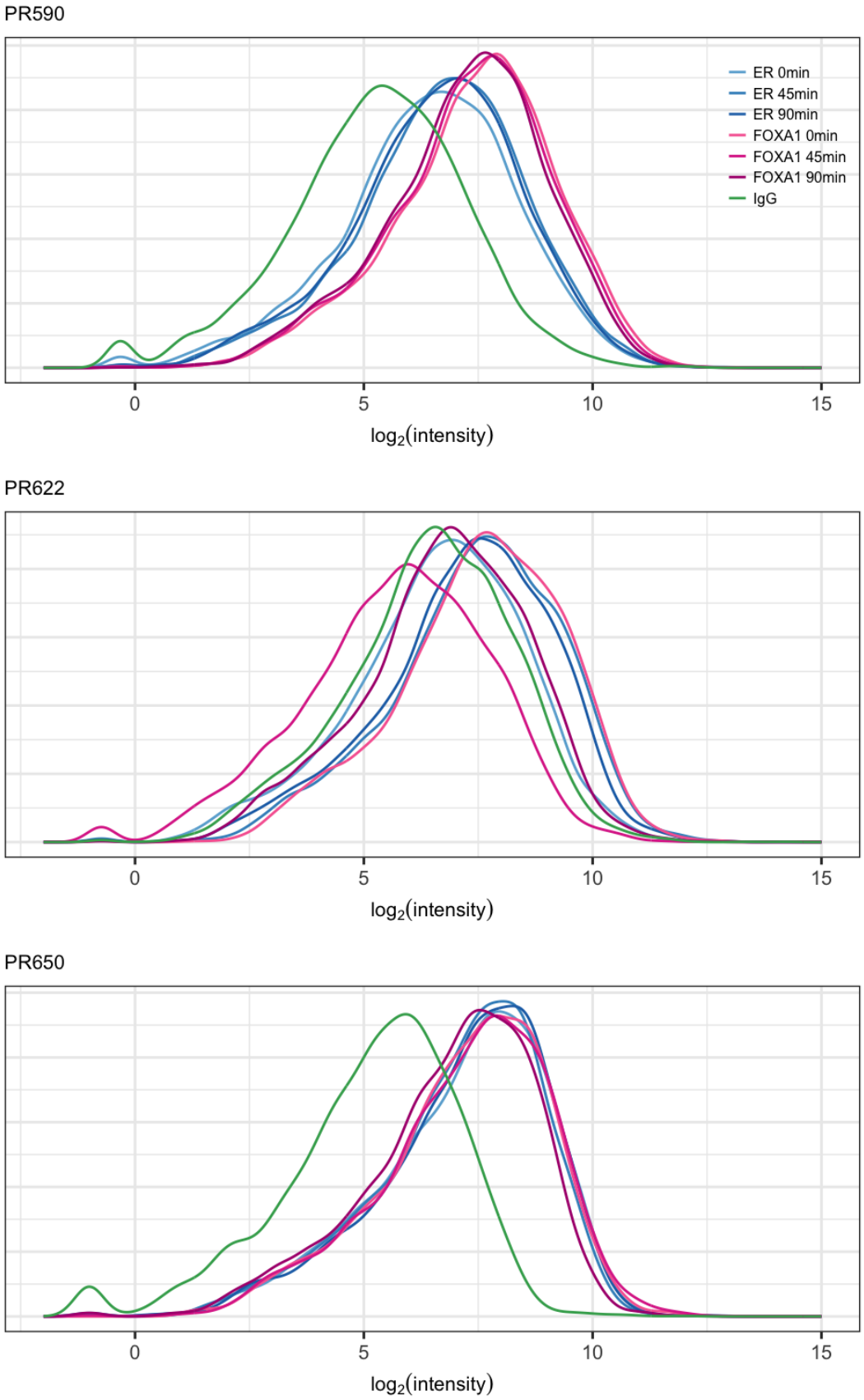


Figure 42: Density plots of intensities from each run following imputation of missing values using the smallest non-missing value in the data for each run.

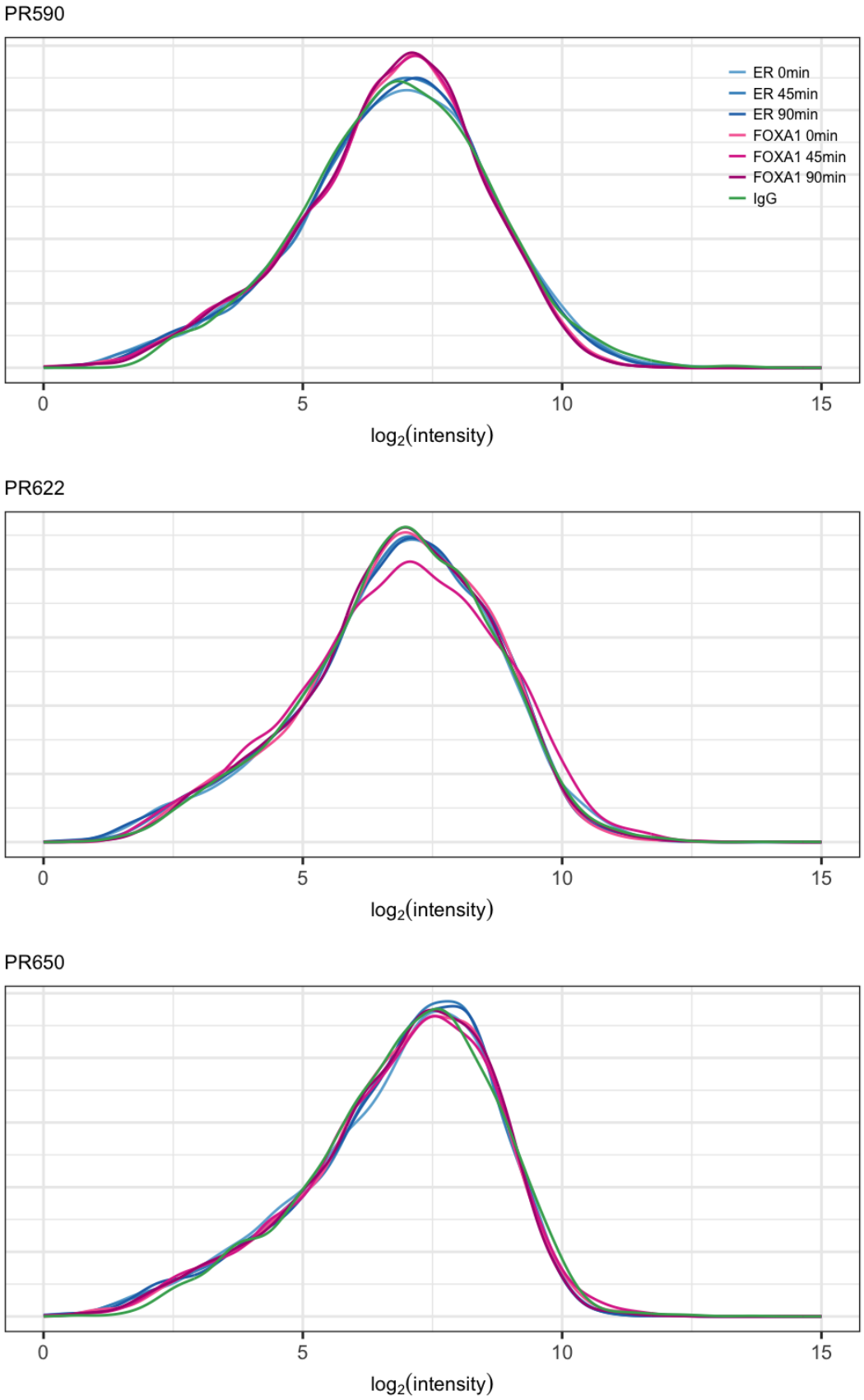


Figure 43: Density plots of normalized intensities from each TMT run where scale normalization was applied to peptide intensities that include misssing values.

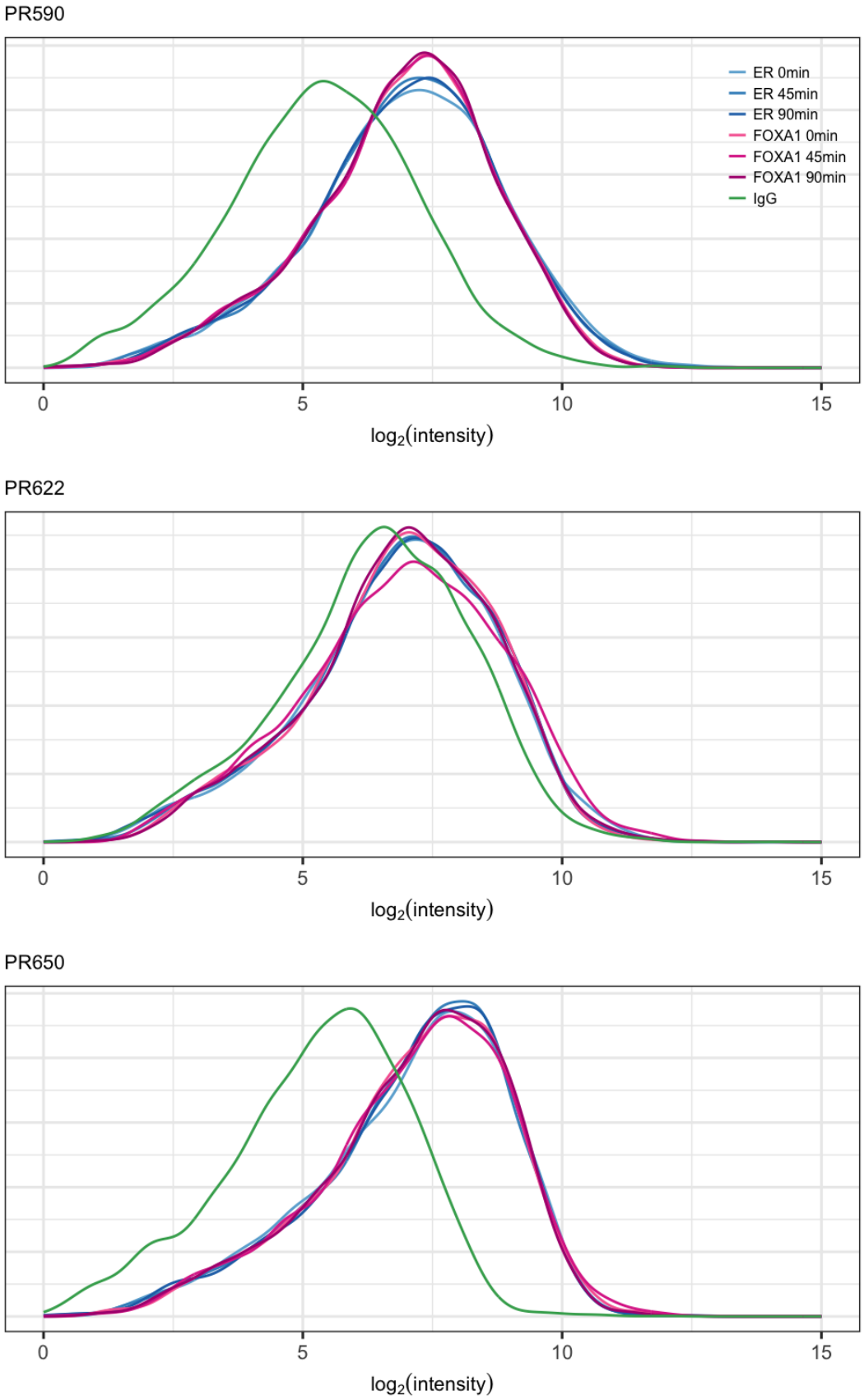


Figure 44: Density plots of normalized intensities from each TMT run where scale normalization was applied to peptide intensities for all samples except the IgG controls.

factor for each sample within a run but the median computed only uses the 10 peptides with the highest IgG measurements. As before, normalization is carried out within each run separately.

Figure 5 shows the resulting normalized intensity distributions. Strikingly, the IgG intensity distribution is shifted to lower values in run PR622, making it more consistent with the other 2 runs.

## 4.4 Protein-level quantification

Protein-level quantification was carried out for each run separately by summing normalized intensity values for all peptides matching to a particular protein. This is similar in principle to the gene-level quantification that is carried out during microarray analysis or the read-counting approach in RNA-Seq. Essentially, all signal attributable to a particular protein is assigned to that protein. Intensity values vary in magnitude depending on the elution profile for the peptide and when the peptide is sampled. Relative intensities for a peptide between the tags or samples within a run should be consistent but the signal may include some contribution from a contaminating, co-eluting peptide, the extent of which may differ for different PSMs. In summing intensities from multiple measurements for the same peptide, those peptides that have higher levels of intensity values will have a greater weight in determining the overall intensity; higher intensity measurements are likely to more accurately reflect differences between samples so this may be advantageous.

When no imputation of missing values was carried out, peptides with missing values in one or more samples were excluded from the summation. Missing values that arise for technical reasons instead of being at undetectable levels in a sample would otherwise reduce the overall intensity in that sample relative to other samples.

The statistical analysis of differential binding between groups that follows requires at least 3 observations per group. Table 3 gives the number of protein identified in just a single run, two runs or all three runs. A total of proteins were identified across all runs of which 527 were observed in all three runs, allowing for a statistical analysis. $\log_2$ fold changes are still computed for proteins identified only in one or two of the runs, but no measure of the statistical significance is given in the differential binding analysis.

| Runs/replicates | 1 | 2 | 3 | total |
|---|---|---|---|---|
| Including missing values | 625 | 401 | 527 | 1553 |
| Excluding missing values | 625 | 398 | 518 | 1541 |

Table 3: Numbers of proteins identified in differing numbers of runs and total number of proteins identified in all runs.

## 4.5 Principal Component Analysis

Protein-level intensities were scaled to sum to 1.0 for each protein within a run, allowing for comparison across runs in a principal component analysis (PCA).

Figure 6 shows a PCA plot for the first two principal components using all proteins that were sampled in all three runs. The plot shows a clear separation of the ER, FOXA1 and IgG control pull-downs. The 0, 45 and 90 minute timepoints within each of the ER and FOXA1 groups are not completely separated in the first two principal components. Figure 7 shows the PCA plot for just the ER samples.

## 4.6 Differential Binding

A statistical analysis of differentially-expressed peptides was carried out using **limma**, a R/Bioconductor package commonly used in the analysis of microarray and RNA-seq data, but applicable to data from any quantitative expression technology.

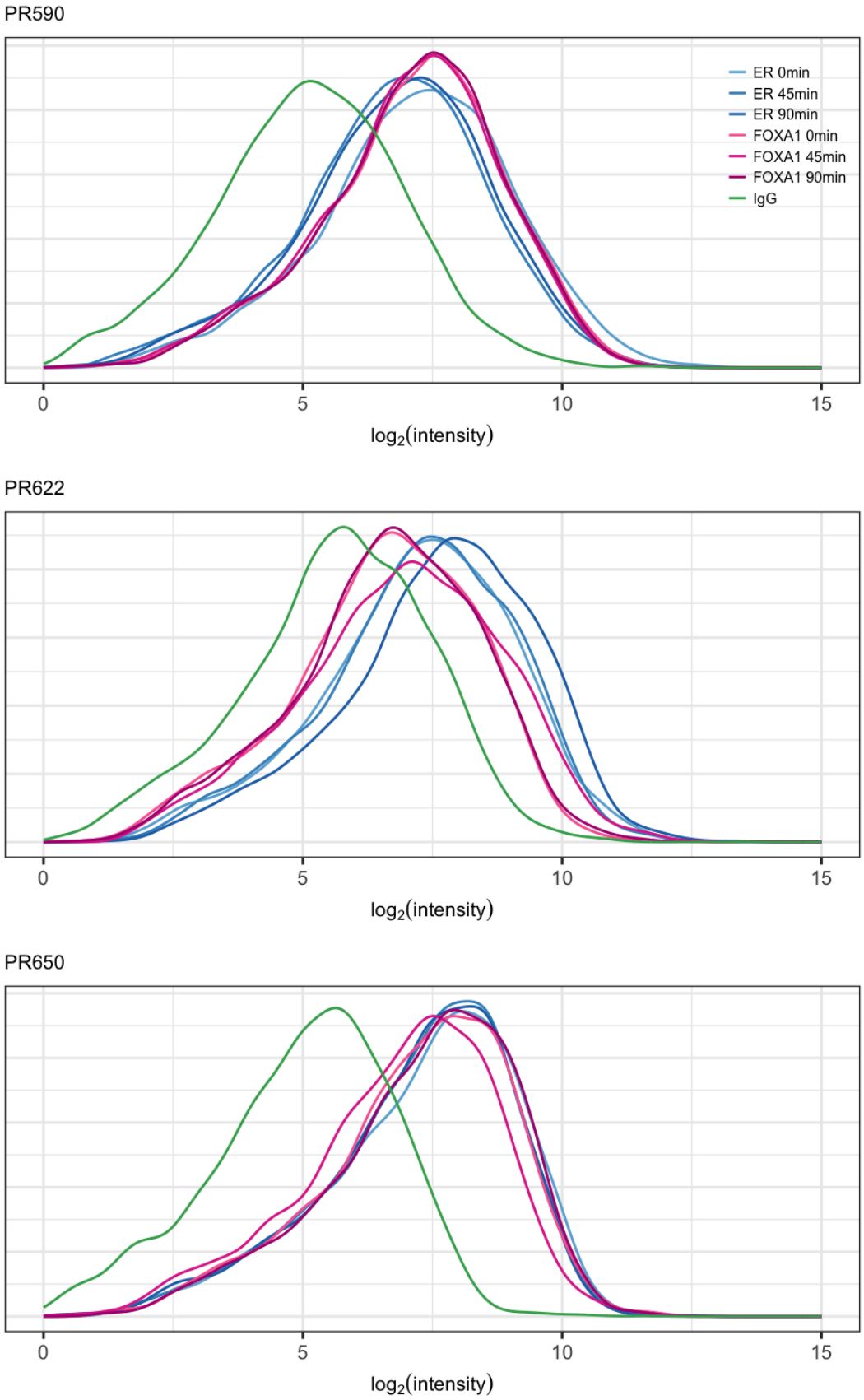


Figure 45: Density plots of normalized intensities from each TMT run where scale normalization is applied based on 10 peptides with the highest IgG intensities in each run.

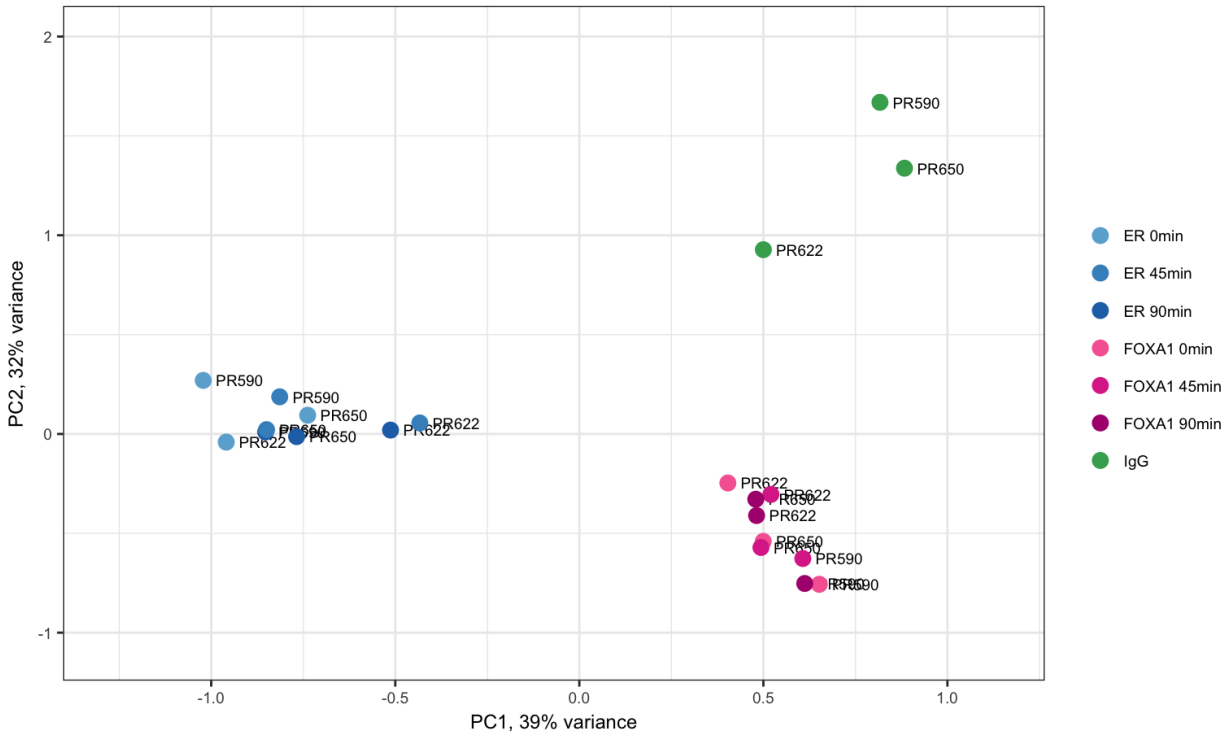


Figure 46: Principal Componenent Analysis for proteins sampled in all 3 runs. The PCA was based on protein-level data resulting from summation of quantile normalized peptide intensities in which missing values were imputed using KNN-based nearest neighbour averaging. The first two principal components are displayed.

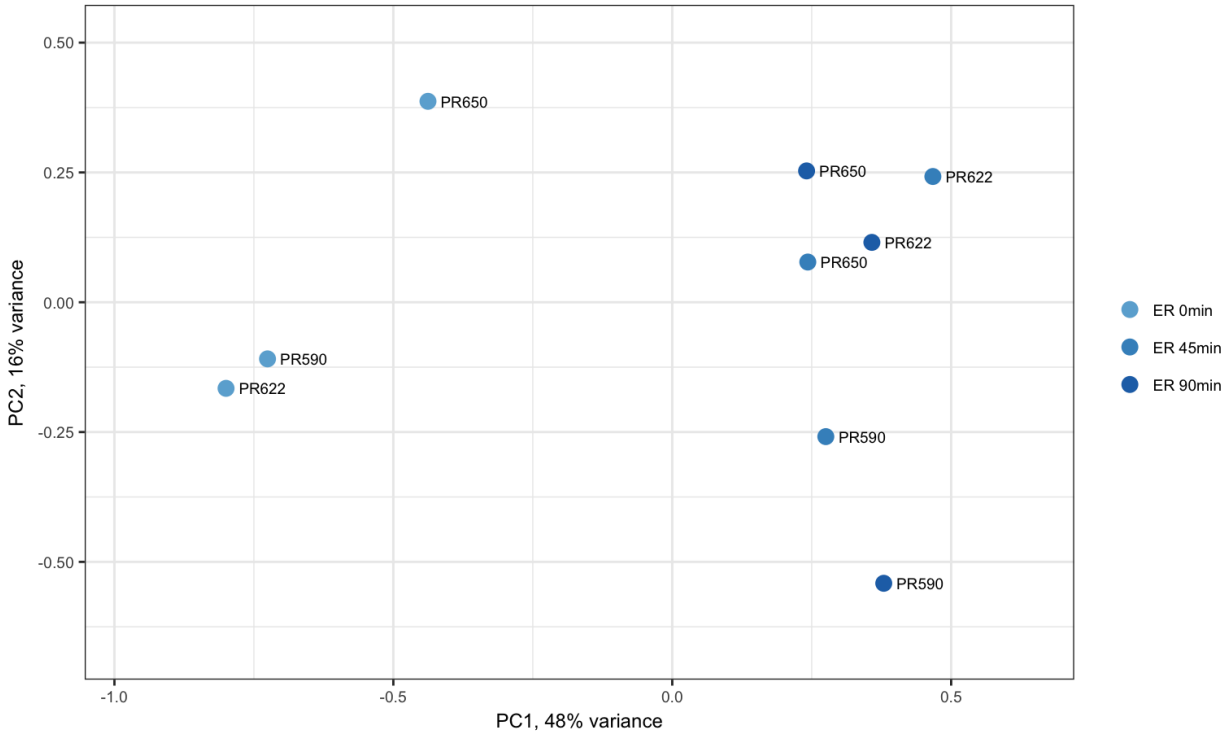


Figure 47: Principal Componenent Analysis for ER-interactng proteins sampled in all 3 runs. The first two principal components are displayed.

Limma uses linear models to assess differential expression in the context of multifactor experimental designs. It is able to analyze comparisons between many RNA targets simultaneously (or in this case many proteins) and has features that make these analyses stable even for experiments with small numbers of samples; this is achieved by borrowing information across genes (proteins).

In this analysis, limma was used to estimate $\log_2$ fold changes and standard errors by fitting a linear model for each protein where the model includes variables for the group (the ER and FOXA1 pull-downs at 0, 45 and 90 minute time points and the IgG control at 45 minutes) and the run. This is essentially a two-way ANOVA, a generalization of a paired analysis, in which comparisons between pull-downs at different time points are made within each run.

Limma employs an empirical Bayes method to moderate the standard errors of the estimated $\log_2$ fold changes; this results in more stable inference and improved power, especially for experiments with small numbers of replicates.

Multiple testing correction of p-values was applied using the Benjamini-Hochberg method to control the false discovery rate (FDR). The adjusted p-value (also known as a q-value) can be understood as follows. If all proteins with q-value below a threshold of 0.05 are selected as differentially expressed, then the expected proportion of false discoveries in the selected group is controlled to be less than the threshold value, in this case 5%.

The B-statistic (lods or B) is the log odds that the protein is differentially expressed. For example, if B = 1.5, the odds of differential expression is $e^{1.5} = 4.48$, i.e, about four and a half to one. The probability that the protein is differentially expressed is $4.48/(1 + 4.48) = 0.82$. A B-statistic of zero corresponds to a 50-50 chance that the gene is differentially expressed. The B-statistic has been automatically adjusted for multiple testing by assuming that 1% of the proteins are expected to be differentially expressed.

The IgG control was used to assess non-specific binding. The binding of a protein is considered to be non-specific if the $\log_2$ fold change relative to the IgG control is less than 1. In the differential binding analysis, protein intensity values are fitted to a linear model and the fitted values for each condition being compared are also compared to the IgG control. For each comparison of two groups, the maximum $\log_2$ fold change from each of the two groups above the IgG control is used to determine if the binding is specific.

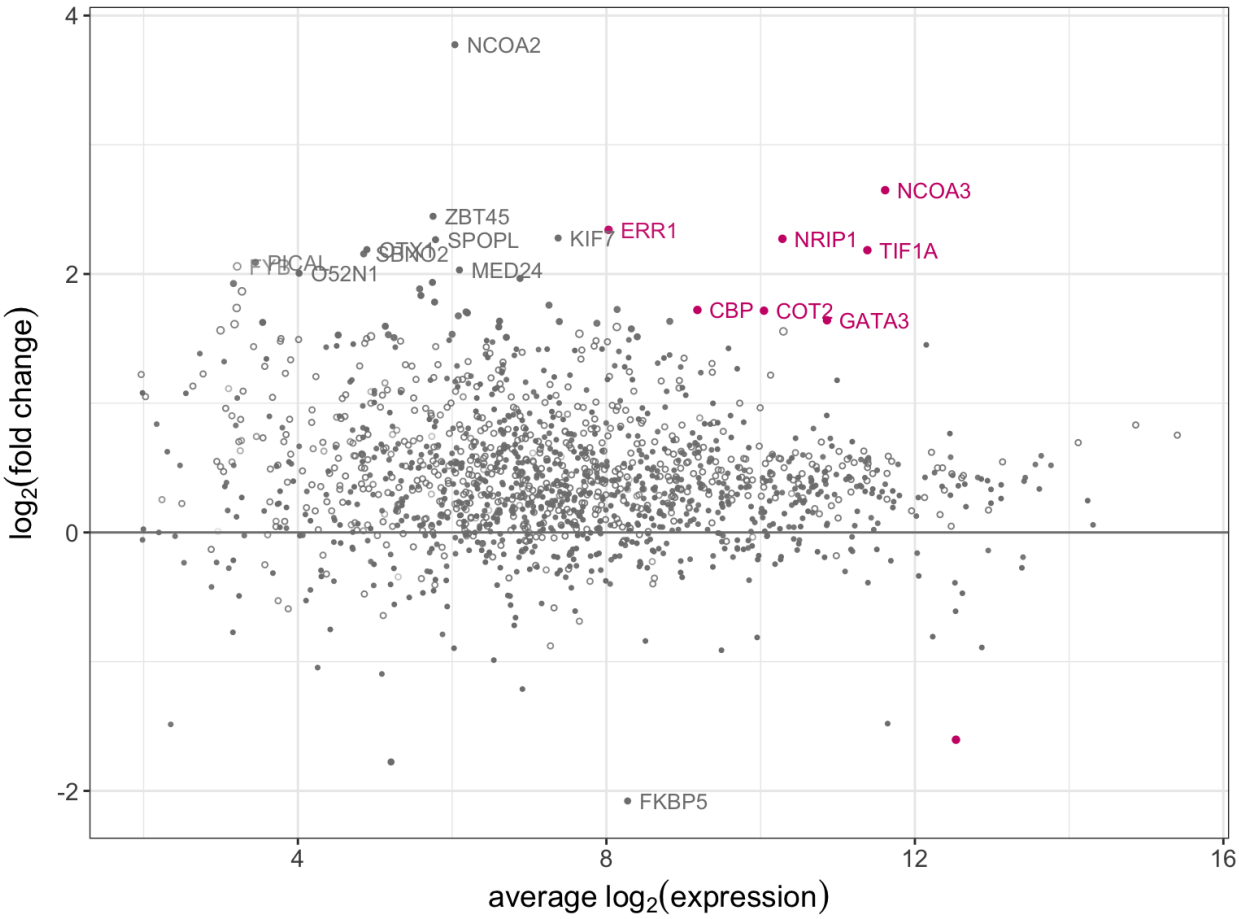


Figure 48: MA plot of the average intensity against log 2 fold change for the ER 45min vs ER 0min comparison (excluding peptides with missing intensities, no normalization). Top ranking differentially-expressed proteins with false discovery rate below 0.05 are highlighted in pink. Open circles indicate that the protein is non-specific from the IgG control comparison.

#### 4.6.1 ER 45min vs ER 0min, excluding peptides with missing intensities, no normalization

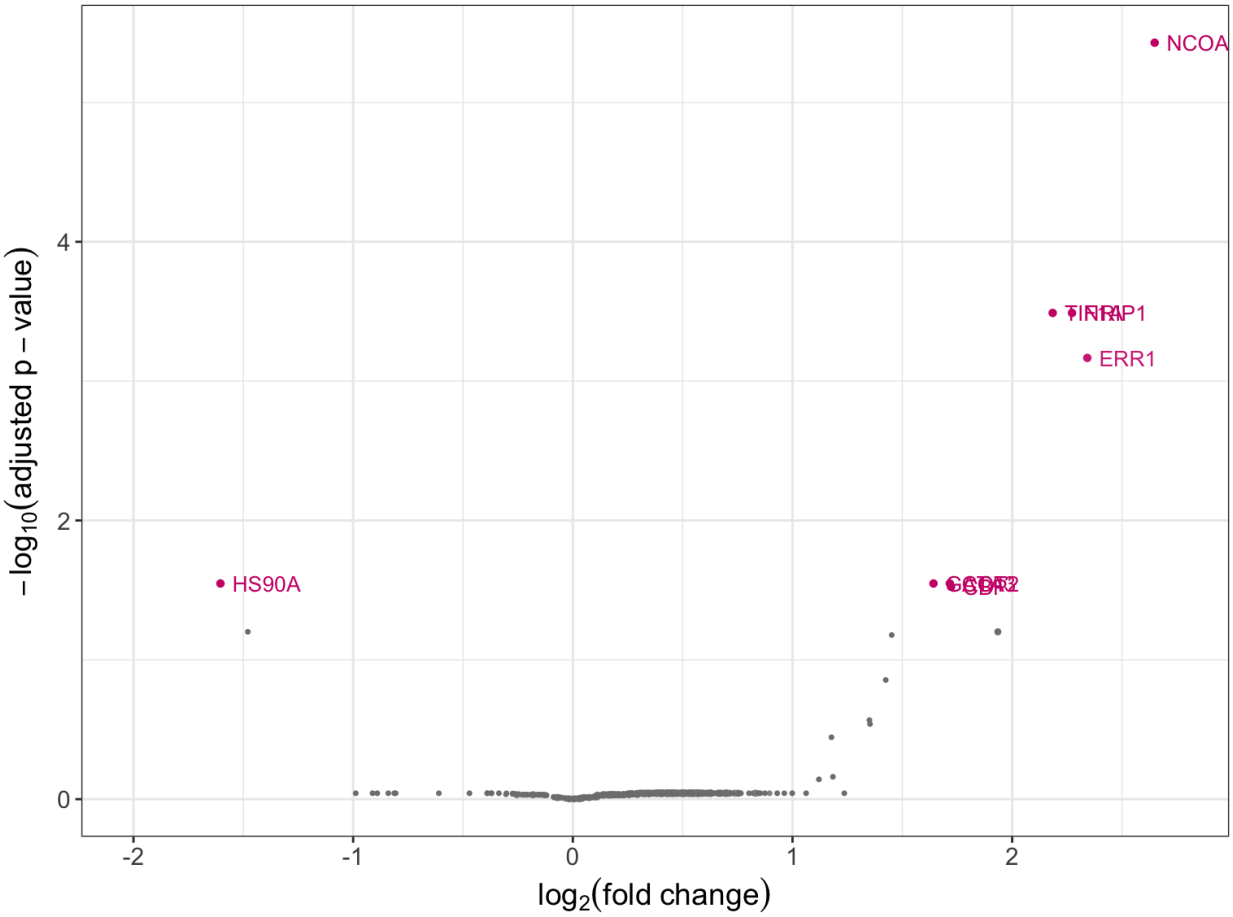


Figure 49: Volcano plot of the average intensity against log 2 fold change for the ER 45min vs ER 0min comparison (excluding peptides with missing intensities, no normalization). Top ranking differentially-expressed proteins with false discovery rate below 0.05 are highlighted in pink. Open circles indicate that the protein is non-specific from the IgG control comparison.

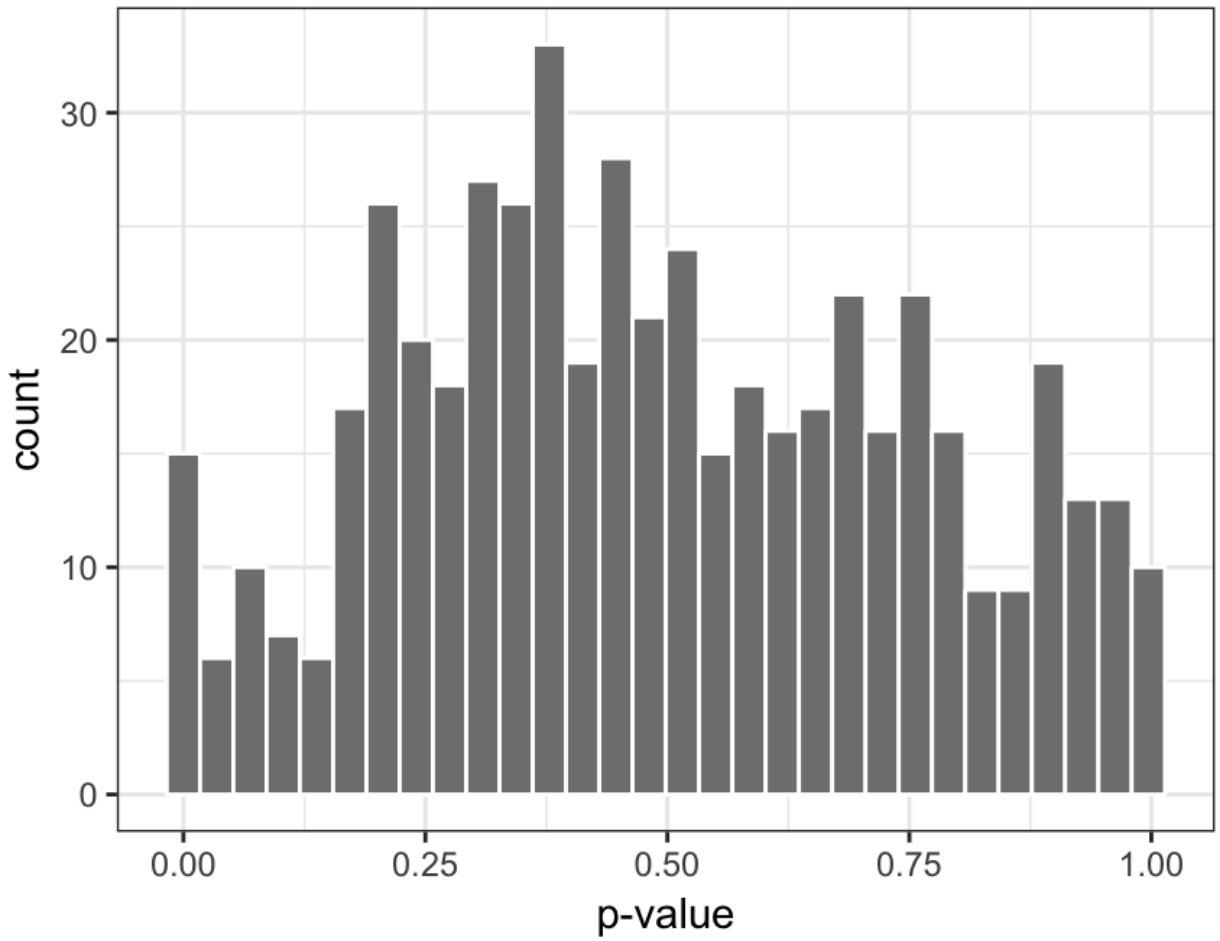


Figure 50: Histogram of p-values for the ER 45min vs ER 0min comparison (excluding peptides with missing intensities, no normalization)

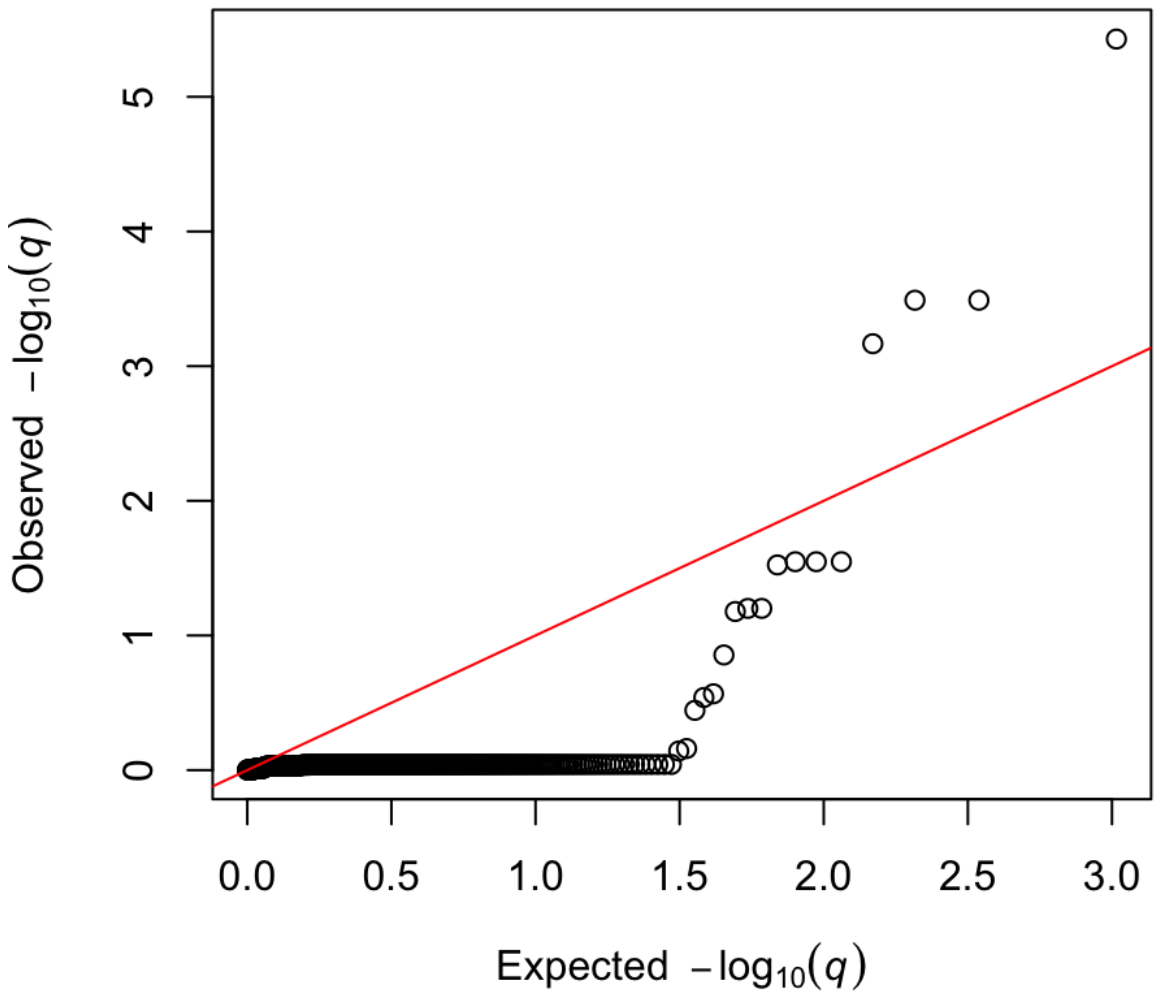


Figure 51: QQ plot of the adjusted p-values for the ER 45min vs ER 0min comparison (excluding peptides with missing intensities, no normalization)

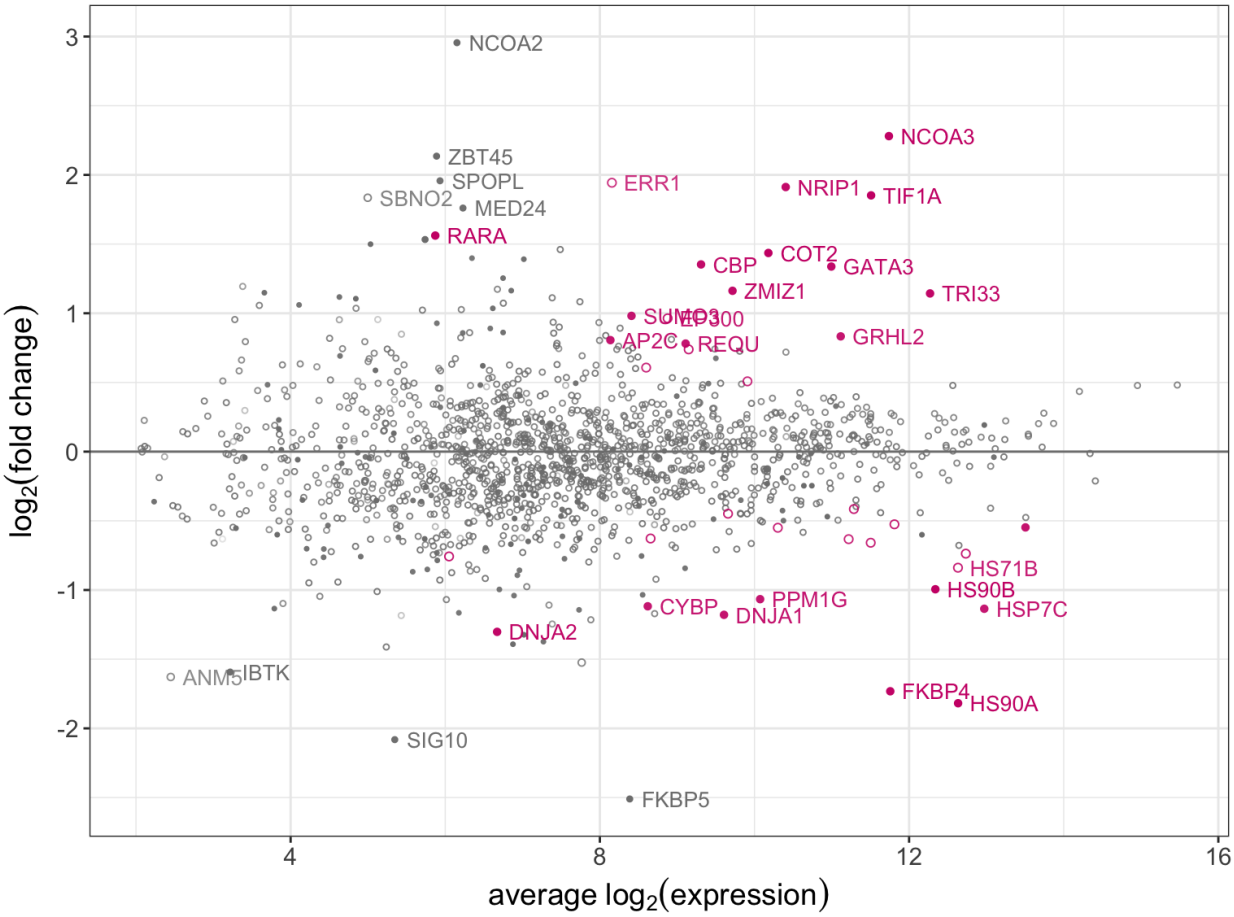


Figure 52: MA plot of the average intensity against log 2 fold change for the ER 45min vs ER 0min comparison (excluding peptides with missing intensities, quantile normalization). Top ranking differentially-expressed proteins with false discovery rate below 0.05 are highlighted in pink. Open circles indicate that the protein is non-specific from the IgG control comparison.

#### 4.6.2 ER 45min vs ER 0min, excluding peptides with missing intensities, quantile normalization

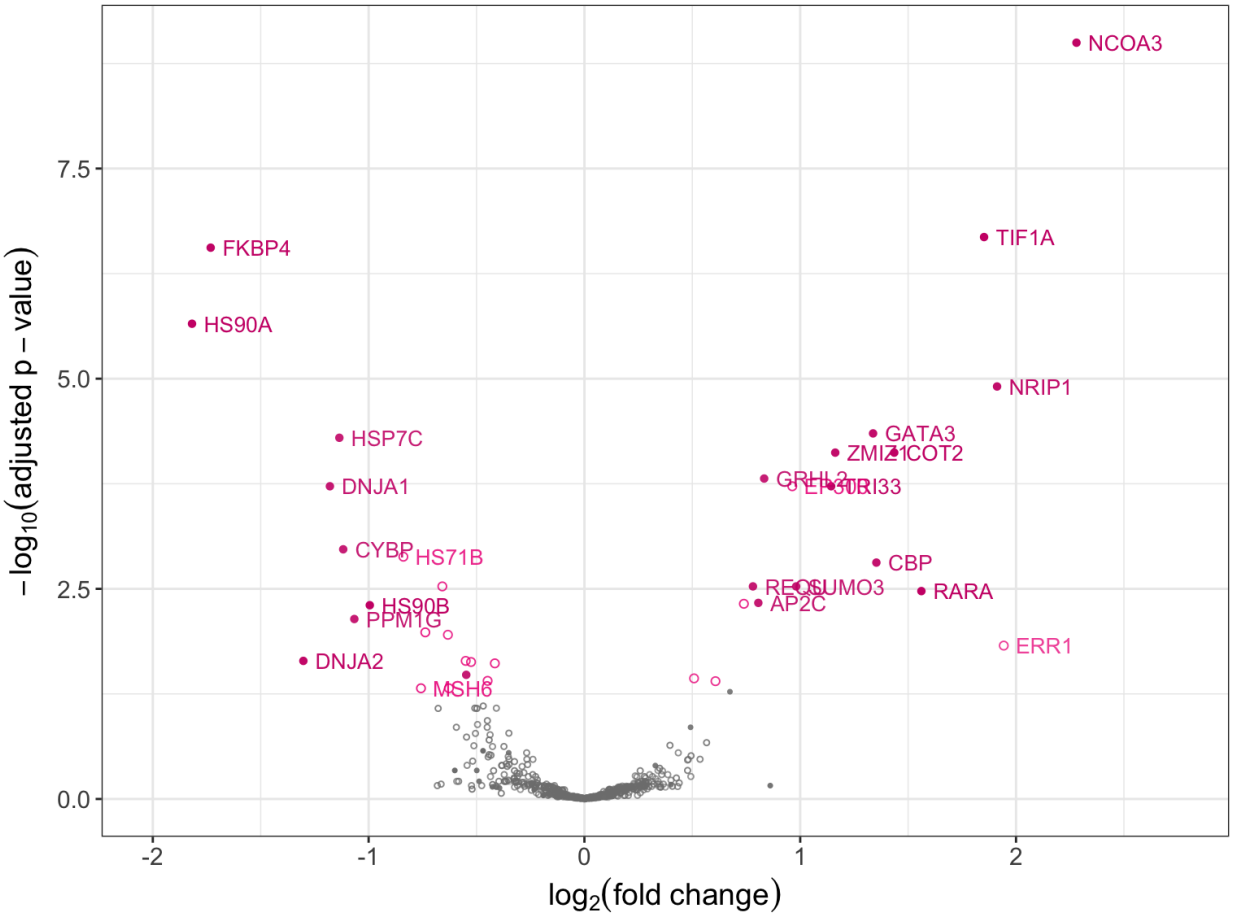


Figure 53: Volcano plot of the average intensity against log 2 fold change for the ER 45min vs ER 0min comparison (excluding peptides with missing intensities, quantile normalization). Top ranking differentially-expressed proteins with false discovery rate below 0.05 are highlighted in pink. Open circles indicate that the protein is non-specific from the IgG control comparison.

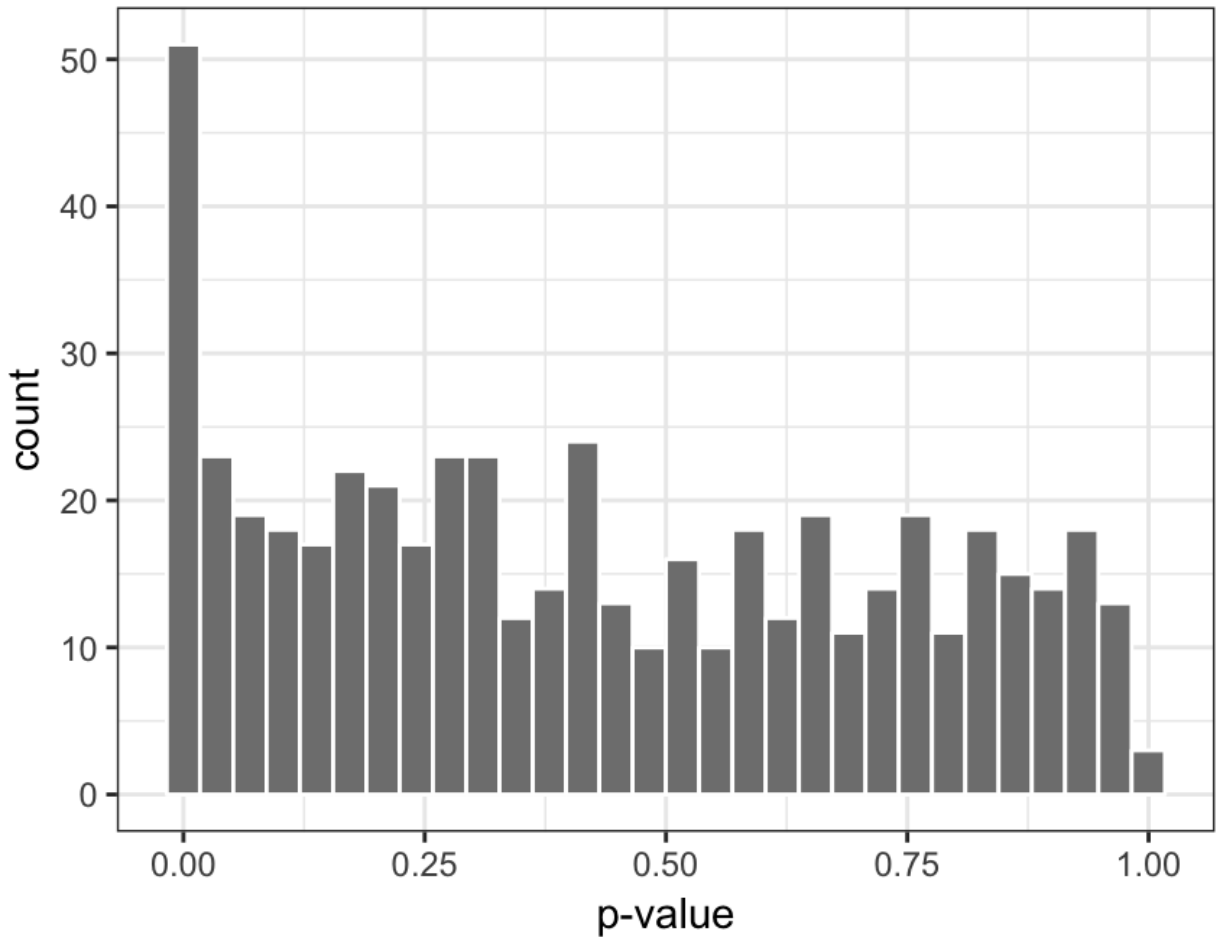


Figure 54: Histogram of p-values for the ER 45min vs ER 0min comparison (excluding peptides with missing intensities, quantile normalization)

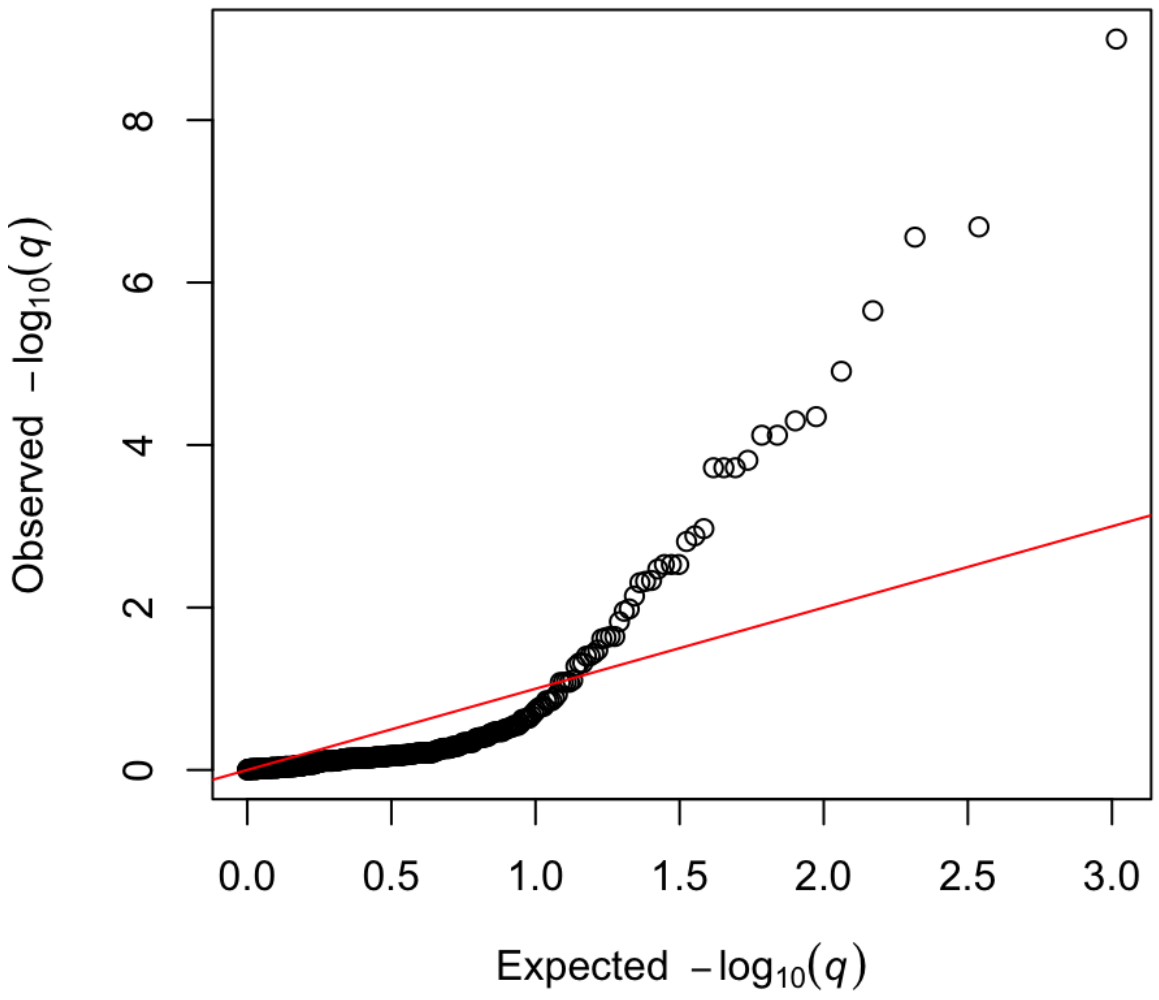


Figure 55: QQ plot of the adjusted p-values for the ER 45min vs ER 0min comparison (excluding peptides with missing intensities, quantile normalization)

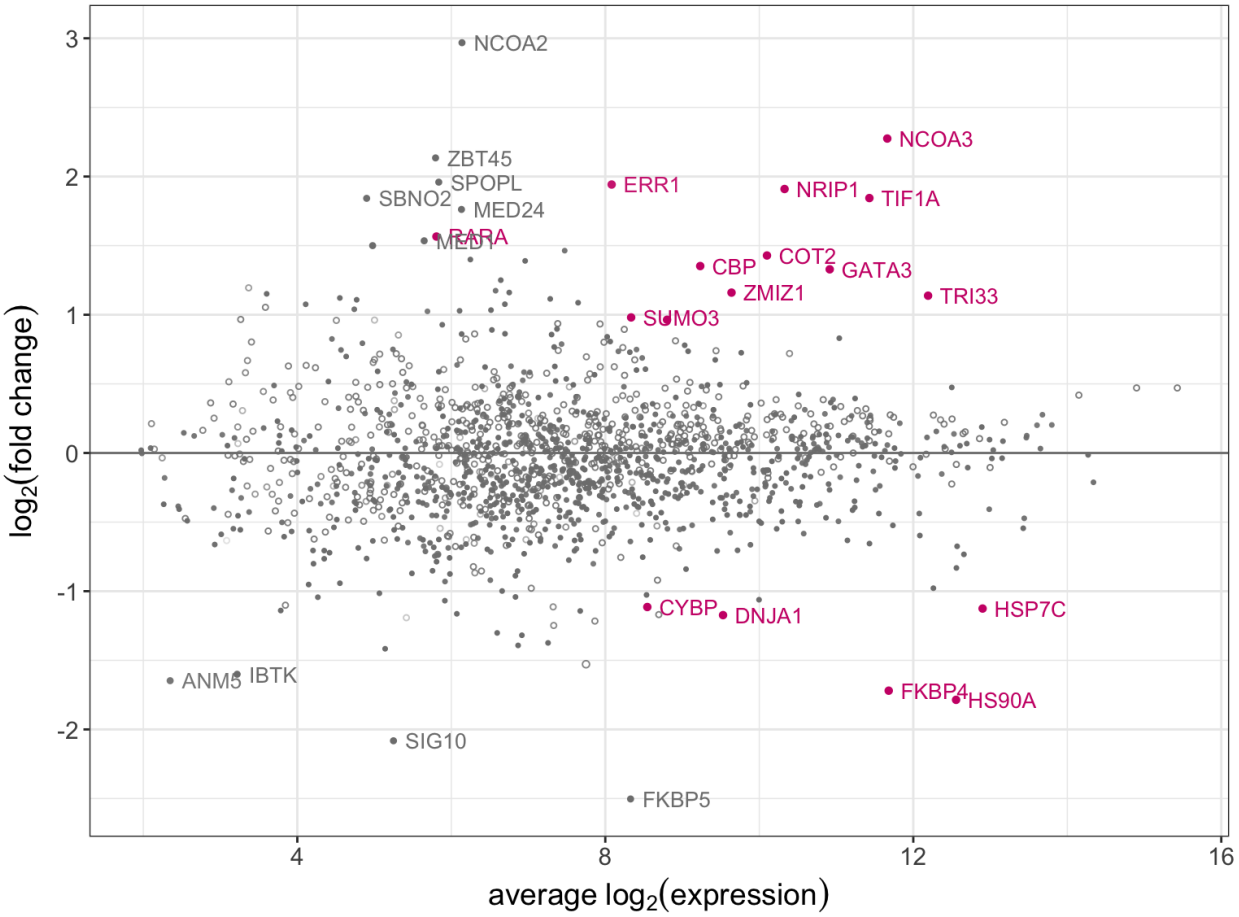


Figure 56: MA plot of the average intensity against log 2 fold change for the ER 45min vs ER 0min comparison (excluding peptides with missing intensities, quantile normalization excluding IgG control). Top ranking differentially-expressed proteins with false discovery rate below 0.05 are highlighted in pink. Open circles indicate that the protein is non-specific from the IgG control comparison.

#### 4.6.3 ER 45min vs ER 0min, excluding peptides with missing intensities, quantile normalization excluding IgG control

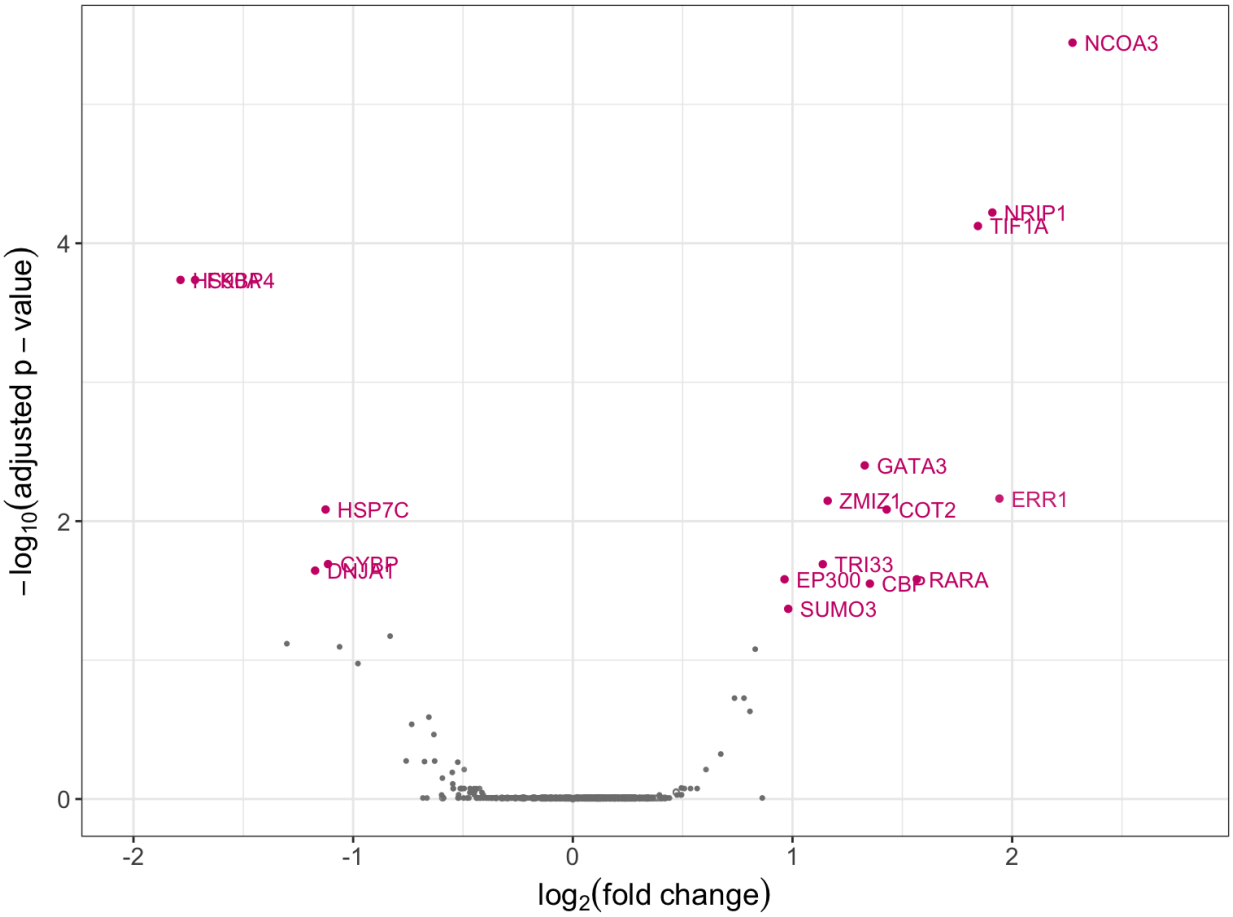


Figure 57: Volcano plot of the average intensity against log 2 fold change for the ER 45min vs ER 0min comparison (excluding peptides with missing intensities, quantile normalization excluding IgG control). Top ranking differentially-expressed proteins with false discovery rate below 0.05 are highlighted in pink. Open circles indicate that the protein is non-specific from the IgG control comparison.

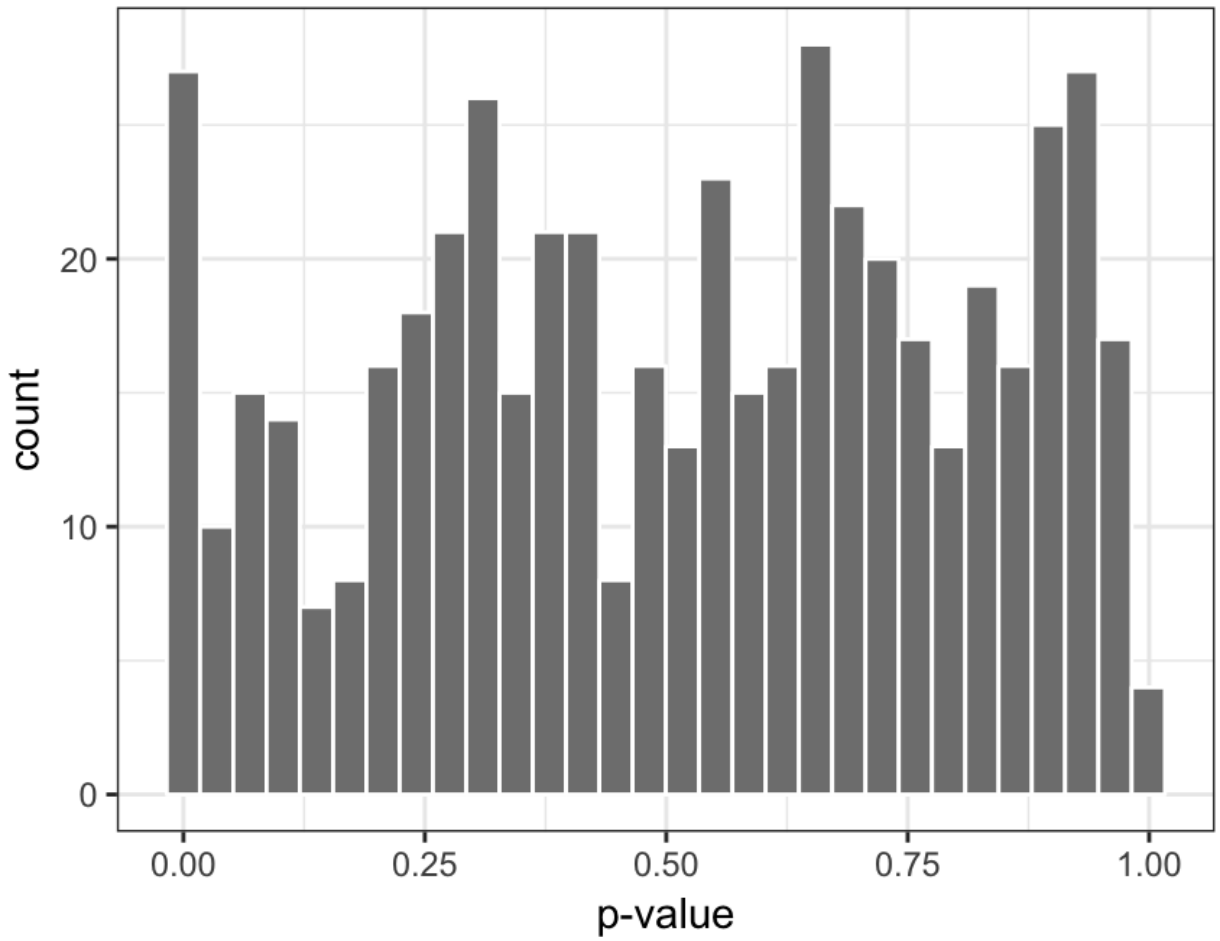


Figure 58: Histogram of p-values for the ER 45min vs ER 0min comparison (excluding peptides with missing intensities, quantile normalization excluding IgG control)

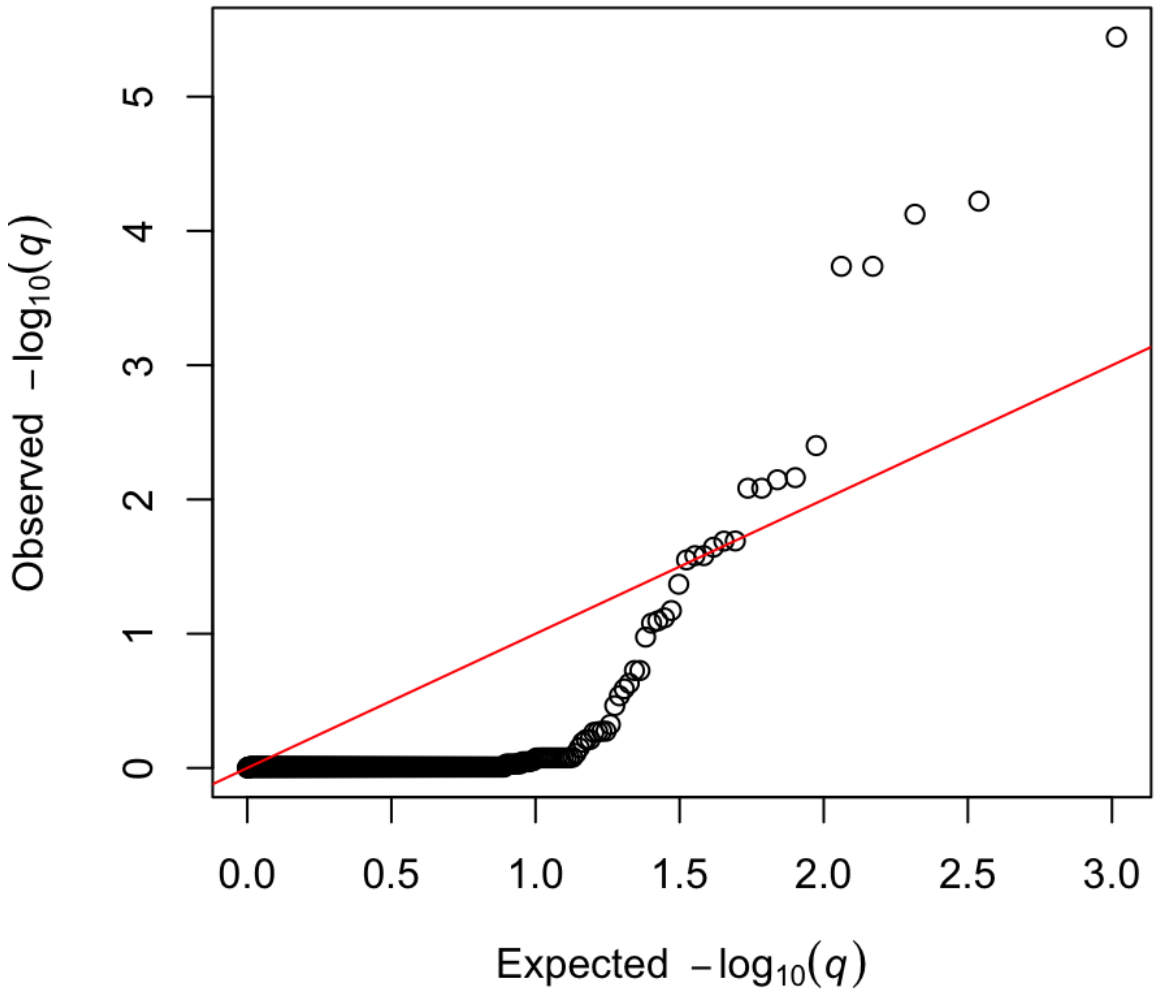


Figure 59: QQ plot of the adjusted p-values for the ER 45min vs ER 0min comparison (excluding peptides with missing intensities, quantile normalization excluding IgG control)

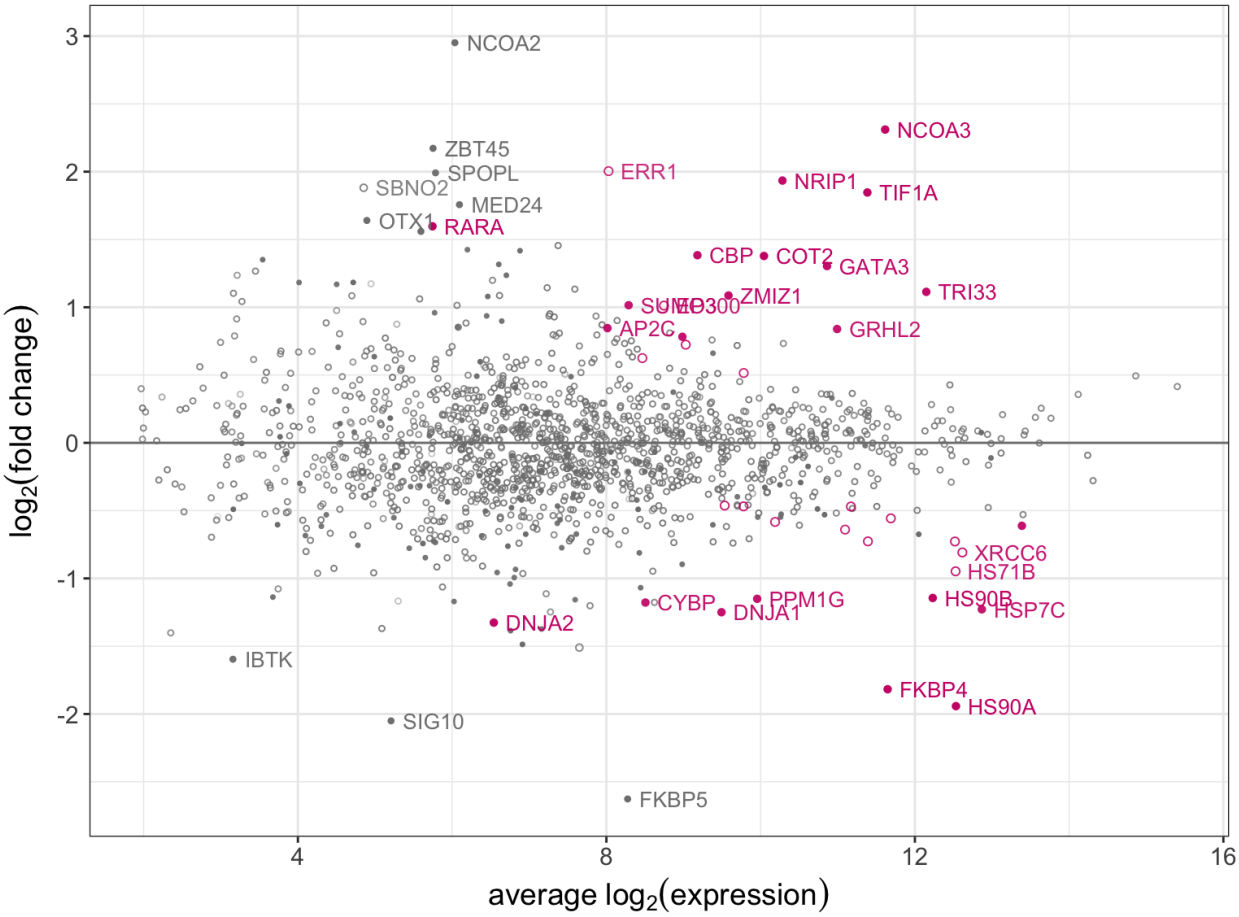


Figure 60: MA plot of the average intensity against log 2 fold change for the ER 45min vs ER 0min comparison (excluding peptides with missing intensities, scale normalization). Top ranking differentially-expressed proteins with false discovery rate below 0.05 are highlighted in pink. Open circles indicate that the protein is non-specific from the IgG control comparison.

#### 4.6.4 ER 45min vs ER 0min, excluding peptides with missing intensities, scale normalization

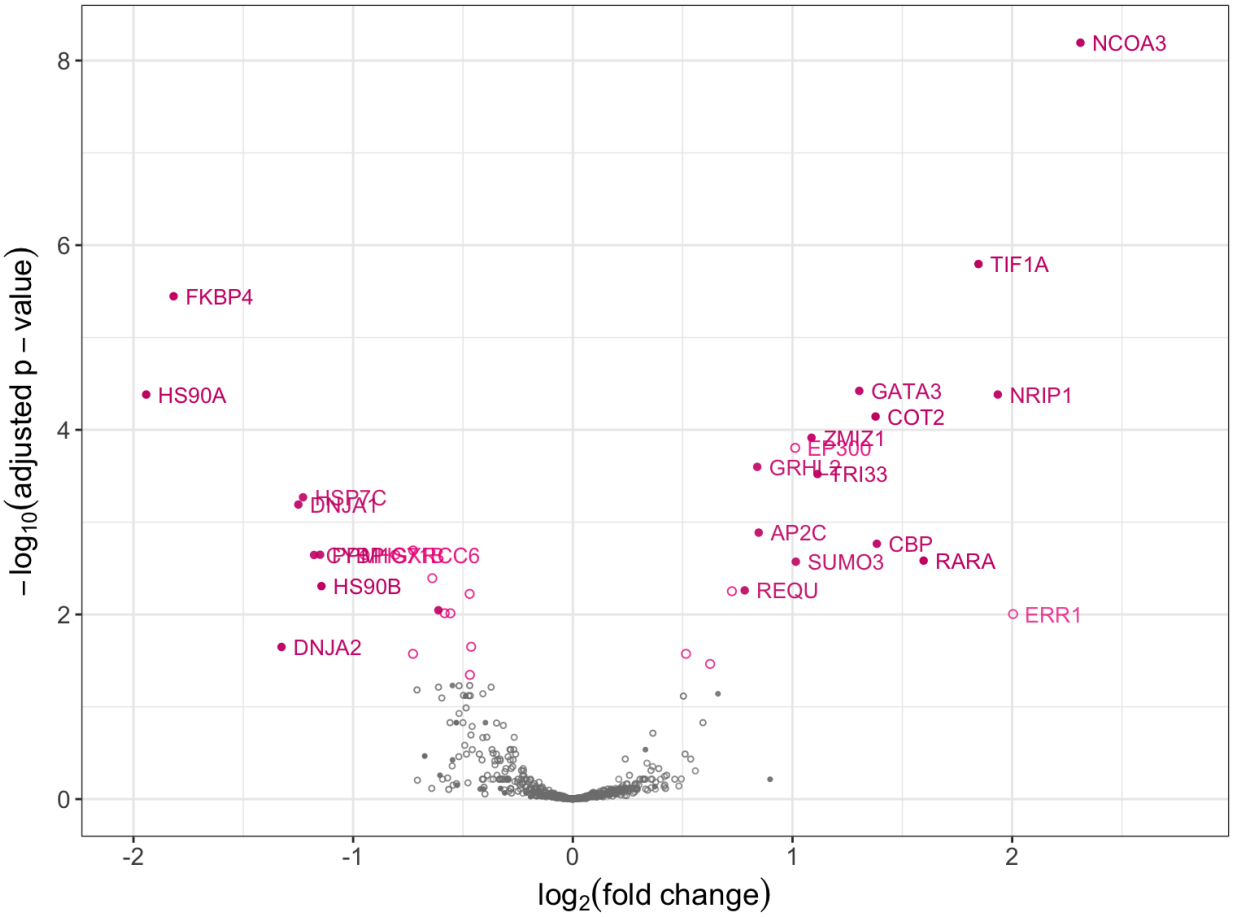


Figure 61: Volcano plot of the average intensity against log 2 fold change for the ER 45min vs ER 0min comparison (excluding peptides with missing intensities, scale normalization). Top ranking differentially-expressed proteins with false discovery rate below 0.05 are highlighted in pink. Open circles indicate that the protein is non-specific from the IgG control comparison.

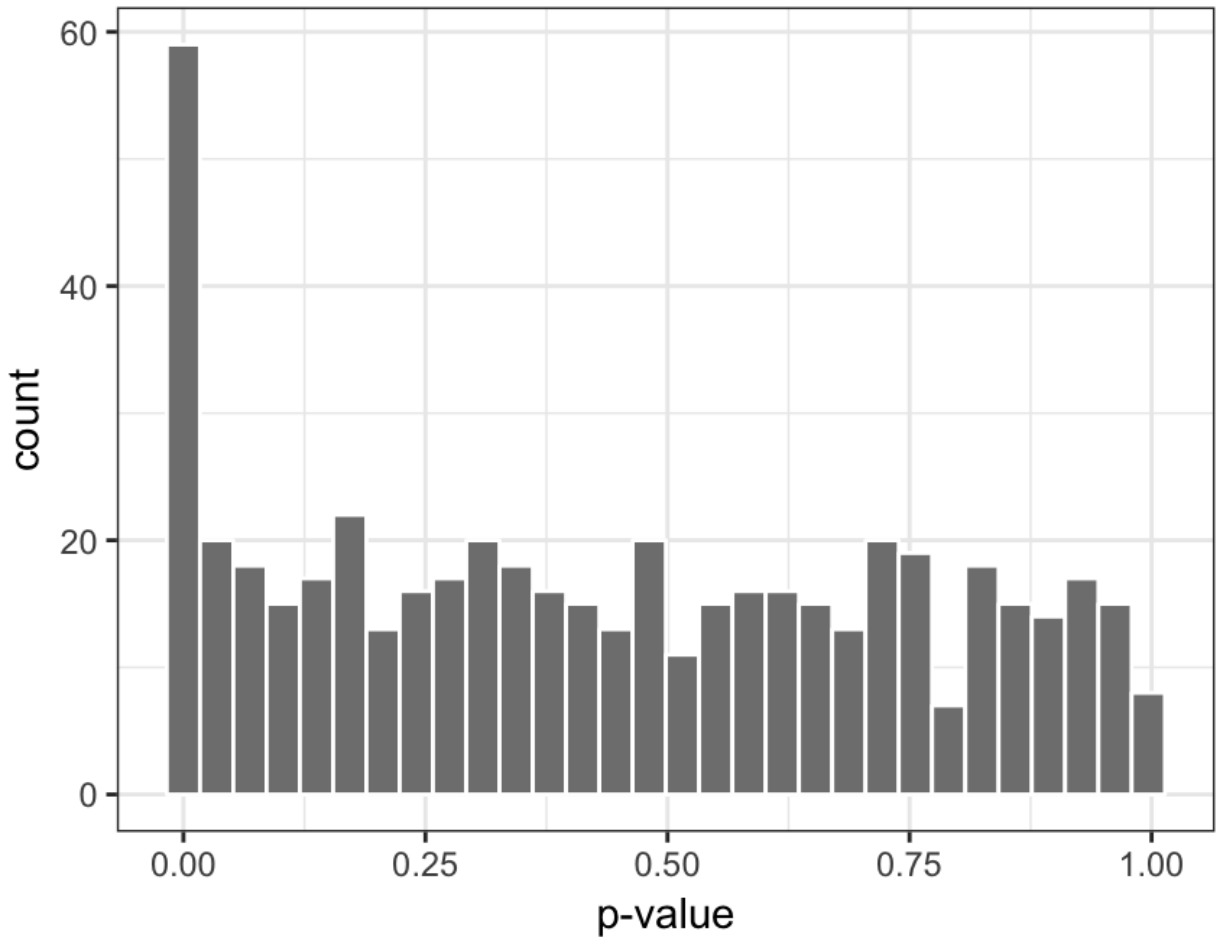


Figure 62: Histogram of p-values for the ER 45min vs ER 0min comparison (excluding peptides with missing intensities, scale normalization)

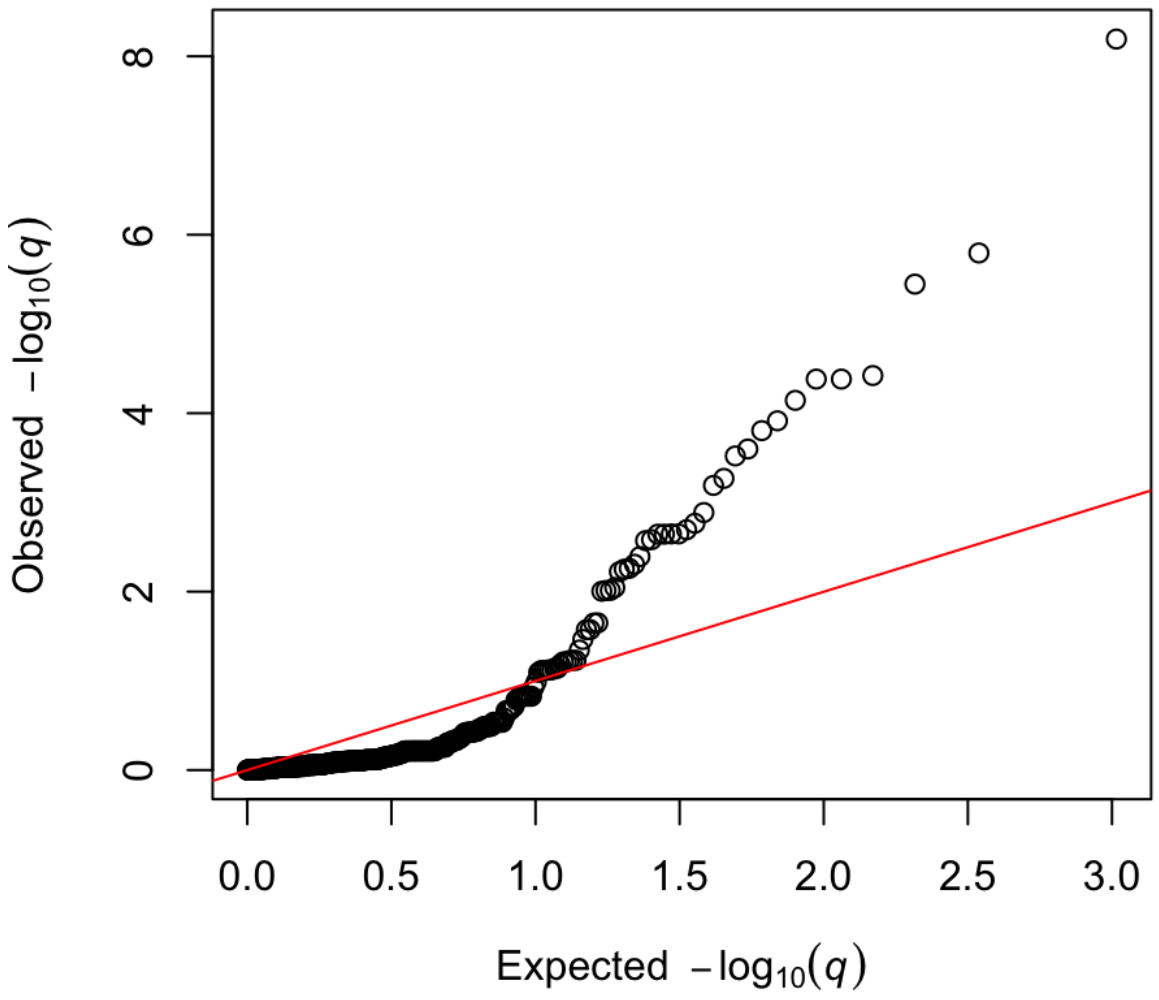


Figure 63: QQ plot of the adjusted p-values for the ER 45min vs ER 0min comparison (excluding peptides with missing intensities, scale normalization)

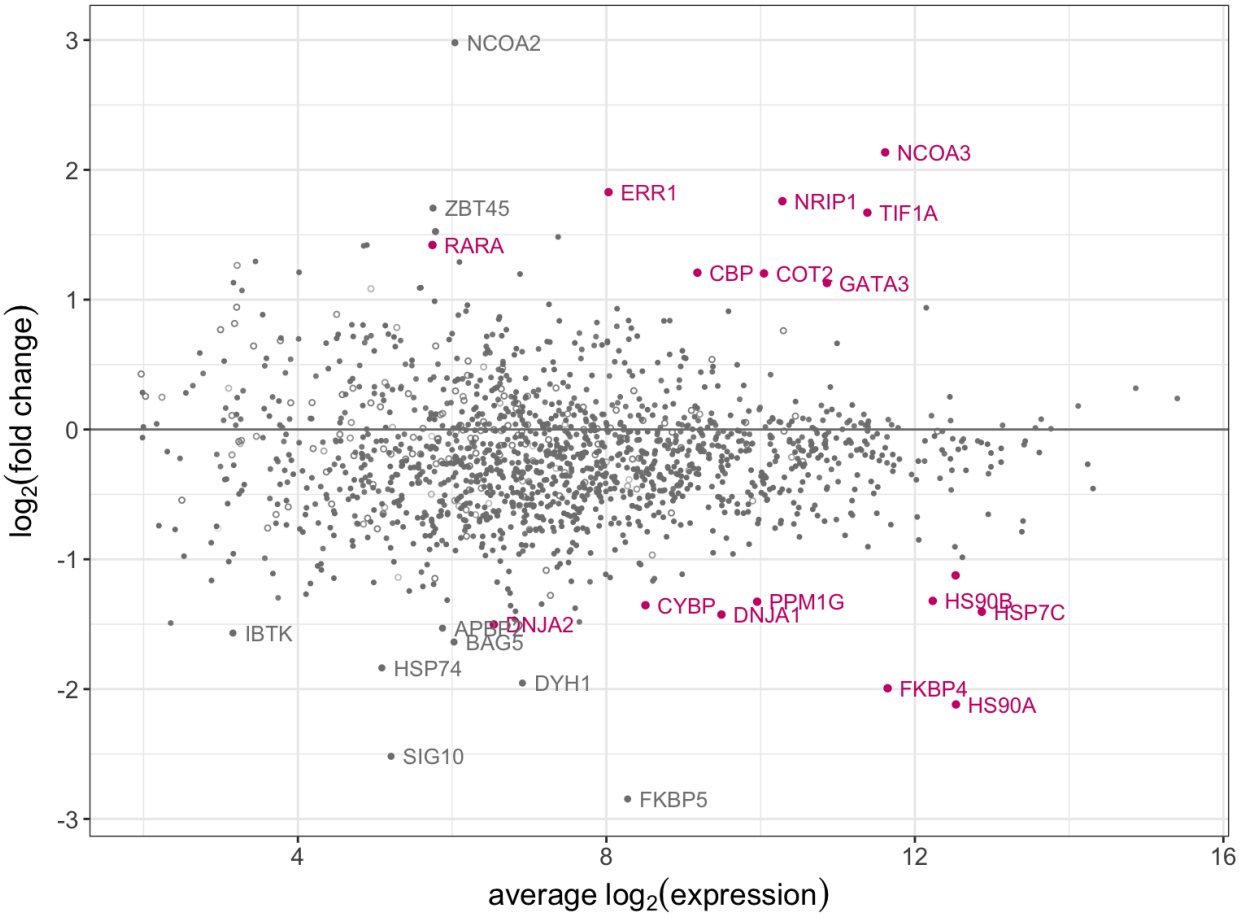


Figure 64: MA plot of the average intensity against log 2 fold change for the ER 45min vs ER 0min comparison (excluding peptides with missing intensities, scale normalization using top 10 IgG peptides). Top ranking differentially-expressed proteins with false discovery rate below 0.05 are highlighted in pink. Open circles indicate that the protein is non-specific from the IgG control comparison.

#### 4.6.5 ER 45min vs ER 0min, excluding peptides with missing intensities, scale normalization using top 10 IgG peptides

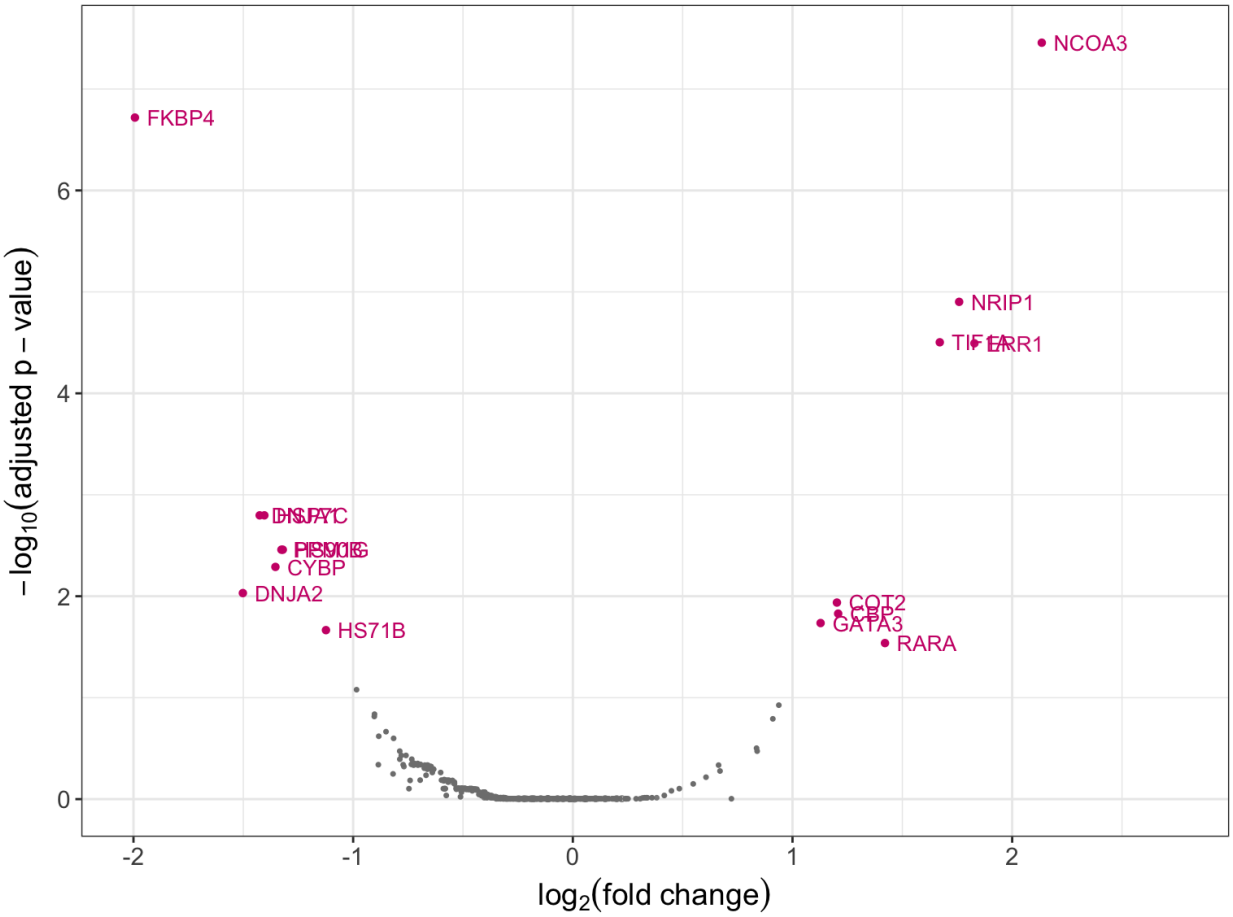


Figure 65: Volcano plot of the average intensity against log 2 fold change for the ER 45min vs ER 0min comparison (excluding peptides with missing intensities, scale normalization using top 10 IgG peptides). Top ranking differentially-expressed proteins with false discovery rate below 0.05 are highlighted in pink. Open circles indicate that the protein is non-specific from the IgG control comparison.

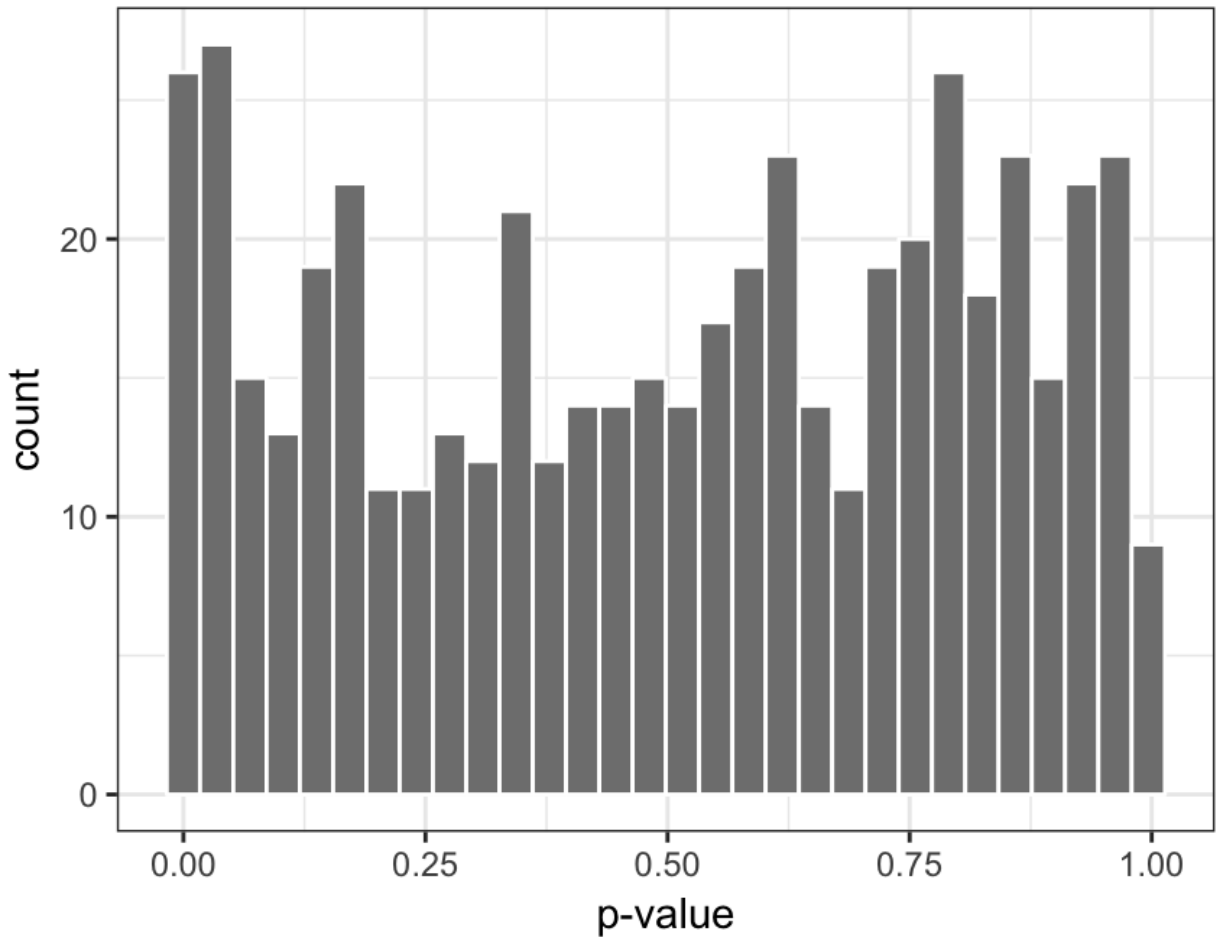


Figure 66: Histogram of p-values for the ER 45min vs ER 0min comparison (excluding peptides with missing intensities, scale normalization using top 10 IgG peptides)

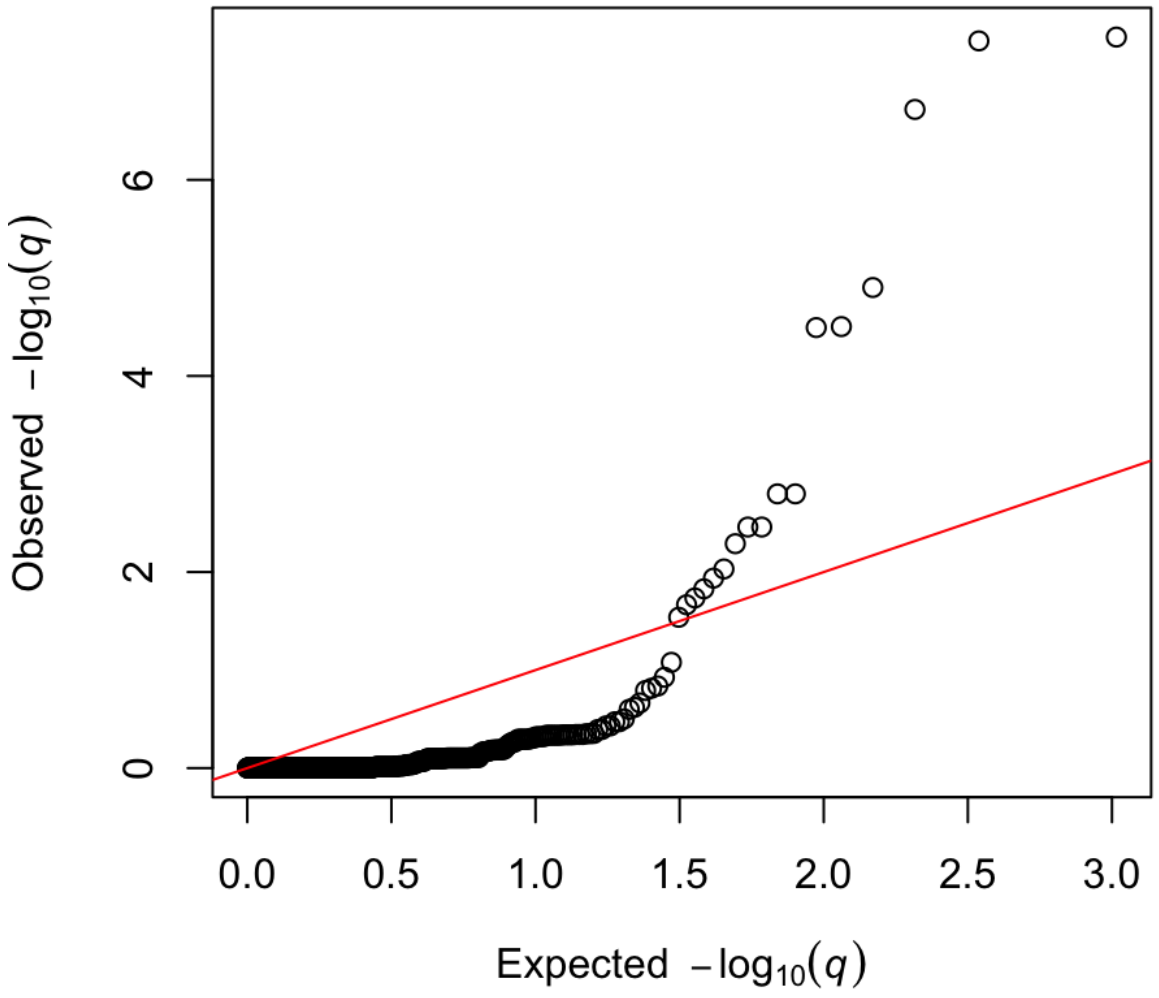


Figure 67: QQ plot of the adjusted p-values for the ER 45min vs ER 0min comparison (excluding peptides with missing intensities, scale normalization using top 10 IgG peptides)

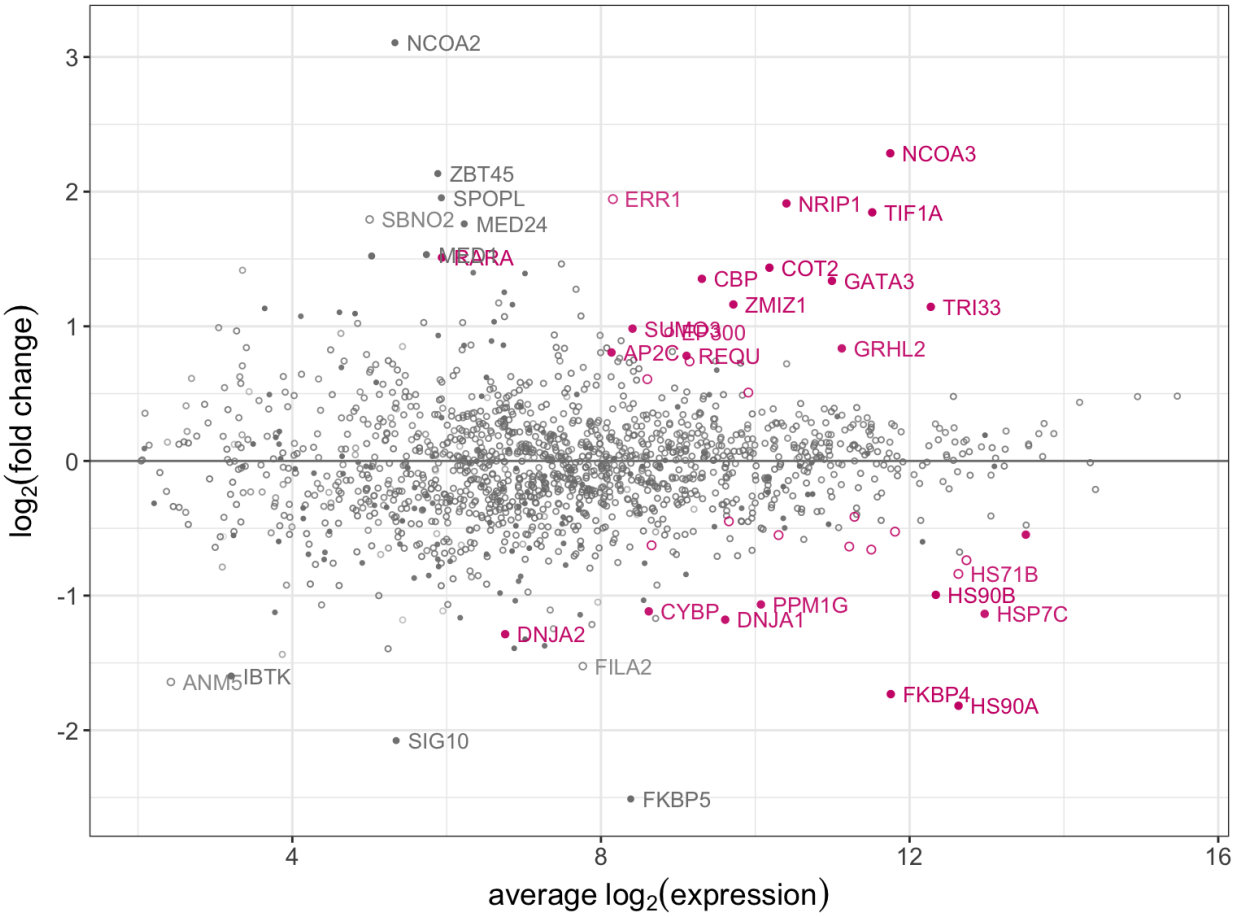


Figure 68: MA plot of the average intensity against log 2 fold change for the ER 45min vs ER 0min comparison (KNN nearest neighbour averaging imputation of missing values, quantile normalization). Top ranking differentially-expressed proteins with false discovery rate below 0.05 are highlighted in pink. Open circles indicate that the protein is non-specific from the IgG control comparison.

#### 4.6.6 ER 45min vs ER 0min, KNN nearest neighbour averaging imputation of missing values, quantile normalization

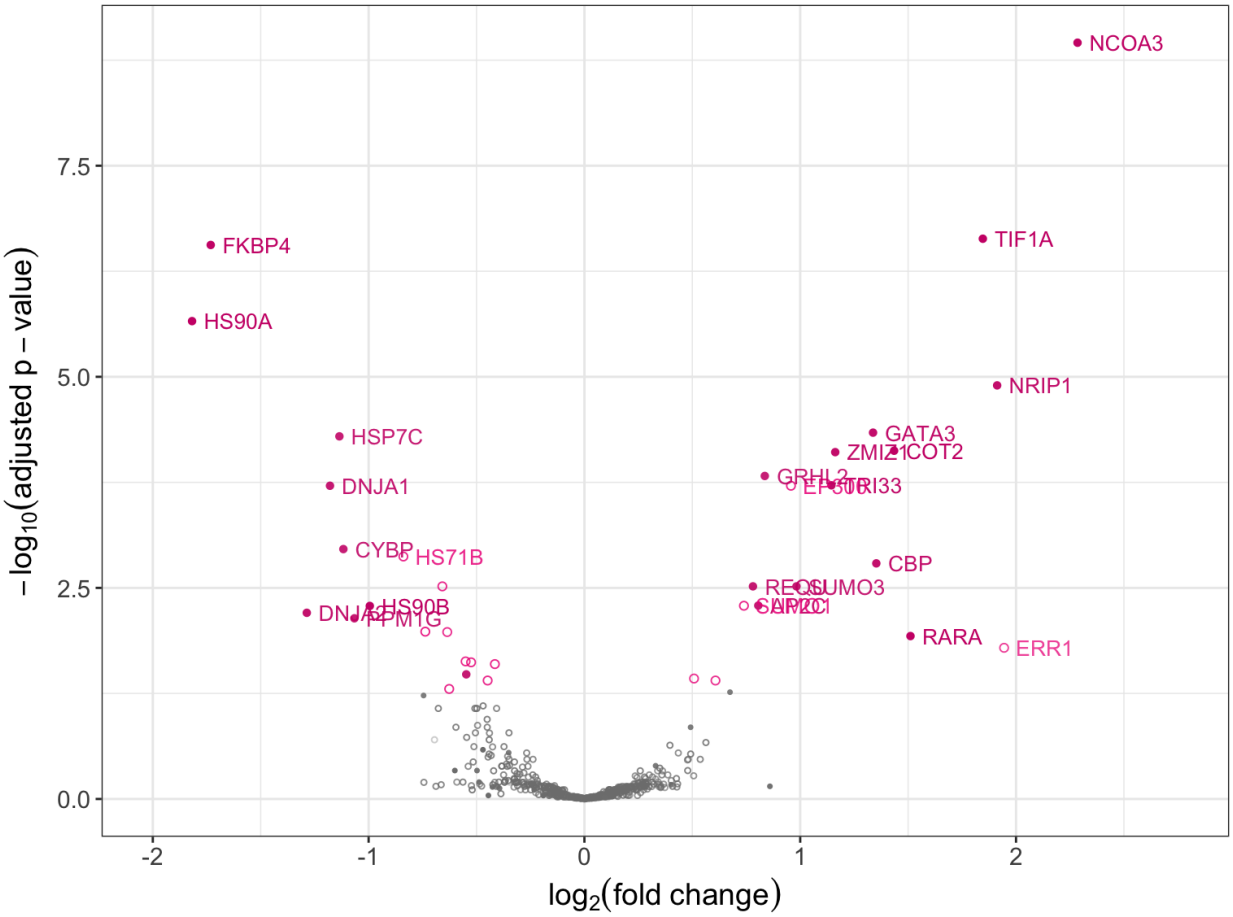


Figure 69: Volcano plot of the average intensity against log 2 fold change for the ER 45min vs ER 0min comparison (KNN nearest neighbour averaging imputation of missing values, quantile normalization). Top ranking differentially-expressed proteins with false discovery rate below 0.05 are highlighted in pink. Open circles indicate that the protein is non-specific from the IgG control comparison.

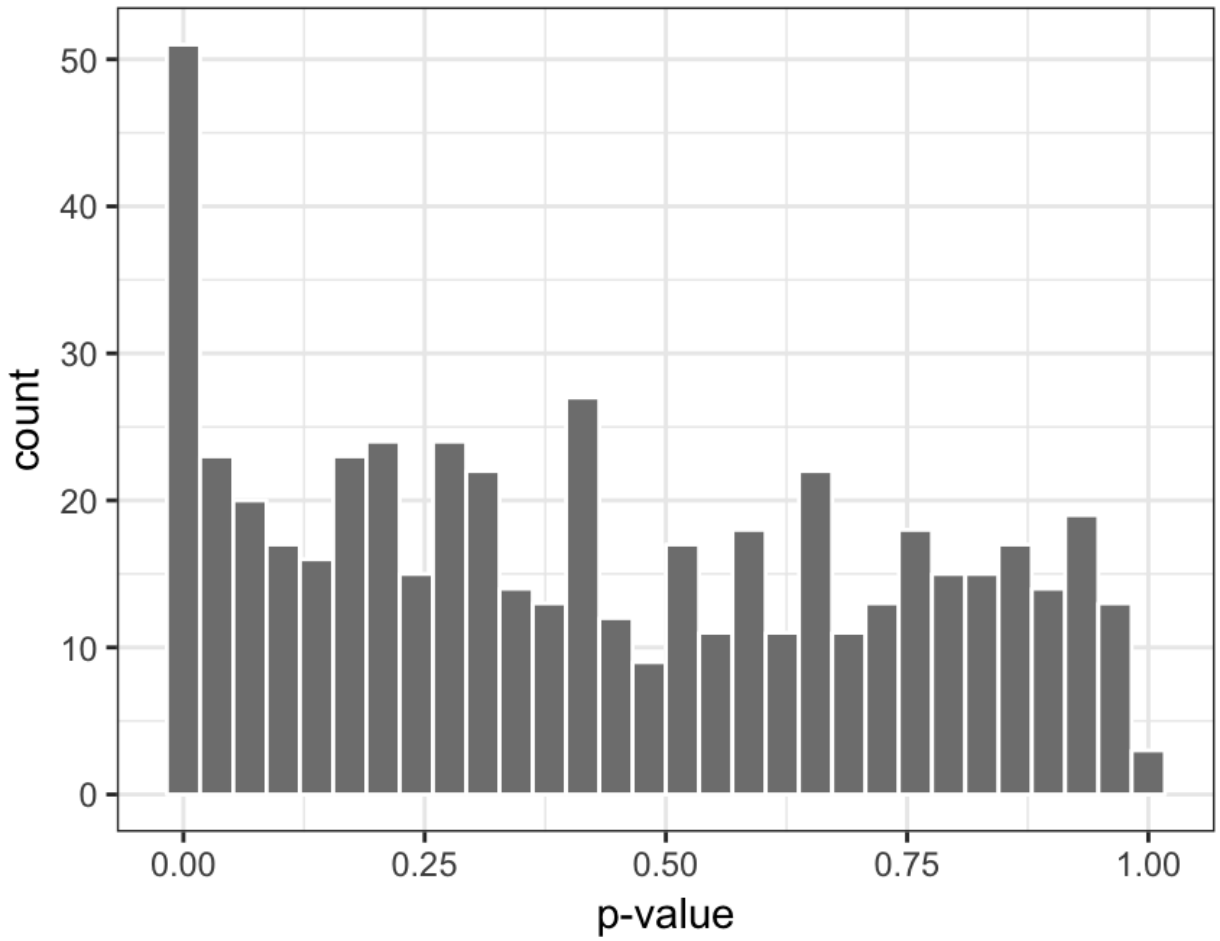


Figure 70: Histogram of p-values for the ER 45min vs ER 0min comparison (KNN nearest neighbour averaging imputation of missing values, quantile normalization)

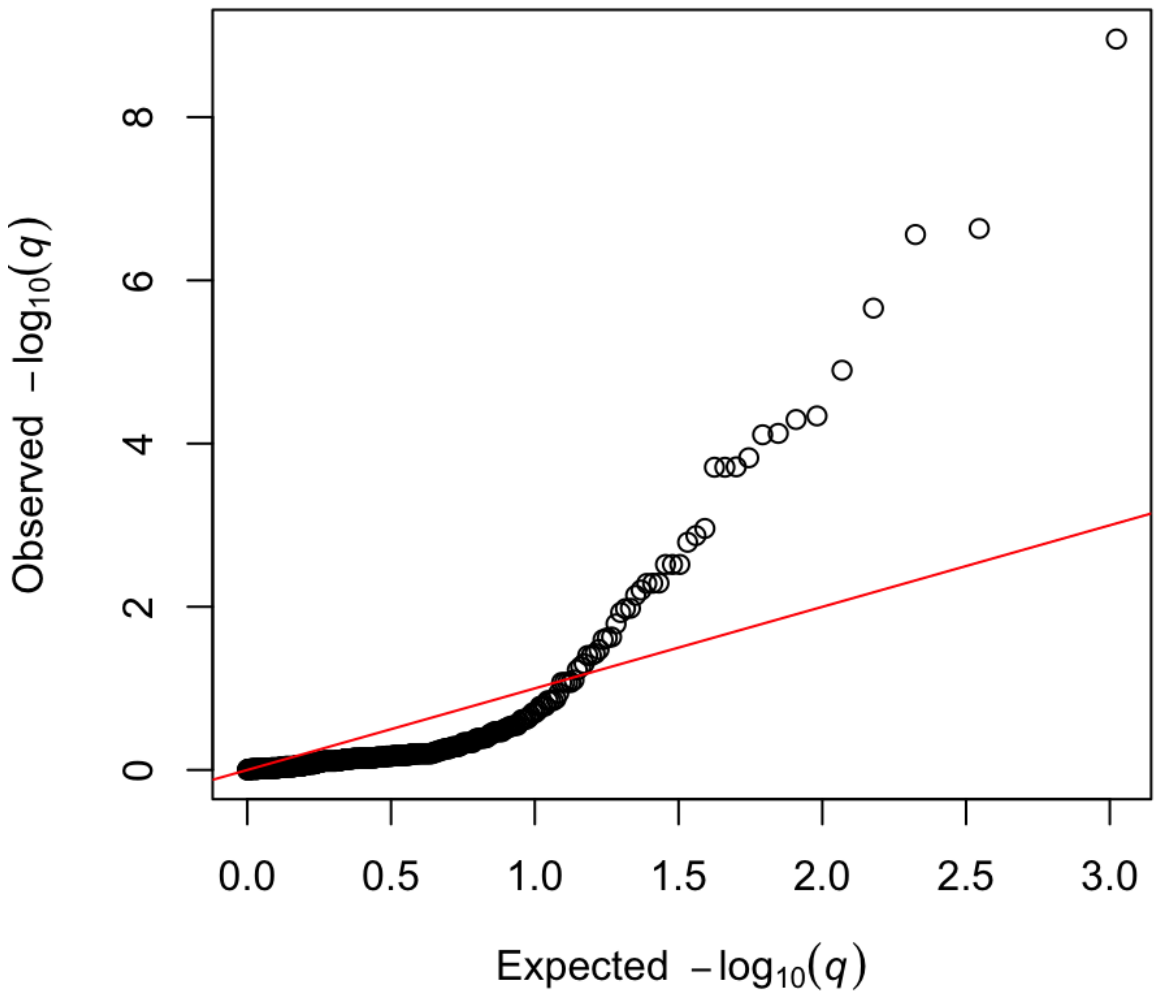


Figure 71: QQ plot of the adjusted p-values for the ER 45min vs ER 0min comparison (KNN nearest neighbour averaging imputation of missing values, quantile normalization)

## 4.7 Comparison of differential binding analysis approaches

In this section, comparisons of the differential binding results obtained using differing methods for handling missing values and varying normalization techniques are presented. The B-statistic (log odds) is used to rank the proteins from most significantly differentially expressed to least significant. Scatter plots of both the B-statistic generated for the two methods being compared and the rank are presented. The protein with the highest B-statistic, i.e. the most significantly differentially expressed protein, is given a rank of 1.

Differing imputation methods have relatively little effect on the results for most proteins. This is largely because only a small proportion of the proteins have peptide-level measurements containing missing values. There are a few proteins that are only represented in the differential binding results when imputation is carried out, for which all peptide-level measurements contain missing values. These proteins are not represented in the comparions with the analysis in which measurements with missing values are removed.

Different normalization approaches have a more substantial impact on the differential binding analysis.

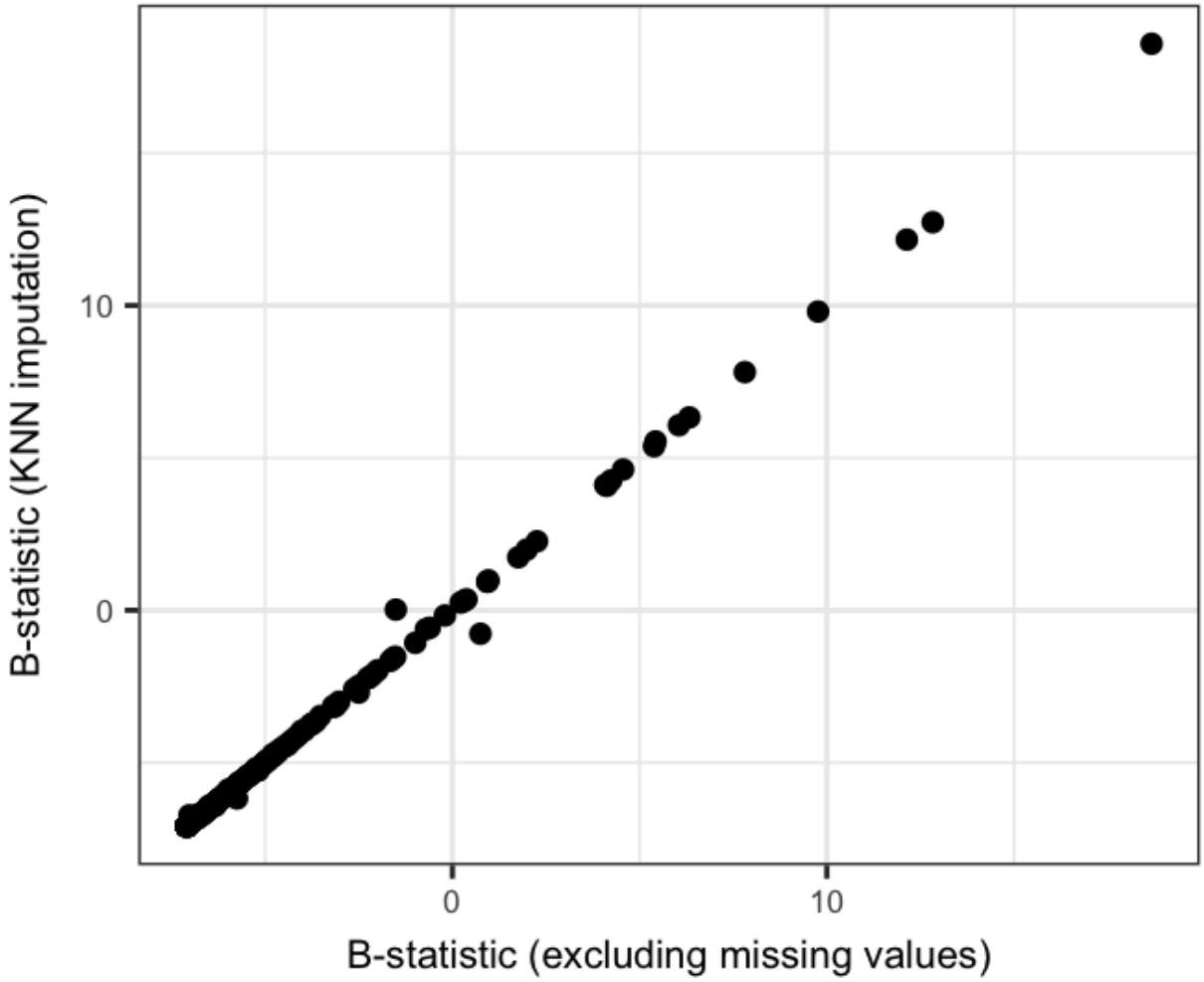


Figure 72: Plot of B-statistic (log odds) for differential expression of proteins for the ER 45min vs ER 0min contrast, comparing results following exclusion of missing values and KNN imputation.

#### 4.7.1 Removal of missing values vs KNN imputation (quantile normalization in both)

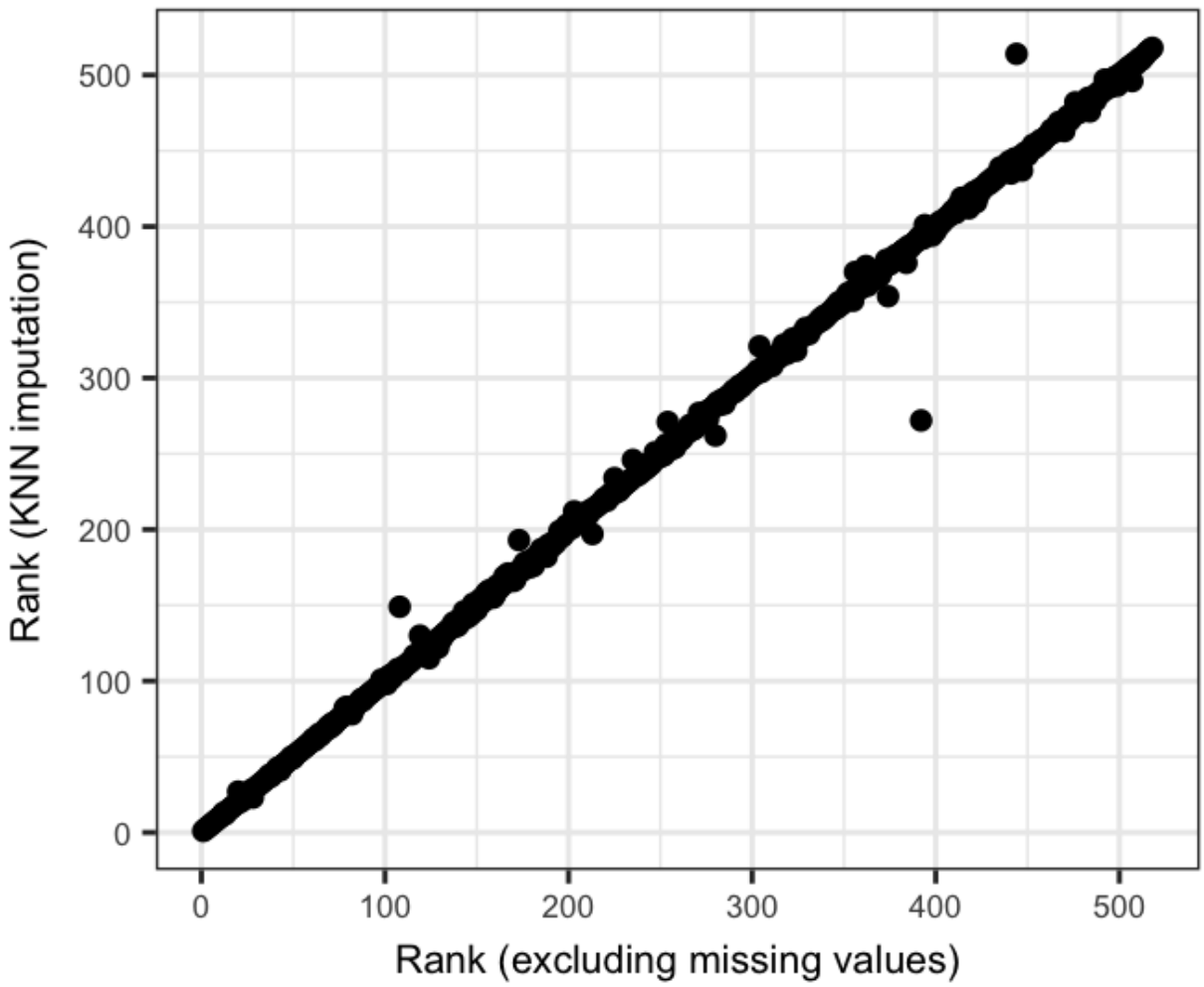


Figure 73: Plot of the rank of differentially-expressed proteins for the ER 45min vs ER 0min contrast, comparing results following exclusion of missing values and KNN imputation.

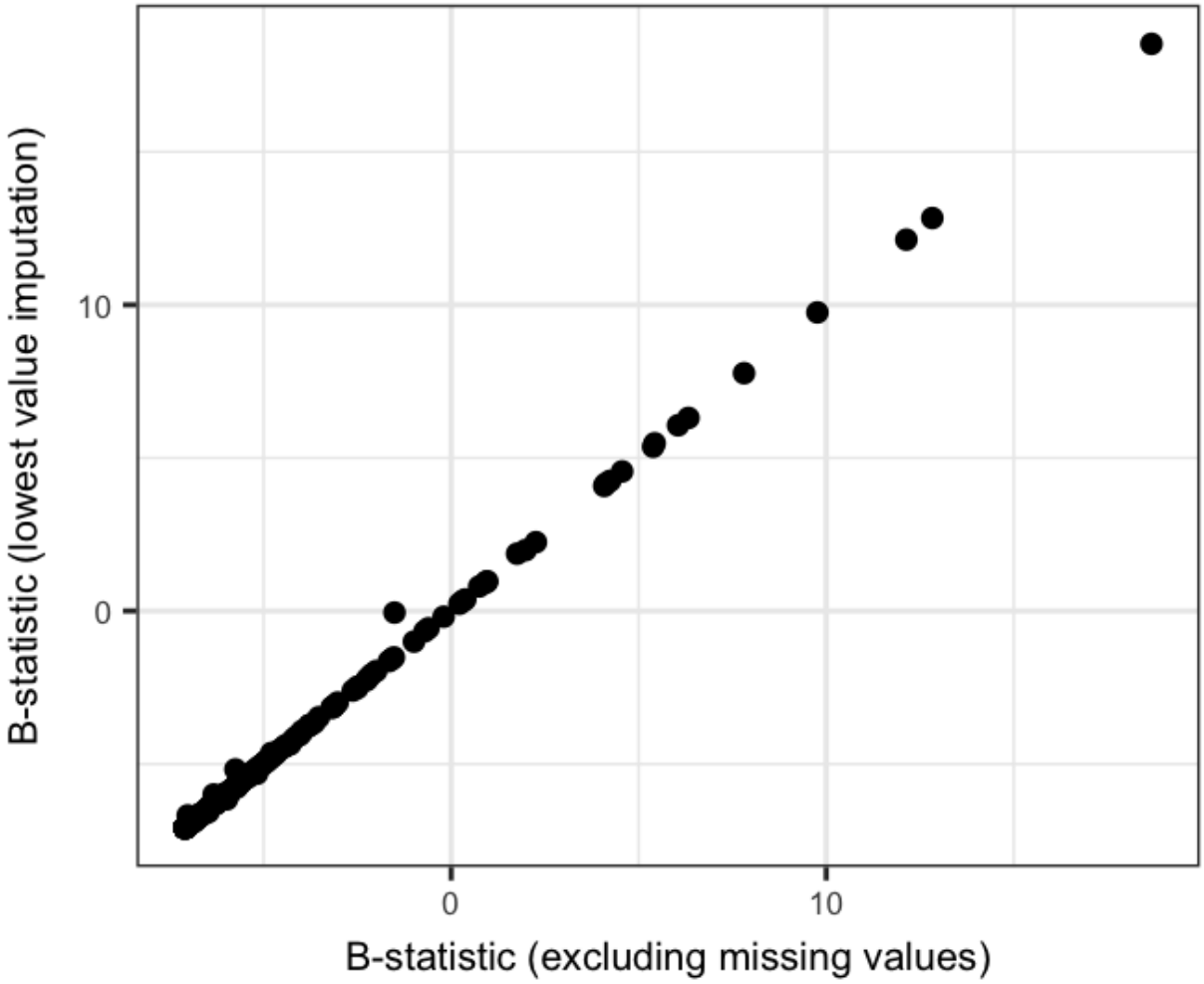


Figure 74: Plot of B-statistic (log odds) for differential expression of proteins for the ER 45min vs ER 0min contrast, comparing results following exclusion of missing values and lowest value imputation.

#### 4.7.2 Removal of missing values vs lowest value imputation (quantile normalization in both)

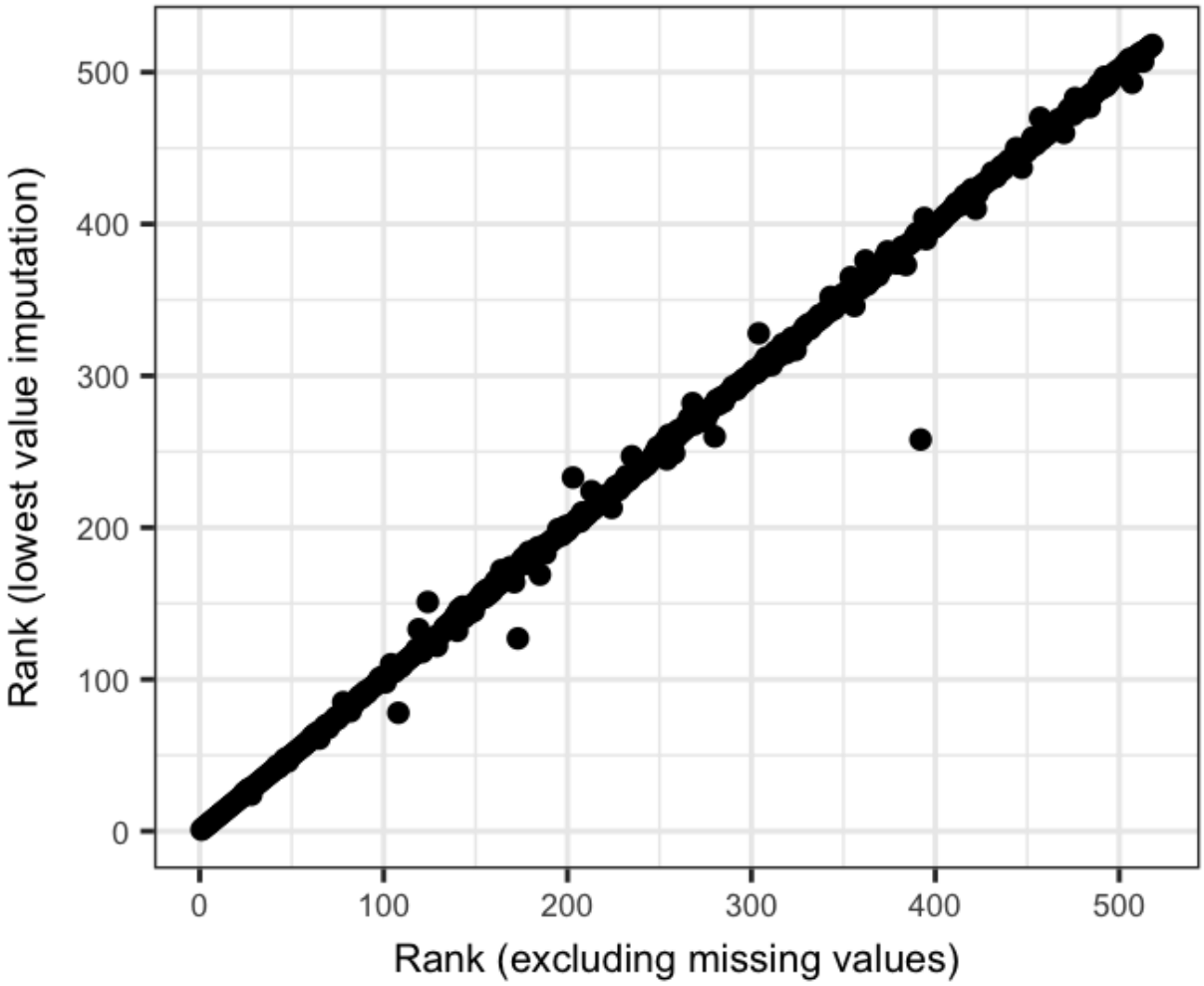


Figure 75: Plot of the rank of differentially-expressed proteins for the ER 45min vs ER 0min contrast, comparing results following exclusion of missing values and lowest value imputation.

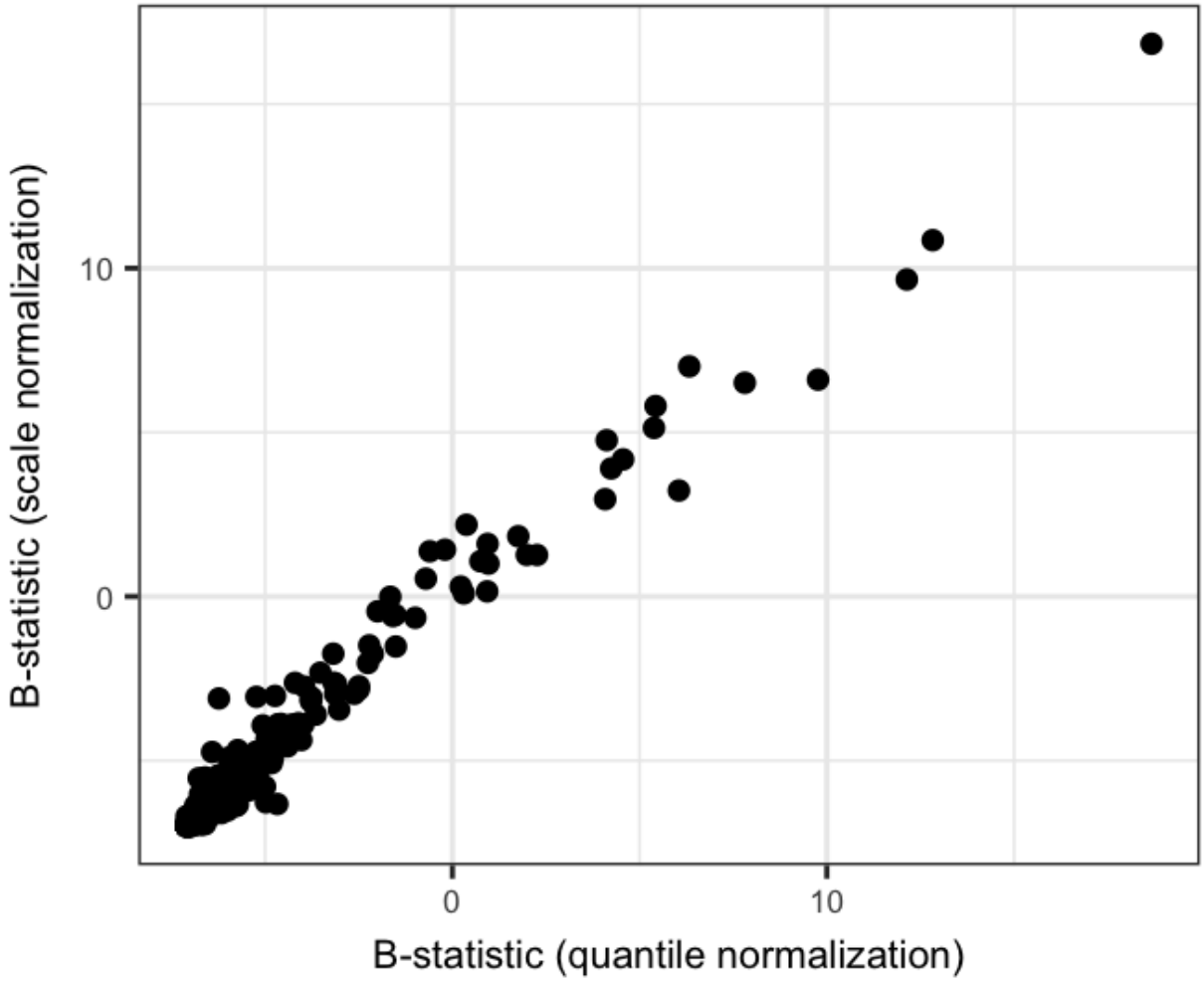


Figure 76: Plot of B-statistic (log odds) for differential expression of proteins for the ER 45min vs ER 0min contrast, comparing results following quantile and scale normalization.

#### 4.7.3 Quantile vs Scale normalization (missing values excluded in both)

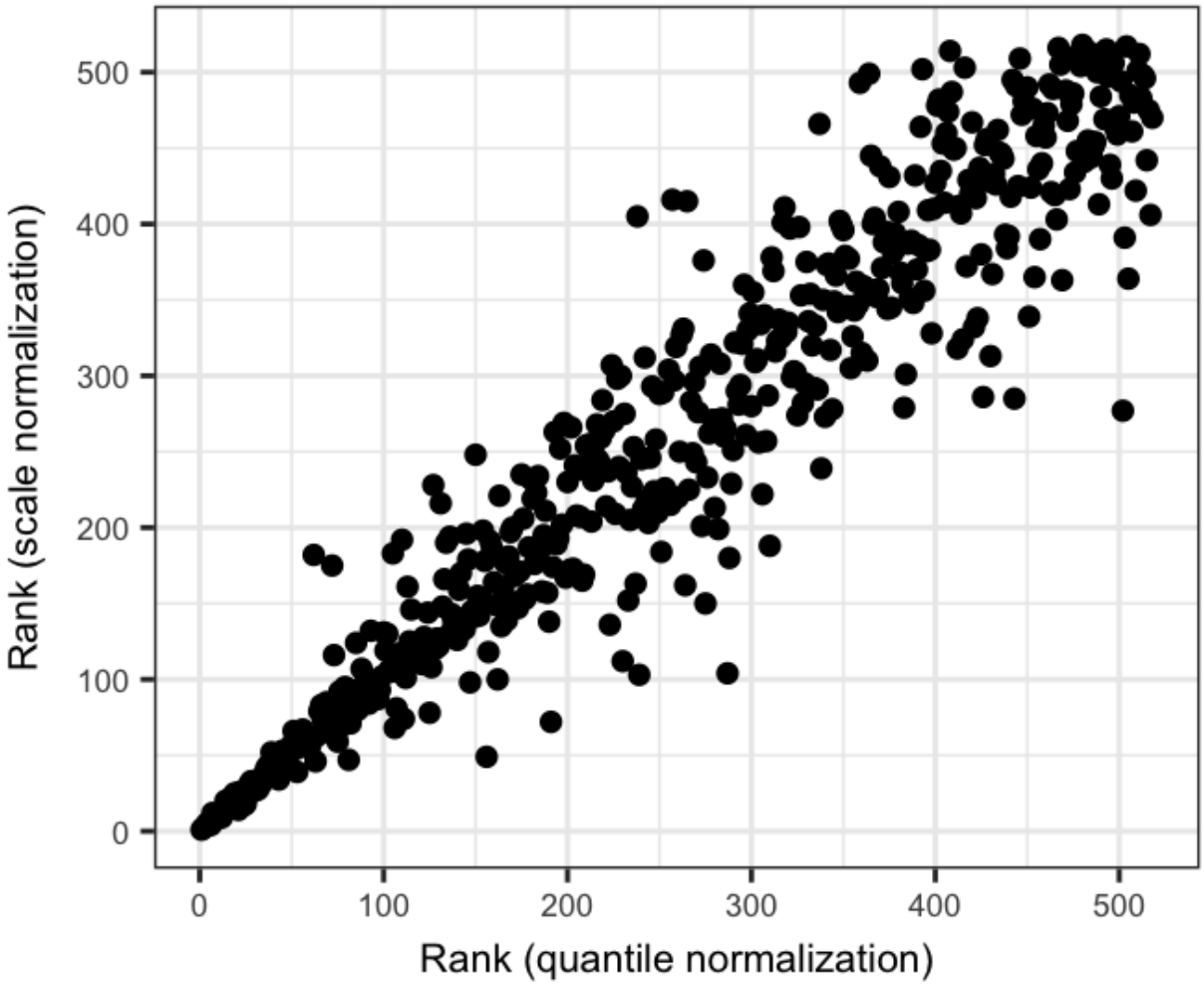


Figure 77: Plot of the rank of differentially-expressed proteins for the ER 45min vs ER 0min contrast, comparing results following quantile and scale normalization.

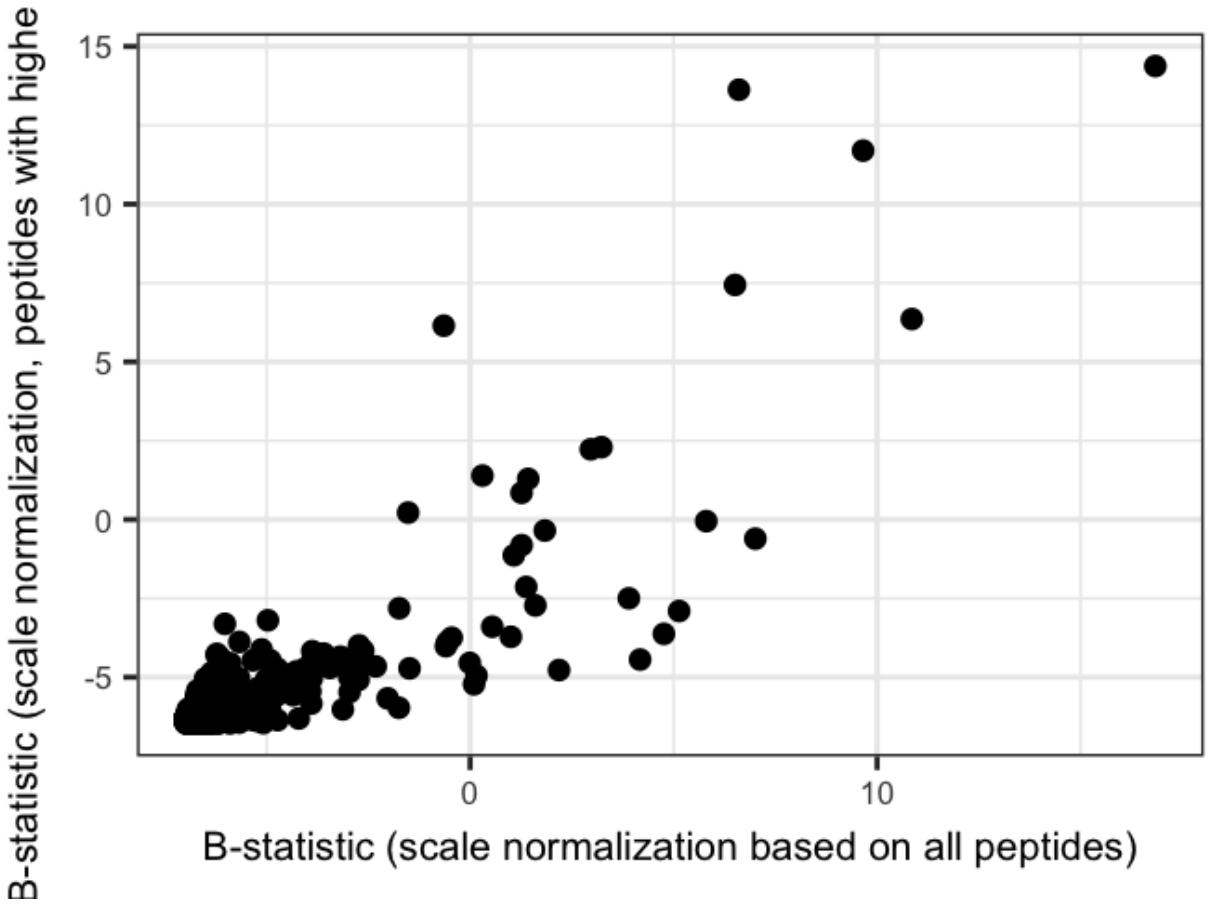


Figure 78: Plot of B-statistic (log odds) for differential expression of proteins for the ER 45min vs ER 0min contrast, comparing results following scale normalization based on all peptides and those with the highest IgG intensities.

#### 4.7.4 Scale normalization based on all peptides vs peptides with highest IgG intensities (missing values excluded in both)

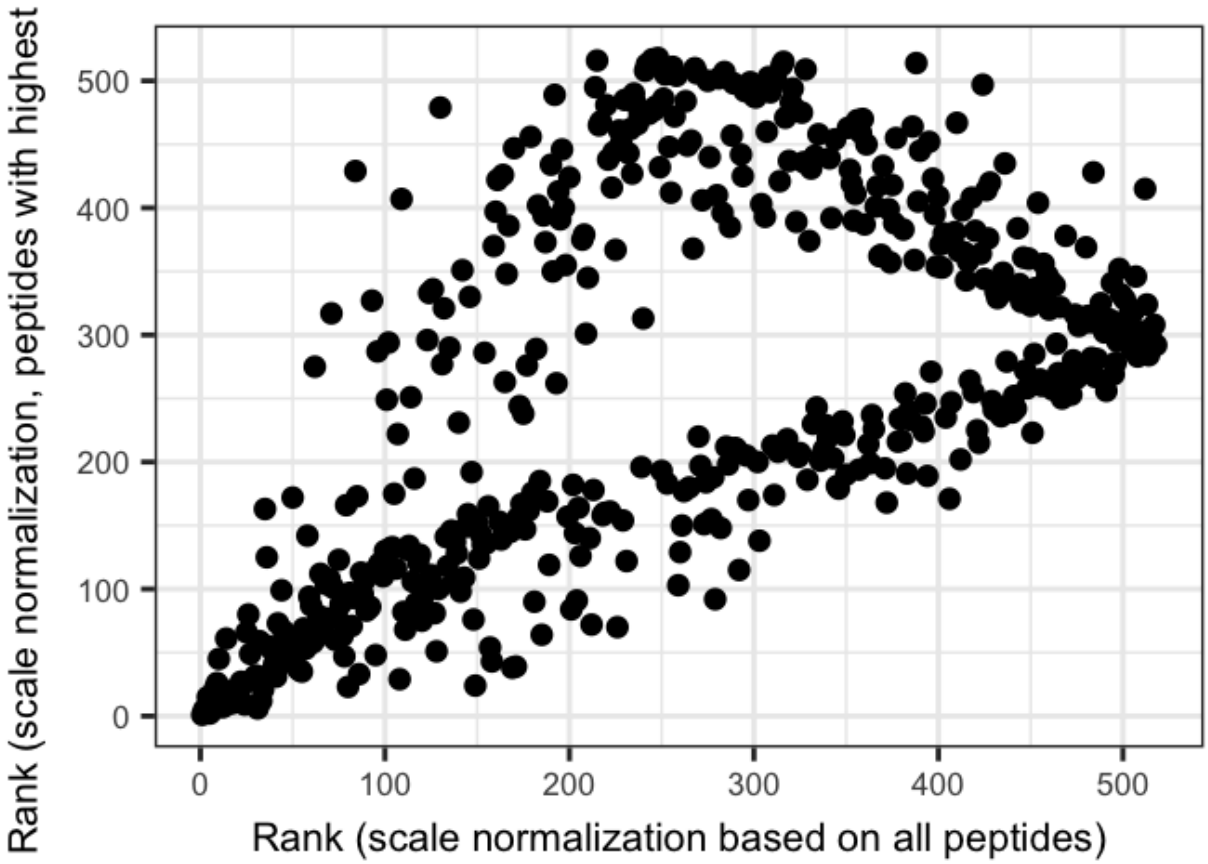


Figure 79: Plot of the rank of differentially-expressed proteins for the ER 45min vs ER 0min contrast, comparing results following scale normalization based on all peptides and those with the highest IgG intensities.

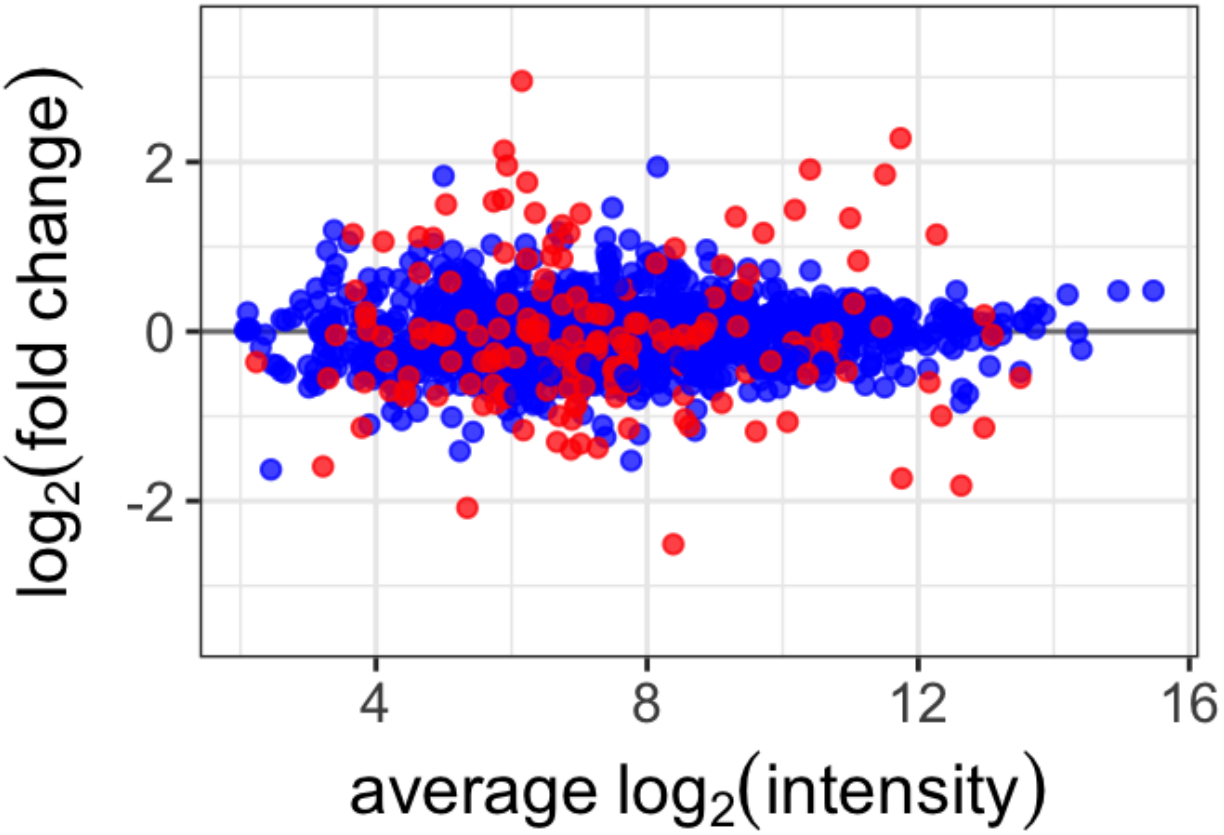


Figure 80: MA plot showing the distribution of non-specific binding. Non-specific binding was identified as proteins that showed less than a log2 enrichment over the IgG channel at either 0 or 45 minutes. The majority of non-specific binding (blue) is found to show less change between time points whereas the specific interactions (red) shows a broader distribution.

### 4.8 Comparisoin of variance between specfic and non-specific binding

```
##
##  F test to compare two variances
##
## data:  tmp$logFC[tmp$group == 1] and tmp$logFC[tmp$group == 0]
## F = 0.18045, num df = 1373, denom df = 166, p-value < 2.2e-16
## alternative hypothesis: true ratio of variances is less than 1
## 95 percent confidence interval:
##  0.0000000 0.2167525
## sample estimates:
## ratio of variances
##          0.1804544
```

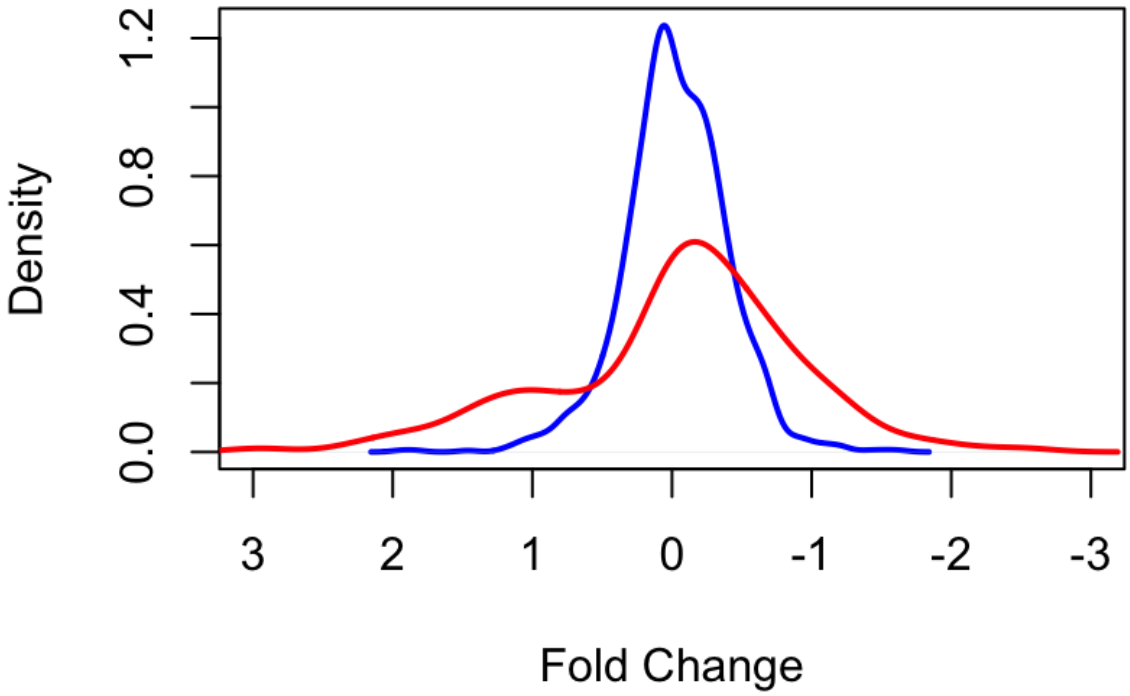


Figure 81: Density plot right showing the distribution of non-specific binding. Non-specific binding was identified as proteins that showed less than a log2 enrichment over the IgG channel at either 0 or 45 minutes. The majority of non-specific binding (blue) is found to show less change between time points whereas the specific interactions (red) shows a broader distribution.

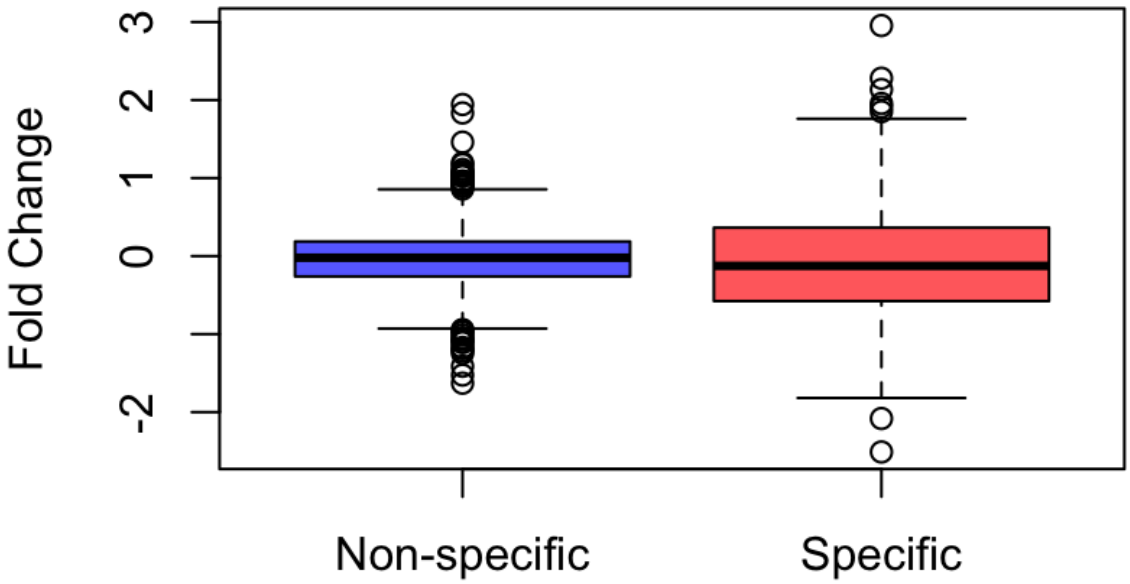


Figure 82: Box plot showing the variance of non-specific vs non-specific binding. Non-specific binding was identified as proteins that showed less than a log2 enrichment over the IgG channel at either 0 or 45 minutes. The the variance of the log fold changes for the non-specific binding interactions was significantly less than that of the specific interactions (F-test, one-sided, p-value $<$ 2.2e*-16).

## 4.9 Differential binding results tables

The following tables contain the top ranking differentially expressed proteins for each comparison. Included are all proteins that reach a statistical signficance of 0.05 in terms of the adjusted p-value and those with an absolute $\log_2$ fold change of 1 or above.

The IgG column gives the larger of the $\log_2$ fold changes for the two groups against the IgG control and an asterisk indicates specific binding where this $\log_2$ fold change is above a threshold of 1. N is the number of replicates in which the protein was observed.

In all cases, peptide intensities were quantile normalized and measurements with missing values were removed prior to summarization at the protein level.

### 4.9.1 ER 45min vs ER 0min

| Protein | Gene | N | log2FC | Avg Expr | p-value | B | IgG | |
|---|---|---|---|---|---|---|---|---|
| Q15596 | NCOA2 | 1 | 2.96 | 6.15 | | | 2.12 | * |
| Q13451 | FKBP5 | 2 | -2.51 | 8.39 | | | 2.55 | * |
| Q9Y6Q9 | NCOA3 | 3 | 2.28 | 11.74 | 1e-09 | 18.67 | 1.90 | * |
| Q96K62 | ZBT45 | 1 | 2.14 | 5.89 | | | 2.58 | * |
| Q96LC7 | SIG10 | 1 | -2.08 | 5.35 | | | 1.79 | * |
| Q6IQ16 | SPOPL | 1 | 1.96 | 5.93 | | | 1.59 | * |
| P11474 | ERR1 | 3 | 1.94 | 8.16 | 0.015 | -0.99 | -0.14 | |
| P48552 | NRIP1 | 3 | 1.91 | 10.40 | 1.2e-05 | 7.81 | 1.56 | * |
| O15164 | TIF1A | 3 | 1.85 | 11.51 | 2.1e-07 | 12.83 | 2.15 | * |
| Q9Y2G9 | SBNO2 | 1 | 1.83 | 5.00 | | | 0.09 | |
| P07900 | HS90A | 3 | -1.82 | 12.63 | 2.2e-06 | 9.77 | 2.23 | * |
| O75448 | MED24 | 1 | 1.76 | 6.23 | | | 1.66 | * |
| Q02790 | FKBP4 | 3 | -1.73 | 11.76 | 2.8e-07 | 12.14 | 1.89 | * |
| O14744 | ANM5 | 1 | -1.63 | 2.45 | | | -0.44 | |
| Q9P2D0 | IBTK | 1 | -1.59 | 3.22 | | | 1.84 | * |
| P10276 | RARA | 3 | 1.56 | 5.87 | 0.0034 | 0.75 | 2.75 | * |
| Q15648 | MED1 | 1 | 1.53 | 5.74 | | | 1.97 | * |
| Q5D862 | FILA2 | 1 | -1.52 | 7.77 | | | -0.29 | |
| P32242 | OTX1 | 2 | 1.50 | 5.03 | | | 1.88 | * |
| Q2M1P5 | KIF7 | 1 | 1.46 | 7.49 | | | 0.71 | |
| P24468 | COT2 | 3 | 1.44 | 10.18 | 7.6e-05 | 5.43 | 2.07 | * |
| P34932 | HSP74 | 1 | -1.41 | 5.24 | | | 0.54 | |
| O14770 | MEIS2 | 1 | 1.40 | 6.35 | | | 1.08 | * |
| P61960 | UFM1 | 1 | -1.39 | 6.88 | | | 1.92 | * |
| Q8N2W9 | PIAS4 | 2 | 1.39 | 7.02 | | | 1.68 | * |
| Q86UV5 | UBP48 | 1 | -1.37 | 7.27 | | | 1.36 | * |
| Q92793 | CBP | 3 | 1.35 | 9.31 | 0.0015 | 1.76 | 1.48 | * |
| P23771 | GATA3 | 3 | 1.34 | 10.99 | 4.5e-05 | 6.33 | 1.61 | * |
| Q9P2D7 | DYH1 | 1 | -1.32 | 7.02 | | | 2.63 | * |
| O60884 | DNJA2 | 3 | -1.30 | 6.67 | 0.023 | -1.51 | 1.76 | * |
| Q9UBW7 | ZMYM2 | 1 | 1.25 | 6.75 | | | 1.46 | * |
| Q01546 | K22O | 2 | -1.25 | 7.38 | | | -1.21 | |
| O60809 | PRA10 | 1 | -1.22 | 7.88 | | | -0.24 | |
| O15117 | FYB | 1 | 1.19 | 3.38 | | | -1.88 | |
| P53990 | IST1 | 1 | -1.18 | 5.43 | | | -4.76 | |
| P31689 | DNJA1 | 3 | -1.18 | 9.61 | 0.00019 | 4.08 | 1.20 | * |
| O00712 | NFIB | 1 | 1.17 | 6.67 | | | -0.34 | |
| Q8N283 | ANR35 | 1 | -1.17 | 8.71 | | | -0.15 | |
| Q9UL15 | BAG5 | 1 | -1.16 | 6.18 | | | 1.11 | * |
| Q6PHW0 | IYD1 | 1 | 1.16 | 6.85 | | | 1.52 | * |
| Q9ULJ6 | ZMIZ1 | 3 | 1.16 | 9.72 | 7.6e-05 | 5.38 | 1.61 | * |
| P15408 | FOSL2 | 1 | 1.15 | 3.66 | | | 1.69 | * |
| Q9UNE7 | CHIP | 2 | -1.14 | 7.73 | | | 1.05 | * |
| Q9UPN9 | TRI33 | 3 | 1.14 | 12.27 | 0.00019 | 4.24 | 1.73 | * |
| P11142 | HSP7C | 3 | -1.14 | 12.97 | 5e-05 | 6.05 | 1.00 | * |
| Q9NWS6 | F118A | 1 | -1.13 | 3.79 | | | 1.60 | * |
| Q9HB71 | CYBP | 3 | -1.12 | 8.62 | 0.0011 | 2.26 | 1.02 | * |
| Q8TCU4 | ALMS1 | 1 | 1.12 | 4.63 | | | 1.44 | * |
| O14686 | KMT2D | 1 | 1.11 | 7.38 | | | 0.39 | |

Continued on next page

| Protein | Gene | N | log2FC | Avg Expr | p-value | B | IgG | |
|---|---|---|---|---|---|---|---|---|
| Q7Z794 | K2C1B | 1 | -1.11 | 7.34 | | | -0.84 | |
| Q6KC79 | NIPBL | 1 | 1.11 | 4.84 | | | 2.63 | * |
| Q68E01 | INT3 | 2 | -1.10 | 3.90 | | | -0.67 | |
| Q8NFD5 | ARI1B | 1 | 1.08 | 7.74 | | | 0.56 | |
| Q9Y6X2 | PIAS3 | 2 | 1.07 | 6.75 | | | 0.71 | |
| Q92624 | APBP2 | 1 | -1.07 | 6.01 | | | 0.05 | |
| O15355 | PPM1G | 3 | -1.07 | 10.07 | 0.0072 | -0.20 | 1.09 | * |
| Q8NH53 | O52N1 | 1 | 1.06 | 4.11 | | | 1.28 | * |
| Q13492 | PICAL | 1 | 1.06 | 3.60 | | | 0.12 | |
| Q4L235 | ACSF4 | 1 | -1.05 | 4.38 | | | -0.13 | |
| O00170 | AIP | 2 | -1.04 | 6.89 | | | 1.13 | * |
| P14625 | ENPL | 2 | 1.04 | 4.85 | | | -0.35 | |
| O60244 | MED14 | 1 | 1.04 | 6.62 | | | 1.56 | * |
| Q15185 | TEBP | 1 | -1.03 | 8.55 | | | 1.29 | * |
| Q6P2C8 | MED27 | 1 | 1.03 | 6.21 | | | -0.01 | |
| Q5VTD9 | GFI1B | 1 | 1.02 | 5.70 | | | 0.42 | |
| O14929 | HAT1 | 2 | -1.01 | 5.12 | | | 0.70 | |
| P08238 | HS90B | 3 | -0.99 | 12.34 | 0.005 | 0.22 | 2.04 | * |
| P55854 | SUMO3 | 3 | 0.98 | 8.41 | 0.003 | 0.96 | 1.13 | * |
| Q09472 | EP300 | 3 | 0.96 | 8.88 | 0.00019 | 4.12 | 0.80 | |
| P0DMV9 | HS71B | 3 | -0.84 | 12.63 | 0.0013 | 1.99 | 0.65 | |
| Q6ISB3 | GRHL2 | 3 | 0.83 | 11.12 | 0.00015 | 4.56 | 1.04 | * |
| Q92754 | AP2C | 3 | 0.81 | 8.14 | 0.0046 | 0.38 | 1.15 | * |
| Q92785 | REQU | 3 | 0.78 | 9.11 | 0.003 | 0.93 | 1.16 | * |
| P52701 | MSH6 | 3 | -0.76 | 6.05 | 0.048 | -2.50 | 0.97 | |
| P63165 | SUMO1 | 3 | 0.74 | 9.15 | 0.0048 | 0.31 | 0.72 | |
| P12956 | XRCC6 | 3 | -0.74 | 12.73 | 0.01 | -0.60 | 0.90 | |
| P31948 | STIP1 | 3 | -0.66 | 11.50 | 0.003 | 0.94 | 0.59 | |
| P78527 | PRKDC | 3 | -0.63 | 11.22 | 0.011 | -0.71 | 0.36 | |
| Q9HAV4 | XPO5 | 3 | -0.63 | 8.66 | 0.048 | -2.50 | 0.72 | |
| O14497 | ARI1A | 3 | 0.61 | 8.60 | 0.04 | -2.26 | 0.29 | |
| Q9Y383 | LC7L2 | 3 | -0.55 | 10.30 | 0.023 | -1.53 | 0.51 | |
| Q13263 | TIF1B | 3 | -0.55 | 13.51 | 0.033 | -2.00 | 1.17 | * |
| P09874 | PARP1 | 3 | -0.53 | 11.81 | 0.023 | -1.59 | 0.63 | |
| Q92925 | SMRD2 | 3 | 0.51 | 9.91 | 0.037 | -2.12 | 0.23 | |
| P25685 | DNJB1 | 3 | -0.45 | 9.66 | 0.039 | -2.22 | 0.60 | |
| Q99873 | ANM1 | 3 | -0.42 | 11.29 | 0.024 | -1.66 | 0.65 | |

Table 4: Top ranking differentially expressed proteins from the ER 45min vs ER 0min comparison, sorted by log2 fold change.

### 4.9.2 ER 90min vs ER 0min

| Protein | Gene | N | log2FC | Avg Expr | p-value | B | IgG | |
|---|---|---|---|---|---|---|---|---|
| Q15596 | NCOA2 | 1 | 2.82 | 6.15 | | | 1.98 | * |
| Q13451 | FKBP5 | 2 | -2.39 | 8.39 | | | 2.55 | * |
| Q96LC7 | SIG10 | 1 | -2.25 | 5.35 | | | 1.79 | * |
| Q9Y6Q9 | NCOA3 | 3 | 2.22 | 11.74 | 1.5e-09 | 18.26 | 1.84 | * |
| Q96K62 | ZBT45 | 1 | 2.19 | 5.89 | | | 2.63 | * |
| Q6IQ16 | SPOPL | 1 | 2.16 | 5.93 | | | 1.79 | * |
| Q9Y2G9 | SBNO2 | 1 | 2.15 | 5.00 | | | 0.41 | |
| P48552 | NRIP1 | 3 | 2.03 | 10.40 | 5e-06 | 8.73 | 1.68 | * |
| Q6UX73 | CP089 | 1 | 2.00 | 8.00 | | | 1.27 | * |
| O75448 | MED24 | 1 | 1.88 | 6.23 | | | 1.77 | * |
| P20393 | NR1D1 | 1 | 1.86 | 8.26 | | | 1.17 | * |
| Q68CL5 | TPGS2 | 2 | -1.85 | 3.12 | | | -6.76 | |
| O15164 | TIF1A | 3 | 1.84 | 11.51 | 2.4e-07 | 12.70 | 2.14 | * |
| P07900 | HS90A | 3 | -1.82 | 12.63 | 2.3e-06 | 9.75 | 2.23 | * |
| P11474 | ERR1 | 3 | 1.81 | 8.16 | 0.024 | -1.59 | -0.28 | |
| O14770 | MEIS2 | 1 | 1.76 | 6.35 | | | 1.44 | * |
| Q2M1P5 | KIF7 | 1 | 1.74 | 7.49 | | | 0.99 | |
| Q02790 | FKBP4 | 3 | -1.72 | 11.76 | 3.2e-07 | 11.99 | 1.89 | * |
| Q15648 | MED1 | 1 | 1.66 | 5.74 | | | 2.09 | * |
| P10276 | RARA | 3 | 1.58 | 5.87 | 0.0033 | 0.87 | 2.77 | * |
| O60229 | KALRN | 1 | 1.57 | 6.32 | | | 0.86 | |
| P15408 | FOSL2 | 1 | 1.57 | 3.66 | | | 2.11 | * |
| Q9UBW7 | ZMYM2 | 1 | 1.55 | 6.75 | | | 1.76 | * |
| P81605 | DCD | 1 | 1.47 | 4.63 | | | -1.79 | |
| P24468 | COT2 | 3 | 1.45 | 10.18 | 7.4e-05 | 5.53 | 2.08 | * |
| Q86UV5 | UBP48 | 1 | -1.44 | 7.27 | | | 1.36 | * |
| P32242 | OTX1 | 2 | 1.43 | 5.03 | | | 1.81 | * |
| Q92624 | APBP2 | 1 | -1.42 | 6.01 | | | 0.05 | |
| Q6KC79 | NIPBL | 1 | 1.42 | 4.84 | | | 2.94 | * |
| Q92793 | CBP | 3 | 1.41 | 9.31 | 0.0011 | 2.27 | 1.54 | * |
| P23771 | GATA3 | 3 | 1.38 | 10.99 | 2.8e-05 | 6.79 | 1.65 | * |
| Q9P2D7 | DYH1 | 1 | -1.37 | 7.02 | | | 2.63 | * |
| O15117 | FYB | 1 | 1.36 | 3.38 | | | -1.71 | |
| P34932 | HSP74 | 1 | -1.29 | 5.24 | | | 0.54 | |
| O60884 | DNJA2 | 3 | -1.28 | 6.67 | 0.024 | -1.61 | 1.76 | * |
| O00712 | NFIB | 1 | 1.28 | 6.67 | | | -0.24 | |
| O76094 | SRP72 | 1 | 1.25 | 3.41 | | | 0.35 | |
| Q9NWS6 | F118A | 1 | -1.25 | 3.79 | | | 1.60 | * |
| O60934 | NBN | 1 | -1.24 | 4.24 | | | 0.84 | |
| Q13492 | PICAL | 1 | 1.24 | 3.60 | | | 0.30 | |
| Q8WX92 | NELFB | 2 | -1.23 | 6.70 | | | 1.26 | * |
| Q8N2W9 | PIAS4 | 2 | 1.21 | 7.02 | | | 1.50 | * |
| Q8N283 | ANR35 | 1 | -1.20 | 8.71 | | | -0.15 | |
| Q6KB66 | K2C80 | 2 | 1.19 | 11.02 | | | 0.73 | |
| Q9UNE7 | CHIP | 2 | -1.17 | 7.73 | | | 1.05 | * |
| O60809 | PRA10 | 1 | -1.17 | 7.88 | | | -0.24 | |
| P31689 | DNJA1 | 3 | -1.16 | 9.61 | 0.00026 | 3.87 | 1.20 | * |
| Q9Y6X2 | PIAS3 | 2 | 1.15 | 6.75 | | | 0.79 | |
| Q4L235 | ACSF4 | 1 | -1.14 | 4.38 | | | -0.13 | |

Continued on next page

| Protein | Gene | N | log2FC | Avg Expr | p-value | B | IgG | |
|---|---|---|---|---|---|---|---|---|
| Q15126 | PMVK | 1 | -1.14 | 5.45 | | | 0.49 | |
| Q9Y4C1 | KDM3A | 1 | -1.11 | 5.93 | | | 0.91 | |
| Q13158 | FADD | 1 | -1.11 | 2.11 | | | -0.90 | |
| Q9ULL5 | PRR12 | 1 | 1.11 | 3.33 | | | -0.10 | |
| P11142 | HSP7C | 3 | -1.11 | 12.97 | 7.3e-05 | 5.69 | 1.00 | * |
| Q9HB71 | CYBP | 3 | -1.10 | 8.62 | 0.0013 | 2.04 | 1.02 | * |
| Q6P2C8 | MED27 | 1 | 1.10 | 6.21 | | | 0.06 | |
| Q9UL15 | BAG5 | 1 | -1.09 | 6.18 | | | 1.11 | * |
| Q6PHW0 | IYD1 | 1 | 1.09 | 6.85 | | | 1.45 | * |
| P07205 | PGK2 | 1 | -1.08 | 6.73 | | | 1.03 | * |
| Q96QK1 | VPS35 | 1 | 1.08 | 4.72 | | | 0.59 | |
| O15355 | PPM1G | 3 | -1.07 | 10.07 | 0.0065 | -0.12 | 1.09 | * |
| Q9UPN9 | TRI33 | 3 | 1.05 | 12.27 | 0.00045 | 3.22 | 1.64 | * |
| P61960 | UFM1 | 1 | -1.05 | 6.88 | | | 1.92 | * |
| Q9ULJ6 | ZMIZ1 | 3 | 1.04 | 9.72 | 0.00025 | 3.98 | 1.49 | * |
| O43866 | CD5L | 2 | -1.04 | 6.17 | | | -2.51 | |
| O14686 | KMT2D | 1 | 1.04 | 7.38 | | | 0.32 | |
| Q5D862 | FILA2 | 1 | -1.03 | 7.77 | | | -0.29 | |
| Q09472 | EP300 | 3 | 1.03 | 8.88 | 0.00011 | 5.00 | 0.86 | |
| Q8NFD5 | ARI1B | 1 | 1.02 | 7.74 | | | 0.50 | |
| P08238 | HS90B | 3 | -1.00 | 12.34 | 0.0047 | 0.32 | 2.04 | * |
| P55854 | SUMO3 | 3 | 0.96 | 8.41 | 0.0034 | 0.71 | 1.11 | * |
| P52701 | MSH6 | 3 | -0.93 | 6.05 | 0.012 | -0.78 | 0.97 | |
| Q6ISB3 | GRHL2 | 3 | 0.85 | 11.12 | 0.00012 | 4.82 | 1.05 | * |
| Q92754 | AP2C | 3 | 0.84 | 8.14 | 0.0033 | 0.88 | 1.19 | * |
| P63165 | SUMO1 | 3 | 0.79 | 9.15 | 0.0033 | 0.98 | 0.77 | |
| Q92785 | REQU | 3 | 0.77 | 9.11 | 0.0034 | 0.81 | 1.15 | * |
| P0DMV9 | HS71B | 3 | -0.75 | 12.63 | 0.0034 | 0.76 | 0.65 | |
| P61956 | SUMO2 | 3 | 0.73 | 9.50 | 0.033 | -2.05 | 1.10 | * |
| P12956 | XRCC6 | 3 | -0.72 | 12.73 | 0.012 | -0.75 | 0.90 | |
| O14497 | ARI1A | 3 | 0.72 | 8.60 | 0.012 | -0.81 | 0.41 | |
| P78527 | PRKDC | 3 | -0.68 | 11.22 | 0.0061 | -0.03 | 0.36 | |
| Q9HAV4 | XPO5 | 3 | -0.65 | 8.66 | 0.037 | -2.19 | 0.72 | |
| P31948 | STIP1 | 3 | -0.62 | 11.50 | 0.0047 | 0.29 | 0.59 | |
| Q04724 | TLE1 | 3 | 0.61 | 9.40 | 0.041 | -2.32 | 1.12 | * |
| Q92925 | SMRD2 | 3 | 0.58 | 9.91 | 0.014 | -1.00 | 0.31 | |
| P55060 | XPO2 | 3 | -0.56 | 10.10 | 0.044 | -2.43 | 0.86 | |
| Q9Y383 | LC7L2 | 3 | -0.51 | 10.30 | 0.037 | -2.18 | 0.51 | |
| P09874 | PARP1 | 3 | -0.50 | 11.81 | 0.033 | -2.01 | 0.63 | |
| Q99873 | ANM1 | 3 | -0.40 | 11.29 | 0.033 | -1.99 | 0.65 | |

Table 5: Top ranking differentially expressed proteins from the ER 90min vs ER 0min comparison, sorted by log2 fold change.

### 4.9.3 ER 90min vs ER 45min

| Protein | Gene | N | log2FC | Avg Expr | p-value | B | IgG | |
|---|---|---|---|---|---|---|---|---|
| Q13158 | FADD | 1 | -1.34 | 2.11 | | | -0.67 | |
| Q68CL5 | TPGS2 | 2 | -1.21 | 3.12 | | | -7.40 | |
| Q6UX73 | CP089 | 1 | 1.20 | 8.00 | | | 1.27 | * |
| P33176 | KINH | 1 | 1.09 | 4.64 | | | 0.78 | |
| O14744 | ANM5 | 1 | 1.06 | 2.45 | | | -1.01 | |
| Q8WXG9 | GPR98 | 1 | 1.02 | 6.85 | | | 2.30 | * |

Table 6: Top ranking differentially expressed proteins from the ER 90min vs ER 45min comparison, sorted by log2 fold change.

### 4.9.4 FOXA1 45min vs FOXA1 0min

| Protein | Gene | N | log2FC | Avg Expr | p-value | B | IgG | |
|---|---|---|---|---|---|---|---|---|
| Q8NH53 | O52N1 | 1 | 4.29 | 4.11 | | | 4.90 | * |
| Q96QK1 | VPS35 | 1 | 3.72 | 4.72 | | | 4.08 | * |
| A6NNA2 | SRRM3 | 1 | 3.69 | 7.45 | | | 4.27 | * |
| P57773 | CXA9 | 1 | 3.12 | 8.22 | | | 2.52 | * |
| A5PLK6 | RGSL | 1 | -3.03 | 6.46 | | | 0.16 | |
| P42356 | PI4KA | 1 | -2.64 | 4.49 | | | -1.42 | |
| Q9NVG8 | TBC13 | 1 | -2.39 | 6.80 | | | 0.41 | |
| O94844 | RHBT1 | 1 | -2.35 | 5.71 | | | 0.20 | |
| P57678 | GEMI4 | 1 | -2.32 | 7.40 | | | -0.16 | |
| Q86UP2 | KTN1 | 1 | 2.23 | 6.69 | | | 2.02 | * |
| P08729 | K2C7 | 1 | -2.19 | 3.89 | | | 0.04 | |
| Q9NW13 | RBM28 | 1 | 2.06 | 6.68 | | | 2.13 | * |
| O94992 | HEXI1 | 2 | -1.70 | 4.22 | | | 0.53 | |
| Q86WI1 | PKHL1 | 1 | -1.69 | 4.09 | | | -0.70 | |
| Q9H2Y7 | ZN106 | 1 | 1.66 | 7.50 | | | -1.73 | |
| Q01813 | PFKAP | 1 | -1.62 | 3.27 | | | -0.69 | |
| Q8IV04 | TB10C | 1 | -1.61 | 6.35 | | | 0.15 | |
| Q9H3P2 | NELFA | 1 | -1.54 | 3.92 | | | 0.55 | |
| Q9NWS6 | F118A | 1 | -1.49 | 3.79 | | | 0.73 | |
| Q9Y3E5 | PTH2 | 1 | 1.49 | 3.11 | | | 0.89 | |
| Q8TDN6 | BRX1 | 1 | 1.46 | 7.29 | | | 1.55 | * |
| Q8NF37 | PCAT1 | 1 | -1.41 | 7.34 | | | -0.42 | |
| Q9H0A0 | NAT10 | 1 | 1.38 | 2.30 | | | 1.61 | * |
| Q96KQ4 | ASPP1 | 1 | -1.38 | 3.41 | | | -0.79 | |
| P33176 | KINH | 1 | -1.36 | 4.64 | | | -0.26 | |
| P20393 | NR1D1 | 1 | -1.32 | 8.26 | | | 0.77 | |
| O60610 | DIAP1 | 1 | -1.32 | 4.23 | | | 0.08 | |
| Q9BQG0 | MBB1A | 1 | 1.30 | 8.49 | | | 1.14 | * |
| Q9HA92 | RSAD1 | 1 | -1.30 | 7.23 | | | 0.48 | |
| Q9UHB6 | LIMA1 | 1 | 1.30 | 3.12 | | | -0.08 | |
| Q9BXD5 | NPL | 1 | -1.29 | 4.27 | | | 0.16 | |
| Q5VTD9 | GFI1B | 1 | -1.29 | 5.70 | | | 0.24 | |
| Q13492 | PICAL | 1 | 1.26 | 3.60 | | | 1.43 | * |
| Q15413 | RYR3 | 1 | -1.26 | 6.19 | | | -5.07 | |
| Q96HY6 | DDRGK | 1 | -1.23 | 3.95 | | | -0.17 | |
| O00487 | PSDE | 1 | 1.23 | 2.15 | | | 0.67 | |
| O15269 | SPTC1 | 1 | -1.18 | 3.96 | | | 0.19 | |
| Q9HDC9 | APMAP | 1 | -1.14 | 7.62 | | | -0.44 | |
| O75179 | ANR17 | 1 | 1.14 | 3.36 | | | 0.61 | |
| Q8ND56 | LS14A | 1 | 1.14 | 3.28 | | | 0.07 | |
| O60229 | KALRN | 1 | -1.13 | 6.32 | | | 0.23 | |
| O95433 | AHSA1 | 1 | 1.13 | 3.19 | | | 1.67 | * |
| Q5T0W9 | FA83B | 1 | 1.13 | 6.88 | | | 0.78 | |
| P00450 | CERU | 1 | 1.12 | 6.76 | | | 0.04 | |
| Q96CT7 | CC124 | 1 | -1.12 | 6.21 | | | -0.32 | |
| Q14677 | EPN4 | 1 | -1.09 | 6.32 | | | -1.86 | |
| Q08J23 | NSUN2 | 2 | -1.09 | 4.80 | | | 0.50 | |
| Q14966 | ZN638 | 1 | 1.08 | 7.79 | | | 1.09 | * |
| Q9H9B1 | EHMT1 | 1 | 1.07 | 3.76 | | | 1.84 | * |

Continued on next page

| Protein | Gene | N | log2FC | Avg Expr | p-value | B | IgG |
|---|---|---|---|---|---|---|---|
| A5YKK6 | CNOT1 | 1 | -1.06 | 5.89 | | | -0.60 |
| Q9HCH5 | SYTL2 | 1 | -1.04 | 6.63 | | | 0.77 |
| P61966 | AP1S1 | 1 | 1.01 | 3.79 | | | 0.46 |
| Q06787 | FMR1 | 1 | -1.01 | 7.26 | | | -0.15 |
| O15117 | FYB | 1 | 1.01 | 3.38 | | | 0.64 |
| P29083 | T2EA | 1 | 1.01 | 5.86 | | | -3.44 |
| Q8IVT2 | MISP | 1 | 1.01 | 5.52 | | | 0.40 |

Table 7: Top ranking differentially expressed proteins from the FOXA1 45min vs FOXA1 0min comparison, sorted by log2 fold change.

#### 4.9.5 FOXA1 90min vs FOXA1 0min

| Protein | Gene | N | log2FC | Avg Expr | p-value | B | IgG |
|---|---|---|---|---|---|---|---|
| A5PLK6 | RGSL | 1 | -1.53 | 6.46 | | | 0.16 |
| Q5T0F9 | C2D1B | 1 | -1.28 | 3.34 | | | 0.00 |
| P04433 | KV309 | 1 | -1.24 | 8.54 | | | 0.36 |
| P55036 | PSMD4 | 1 | -1.22 | 4.17 | | | 0.15 |
| O95433 | AHSA1 | 1 | -1.13 | 3.19 | | | 0.54 |
| O00487 | PSDE | 1 | -1.08 | 2.15 | | | -0.56 |

Table 8: Top ranking differentially expressed proteins from the FOXA1 90min vs FOXA1 0min comparison, sorted by log2 fold change.

### 4.9.6 FOXA1 90min vs FOXA1 45min

| Protein | Gene | N | log2FC | Avg Expr | p-value | B | IgG | |
|---|---|---|---|---|---|---|---|---|
| Q8NH53 | O52N1 | 1 | -4.27 | 4.11 | | | 4.90 | * |
| Q96QK1 | VPS35 | 1 | -4.20 | 4.72 | | | 4.08 | * |
| P42356 | PI4KA | 1 | 3.49 | 4.49 | | | -0.57 | |
| P57773 | CXA9 | 1 | -2.97 | 8.22 | | | 2.52 | * |
| A6NNA2 | SRRM3 | 1 | -2.88 | 7.45 | | | 4.27 | * |
| Q86UP2 | KTN1 | 1 | -2.69 | 6.69 | | | 2.02 | * |
| Q9NVG8 | TBC13 | 1 | 2.67 | 6.80 | | | 0.69 | |
| O94844 | RHBT1 | 1 | 2.51 | 5.71 | | | 0.36 | |
| O00487 | PSDE | 1 | -2.31 | 2.15 | | | 0.67 | |
| O95433 | AHSA1 | 1 | -2.26 | 3.19 | | | 1.67 | * |
| Q15413 | RYR3 | 1 | 2.13 | 6.19 | | | -4.20 | |
| P08729 | K2C7 | 1 | 2.04 | 3.89 | | | -0.11 | |
| Q9H0A0 | NAT10 | 1 | -1.98 | 2.30 | | | 1.61 | * |
| O75179 | ANR17 | 1 | -1.91 | 3.36 | | | 0.61 | |
| Q9HDC9 | APMAP | 1 | 1.89 | 7.62 | | | 0.31 | |
| P57678 | GEMI4 | 1 | 1.88 | 7.40 | | | -0.60 | |
| Q8ND56 | LS14A | 1 | -1.81 | 3.28 | | | 0.07 | |
| Q9H3P2 | NELFA | 1 | 1.74 | 3.92 | | | 0.76 | |
| O94992 | HEXI1 | 2 | 1.69 | 4.22 | | | 0.51 | |
| Q8IV04 | TB10C | 1 | 1.67 | 6.35 | | | 0.20 | |
| P33176 | KINH | 1 | 1.65 | 4.64 | | | 0.03 | |
| P61966 | AP1S1 | 1 | -1.62 | 3.79 | | | 0.46 | |
| Q9NWS6 | F118A | 1 | 1.51 | 3.79 | | | 0.75 | |
| A5PLK6 | RGSL | 1 | 1.50 | 6.46 | | | -1.37 | |
| Q13492 | PICAL | 1 | -1.46 | 3.60 | | | 1.43 | * |
| Q8TE85 | GRHL3 | 1 | 1.43 | 4.85 | | | -0.03 | |
| Q9HCH5 | SYTL2 | 1 | 1.43 | 6.63 | | | 1.16 | * |
| Q9H2Y7 | ZN106 | 1 | -1.40 | 7.50 | | | -1.73 | |
| Q9Y6E0 | STK24 | 1 | -1.39 | 3.66 | | | 0.52 | |
| Q14677 | EPN4 | 1 | 1.37 | 6.32 | | | -1.58 | |
| P23677 | IP3KA | 1 | 1.35 | 7.05 | | | -0.42 | |
| Q9NW13 | RBM28 | 1 | -1.33 | 6.68 | | | 2.13 | * |
| Q9Y3E5 | PTH2 | 1 | -1.32 | 3.11 | | | 0.89 | |
| Q5T0F9 | C2D1B | 1 | -1.32 | 3.34 | | | 0.04 | |
| Q9HA92 | RSAD1 | 1 | 1.31 | 7.23 | | | 0.49 | |
| P04004 | VTNC | 1 | 1.29 | 6.39 | | | -0.30 | |
| O60229 | KALRN | 1 | 1.29 | 6.32 | | | 0.38 | |
| Q8NF37 | PCAT1 | 1 | 1.28 | 7.34 | | | -0.55 | |
| Q86WI1 | PKHL1 | 1 | 1.26 | 4.09 | | | -1.13 | |
| Q5T1M5 | FKB15 | 1 | -1.25 | 6.17 | | | -0.05 | |
| Q8IUE6 | H2A2B | 2 | 1.23 | 7.40 | | | 0.00 | |
| Q9H0S4 | DDX47 | 1 | 1.18 | 7.09 | | | -0.14 | |
| Q96KQ4 | ASPP1 | 1 | 1.16 | 3.41 | | | -1.01 | |
| Q8IVT2 | MISP | 1 | -1.15 | 5.52 | | | 0.40 | |
| Q9H9B1 | EHMT1 | 1 | -1.13 | 3.76 | | | 1.84 | * |
| Q13158 | FADD | 1 | -1.10 | 2.11 | | | 0.37 | |
| P07384 | CAN1 | 1 | -1.09 | 5.85 | | | 0.49 | |
| P32242 | OTX1 | 2 | -1.09 | 5.03 | | | 2.36 | * |
| P02656 | APOC3 | 3 | 1.08 | 6.97 | 1 | -4.11 | -0.76 | |

Continued on next page

| Protein | Gene | N | log2FC | Avg Expr | p-value | B | IgG | |
|---|---|---|---|---|---|---|---|---|
| P35580 | MYH10 | 1 | 1.07 | 7.89 | | | -0.23 | |
| O00442 | RTCA | 1 | -1.06 | 2.48 | | | 1.26 | * |
| P39019 | RS19 | 2 | -1.06 | 8.37 | | | -0.10 | |
| P14770 | GPIX | 2 | 1.06 | 6.28 | | | -0.01 | |
| Q9UHB6 | LIMA1 | 1 | -1.03 | 3.12 | | | -0.08 | |
| O14745 | NHRF1 | 1 | -1.02 | 5.90 | | | 0.31 | |

Table 9: Top ranking differentially expressed proteins from the FOXA1 90min vs FOXA1 45min comparison, sorted by log2 fold change.

# 5 GRHL2 ChIP-Seq Analysis

## 5.1 Pre-processing

### 5.1.1 Download files

```
#!/bin/sh
java -jar ../java/clarity-tools.jar -l SLX-14333
```

### 5.1.2 Removal of reads in blacklisted sites

```
#downloaded from http://mitra.stanford.edu/kundaje/akundaje/release/blacklists/hg38-human/hg38.blacklis

bl=../blacklists/hg38.blacklist.bed


mkdir ./blacklist_filtered
cd SLX-14333
for f in *.bam
do
    echo $f
    bedtools intersect -v -abam $f -b $bl  > ../blacklist_filtered/$f
done

### Re-index

cd ../blacklist_filtered
for f in *.bam
do
samtools index $f
done
```

### 5.1.3 Peak Calling

```
### MACS peak caller

### Run macs on the blacklisted data
```

```
mkdir ./peaks
cd peaks
control=../GRHL2_filtered/SLX-14333.D701_D503.bam
for bam in ../GRHL2_filtered/*.bam
do
root=`basename $bam .bam`
macs2 callpeak -t $bam -c $control -f BAM -n $root -g hs &
done
```

## 5.2 Differntial binding analysis

### 5.2.1 MA plot

```
suppressMessages(library(DiffBind))

if(!file.exists("rdata/003_diffbind.rda")) {
    GRHL2 <- dba(sampleSheet="samplesheet/samplesheet.csv")
    GRHL2 <- dba.count(GRHL2, summits=250)
    GRHL2 <- dba.contrast(GRHL2)
    GRHL2 <- dba.analyze(GRHL2)
    save(GRHL2,file="rdata/003_diffbind.rda")
} else {
    load("rdata/003_diffbind.rda")
}


dba.plotMA(GRHL2, bFlip=1)
```

### 5.2.2 PCA

```
dba.plotPCA(GRHL2,components = 2:3)
```

### 5.2.3 Table of differntiall bound sites

```
library(knitr)
kable(head(as.data.frame(dba.report(GRHL2))))
```

| | seqnames | start | end | width | strand | Conc | Conc_none | Conc_ER | Fold | p.value | FDR |
|---|---|---|---|---|---|---|---|---|---|---|---|
| 12123 | 14 | 93959394 | 93959894 | 501 | * | 7.63 | 6.04 | 8.37 | -2.33 | 0 | 0e+00 |
| 9047 | 12 | 75706270 | 75706770 | 501 | * | 6.74 | 4.93 | 7.52 | -2.60 | 0 | 0e+00 |
| 24493 | 21 | 31529399 | 31529899 | 501 | * | 6.50 | 4.86 | 7.25 | -2.39 | 0 | 0e+00 |
| 129 | 1 | 7447769 | 7448269 | 501 | * | 4.98 | 2.44 | 5.85 | -3.41 | 0 | 0e+00 |
| 40054 | 9 | 75101020 | 75101520 | 501 | * | 6.94 | 4.80 | 7.76 | -2.96 | 0 | 0e+00 |
| 28564 | 3 | 176953741 | 176954241 | 501 | * | 5.53 | 3.80 | 6.30 | -2.50 | 0 | 1e-07 |

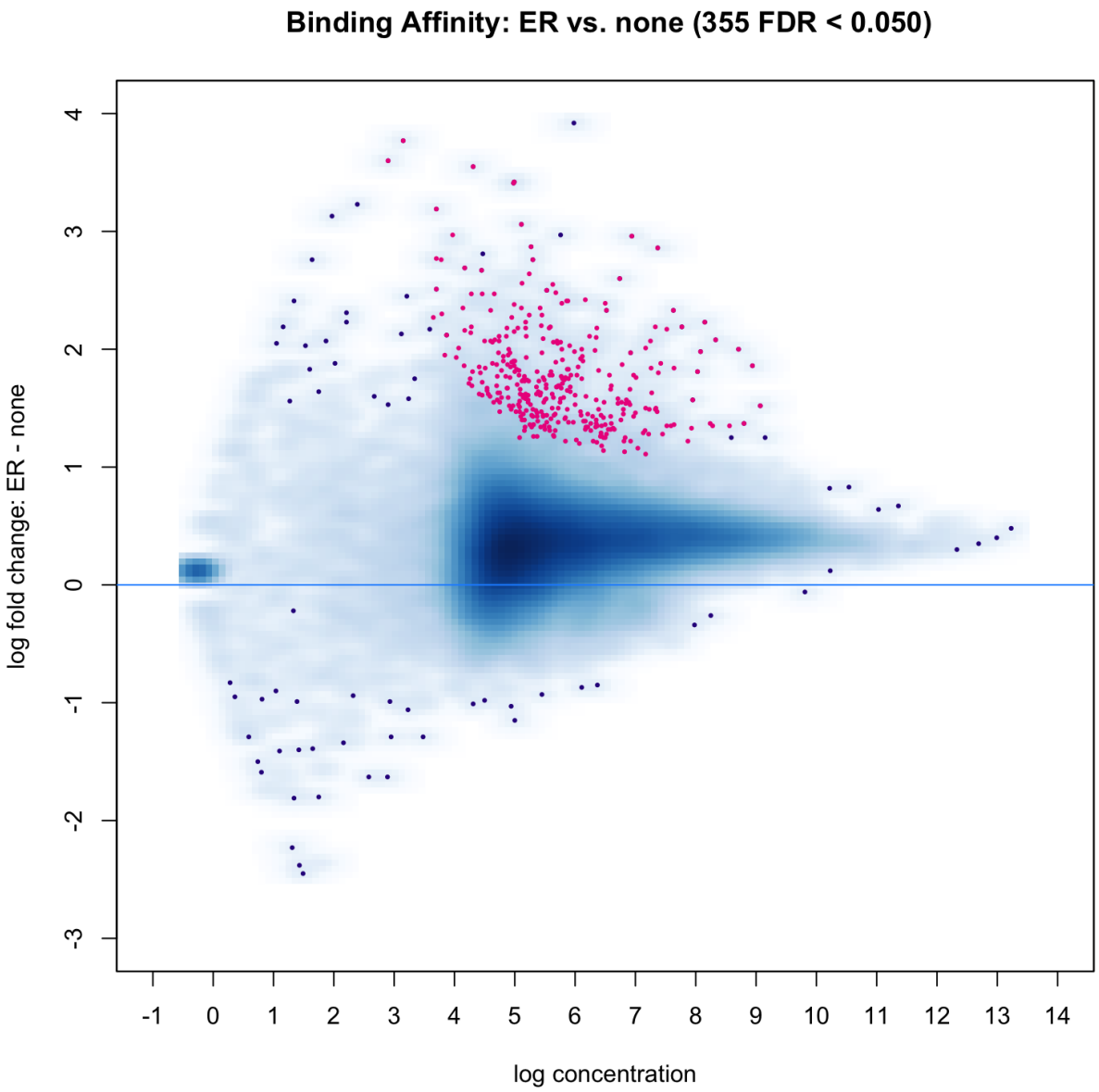


Figure 83: MA plot showing changes in GRHL2 binding before and after treatment with 100nM E2.

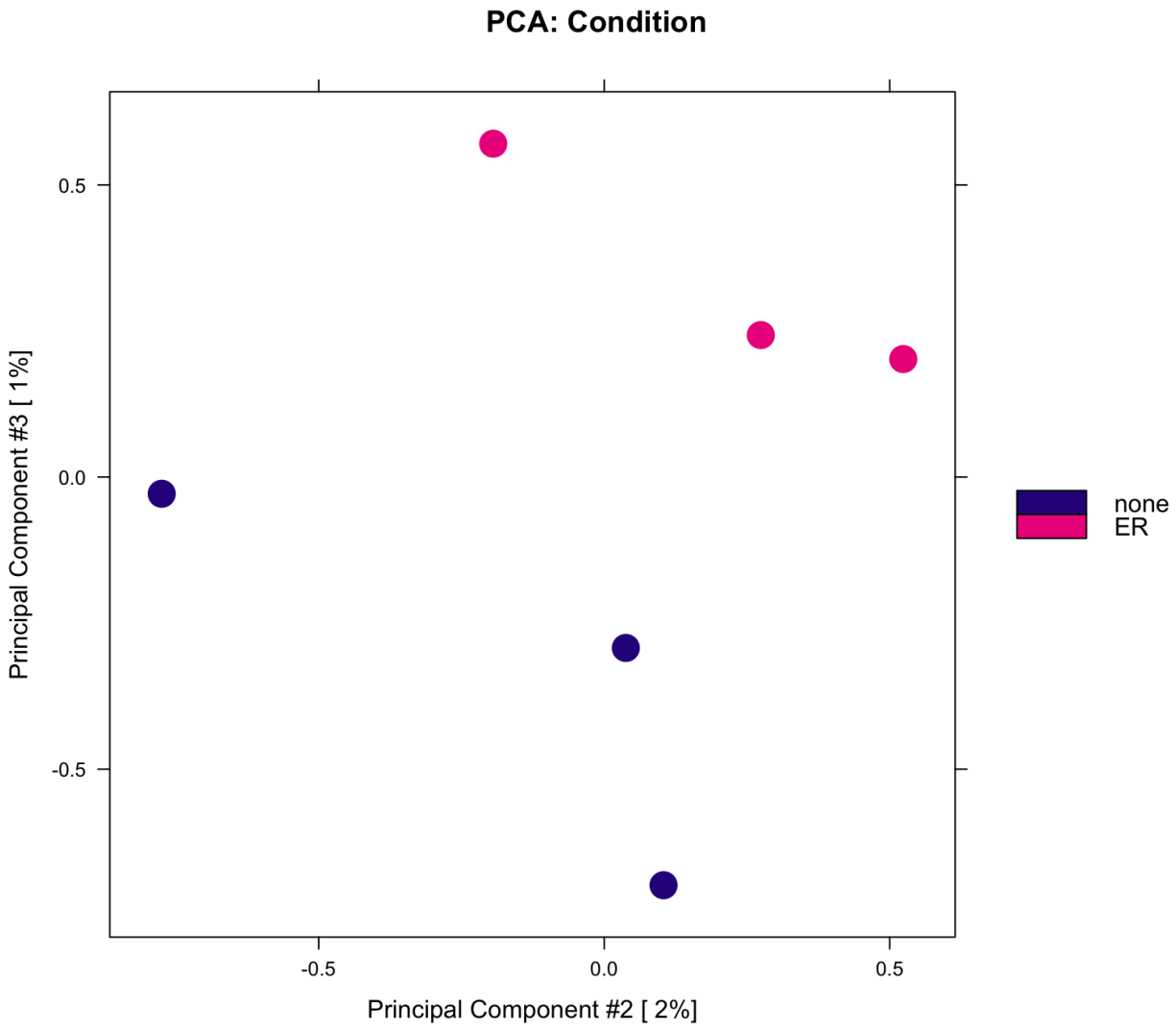


Figure 84: PCA Plot showing clustering of samples by condition

### 5.2.4 Number of sites with increased or decreased binding

```
r<-dba.report(GRHL2,th=1)
length(r[r$Fold>0])
```

```
## [1] 4973
```

```
length(r[r$Fold<0])
```

```
## [1] 37496
```

## 5.3 Quality Control

### 5.3.1 Reproducability of peaks

```
dba.plotVenn(GRHL2,GRHL2$masks$ER, label1="Rep1", label2="Rep2", main="GRHL2 +E2")
```

```
dba.plotVenn(GRHL2,GRHL2$masks$none, label1="Rep1", label2="Rep2", main="GRHL2 -E2")
```

```
called_none<-rowSums(GRHL2$called[,c(1:3)])
called_ER<-rowSums(GRHL2$called[,c(4:6)])
print(paste("Peaks called in -E2 samples:", length(called_none[called_none>0])))
```

```
## [1] "Peaks called in -E2 samples: 38763"
```

```
print(paste("Peaks called in +E2 samples:", length(called_ER[called_ER>0])))
```

```
## [1] "Peaks called in +E2 samples: 42565"
```

```
called_both<-called_none*called_none
print(paste("Peaks called in both settings:", length(called_both[called_both>0])))
```

```
## [1] "Peaks called in both settings: 38763"
```

## 5.4 VULCAN Analysis

```
suppressMessages(library(vulcan))

dist_calc<-function(method,dfanno,genematrix,genesmore,allsamples){
    # This function structure was strongly suggested
    # by the Bioconductor reviewer
    supportedMethods<-c(
        "closest",
        "strongest",
        "sum",
        "topvar",
        "farthest",
        "lowvar"
    )
    if(!method%in%supportedMethods){
        stop("unsupported method ", method)
    }

    for (gene in genesmore) {
```

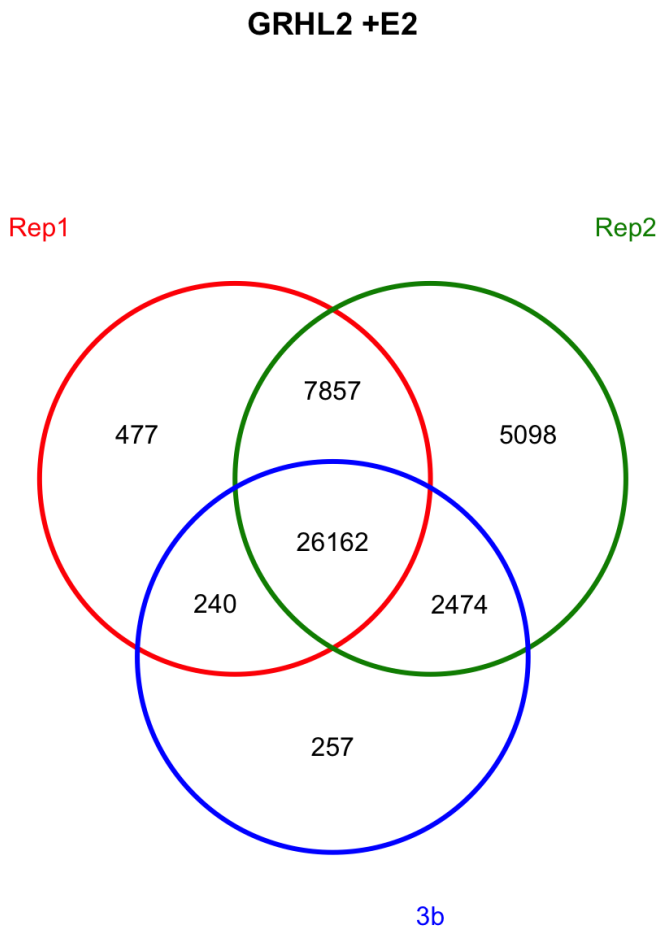


Figure 85: Peak overlap +E2

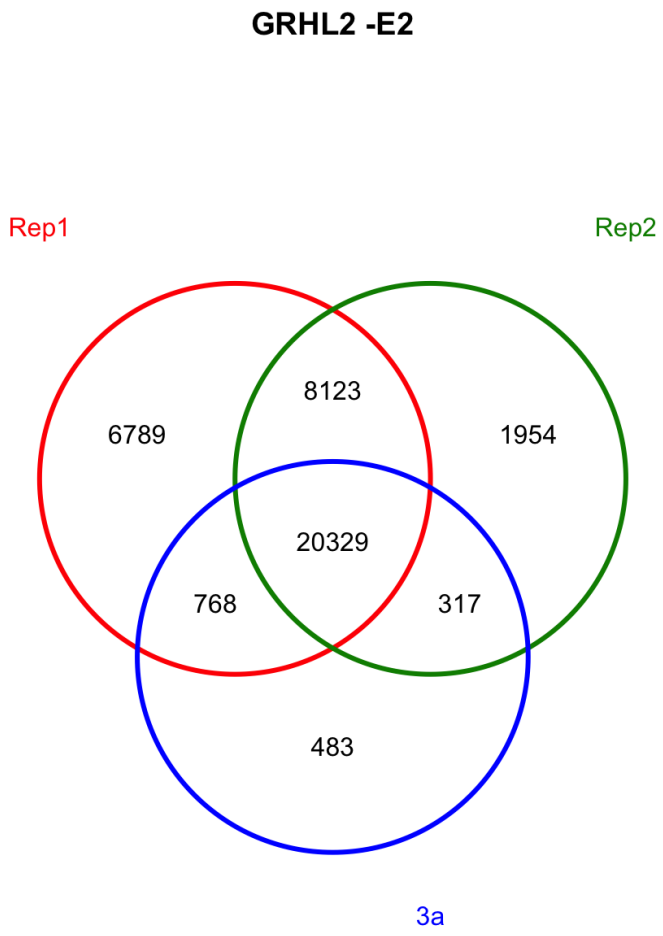


Figure 86: Peak overlap -E2

```
        subanno <- dfanno[dfanno$feature == gene, ]

        if (method == "closest") {
            closest <- which.min(subanno$distanceToStart)
            genematrix[gene, allsamples] <- as.numeric(subanno[closest,
                                                               allsamples])
        }

        if (method == "farthest") {
            farthest <- which.max(subanno$distanceToStart)
            genematrix[gene, allsamples] <- as.numeric(subanno[farthest,
                                                               allsamples])
        }

        if (method == "sum") {
            sums <- apply(subanno[, allsamples], 2, sum)
            genematrix[gene, allsamples] <- as.numeric(sums)
        }

        if (method == "strongest") {
            sums <- apply(subanno[, allsamples], 1, sum)
            top <- which.max(sums)
            genematrix[gene, allsamples] <- as.numeric(subanno[top,
                                                               allsamples])
        }

        if (method == "topvar") {
            vars <- apply(subanno[, allsamples], 1, var)
            top <- which.max(vars)
            genematrix[gene, allsamples] <- as.numeric(subanno[top,
                                                               allsamples])
        }

        if (method == "lowvar") {
            vars <- apply(subanno[, allsamples], 1, var)
            top <- which.min(vars)
            genematrix[gene, allsamples] <- as.numeric(subanno[top,
                                                               allsamples])
        }

    }
    return(genematrix)
}


vulcan.import.dba<- function (dbaobj, samples,intervals = NULL)
{
    dbcounts <- dbaobj
    listcounts <- dbcounts$peaks
    names(listcounts) <- dbcounts$samples[, 1]
    first <- listcounts[[1]]
    rawmat <- matrix(NA, nrow = nrow(first), ncol = length(listcounts) +
                         3)
```

```
    colnames(rawmat) <- c("Chr", "Start", "End", names(listcounts))
    rownames(rawmat) <- 1:nrow(rawmat)
    rawmat <- as.data.frame(rawmat)
    rawmat[, 1] <- as.character(first[, 1])
    rawmat[, 2] <- as.integer(first[, 2])
    rawmat[, 3] <- as.integer(first[, 3])
    for (i in 1:length(listcounts)) {
        rawmat[, names(listcounts)[i]] <- as.numeric(listcounts[[i]]$RPKM)
    }
    peakrpkms <- rawmat
    rm(rawmat)
    first <- listcounts[[1]]
    rawmat <- matrix(NA, nrow = nrow(first), ncol = length(listcounts) +
                        3)
    colnames(rawmat) <- c("Chr", "Start", "End", names(listcounts))
    rownames(rawmat) <- 1:nrow(rawmat)
    rawmat <- as.data.frame(rawmat)
    rawmat[, 1] <- as.character(first[, 1])
    rawmat[, 2] <- as.integer(first[, 2])
    rawmat[, 3] <- as.integer(first[, 3])
    for (i in 1:length(listcounts)) {
        rawmat[, names(listcounts)[i]] <- as.integer(listcounts[[i]]$Reads)
    }
    peakcounts <- rawmat
    rm(rawmat)
    vobj <- list(peakcounts = peakcounts, samples = samples,
                 peakrpkms = peakrpkms)
    return(vobj)
}

prependSampleNames <- function(vobj,prependString){
    colnames(vobj$peakcounts)[0:-3]<-paste0(prependString,colnames(vobj$peakcounts)[0:-3])
    vobj$samples[[2]]<-paste0(prependString,vobj$samples[[2]])
    vobj$samples[[1]]<-paste0(prependString,vobj$samples[[1]])
    colnames(vobj$peakrpkms)[0:-3]<-paste0(prependString,colnames(vobj$peakrpkms)[0:-3])
    return(vobj)
}

loadVulcanNetworks<-function(){
    regulons<-list()
    load("networks/laml-tf-regulon.rda")
    regulons$laml<-regul
    rm(regul)
    load("networks/brca-tf-regulon.rda")
    regulons$tcga<-regul
    rm(regul)
    load("networks/metabric-regulon-tfs.rda")
    regulons$metabric<-regulon
    rm(regulon)
    return(regulons)
}
```

```r
#Slow so just load the file below
#vobj<-vulcan.import("samplesheet/samplesheet.csv")
#load(file="003_vobj.Rda")
samples <- list()
samples[['ER']]<-c('1a','2a','3a')
samples[['none']]<-c('1b','2b','3b')

vobj <-vulcan.import.dba(GRHL2,samples)

#vobj<-vulcan.annotate(vobj,lborder=-10000,rborder=10000,method='sum')

vobj <-prependSampleNames(vobj,"X")

lborder=-10000
rborder=10000
method='sum'
#DEBUG
#source("https://bioconductor.org/biocLite.R")
#biocLite("TxDb.Hsapiens.UCSC.hg38.knownGene")
suppressMessages(library("TxDb.Hsapiens.UCSC.hg38.knownGene"))

annotation <- toGRanges(TxDb.Hsapiens.UCSC.hg38.knownGene,
                        feature = "gene")
gr <- GRanges(vobj$peakcounts)
seqlevels(annotation)<- sub('chr','',seqlevels(annotation))
anno <- annotatePeakInBatch(gr, AnnotationData = annotation,
                            output = "overlapping", FeatureLocForDistance = "TSS",
                            bindingRegion = c(lborder, rborder))
```

```
## Annotate peaks by annoPeaks, see ?annoPeaks for details.

## maxgap will be ignored.
```

```r
dfanno <- anno
names(dfanno) <- seq_len(length(dfanno))
dfanno <- as.data.frame(dfanno)
allsamples <- unique(unlist(vobj$samples))
genes <- unique(dfanno$feature)
peakspergene <- table(dfanno$feature)
rawcounts <- matrix(NA, nrow = length(genes), ncol = length(allsamples))
colnames(rawcounts) <- allsamples
rownames(rawcounts) <- genes
genesone <- names(peakspergene)[peakspergene == 1]
for (gene in genesone) {
    rawcounts[gene, allsamples] <- as.numeric(dfanno[dfanno$feature ==
                                                        gene, allsamples])
}

genesmore <- names(peakspergene)[peakspergene > 1]
rawcounts <- dist_calc(method, dfanno, rawcounts, genesmore,
                       allsamples)

gr <- GRanges(vobj$peakrpkms)
anno <- annotatePeakInBatch(gr, AnnotationData = annotation,
                            output = "overlapping", FeatureLocForDistance = "TSS",
```

```
                                bindingRegion = c(lborder, rborder))
```

```
## Annotate peaks by annoPeaks, see ?annoPeaks for details.
## maxgap will be ignored.
```

```
dfanno <- anno
names(dfanno) <- seq_len(length(dfanno))
dfanno <- as.data.frame(dfanno)
allsamples <- unique(unlist(vobj$samples))
genes <- unique(dfanno$feature)
peakspergene <- table(dfanno$feature)
rpkms <- matrix(NA, nrow = length(genes), ncol = length(allsamples))
rownames(rpkms) <- genes
genesone <- names(peakspergene)[peakspergene == 1]
colnames(rpkms)<-allsamples
for (gene in genesone) {
    rpkms[gene, allsamples] <- as.numeric(dfanno[dfanno$feature ==
                                                    gene, allsamples])
}
genesmore <- names(peakspergene)[peakspergene > 1]

rpkms <- dist_calc(method, dfanno, rpkms, genesmore, allsamples)
rawcounts <- matrix(as.numeric(rawcounts), nrow = nrow(rawcounts),
                    dimnames = dimnames(rawcounts))
rpkms <- matrix(as.numeric(rpkms), nrow = nrow(rpkms), dimnames = dimnames(rpkms))
vobj$rawcounts <- rawcounts
colnames(rpkms)<-allsamples
vobj$rpkms <- rpkms

#DEBUG ENDS

vobj<-vulcan.normalize(vobj)

load(file="networks/metabric-regulon-tfs.rda")

regulons <- loadVulcanNetworks()
suppressMessages(library("org.Hs.eg.db"))
list_eg2symbol<-as.list(org.Hs.egSYMBOL[mappedkeys(org.Hs.egSYMBOL)])

vobj_results<-list()

#test<-vulcan(vobj,       network=regulon, contrast=c("none","ER")    )

networks<-c("tcga","metabric") #,"laml")

for (network in networks) {
    vobj_results[[network]]<-vulcan(vobj,
                                    network=regulons[[network]],
                                    contrast=c("none","ER"),
                                    annotation=list_eg2symbol)
}
```

```
## Mon Mar 12 21:12:48 2018
## Computing the null model distribution by 1000 permutations.
```

```
## ------------------------------------------------------------
## Mon Mar 12 21:13:00 2018
## Computing regulon enrichment with aREA algorithm
##
## Estimating the normalized enrichment scores
## Mon Mar 12 21:13:35 2018
## Computing the null model distribution by 1000 permutations.
## ------------------------------------------------------------
## Mon Mar 12 21:13:47 2018
## Computing regulon enrichment with aREA algorithm
##
## Estimating the normalized enrichment scores
```

```
vobj_objects<-list(vobj_results)
names(vobj_objects)<-c("GRHL2")
networks<-c("tcga","metabric")
```

### 5.4.1 Transcription factor activity

```
plotVulcan <-function(vobj,threshold,network_title,title,plotTF,xlim,ylim) {
    threshold<-sign(threshold)*p2z(abs(threshold))
    network=vobj$mrs[,"NES"]
    tfs<-names(network)
    networkmat<-cbind(rep(0,length(network)),network[tfs])
    colnames(networkmat)<-c("0h","45min")
    matplot(t(networkmat),type="l",col="grey",ylab="VULCAN NES",xaxt="n",lty=1,main=title,xlim=xlim,yli
    axis(1,at=c(1:2),labels=colnames(networkmat))
    abline(h=c(0,threshold,-threshold),lty=2)
    text(2,networkmat[plotTF,2],label=names(networkmat[,2][plotTF]),pos=4,cex=0.6,font=2,col="red3")
    mtext(network_title)
}

par(mfrow=c(2,3))
for(network in networks){
    for (vobj_name in names(vobj_objects))
    {

        vobj<-vobj_objects[[vobj_name]]
        vobj<-vobj[[network]]
        #TFs<-getTFs(vobj)
        TFs=c("ESR1","PGR","FOXA1","GRHL2") #Overide TFS
        plotVulcan(vobj,0.05, paste0(network," Network"),vobj_name,TFs,xlim=c(1,2.3), ylim=c(min(vobj$m

        #TFs<-getTFs(vobj,0.05)
        plotVulcan(vobj,0.05, paste0(network," Network"),vobj_name,TFs,xlim=c(1,2.3), ylim=c(0,max(vobj

        #TFs<-getTFs(vobj,-0.05)
        plotVulcan(vobj,-0.05, paste0(network," Network"),vobj_name,TFs,xlim=c(1,2.3), ylim=c(min(vobj$
    }
}
```

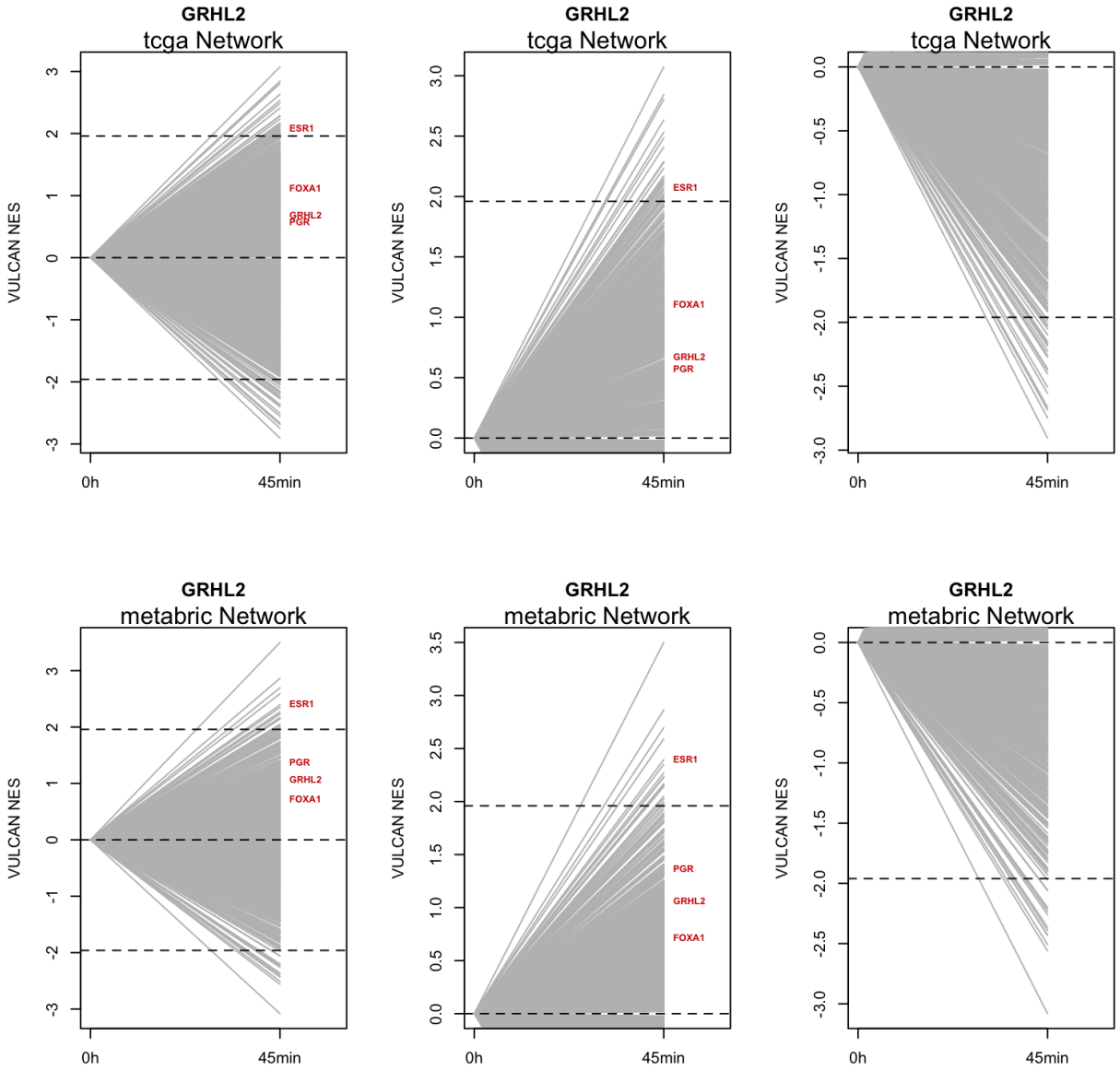


### 5.4.2 METABRIC TGCA comparison

```
interect<-intersect(rownames(vobj_results$metabric$mrs),
                    rownames(vobj_results$tcga$mrs))
plot(-log10(vobj_results$metabric$mrs[interect,"pvalue"]),
     -log10(vobj_results$tcga$mrs[interect,"pvalue"]),
     pch=20, xlab="Metabric Network Enrichment Score", ylab="TCGA Network Enrichment Score",main="VULCA
     col="gray"
     )

filtered<-(log10(vobj_results$metabric$mrs[interect,"pvalue"])^2+log10(vobj_results$tcga$mrs[interect,"
filtered[c("GATA3","PGR","FOXA1","ESR1","GRHL2")]<-rep(FALSE,5)
```

```
points(-log10(vobj_results$metabric$mrs[interect,"pvalue"][filtered]),
     -log10(vobj_results$tcga$mrs[interect,"pvalue"][filtered]),
     labels=interect[filtered],cex=1)

text(-log10(vobj_results$metabric$mrs[interect,"pvalue"][filtered]),
     -log10(vobj_results$tcga$mrs[interect,"pvalue"][filtered])-0.1,
     labels=interect[filtered],cex=1)

points(-log10(vobj_results$metabric$mrs[interect,"pvalue"][c("GATA3","PGR","FOXA1","ESR1","GRHL2")]),
       -log10(vobj_results$tcga$mrs[interect,"pvalue"][c("GATA3","PGR","FOXA1","ESR1","GRHL2")]),pch=20
text(-log10(vobj_results$metabric$mrs[interect,"pvalue"][c("FOXA1","ESR1","GRHL2")]),
     -log10(vobj_results$tcga$mrs[interect,"pvalue"][c("FOXA1","ESR1","GRHL2")])+0.2,col="red",
     labels=c("FOXA1","ESR1","GRHL2"),cex=1.25,font=2)
text(-log10(vobj_results$metabric$mrs[interect,"pvalue"][c("GATA3","PGR")])+0.2,
     -log10(vobj_results$tcga$mrs[interect,"pvalue"][c("GATA3","PGR")]),col="red",
     labels=c("GATA3","PGR"),cex=1.25,font=2)
```

## 5.5 Motif Analysis

### 5.5.1 Export bed files

```
#Note homer needs this as Hg format so you need to change from "1" to "chr1" etc.
df<-as.data.frame(dba.report(GRHL2))
df$seqnames<-paste0("chr",df$seqnames)

kable(head(df))
```

| | seqnames | start | end | width | strand | Conc | Conc_none | Conc_ER | Fold | p.value | FDR |
|---|---|---|---|---|---|---|---|---|---|---|---|
| 12123 | chr14 | 93959394 | 93959894 | 501 | * | 7.63 | 6.04 | 8.37 | -2.33 | 0 | 0e+00 |
| 9047 | chr12 | 75706270 | 75706770 | 501 | * | 6.74 | 4.93 | 7.52 | -2.60 | 0 | 0e+00 |
| 24493 | chr21 | 31529399 | 31529899 | 501 | * | 6.50 | 4.86 | 7.25 | -2.39 | 0 | 0e+00 |
| 129 | chr1 | 7447769 | 7448269 | 501 | * | 4.98 | 2.44 | 5.85 | -3.41 | 0 | 0e+00 |
| 40054 | chr9 | 75101020 | 75101520 | 501 | * | 6.94 | 4.80 | 7.76 | -2.96 | 0 | 0e+00 |
| 28564 | chr3 | 176953741 | 176954241 | 501 | * | 5.53 | 3.80 | 6.30 | -2.50 | 0 | 1e-07 |

```
#write.bed(df,"bed/up.bed")
```

```
df_all<-as.data.frame(dba.report(GRHL2, th=1))
df_all$seqnames<-paste0("chr",df_all$seqnames)

kable(head(df_all))
```

| | seqnames | start | end | width | strand | Conc | Conc_none | Conc_ER | Fold | p.value | FDR |
|---|---|---|---|---|---|---|---|---|---|---|---|
| 12123 | chr14 | 93959394 | 93959894 | 501 | * | 7.63 | 6.04 | 8.37 | -2.33 | 0 | 0e+00 |
| 9047 | chr12 | 75706270 | 75706770 | 501 | * | 6.74 | 4.93 | 7.52 | -2.60 | 0 | 0e+00 |
| 24493 | chr21 | 31529399 | 31529899 | 501 | * | 6.50 | 4.86 | 7.25 | -2.39 | 0 | 0e+00 |
| 129 | chr1 | 7447769 | 7448269 | 501 | * | 4.98 | 2.44 | 5.85 | -3.41 | 0 | 0e+00 |
| 40054 | chr9 | 75101020 | 75101520 | 501 | * | 6.94 | 4.80 | 7.76 | -2.96 | 0 | 0e+00 |
| 28564 | chr3 | 176953741 | 176954241 | 501 | * | 5.53 | 3.80 | 6.30 | -2.50 | 0 | 1e-07 |

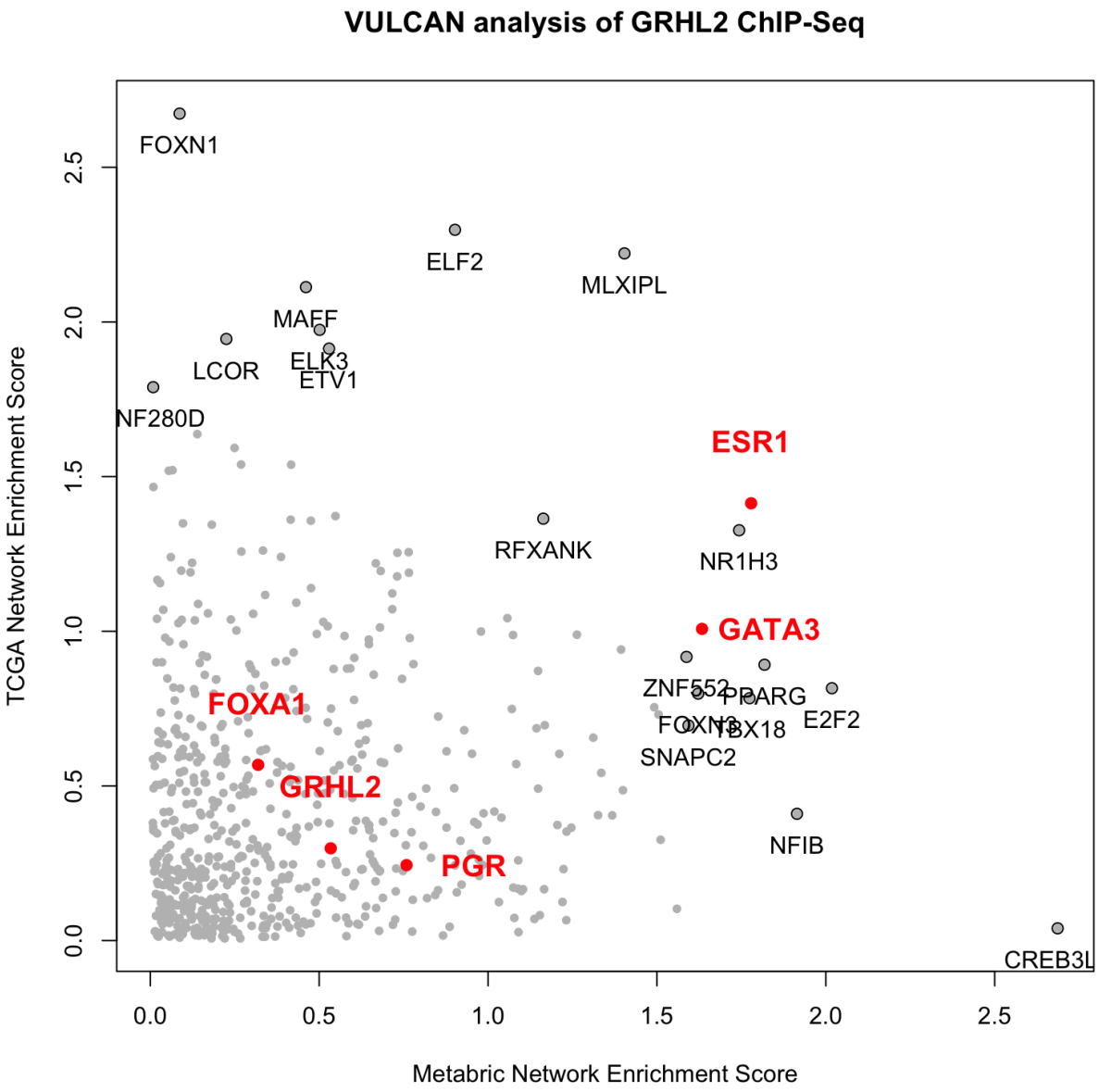


Figure 87: Comparision of results of VULCAN analysis for METABRIC and TGCA

```
#write.bed(df_all,"bed/all.bed")
```

### 5.5.2 Homer

```
#Homer

mkdir motifAnalysis
cd motifAnalysis
findMotifsGenome.pl ../bed/up.bed hg38 grhl2UpSites
findMotifsGenome.pl ../bed/all.bed hg38 grhl2AllSites
```

### 5.5.3 Generate promoter locations

Generate Bed file of Promoters

```
require(TxDb.Hsapiens.UCSC.hg38.knownGene)
txdb <- TxDb.Hsapiens.UCSC.hg38.knownGene
p<-promoters(genes(txdb), upstream = 1500, downstream = 500)

write.bed<-function(df, filename){
    write.table(as.data.frame(df)[,1:3],
                filename, quote=FALSE, sep="\t",
                row.names=FALSE, col.names=FALSE)
}

write.bed(p,"bed/promoter.bed")
```

## 5.6 Ovlerap of GRHL2 binding sites with published data

### 5.6.1 Extract ChIA-PET Data

```
#ChIA-pet all 3 https://www.encodeproject.org/experiments/ENCSR000BZZ/
cd bed
multiIntersectBed -i *bed6_sorted.bed | awk '{if ($4 > 1) {print} }' > hglft_ChIA_combined.bed
```

### 5.6.2 Find overlapping sites

```
#p300 from Zwart, EMBO, 2011
#ER from Hurtado 2011
#gro-seq GSE43835
#Rest from Caroll MLL3 paper

cd bed
mkdir overlaps

#generate gro-seq interect
#file1=hglft_E2.40m.rep1.bed
```

```
#file2=hglft_E2.40m.rep2.bed
#output=gro-seq.bed
#bedtools intersect -sorted -a $file1 -b $file2 > overlaps/$output

file1=hglft_foxa1.bed
file2=up.bed
output=foxa1-up.bed
bedtools intersect -a $file1 -b $file2 > overlaps/$output

file1=hglft_ER_Hurtado_2011.bed
output=er-up.bed
bedtools intersect -a $file1 -b $file2 > overlaps/$output

#file1=gro-seq.bed
#output=gro-up.bed
#bedtools intersect -a $file1 -b $file2 > overlaps/$output


file1=hglft_ChIA_combined.bed
output=ChIAPet_up.bed
bedtools intersect -a $file1 -b $file2 > overlaps/$output

file1=hglft_h3k4me1.bed
output=h3k4me1-up.bed
bedtools intersect -a $file1 -b $file2 > overlaps/$output

file1=hglft_h3k4me3.bed
output=h3k4me3-up.bed
bedtools intersect -a $file1 -b $file2 > overlaps/$output

file1=hglft_p300_ctrl.bed
output=p300_ctrl_up.bed
bedtools intersect -a $file1 -b $file2 > overlaps/$output

file1=hglft_p300_e2.bed
output=p300_e2_up.bed
bedtools intersect -a $file1 -b $file2 > overlaps/$output


#all peaks

file1=hglft_foxa1.bed
file2=all.bed
output=foxa1-all.bed
bedtools intersect -a $file1 -b $file2 > overlaps/$output

file1=hglft_ER_Hurtado_2011.bed
output=er-all.bed
bedtools intersect -a $file1 -b $file2 > overlaps/$output

#file1=gro-seq.bed
#output=gro-all.bed
#bedtools intersect -a $file1 -b $file2 > overlaps/$output
```

```
file1=hglft_ChIA_combined.bed
output=ChIAPet_all.bed
bedtools intersect -a $file1 -b $file2 > overlaps/$output

file1=hglft_h3k4me1.bed
output=h3k4me1-all.bed
bedtools intersect -a $file1 -b $file2 > overlaps/$output

file1=hglft_h3k4me3.bed
output=h3k4me3-all.bed
bedtools intersect -a $file1 -b $file2 > overlaps/$output

file1=hglft_p300_ctrl.bed
output=p300_ctrl_all.bed
bedtools intersect -a $file1 -b $file2 > overlaps/$output

file1=hglft_p300_e2.bed
output=p300_e2_all.bed
bedtools intersect -a $file1 -b $file2 > overlaps/$output

##Overlap with promoters

file1=overlaps/ChIAPet_up.bed
file2=promoter.bed
output=ChIAPet_up_prom.bed
bedtools intersect -a $file1 -b $file2 > overlaps/$output

file1=overlaps/ChIAPet_all.bed
file2=promoter.bed
output=ChIAPet_all_prom.bed
bedtools intersect -a $file1 -b $file2 > overlaps/$output
```

### 5.6.3 Count number of overlaping sites

```
cd bed/overlaps
wc -l *.bed > overlaps.txt
```

### 5.6.4 Table of number of overlaping sites for each factor

```
overlaps<-read.table("bed/overlaps/overlaps.txt")
kable(overlaps)
```

| V1 | V2 |
|---|---|
| 1764 | ChIAPet_all.bed |
| 109 | ChIAPet_all_prom.bed |
| 214 | ChIAPet_up.bed |
| 8 | ChIAPet_up_prom.bed |
| 5539 | er-all.bed |
| 318 | er-up.bed |
| 13422 | foxa1-all.bed |

| V1 | V2 |
|---|---|
| 255 | foxa1-up.bed |
| 33831 | h3k4me1-all.bed |
| 343 | h3k4me1-up.bed |
| 10234 | h3k4me3-all.bed |
| 55 | h3k4me3-up.bed |
| 7072 | p300_ctrl_all.bed |
| 155 | p300_ctrl_up.bed |
| 13588 | p300_e2_all.bed |
| 337 | p300_e2_up.bed |
| 87244 | total |

### 5.6.5 GRHL2 binding overlap with known factors

```
overlapsDF<-cbind(overlaps[1:16,],c('all','all','up','up','all','up','all','up','all','up','all','up','a
overlapsDF<-cbind(overlapsDF,c('all','promoter','all','promoter',rep("all",12)))
overlapsDF<-cbind(overlapsDF,c(rep("None",14),"E2","E2"))
colnames(overlapsDF)<-c("Number","Factor","GRHL2","Feature","Treatment")
overlapsDF$Factor<-c(rep("ChIAPet",4),rep("ER",2),rep("FOXA1",2),rep("H3K4Me1",2),rep("H3K4Me3",2),rep(
overlapsDF$Number<-as.numeric(overlapsDF$Number)
ChIAPet<-overlapsDF[overlapsDF$Factor=='ChIAPet' & overlapsDF$Feature=='all',]
ChIAPet$Number<-overlapsDF[overlapsDF$Factor=='ChIAPet' & overlapsDF$Feature=='all',]$Number - overlapsD
ChIAPet$Feature<-c('enchancer','enchancer')
overlapsDF<-rbind(overlapsDF,ChIAPet)
overlapsDF<-data.frame(overlapsDF)
overlapsDF[overlapsDF$GRHL2=='up',]$Number<-(overlapsDF[overlapsDF$GRHL2=='up',]$Number/355)*100 #355 i
overlapsDF[overlapsDF$GRHL2=='all',]$Number<-(overlapsDF[overlapsDF$GRHL2=='all',]$Number/42721)*100 #T

library(lattice)

barchart(Number ~ Factor ,data=overlapsDF[overlapsDF$Factor != 'ChIAPet',],
         par.settings = simpleTheme(col=c("lightblue","pink")),
         group=GRHL2,auto.key=list(space="top", columns=2, text=c('All GRHL2 Sites','GRHL2 Sites Respons
         main="GRHL2 Binding Overlap with Known Factors", ylab="Percentage of GRHL2 sites that overlap"
         xlab="Factor")
```

### 5.6.6 GRHL2 binding overlap with P300 binding sites

```
barchart(Number ~ Treatment ,data=overlapsDF[overlapsDF$Factor=='P300',],
         group=GRHL2,
         auto.key=list(space="top",columns=2, text=c('All GRHL2 Sites','GRHL2 Responsive to E2')),
         par.settings = simpleTheme(col=c("lightblue","pink")),
         main="GRHL2 overlap with P300 binding sites",
         xlab="P300 ChIP-Seq Condition",
         ylab="Percentage of GRHL2 sites that overlap")
```

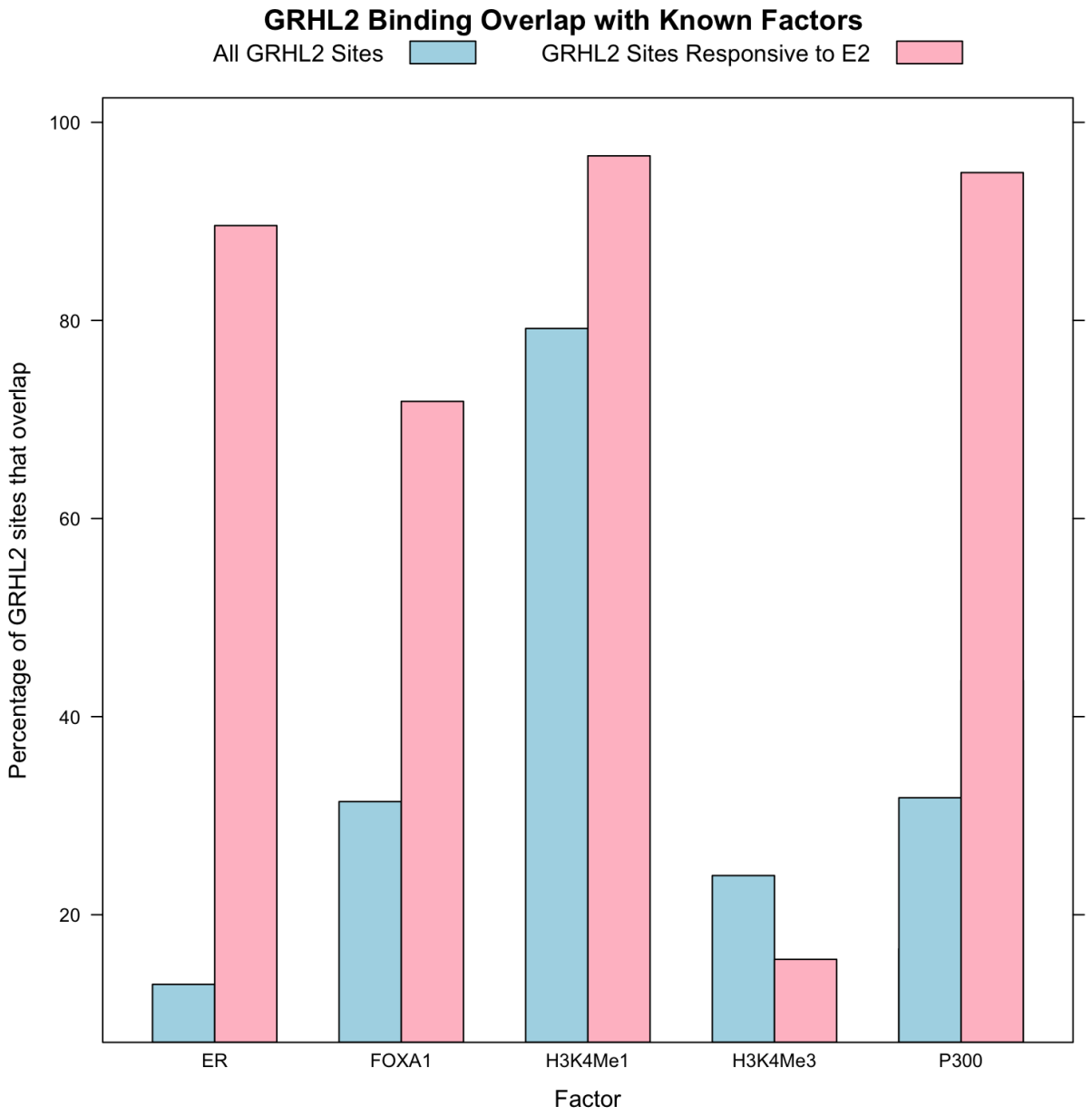


Figure 88: GRHL2 binding overlap with known factors

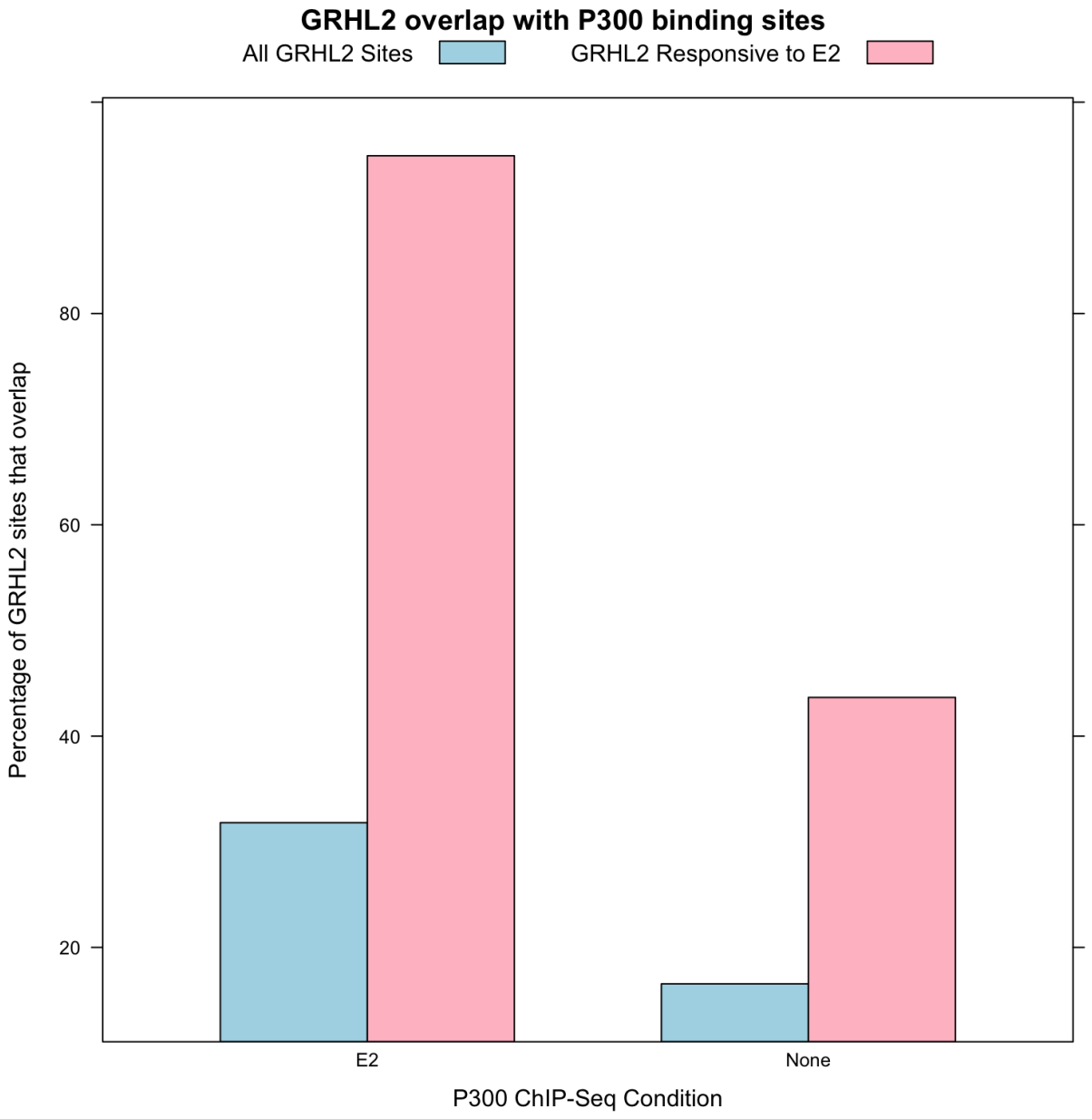


Figure 89: GRHL2 binding overlap with P300 binding sites

### 5.6.7 GRHL2 overlap with ChIA-PET sites

```
barchart(Number ~ Feature ,data=overlapsDF[overlapsDF$Factor=='ChIAPet',],
         group=GRHL2,
         auto.key=list(space="top",columns=2, text=c('All GRHL2 Sites','GRHL2 Sites Responsive to E2'))
         par.settings = simpleTheme(col=c("lightblue","pink")),
         main="GRHL2 overlap with ChIA-PET sites",
         xlab="Genomic Feature ChIP-Seq Condition",
         ylab="Percentage of GRHL2 sites that overlap")
```

### 5.6.8 GRHL2 overlap with Gro-SEQ data

```
allPeaks<-read.csv("txt/All_GRHL2_peaks_GSE43836.csv")
upPeaks<-read.csv("txt/Up_GRHL2_peaks_GSE43836.csv")


par(mfrow=c(1,2))

plot(allPeaks[1:2],ylim=c(0,6),type="n", lwd=2, ylab="Read Depth", main="All GRHL2 Sites")
lines(allPeaks[c(1,2)], lwd=2, col="lightblue")
lines(allPeaks[c(1,3)], lwd=2,  col="lightblue")
lines(allPeaks[c(1,4)], lwd=2,  col="pink")
lines(allPeaks[c(1,5)],  lwd=2, col="pink")

plot(upPeaks[c(1,5)],ylim=c(0,6),type="n", ylab="Read Depth", main="E2 responsive GRHL2 Sites")
lines(upPeaks[c(1,2)], lwd=2,col="lightblue")
lines(upPeaks[c(1,3)], lwd=2, col="lightblue")
lines(upPeaks[c(1,4)], lwd=2, col="pink")
lines(upPeaks[c(1,5)],  lwd=2,col="pink")
```

### 5.6.9 GRHL2 overlap with Gro-SEQ data is reproducible between studies

```
GSE43836<-read.csv("txt/averaged_GSE43836.csv")

colnames(GSE43836)[1]<-"Distance from Center/bp"

par(mfrow=c(2,2))

plot(GSE43836[1:2],ylim=c(0,6),type="n", lwd=2, ylab="Read Depth", main="All GRHL2 Sites [GSE43836]")
lines(GSE43836[c(1,2)], lwd=2, col="lightblue")
lines(GSE43836[c(1,3)], lwd=2,  col="pink")
lines(GSE43836[c(1,4)], lwd=2,  col="deeppink")
legend("topright", legend=c("0 min", "45 min", "90 min"),
       col=c("lightblue","pink","deeppink"),pch=20, cex=0.5, horiz = TRUE)

plot(GSE43836[1:2],ylim=c(0,6),type="n", lwd=2, ylab="Read Depth", main="Resonsive GRHL2 Sites [GSE4383
lines(GSE43836[c(1,5)], lwd=2, col="lightblue")
lines(GSE43836[c(1,6)], lwd=2,  col="pink")
lines(GSE43836[c(1,7)], lwd=2,  col="deeppink")
legend("topright", legend=c("0 min", "45 min", "90 min"),
```

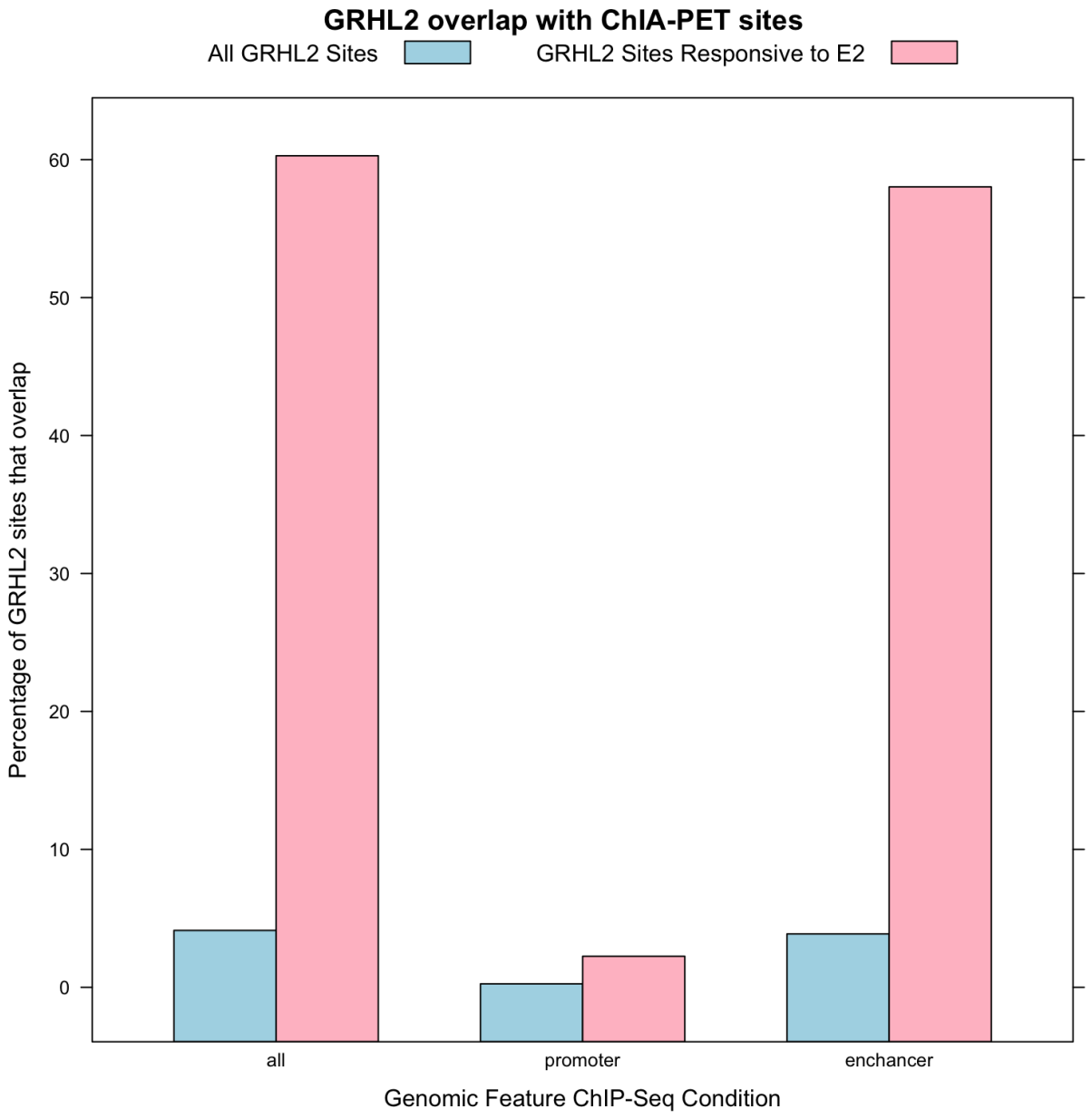


Figure 90: GRHL2 overlap with ChIA-PET sites

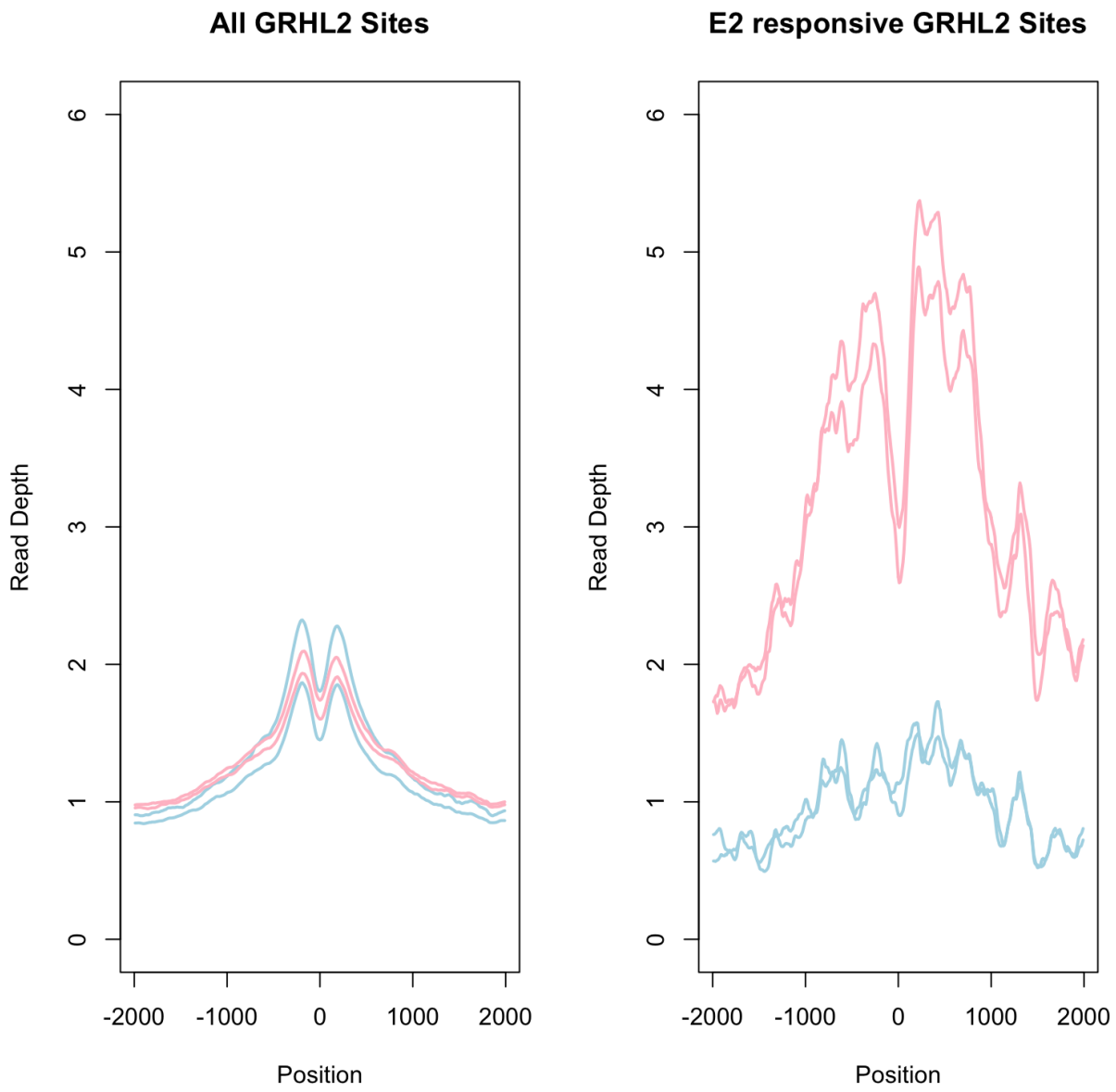


Figure 91: Gro-Seq data at GRHL2 sites. Blue is control samples, pink is E2 treated samples. Data from GSE43836.

```
       col=c("lightblue","pink","deeppink"),pch=20, cex=0.5,horiz = TRUE)

GSE45822<-read.csv("txt/averaged_GSE45822.csv")

colnames(GSE45822)[1]<-"Distance from Center/bp"


plot(GSE45822[1:2],ylim=c(0,6),type="n", lwd=2, ylab="Read Depth", main="All GRHL2 Sites [GSE45822]")
lines(GSE45822[c(1,3)], lwd=2, col="lightblue")
lines(GSE45822[c(1,2)], lwd=2,  col="deeppink")
legend("topright", legend=c("Veh", "E2"),
       col=c("lightblue","deeppink"),pch=20, cex=0.5,horiz = TRUE)

plot(GSE45822[1:2],ylim=c(0,6),type="n", lwd=2, ylab="Read Depth", main="All GRHL2 Sites [GSE45822]")
lines(GSE45822[c(1,5)], lwd=2, col="lightblue")
lines(GSE45822[c(1,4)], lwd=2,  col="deeppink")
legend("topright", legend=c("Veh", "E2"),
       col=c("lightblue","deeppink"),pch=20, cex=0.5,horiz = TRUE)
```

# 6 GRHL2 qPLEX-RIME Analysis

## 6.1 Introduction

This report provides a summary of the results of your proteomics experiment.

Your experiment has **11** samples. **9032** peptides from **1514** unique proteins were captured in the experiment. Each protein is represented by **1** to **255** peptides, but median number of peptides per protein was **2**.

## 6.2 Raw data QC

### 6.2.1 Coverage plot

Figure 1 shows the coverage of the bait protein, GRHL2, in terms of peptides detected.

### 6.2.2 Intensity Plot

Figure 2 shows the distribution of raw peptide intensities for each sample.

### 6.2.3 Peptide intensities for GHRL2

Figure 3 shows the raw intensities for each peptide detected for the bait protein GRHL2 in each sample.

### 6.2.4 Correlation Plot

Figure 4 shows a correlation matrix to visualize the level of linear association of samples within and between groups based on the raw peptide intensities.

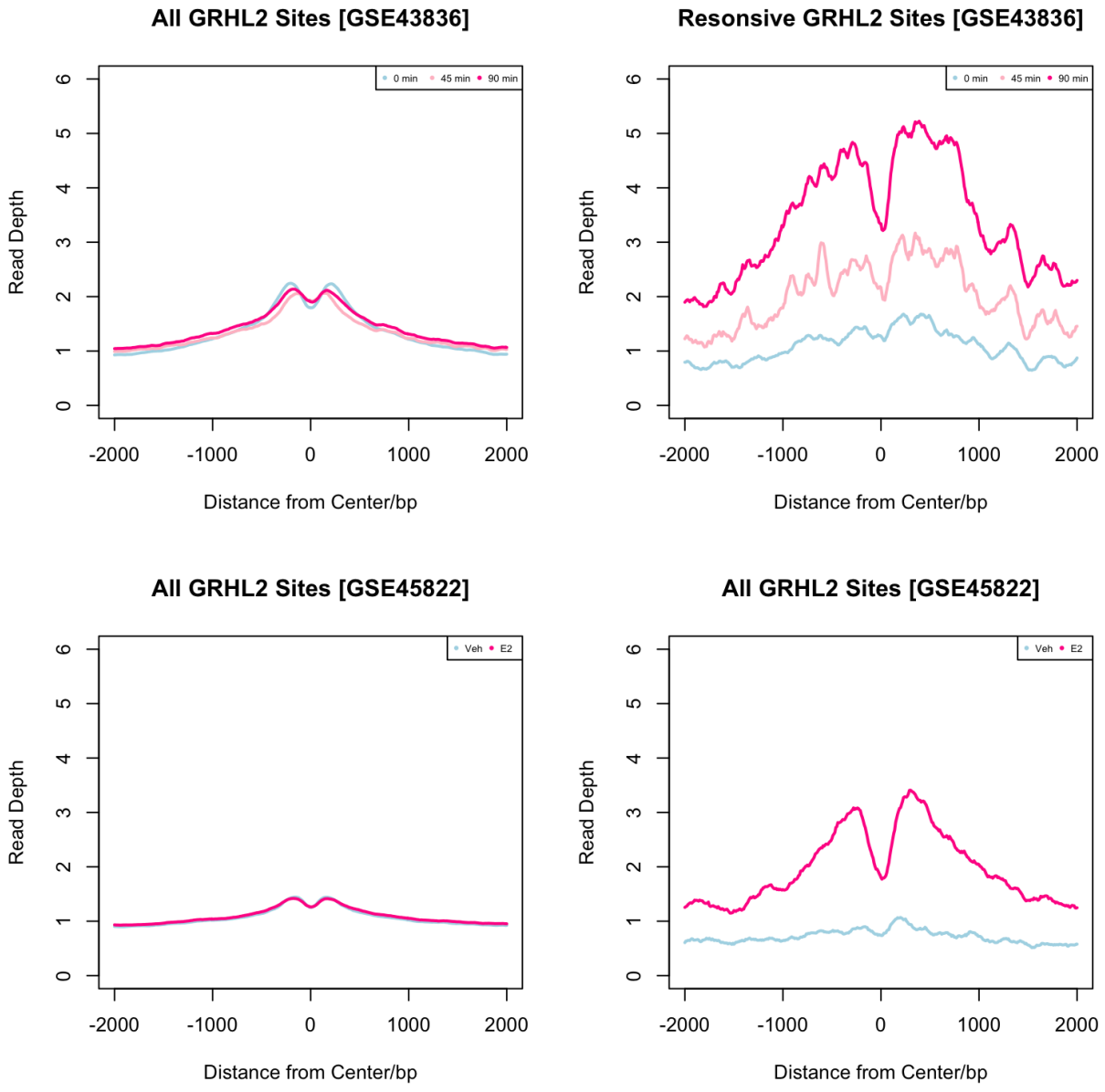


Figure 92: Analysis of GRHL2 sites of Gro-Seq data from GSE43836 and GSE45822 both showed that E2 responsive GRHL2 resonsive sites are transcriptionally responsive to E2.

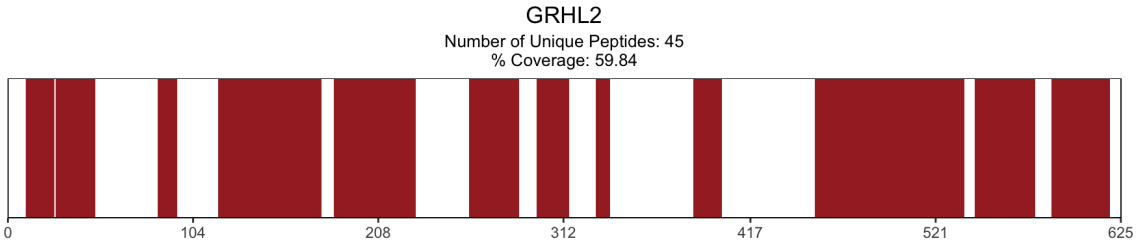


Figure 93: **Figure 1. Plot of peptide coverage for GRHL2 (UniprotID: Q6ISB3) **

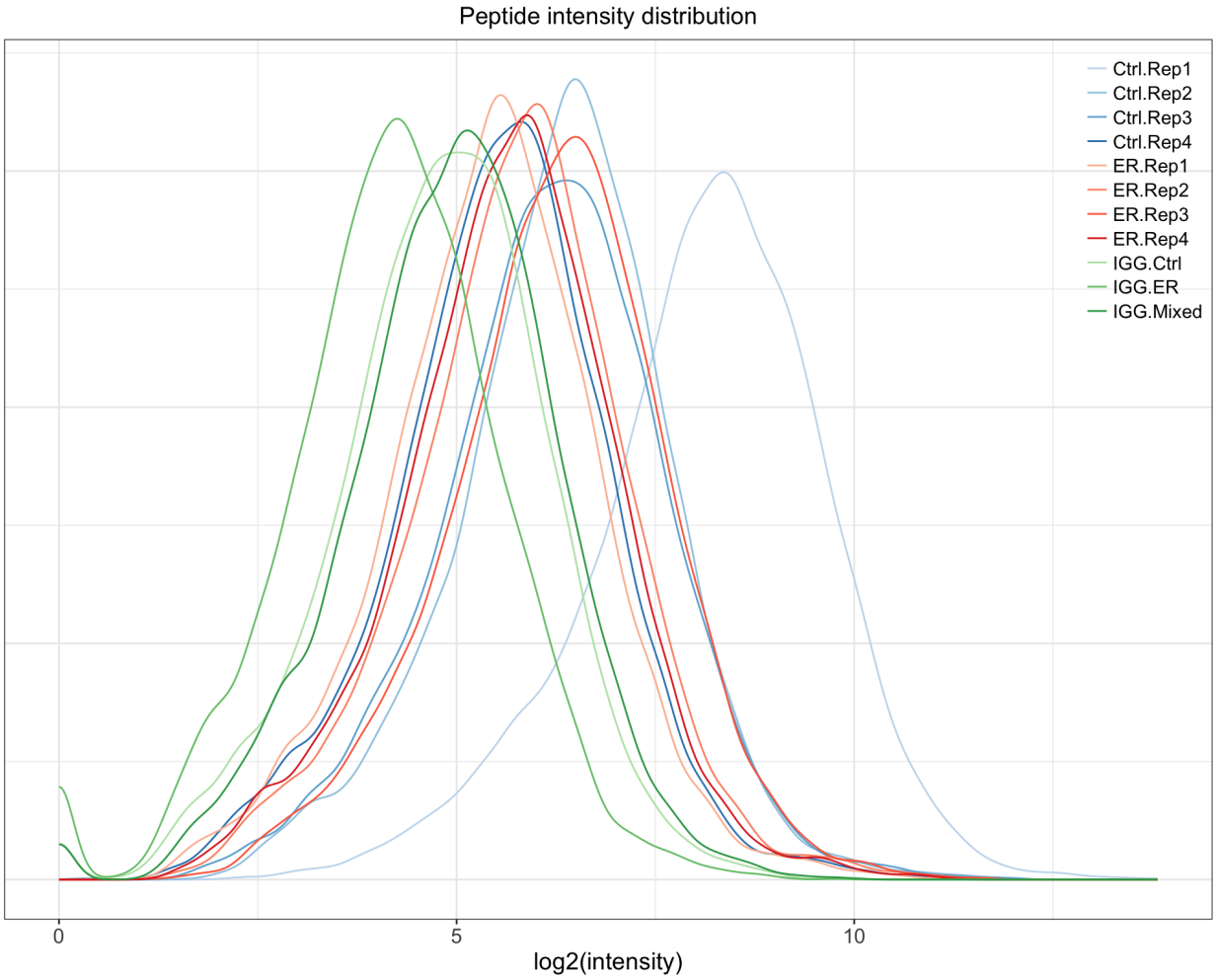


Figure 94: **Figure 2. Raw intensities plot. **

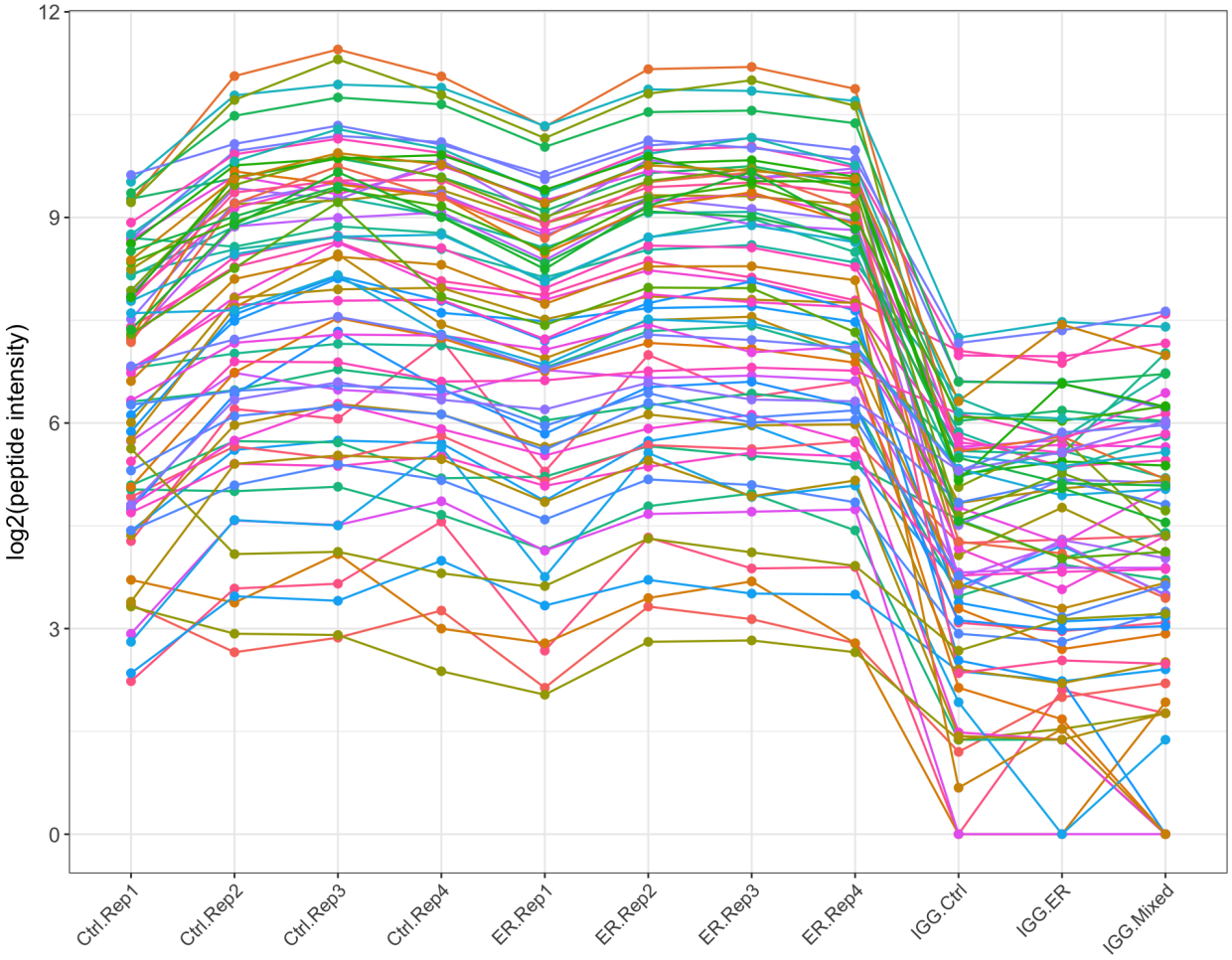


Figure 95: **Figure 3. Peptide intensities for GRHL2. **

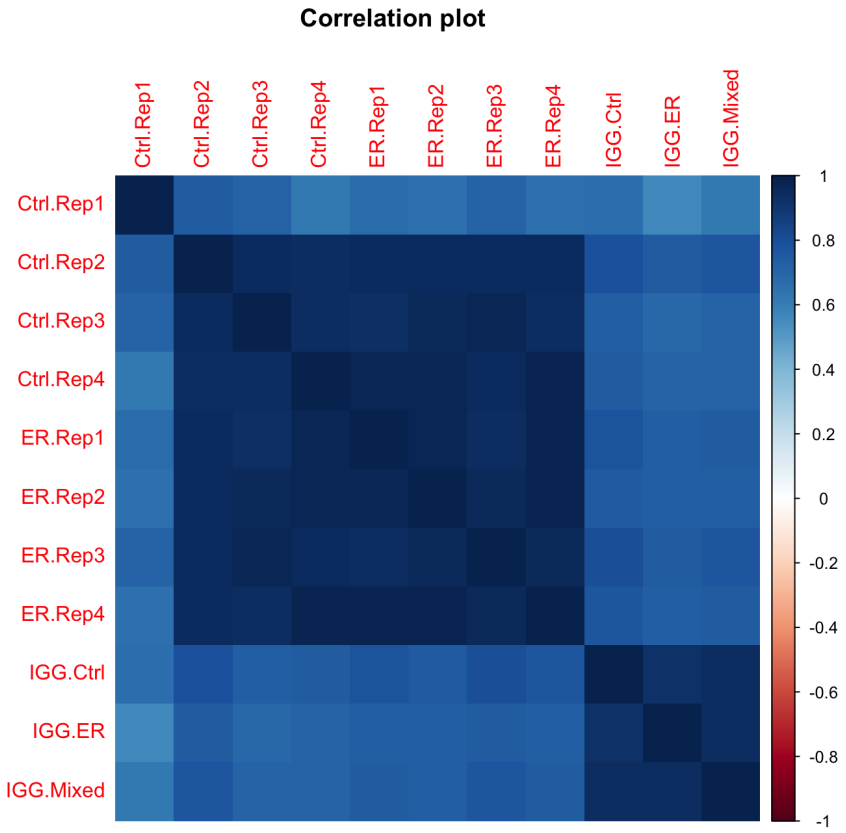


Figure 96: **Figure 4. Correlation plot based on raw intensities. **

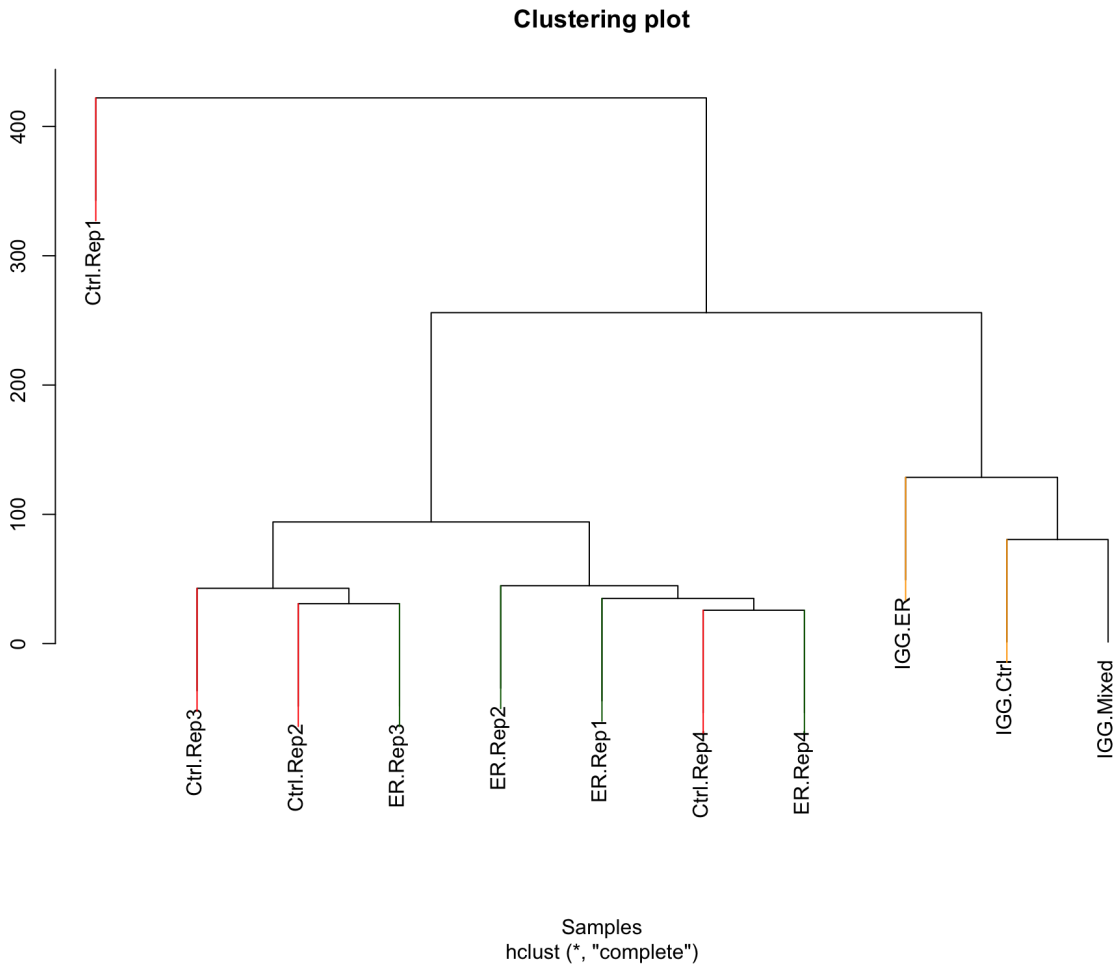


Figure 97: **Figure 5. Hierachical clustering based on raw intensities. **

### 6.2.5 Hierichical clustering dendrogram

Figure 5 shows a dendrogram displaying the hierarchical relationship among samples. The vertical axis shows the dissimilarity (measured by means of the Euclidean distance) between samples: similar samples appear on the same branches. Colors correspond to sample groups.

### 6.2.6 PCA Plot

Figure 6 shows a visual representation of the scaled loading of the first two dimensions of a principle component analysis of the raw peptide intensities.

List of 1 $ aspect.ratio: num 1 - attr(, *"class")= chr [1:2] "theme" "gg" - attr(*, "complete")= logi FALSE - attr(*, "validate")= logi TRUE

### 6.2.7 QC Conclusion

The sample Ctrl rep 1 appears to be an outlier. The differential anlaysis was carried out twice, first with this sample included and then again with the sample excluded.

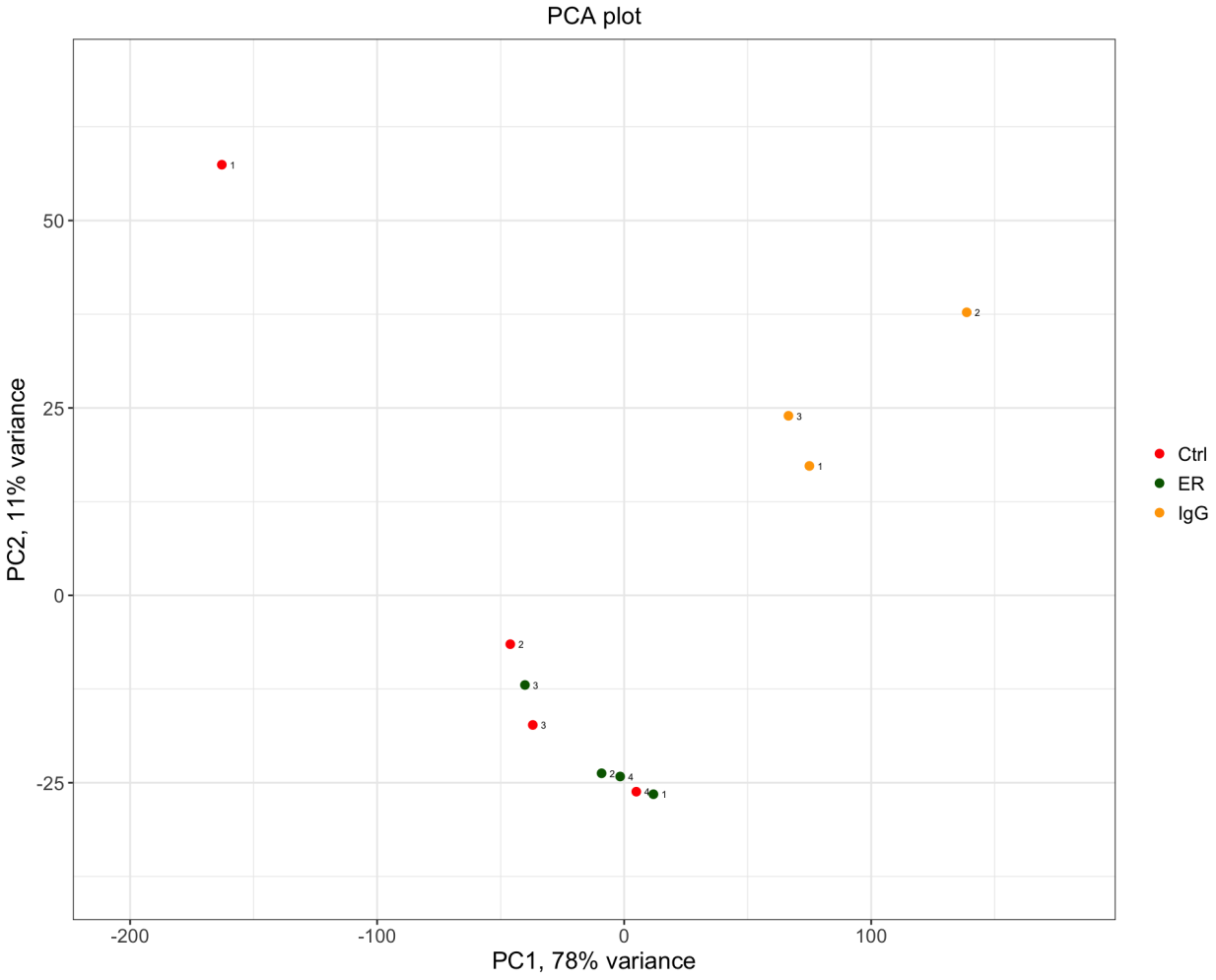


Figure 98: **Figure 6. Principle Component Analysis based on raw intensities. **

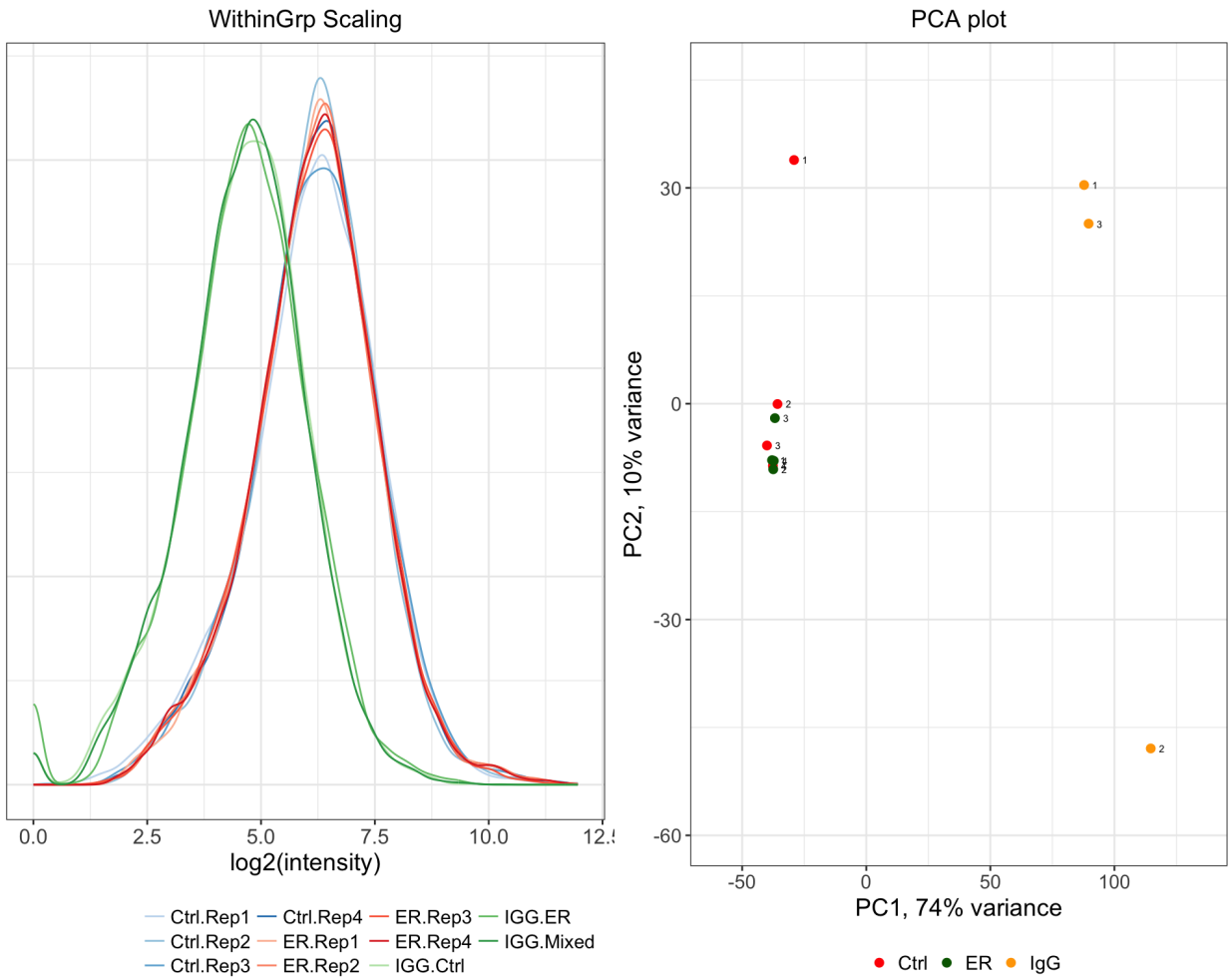


Figure 99: **Figure 7. Effects of normalisation on peptide intensities. **

## 6.3 Full data set analysis

The following section shows the results for analysis of all 8 samples.

### 6.3.1 Effect of within group normalisation

Normalisation was carried out using median scaling. The experimental samples and the IgG control samples were normalised separately. Figure 7 show the effects of normalisation on the intensity plots and the principle component analysis.

### 6.3.2 Differential analysis results

Figure 8 shows differential abundancy results. No proteins were statistically differentially abundant. Figure 7 shows an MA plot and a volcano plot of the differental analysis results.

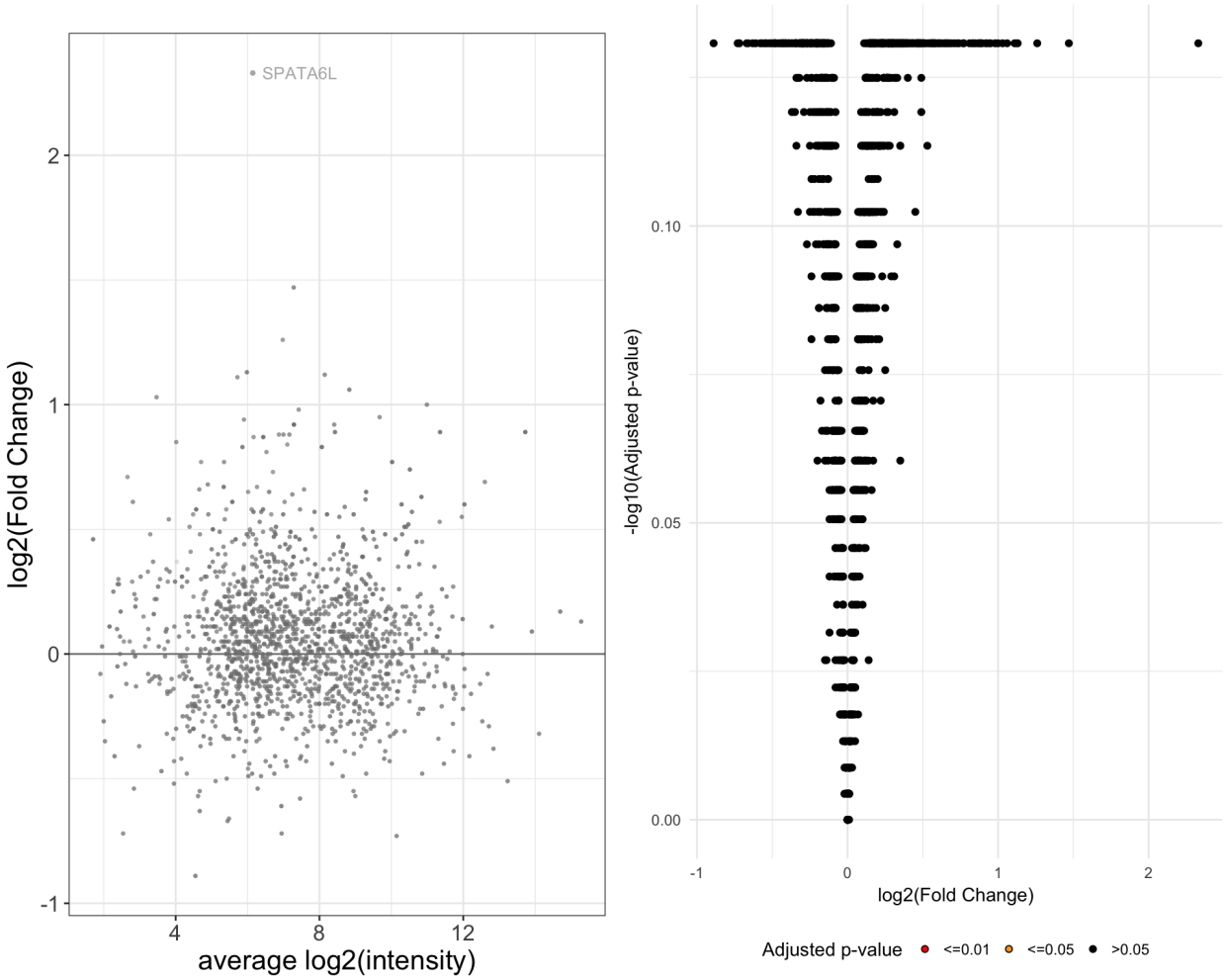


Figure 100: **Figure 9. MA plot and volcano plot of differential protein abundancy. **

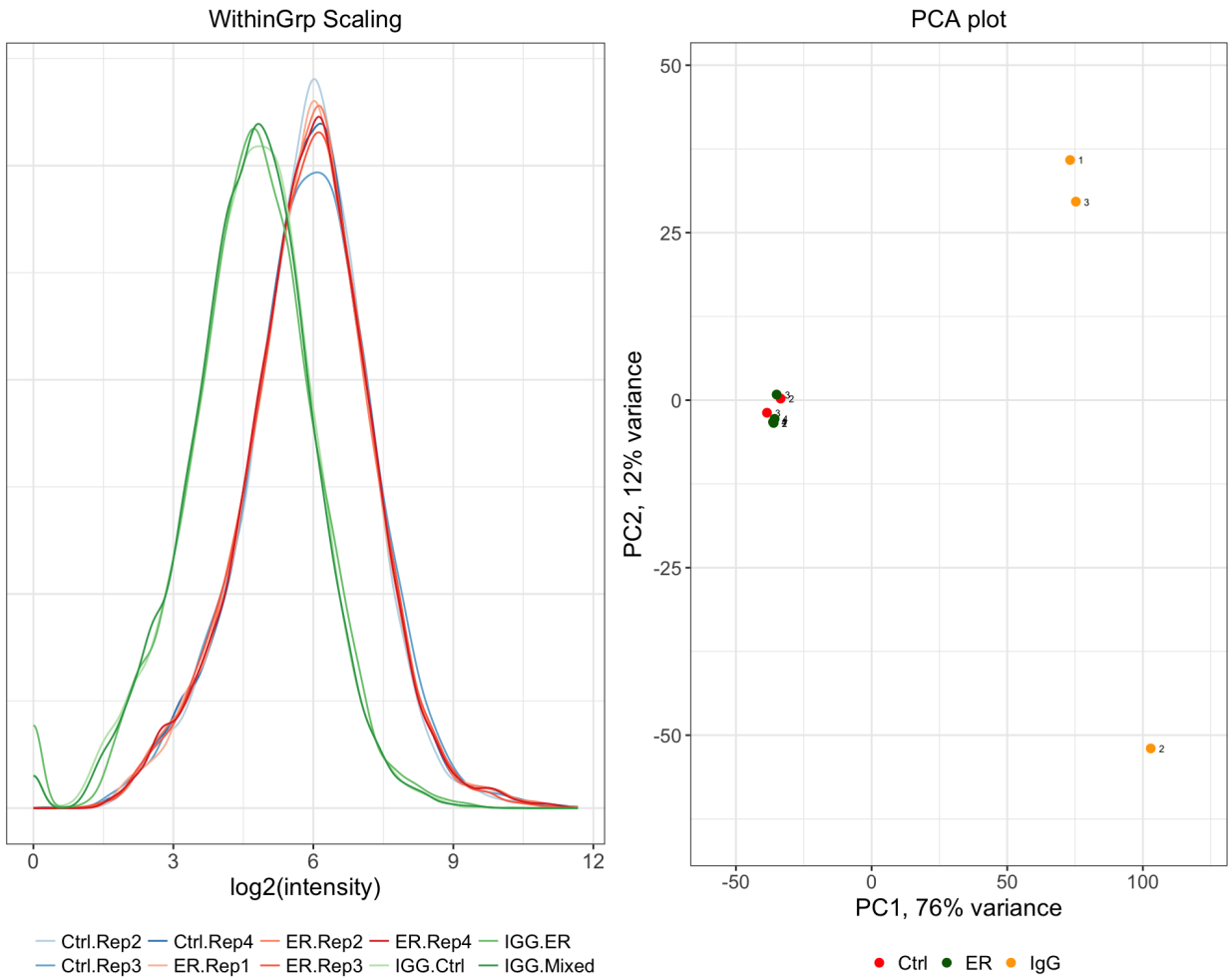


Figure 101: **Figure 10. Effects of normalisation on peptide intensities. **

## 6.4 Remove sample Ctrl 1

The following section shows the same analysis, but with the Ctrl rep 1 sample removed

### 6.4.1 Effect of within group normalisation

Normalisation was carried out using median scaling. The experimental samples and the IgG control samples were normalised separately. Figure 10 show the effects of normalisation on the intensity plots and the principle component analysis.

### 6.4.2 ER - Ctrl

Figure 11 shows differential abundancy results for the contrasts ER_v_Ctrl. Figure 10 shows an MA plot and a volcano plot of the differental analysis results

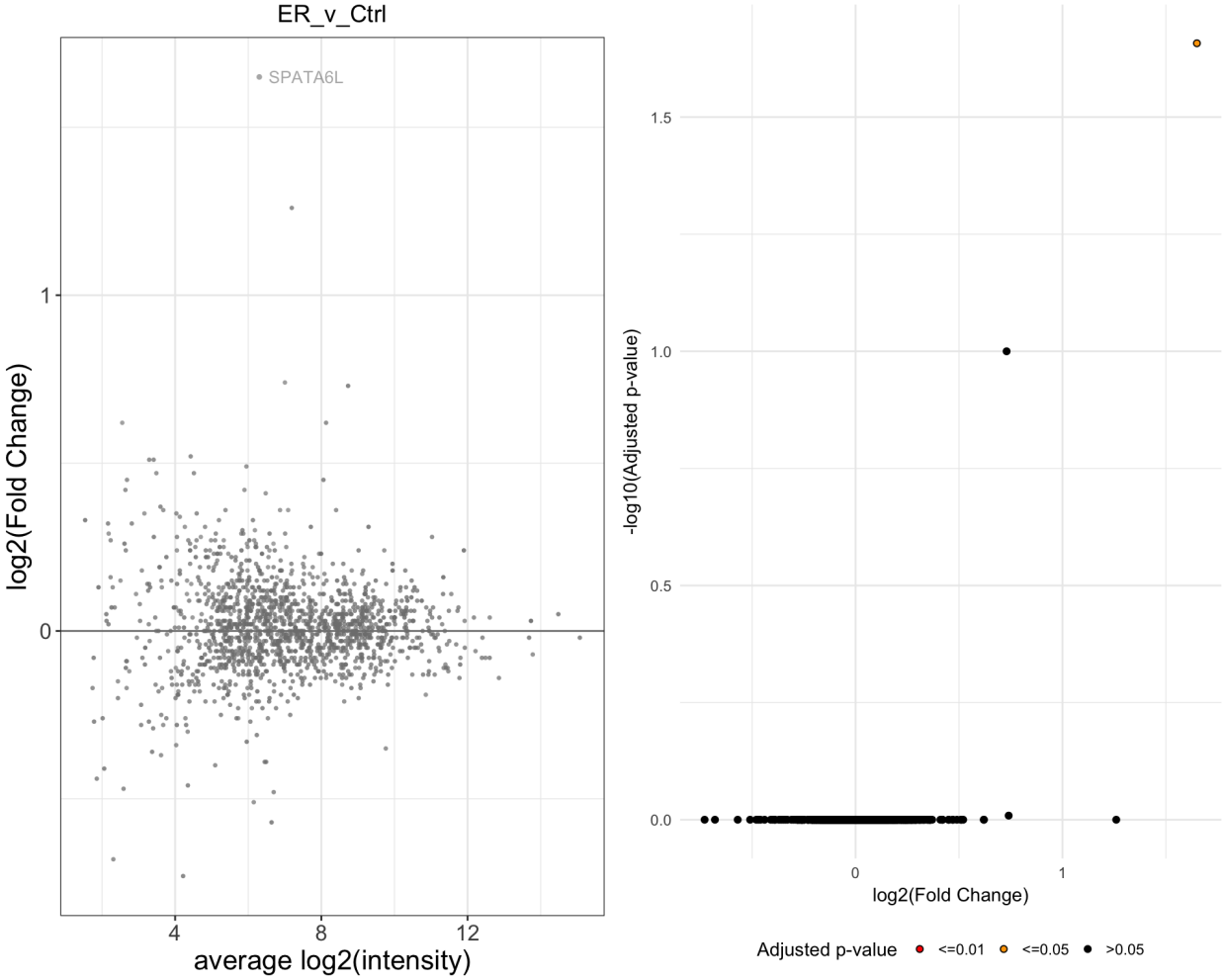


Figure 102: **Figure 12. MA plot and volcano plot of differential protein abundancy. **

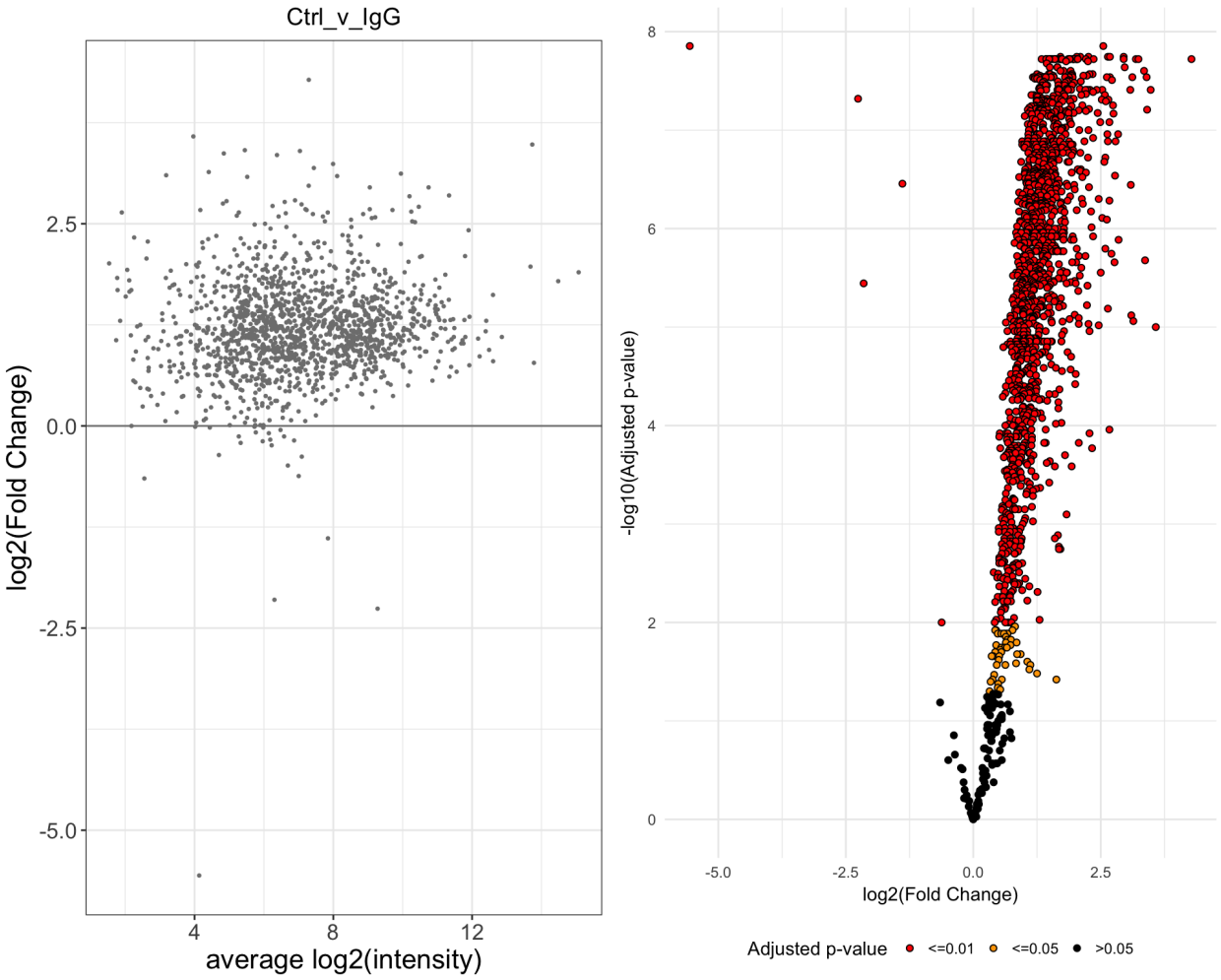


Figure 103: **Figure 15. MA plot and volcano plot of differential protein abundancy. **

### 6.4.3 Ctrl - IgG

Figure 13 shows differential abundancy results for the contrasts Ctrl_v_IgG. Figure 14 shows an MA plot and a volcano plot of the differental analysis results.

### 6.4.4 ER - IgG

Figure 16 shows differential abundancy results for the contrasts ER_v_IgG. Figure 17 shows an MA plot and a volcano plot of the differental analysis results.

# 7 Effect of GRHL2 expression on eRNA and mRNA

## 7.1 Effect of GRHL2 overexpression on eRNA transcription

```
library("ggpubr")
```

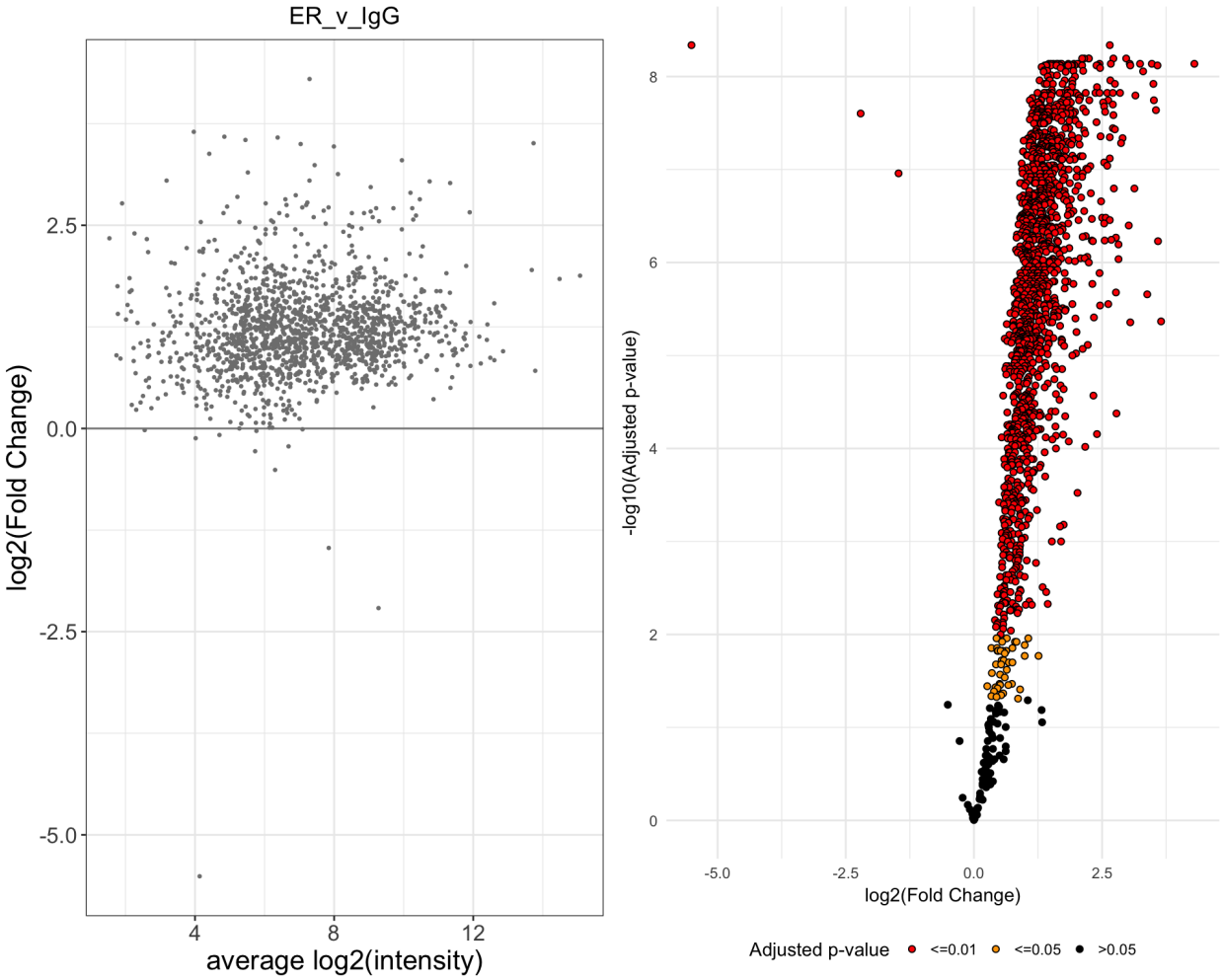


Figure 104: **Figure 18. MA plot and volcano plot of differential protein abundancy. **

```
eRNA<-read.csv("txt/eRNA_values.csv")

oe<-eRNA[eRNA$Experiment=="overexpression",]

oe_comparisons <- list( c("Control","GRHL2") )
oe_p <- ggboxplot(oe, x = "Treatment", y = "eRNA",
               add = "jitter", color="Treatment",
               facet.by="Gene", ylab="Relative eRNA levels")
oe_p <- oe_p + stat_compare_means(comparisons = oe_comparisons,
                       method = "wilcox.test" ,
                       paired=TRUE)
oe_p
```

## 7.2 Effect of GRHL2 knockdown on eRNA transcription

```
si<-eRNA[eRNA$Experiment=="knockdown",]

si_comparisons <- list( c("siCtrl","siGRHL2") )
p <- ggboxplot(si, x = "Treatment", y = "eRNA",
               add = "jitter", color="Treatment",
               facet.by="Gene", ylab="Relative eRNA levels")
p + stat_compare_means(comparisons = si_comparisons,
                       method = "wilcox.test" ,
                       paired = TRUE)
```

### 7.2.1 siRNA combined test

```
wilcox.test(si$eRNA[si$Treatment=='siCtrl'],
            si$eRNA[si$Treatment=='siGRHL2'],
            paired=TRUE, alternative="less")
```

```
##
##  Wilcoxon signed rank test
##
## data:  si$eRNA[si$Treatment == "siCtrl"] and si$eRNA[si$Treatment == "siGRHL2"]
## V = 45, p-value = 0.04071
## alternative hypothesis: true location shift is less than 0
```

## 7.3 Effect of GRHL2 overexpression on mRNA transcription

```
qpcr<-read.csv("txt/QPCR GREB1 XBP1 TFF1.csv", header=TRUE)
df<-data.frame(qpcr)

p <- ggboxplot(df, x = "Sample", y = "Expression", ylab="Relative Expression",
               xlab="Condition",
               color = "Sample", palette =c("#00AFBB", "#E7B800", "#FC4E07"),
               add = "jitter", shape = "Sample", facet.by="Target",
               outlier=FALSE)
```

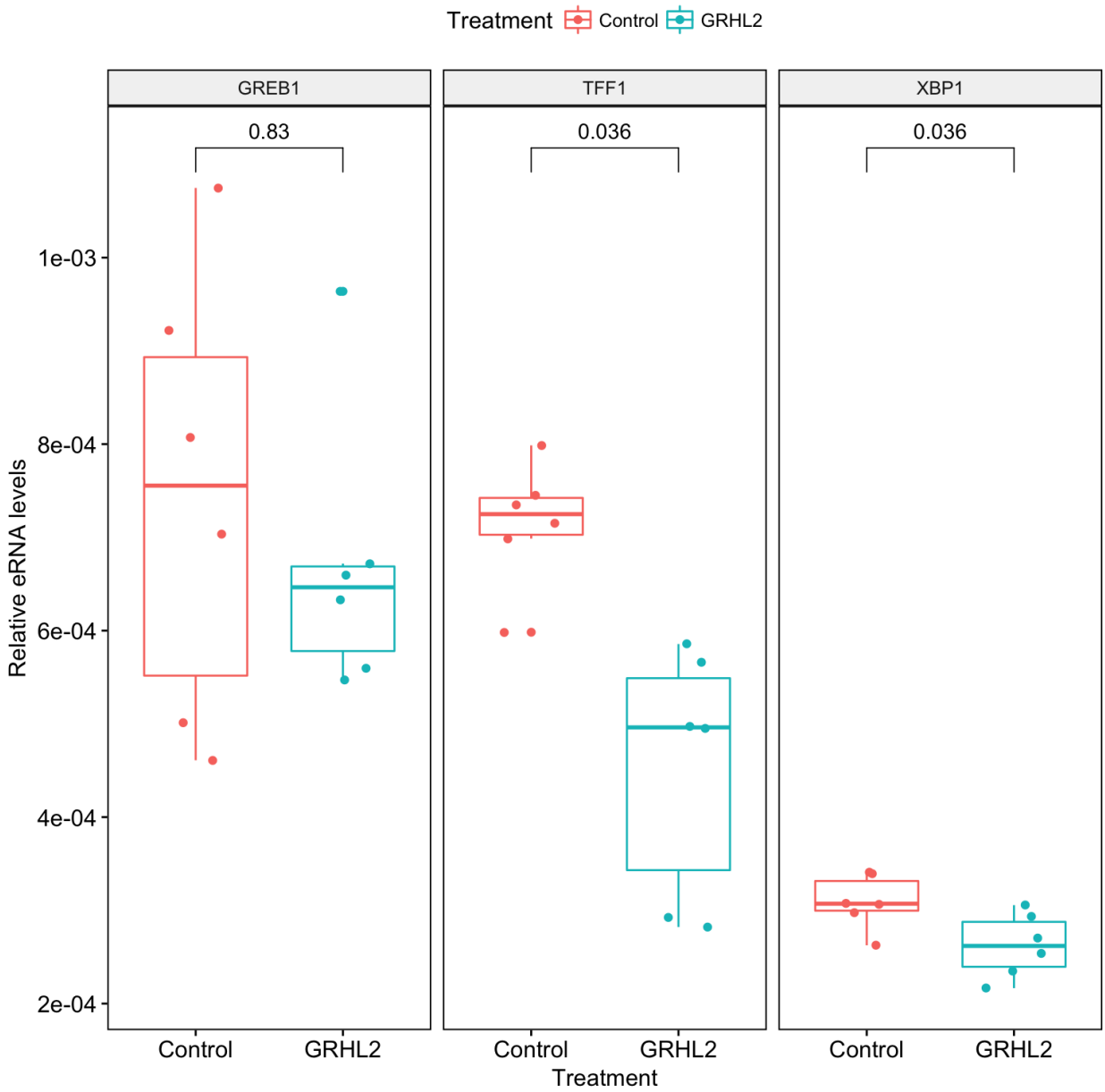


Figure 105: Effect of Overexpression of GRHL2 on eRNA at E2 responsive binding sites.

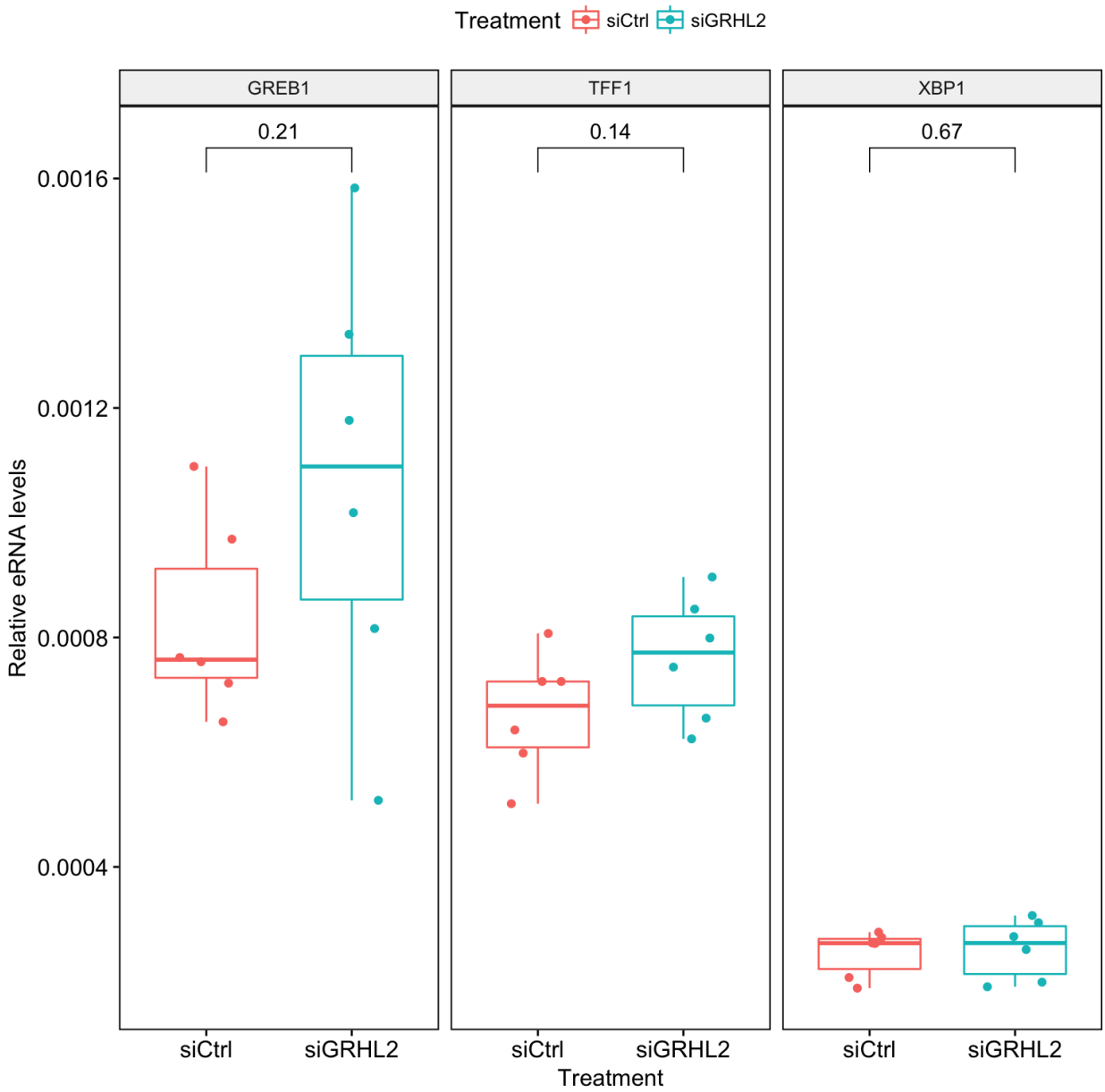


Figure 106: Effect of knockdown of GRHL2 on eRNA at E2 responsive binding sites.

```r
my_comparisons <- list( c("Ctrl", "siGRHL2"), c("Ctrl","GRHL2-DDK"))
p +
    stat_compare_means(comparisons = my_comparisons,method="t.test", paired=TRUE)  +
    theme(axis.text.x = element_text(angle = 90, hjust = 1))
```

# 8 Technical Session Info

The following code describes the R environment used to generate this document and will help making it fully reproducible should there be future updates in any of the packages.

```r
sessionInfo()
```

```
## R version 3.4.1 (2017-06-30)
## Platform: x86_64-apple-darwin15.6.0 (64-bit)
## Running under: OS X El Capitan 10.11.6
##
## Matrix products: default
## BLAS: /Library/Frameworks/R.framework/Versions/3.4/Resources/lib/libRblas.0.dylib
## LAPACK: /Library/Frameworks/R.framework/Versions/3.4/Resources/lib/libRlapack.dylib
##
## locale:
## [1] en_GB.UTF-8/en_GB.UTF-8/en_GB.UTF-8/C/en_GB.UTF-8/en_GB.UTF-8
##
## attached base packages:
##  [1] grid      stats4    parallel  stats     graphics  grDevices utils
##  [8] datasets  methods   base
##
## other attached packages:
##  [1] rmarkdown_1.6
##  [2] DT_0.2
##  [3] readxl_1.0.0
##  [4] qPLEXanalyzer_1.0.0
##  [5] statmod_1.4.30
##  [6] plyr_1.8.4
##  [7] UniProt.ws_2.16.0
##  [8] RCurl_1.95-4.8
##  [9] bitops_1.0-6
## [10] RSQLite_2.0
## [11] TxDb.Hsapiens.UCSC.hg38.knownGene_3.4.0
## [12] knitr_1.17
## [13] bindrcpp_0.2
## [14] preprocessCore_1.38.1
## [15] limma_3.32.10
## [16] xtable_1.8-2
## [17] kfigr_1.2
## [18] MSnbase_2.2.0
## [19] ProtGenerics_1.8.0
## [20] mzR_2.10.0
## [21] Rcpp_0.12.13
## [22] tibble_1.3.4
## [23] dplyr_0.7.4
## [24] tidyr_0.7.2
```

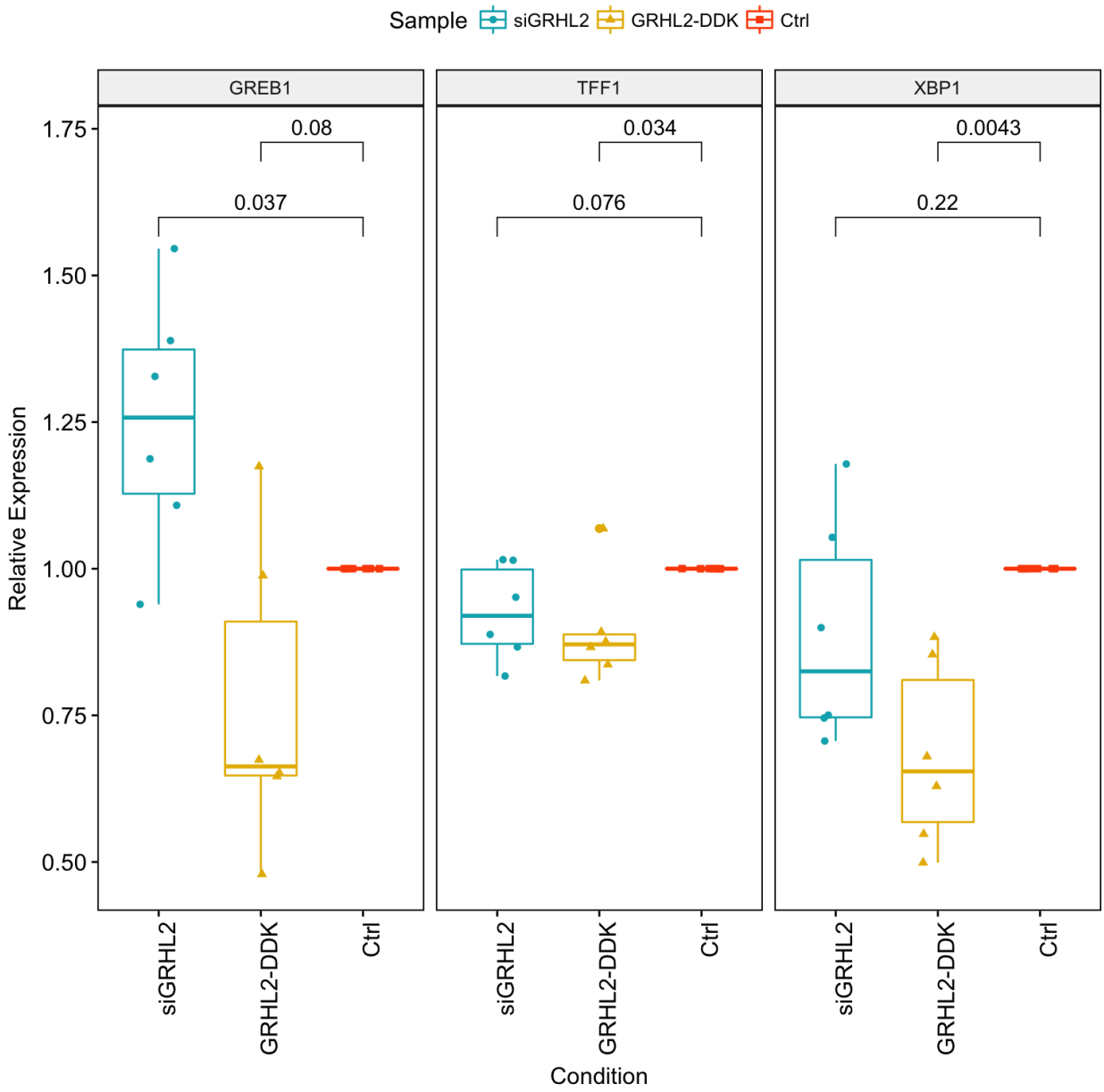


Figure 107: Effect of GRHL2 expression on E2 responsive genes.

```
## [25] GeneNet_1.2.13
## [26] fdrtool_1.2.15
## [27] longitudinal_1.1.12
## [28] corpcor_1.6.9
## [29] gridExtra_2.3
## [30] org.Hs.eg.db_3.4.1
## [31] vulcan_0.99.36
## [32] caTools_1.17.1
## [33] csaw_1.10.0
## [34] BiocParallel_1.10.1
## [35] wordcloud_2.5
## [36] RColorBrewer_1.1-2
## [37] zoo_1.8-0
## [38] DESeq_1.28.0
## [39] lattice_0.20-35
## [40] locfit_1.5-9.1
## [41] TxDb.Hsapiens.UCSC.hg19.knownGene_3.2.2
## [42] GenomicFeatures_1.28.5
## [43] AnnotationDbi_1.38.2
## [44] gplots_3.0.1
## [45] ChIPpeakAnno_3.10.2
## [46] VennDiagram_1.6.17
## [47] futile.logger_1.4.3
## [48] Biostrings_2.44.2
## [49] XVector_0.16.0
## [50] viper_1.10.0
## [51] DiffBind_2.5.6
## [52] SummarizedExperiment_1.6.5
## [53] DelayedArray_0.2.7
## [54] matrixStats_0.52.2
## [55] Biobase_2.36.2
## [56] GenomicRanges_1.28.6
## [57] GenomeInfoDb_1.12.3
## [58] IRanges_2.10.5
## [59] S4Vectors_0.14.7
## [60] BiocGenerics_0.22.1
## [61] ggpubr_0.1.6
## [62] magrittr_1.5
## [63] ggplot2_2.2.1
##
## loaded via a namespace (and not attached):
##   [1] sendmailR_1.2-1               highcharter_0.5.0
##   [3] rtracklayer_1.36.6            AnnotationForge_1.18.2
##   [5] vioplot_0.2                   acepack_1.4.1
##   [7] bit64_0.9-7                   data.table_1.10.4-2
##   [9] rpart_4.1-11                  hwriter_1.3.2
##  [11] AnnotationFilter_1.0.0        doParallel_1.0.11
##  [13] lambda.r_1.2                  rlist_0.4.6.1
##  [15] bit_1.1-12                    lubridate_1.7.1
##  [17] httpuv_1.3.5                  assertthat_0.2.0
##  [19] amap_0.8-14                   evaluate_0.10.1
##  [21] BiocInstaller_1.26.1          Rhtslib_1.8.0
##  [23] quantmod_0.4-12               igraph_1.1.2
##  [25] DBI_0.7                       geneplotter_1.54.0
```

```
##  [27] htmlwidgets_0.9              purrr_0.2.4
##  [29] corrplot_0.84                backports_1.1.1
##  [31] BatchJobs_1.6                geepack_1.2-1
##  [33] annotate_1.54.0              biomaRt_2.32.1
##  [35] imputeLCMD_2.0               TTR_0.23-2
##  [37] ensembldb_2.0.4              Cairo_1.5-9
##  [39] fail_1.3                     BSgenome_1.44.2
##  [41] checkmate_1.8.4              GenomicAlignments_1.12.2
##  [43] xts_0.10-1                   mnormt_1.5-5
##  [45] sparcl_1.0.3                 cluster_2.0.6
##  [47] segmented_0.5-2.2            lazyeval_0.2.0
##  [49] genefilter_1.58.1            edgeR_3.18.1
##  [51] pkgconfig_2.0.1              slam_0.1-40
##  [53] labeling_0.3                 nlme_3.1-131
##  [55] nnet_7.3-12                  bindr_0.1
##  [57] rlang_0.1.2                  sandwich_2.4-0
##  [59] seqinr_3.4-5                 affyio_1.46.0
##  [61] GOstats_2.42.0               AnnotationHub_2.8.3
##  [63] cellranger_1.1.0             rprojroot_1.2
##  [65] graph_1.54.0                 Matrix_1.2-11
##  [67] base64enc_0.1-3              pheatmap_1.0.8
##  [69] png_0.1-7                    rjson_0.2.15
##  [71] KernSmooth_2.23-15           geeM_0.10.0
##  [73] blob_1.1.0                   qvalue_2.8.0
##  [75] stringr_1.2.0                regioneR_1.8.1
##  [77] ShortRead_1.34.2             brew_1.0-6
##  [79] tmvtnorm_1.4-10              ggsignif_0.4.0
##  [81] scales_0.5.0                 memoise_1.1.0
##  [83] GSEABase_1.38.2              cp4p_0.3.5
##  [85] gdata_2.18.0                 zlibbioc_1.22.0
##  [87] compiler_3.4.1               pcaMethods_1.68.0
##  [89] DESeq2_1.16.1                Rsamtools_1.28.0
##  [91] ade4_1.7-8                   affy_1.54.0
##  [93] systemPipeR_1.10.2           DAPARdata_1.4.0
##  [95] Category_2.42.1              htmlTable_1.9
##  [97] Formula_1.2-2                MASS_7.3-47
##  [99] tidyselect_0.2.3             vsn_3.44.0
## [101] stringi_1.1.5                highr_0.6
## [103] yaml_2.1.14                  norm_1.0-9.5
## [105] latticeExtra_0.6-28          MALDIquant_1.17
## [107] ggrepel_0.7.0                tools_3.4.1
## [109] DAPAR_1.8.7                  imp4p_0.5
## [111] foreach_1.4.4                foreign_0.8-69
## [113] idr_1.2                      mzID_1.14.0
## [115] digest_0.6.12                Iso_0.0-17
## [117] shiny_1.0.5                  broom_0.4.3
## [119] MESS_0.5.0                   httr_1.3.1
## [121] psych_1.7.8                  colorspace_1.3-2
## [123] XML_3.98-1.9                 truncnorm_1.0-7
## [125] splines_3.4.1                RBGL_1.52.0
## [127] multtest_2.32.0              gmm_1.6-1
## [129] jsonlite_1.5                 futile.options_1.0.0
## [131] BBmisc_1.11                  R6_2.2.2
## [133] Hmisc_4.0-3                  htmltools_0.3.6
```

```
## [135] mime_0.5                      glue_1.1.1
## [137] class_7.3-14                  interactiveDisplayBase_1.14.0
## [139] codetools_0.2-15              mvtnorm_1.0-6
## [141] mixtools_1.1.0                curl_3.0
## [143] gtools_3.5.0                  openxlsx_4.0.17
## [145] GO.db_3.4.1                   survival_2.41-3
## [147] munsell_0.4.3                 e1071_1.6-8
## [149] GenomeInfoDbData_0.99.0       iterators_1.0.9
## [151] impute_1.50.1                 reshape2_1.4.2
## [153] gtable_0.2.0
```